Distribution Agreement

Signature:

______________________________ _______________
Elizabeth Marie Kline Date

Innate and Adaptive Immune System Crosstalk in Parkinson's Disease

By

Elizabeth Marie Kline
Doctor of Philosophy

Graduate Division of Biological and Biomedical Science
Neuroscience

Malú G. Tansey
Advisor

Francisco Alvarez
Committee Member

Jacob Kohlmeier
Committee Member

Jeremy Boss
Committee Member

Gary Miller
Committee Member

W. Michael Caudle
Committee Member

Accepted:

Lisa A. Tedesco, Ph.D.
Dean of the James T. Laney School of Graduate Studies

Date

Innate and Adaptive Immune System Crosstalk in Parkinson's Disease

By

Elizabeth Marie Kline
B.S. University of Pittsburgh, 2013
B.A. University of Pittsburgh, 2013

Advisor: Malú G. Tansey, PhD

An abstract of
A dissertation submitted to the Faculty of the
James T. Laney School of Graduate Studies of Emory University
in partial fulfillment of the requirements for the degree of
Doctor of Philosophy
in Neuroscience
2019

Abstract

Innate and Adaptive Immune System Crosstalk in Parkinson's Disease

By Elizabeth Marie Kline

Parkinson's disease is a neurodegenerative movement disorder characterized by degeneration of dopaminergic neurons in the substantia nigra and aggregation of α-synuclein. The cause of Parkinson's disease (PD) is unknown, although genetic and environmental risk factors have been identified. The signaling pathways downstream of antigen presentation and mixed lineage kinases regulate a multitude of neuronal and immune functions and are of interest in PD.

Mixed lineage kinases (MLKs) are expressed by both neuronal and glial cells. Because they are upstream of cell death pathways, previous work focused on inhibition as a possible therapeutic strategy. In this work, a neuroprotection study is presented in which specific inhibition of mixed lineage kinase 3 was tested in a neurotoxin model of PD in mice. It was found that the mixed lineage kinase 3 (MLK3) inhibitor did not interfere with the neurotoxin, was able to cross the blood-brain barrier, and did inhibit phosphorylation of an MLK3 target (JNK). By targeting MLK3 with the inhibitor CLFB-1134, protection of dopaminergic cell bodies and terminals was achieved, although striatal levels of dopamine were not restored to the level observed in control animals.

Antigen presentation via the protein major histocompatibility complex class II (MHCII) is suspected to contribute to PD pathology based on genome-wide association studies, post-mortem histology, and evidence from animal models of PD. Here it is reported that mice with peripheral myeloid deletion of MHCII display changes in T cell frequencies and maintain tyrosine hydroxylase expression in the striatum following nigral human α-synuclein expression. The pesticide cypermethrin, a member of the pyrethroid family known to increase risk for PD in humans, did not robustly exacerbate the inflammation or degeneration caused by human α-synuclein expression. This work also describes an investigation of the effects of an MHCII single nucleotide polymorphism genotype on T cell subsets in PD patients.

MLK3 kinase function and MHCII antigen presentation regulate key neuronal and immune functions that appear to influence the neurodegenerative process in PD. Anti-inflammatory therapeutic interventions that attempt to diminish MHCII expression and inhibition of MLK3 represent different approaches to preserve nigrostriatal dopamine and prevent the progression of degeneration.

Innate and Adaptive Immune System Crosstalk in Parkinson's Disease

By

Elizabeth Marie Kline
B.S. University of Pittsburgh, 2013
B.A. University of Pittsburgh, 2013

Advisor: Malú G. Tansey, PhD

A dissertation submitted to the Faculty of the
James T. Laney School of Graduate Studies of Emory University
in partial fulfillment of the requirements for the degree of
Doctor of Philosophy
in Neuroscience
2019

ACKNOWLEDGEMENTS

Thank you to all the people who volunteered their time and tissue to make these studies possible. Thank you to Emory University's Department of Animal Research. Thank you to our funding sources: MJFF, NIH NINDS 5R01NS092122-03.

My Lab-mates: Thank you to the entire Tansey Lab. I could not have done this work without the help of Jianjun Chang, Billie Jeanne Duke, Yuan Yang, Matthew Goodson, and Danielle Oliver. Thank you to those who came before me and who left an amazing trail and guided me along my way: Drs. George Kannarkat, Kathryn MacPherson, and Darcie Anna Cook. Thank you also to Dr. Madelyn Houser for all you have taught me. Thank you, Mary Herrick, for encouraging me and answering all of my flow cytometry questions. Sean Kelly and Rachel Egger Kelly, thank you for your help. Thank you to Dr. Lori Eidson (and Mac!) for cheering me on and cheering me up. Thank you to Laura Butkovich for being one of the kindest, most interesting people I have ever met. It was an honor to work with you. Dr. Valerie Joers: you are a treasured friend and a wonderful role model. Thank you for keeping me company and guiding me.

My Friends: Thank you to Dr. Brandi Wynne for fueling my work with happy times. Isabella Salamone deserves special thanks for all she has done to help me be a better person. Em Maier deserves many thanks, as well, for taking care of me. Dr. Maria Briscione, Paul Vizza, and Michael Vizza: thank you for the gorgeous sunshine you brought into my life and for still inviting me out when I was very rainy. Maria, you have been the roof over and the voice in my head so many times during graduate school. I am very grateful for you. Dr. Erica Landis

and Rebekah Blakney are co-authors of my adulthood and deserve many thanks. It has been enormously fun to share this time with you. Thank you.

My Partner: Thank you for being an accepting, supportive, inspiring presence every day and for loving me the way you do, Daniel John Healy.

Dr. Malú Tansey: Thank you for taking me on as a trainee. Thank you for helping me become the scientist, thinker, teacher, and person I am today. I am forever grateful to have been on your team.

My Family: I would like to thank my grandparents, Carl Kline, Thomas Maroon, Gaylona Kline, and Lou Maroon, who supported my education. My parents, Bill and Mary Ann Kline, and my sister, Emily Kline, are to be thanked for their overwhelming love, encouragement, and guidance. Thank you for listening to me and for helping me grow.

TABLE OF CONTENTS

1. **INTRODUCTION** 1

1.1 Genetic and environmental factors converge to disrupt immune function and increase risk for Parkinson's disease. 1

1.1a) Parkinson's disease background 2

1.1b) Brain inflammation in PD and animal models of PD 4

1.1c) PD immunophenotype 13

1.1d) PD genetic factors with known immune system effects 21

1.1e) PD environmental risk factors with known immune system effects 34

1.1f) PD gene-environment interactions with known effects on the immune system 43

1.1g) Conclusion 45

1.2 Mixed-lineage kinase 3 46

2. **THE SECOND GENERATION MIXED-LINEAGE KINASE-3 (MLK3) INHIBITOR CLFB-1134 PROTECTS AGAINST NEUROTOXIN-INDUCED NIGRAL DOPAMINERGIC NEURON LOSS** 50

2.1 Introduction 50

2.2 Materials and Methods 52

2.2a) Screening pharmacokinetics in mice and rats 52

2.2b) 1-methyl-4-phenyl-1,2,3,6-tetrahydropyridine studies 52

2.2c) High performance liquid chromatography of striatal neurochemistry 56

2.2d) Phospho-JNK and total JNK immunoassay 56

2.2e) Western blot 57

2.2f) Histology and stereology 58

2.2g) Statistics 59

2.3 Results 59

2.3a) CLFB-1134 displays a favorable pharmacokinetic profile with high brain penetrance in rats and mice 59

2.3b) MLK3 inhibition *in vivo* with CLFB-1134 does not interfere with MPTP metabolism to MPP+ 63

2.3c) *In vivo* administration of CLFB-1134 engages the target MLK3 and results in attenuated JNK phosphorylation. 65

2.3d) CLFB-1134 protects against MPTP-induced loss of striatal dopaminergic terminals 67

2.3e) MLK3 inhibition *in vivo* with CLFB-1134 did not protect against MPTP-induced striatal DA depletion 69

2.3f) MLK3 inhibition *in vivo* with CLFB-1134 protects against MPTP-induced nigral dopaminergic degeneration. 69

2.4 Discussion 72

3. PERIPHERAL MYELOID CELL MHCII EXPRESSION IN MICE AFFECTS IMMUNOPHENOTYPE AND HUMAN WT α-SYNUCLEIN-INDUCED NEURODEGENERATION AND INFLAMMATION 77

3.1 Introduction 77

3.2 Materials and Methods 82

3.2a) Mice 82

3.2b) Virus and stereotaxic injection 83

3.2c) Immunofluorescence 84

3.2d) Western blot 85

3.2e) Immune cell isolation and flow cytometry 86

3.2f) Mesoscale Discovery multiplex enzyme linked immunosorbent assay 88

3.2g) Quantitative real time polymerase chain reaction 89

3.2h) Statistics 90

3.3 Results 90

3.3a) Verification of MHCII deletion in peripheral myeloid cells in LysMCre+ IAbfl/fl mice 90

3.3b) Immunophenotyping of LysMCre±IAb$^{fl/f}$ mouse peripheral blood mononuclear cells 97

3.3c) Immunophenotyping of LysMCre±IAb$^{fl/f}$ following 3 weeks of cypermethrin treatment 100

3.3d) T cell subsets in the peripheral blood and deep cervical lymph nodes of LysMCre±IAb$^{fl/f}$ mice 103

3.3e) T cell subsets of LysMCre±IAb$^{fl/}$ mice following 3 weeks of cypermethrin treatment 111

3.3f) LysMCre-IAb$^{fl/f}$ mice do not differ in plasma levels of inflammatory cytokines 4 months post-rAAV2/9 human WT α-synuclein injection 116

3.3g) Cypermethrin treatment increases plasma IL-1β in LysMCre+I-Ab$^{fl/fl}$ mice 118

3.3h) Demonstration of human α-synuclein expression in the SN following viral vector injection 121

3.3i) Inflammatory gene expression in the striatum 4 months after nigral rAAV2/9 human WT α-synuclein injection 124

3.3j) Assessment of striatal dopaminergic terminals 4 months after rAAV2/9 human WT WT α-synuclein injection 128

3.3k) Short-term cypermethrin exposure does not decrease tyrosine hydroxylase or dopamine transporter protein expression, even in the presence of human WT α-synuclein 131

3.4 Discussion 133

4. CHARACTERIZATION OF T CELL SUBSETS ASSOCIATED WITH rs3129882 GENOTYPE IN PARKINSON'S DISEASE PATIENTS AND CONTROLS 143

4.1 Introduction 143

4.2 Materials and Methods 146

4.2a) Cohort subject recruitment and genotyping 146

4.2b) Peripheral blood mononuclear cell isolation, cryopreservation, and thaw 147

4.2c) Flow cytometry 147

4.2d) Study approval 148

4.2e) Statistics 148

4.3 Results 148

4.3a) Characteristics of human study population 148

4.3b) High-risk *rs3129882* genotype is associated with decreased number of Tregs, and interactions between SNP and PD affect effector memory subset counts 150

4.4 Discussion 159

5. CONCLUSIONS 162

APPENDIX 168

Antibodies used in Chapters 2-4 168

List of Figures and Tables

Figure 1. Working model of innate and adaptive immune crosstalk via MHCII in PD 33

Figure 2. CLFB-1134 does not interfere with MPTP metabolism 64

Figure 3. *In vivo* target engagement by CLFB-1134 66

Figure 4. CLFB-1134 protects against MPTP-induced loss of striatal TH 68

Figure 5. CLFB-1134 does not protect against MPTP-induced striatal DA depletion 70

Figure 6. CLFB-1134 protects against MPTP-induced nigral dopaminergic cell loss 71

Figure 7. Flow cytometry gating strategies for mouse splenocytes and mouse peritoneal immune cells 92-93

Figure 8. MHCII deletion in peripheral myeloid cells of naïve LysMCre+I-Ab$^{fl/fl}$ mice 94

Figure 9. Flow cytometry gating strategies for mouse PBMC general immune cell types and PBMC and DCLN T cell subsets 95-96

Figure 10. MHCII deletion in LysMCre+I-Ab$^{fl/fl}$ PBMCs 98-99

Figure 11. No difference in MHCII+ cell frequency or number between LysMCre-I-Ab$^{fl/fl}$ and LysMCre+I-Ab$^{fl/fl}$ PBMCs following 3 weeks of cypermethrin or vehicle treatment. 101-102

Figure 12. CD4+ T cell subsets are affected by LysMCre-mediated deletion of MHCII 104-107

Figure 13. The frequency of effector memory CD4+ T cells in mouse deep cervical lymph nodes is affected by LysMCre-mediated deletion of MHCII 108-110

Figure 14. Cypermethrin and LysMCre genotype affect PBMC T cell frequencies 112-114

Figure 15. Cypermethrin and LysMCre affect the frequency of total T cells and central memory CD4s in the deep cervical lymph nodes 114-115

Figure 16. Plasma cytokine and chemokine levels do not differ between LysMCre- and LysMCre+I-Ab$^{fl/fl}$ mice 117-118

Figure 17. Plasma IL-1β levels increase with cypermethrin treatment in LysMCre+I-Ab$^{fl/fl}$ mice 119-120

Figure 18. Targeting of rAAV2/9 human WT α-synuclein to the mouse substantia nigra 122

Figure 19. Targeting of rAAV2/5 human WT α-synuclein to the mouse substantia nigra 123

Figure 20. Inflammatory gene expression in the striatum 4 months after nigral rAAV2/9 human WT α-synuclein injection 125-127

Figure 21. Tyrosine hydroxylase and dopamine transporter protein expression are decreased ipsilateral to rAAV2/9 human WT α-synuclein injection in LysMCre-I-Ab$^{fl/fl}$ striatum. 129-130

Figure 22. Short-term cypermethrin exposure does not decrease tyrosine hydroxylase or dopamine transporter protein expression, even in the presence of human WT α-synuclein 132

Figure 23. Human T cell subset gating strategy 151

Figure 24. High-risk *rs3129882* genotype is associated with decreased number of Tregs, and interactions between SNP genotype and PD affect effector memory counts. 152-158

Table 1. Experimental groups for MPTP studies 55

Table 2. CLFB-1134 pharmacokinetic properties in mice and rats 60-62

Table 3. Primers for mouse striatal qPCR 89

Table 4. Characteristics of human study population 149

CHAPTER 1. INTRODUCTION

1.1 Genetic and environmental factors converge to disrupt immune function and increase risk for Parkinson's disease.

The goal of this introductory chapter is to describe Parkinson's as a disease of neuroimmune dysfunction, arising, in part, from interactions between genetic factors and environmental exposures arbitrated by the immune system. While age is the greatest risk factor for Parkinson's disease (PD), genetic and environmental factors contribute to risk as well, although mechanisms remain unclear. Despite awareness of PD for over two hundred years, no therapies capable of modifying disease progression exist. It may be the case that failure of experimental clinical interventions could be attributed to the categorization of PD patients as a relatively uniform group rather than subdividing patients based on genetic variations and environmental exposures. Enriching trials for subjects with specific genetic risk factors and/or specific environmental exposures may reveal contexts in which some therapeutic strategies can be successful. The immune system mediates outcomes to environmental exposures based on specific heritable trains that influence immune function, and this will be the focus of the review, rather than the direct effects of environmental exposures on the neurons that degenerate in PD. By synthesizing the information in this way and focusing on the critical role of the immune system, we seek to further the development of immunomodulatory approaches to prevent or delay onset of PD and to push the field toward greater consideration of the gene-environment context of individual PD patients. In this way, PD patients may receive more precision medical care suitable for their specific genetics and environmental exposures.

1.1a) Parkinson’s disease background

In 1817, James Parkinson, a medical doctor, described a “shaking palsy”. The condition was detailed and named after Parkinson by the scientist Jean-Martin Charcot in 1872. At that time, the pathology of the disease was unknown, but by 1893, a patient with a tumor in the substantia nigra was described in a case study by Paul Blocq and Georges Marinesco (Hostiuc et al., 2016). Because this patient had a resting tremor, like the patients described by Parkinson in his essay, the connection between the substantia nigra and parkinsonism emerged. Fritz Heinrich Lewy, writing in 1912, first published a characterization of the proteinaceous aggregates in PD brain, including areas outside the substantia nigra. The observation was corroborated by Konstantin Nikolaevich Tretiakoff in 1919, and Tretiakoff named the structures “Lewy bodies” (LBs). Decades later, in the 1990s, the 140 amino acid protein α-synuclein was identified as a primary component of LBs in PD as well as dementia with LBs and the synucleinopathy multiple system atrophy. The field shifted significantly in how α-synuclein is regarded within the mechanism of PD pathogenesis in 1997 when a missense mutation in the gene for α-synuclein was identified in an Italian family with multiple cases of early onset PD (Polymeropoulos et al., 1997). Braak and colleagues, in 2003, published a staging system for idiopathic PD based on the localization of α-synuclein-containing LBs (Braak et al., 2003). The dorsal motor nucleus of the vagal nerve was identified as a possible point of origin for LB formation in the brain. Since then, genome wide association studies (GWASs) have shown that variations in *SNCA* are associated with increased risk for idiopathic PD (Satake et al., 2009; Simon-Sanchez et al., 2009). In terms of the field's awareness of PD as a neuroimmune dysfunction, activated microglia were first observed in post-mortem PD brain tissue in 1988 (McGeer et al., 1988b; McGeer et al., 1988a). This was followed by the measurement of inflammatory cytokines including IL-1β, IL-6, epidermal growth factor, and transforming growth factor-α in PD brain (Mogi et al., 1994b).

Currently, PD is the most common neurodegenerative movement disorder, affecting approximately 10 million patients worldwide (Dorsey et al., 2007). There are approximately 50,000 new diagnoses of PD per year and the number of patients is expected to double by 2030 (Dorsey et al., 2007). PD is diagnosed in the clinic based on motor symptoms including resting tremor, gait abnormalities, postural instability, and bradykinesia (Poewe et al., 2017). These motor symptoms are brought on by deficiency in the neurotransmitter dopamine (DA) induced by degeneration of striatal dopaminergic terminals and death of neurons in the substantia nigra (SN), a midbrain nucleus, although this is not the only brain region affected by the disease. The other neuropathological hallmark of PD is the presence of proteinaceous aggregations called Lewy bodies (LBs), or, when present in neuronal processes, Lewy neurites. The protein α-synuclein is the main component of LBs (Ingelsson, 2016). In humans, non-human primates, and rodents, DA neurons in the SN project to the medium spiny neurons of the striatum, a brain region within a network known as the basal ganglia. Currently, the main treatment for PD is DA replacement by dosing with levodopa which can be converted to dopamine by DOPA decarboxylase. Deep brain stimulation (DBS) surgeries are offered to some PD patients whose symptoms are not successfully managed by levodopa treatment. These interventions have existed for a relatively long time and can address motor symptoms, but do not modify the progression of dopamine loss (Birkmayer and Hornykiewicz, 1961; Benabid et al., 1987).

Idiopathic PD likely originates from diverse underlying mechanisms, making assessment of risk, evaluation of prognosis, and design of treatment challenging. Because of the complex nature of neuroimmune interactions and differences between PD models and PD patients, there is no consensus in the field definitively establishing whether the various phases of the immune response in PD are adaptive and ought to be enhanced for therapeutic outcomes or are disease-promoting and should be inhibited. Here we review several inflammation-related phenomena in PD, the peripheral blood immunophenotype changes associated with PD, genetic and environmental factors known to engage the immune system in PD, and, finally, synergy between genetic and environmental factors that converge on the immune system and are likely to affect the progression of disease.

1.1b) Brain inflammation in PD and animal models of PD

Using positron-emission tomography (PET) imaging, radioligands that bind microglial surface markers such as ^{11}C-PH1195, ^{11}C-PBR, or ^{18}F-FEPPA, can detect ongoing neuroinflammation in living PD patients (Banati et al., 1997; Papadopoulos et al., 2006). These studies reported that PD brains are characterized by increased microglial activation in the pons, basal ganglia, frontal and temporal cortex. Importantly, while the observed PET signal has been attributed to microglia, distinguishing between microglia and macrophage from the peripheral immune system has not been possible in these studies. The importance of identifying cells in the brain as microglia or infiltrating peripheral immune cells will be discussed in later sections of this review. Regardless, the magnitude of PET ligand signal does not correlate with UPDRS score in all studies, but does in some (Ouchi et al., 2005). Thus, via PET, determining whether neuroinflammation is directly associated with degree of motor impairment is not currently possible in humans. PET studies of PD are limited by substantial inter-individual variability, and because fluctuations in microglial or macrophage phenotype throughout disease likely exist, studies have to control for factors such as age of onset and disease duration to more accurately interpret PET findings (Joers et al., 2017).

Post-mortem comparisons of PD and age-matched healthy control brains describe the presence of cells positive for the antigen presentation protein major histocompatibility complex class II (MHCII) in the PD SN, indicating immune activation within an area of degeneration (McGeer et al., 1988a). MHC-II expression in PD brain has been shown to correlate with deposition of α-synuclein (Croisier et al., 2005). Other specific indicators of immune activation in the PD brain include increased caspase activity and increased expression of tumor necrosis factor receptor 1 (TNFR1), p53 protein, interferon-γ (IFNγ), and nuclear factor kappa-light-chain-enhancer of activated B cells (NFκB) (Boka et al., 1994; Mogi et al., 2000; Mogi et al., 2007). In a case where humans unknowingly self-administered a synthetic analogue of meperidine, the neurotoxin 1-methyl-4-phenyl-1,2,3,6-tetrahydropyridine (MPTP) which is toxic to DA neurons, the SN was characterized by MHCII+ cells upon post-mortem examination (Langston et al., 1999). The evidence from Langston et al. and

McGeer et al. suggests that that DA degeneration arising from acute neurotoxin exposure or PD both can result in antigen presentation (McGeer et al., 1988b; Langston et al., 1999).

Antigen presentation involves the uptake of pathogens, proteins, or cellular debris by antigen presenting cells (dendritic cells, macrophages, microglia, etc.) via phagocytosis or macropinocytosis. These internalized molecules are processed into peptides through endolysosomal pathways, resulting in peptide loading onto MHC complexes for presentation to naïve T cells (Roche and Furuta, 2015). In antigen presentation via MHCII, the peptide-MHCII complex is recognized by the T cell receptors on CD4+ T cells. Structurally, MHCII molecules are heterodimeric, consisting of an α chain and a β chain (Trowsdale, 1993). The genetic locus for MHCII codes for three α/β heterodimeric isotypes known as HLA-DR, -DQ, and DP (Trowsdale, 1993). The type of antigen loaded into MHCII is dependent upon the MHCII isotype. T cells in turn bind the peptide-MHC complex via their clonotypic T cell receptor with support from coreceptors (Pennock et al., 2013). Cytolytic CD8+ T cells recognize antigenic peptides loaded onto MHCI and kill infected or marked target cells through direct cell-to-cell contact and cell lysis via release of granzyme B and other proteases. CD4+ T cells take on helper phenotypes and release a blend of cytokines that can act directly on cellular receptors to activate cell death pathways, recruit innate immune cells, and drive B cell activation (Pennock et al., 2013).

Identifying the antigen presenting cells observed in post-mortem PD tissue as immune cells that are brain resident (microglia) or infiltrators from the peripheral immune system has been a challenge. Doing so remains an important goal because of the meaning for treatment; for example, it is useful to know whether a drug needs to cross the blood-brain barrier. Peripheral and brain-resident immune cells are likely to be functionally distinct, having originated in developmentally separate tissues and matured in a different cellular neighborhood, and this must be taken into consideration in the identification of druggable targets. While the cells of the peripheral immune system arise from and are renewed by a shared, pluripotent hematopoietic precursor cell population in the bone marrow, microglia are developmentally distinct, originating from progenitors in the yolk sac during embryogenesis (Alliot et al., 1999; Ginhoux et al., 2013). Surface protein and gene expression overlap between microglia and macrophages is extensive. However, in their responses to inflammatory signals such as IL-4, LPS, IFNγ, and dexamethasone, microglia and macrophages exhibit major differences in protein upregulation and cytokine secretion (Michelucci et al., 2009). Even among microglia, there is regional heterogeneity in function, morphology, and cell density (Lawson et al., 1990; Mittelbronn et al., 2001; Kim et al., 2004), with a notable increase in microglia density in the SN and striatum (12% of total cells rather than 5% in other brain regions, (Lawson et al., 1990)). Microglia are not the only central nervous system (CNS) tissue macrophage. There also exists perivascular macrophages, meningeal macrophages, and choroid plexus macrophages, all of which have Iba-1, F4/80, and CX3CR1 expression in common with microglia. Review of the innate immune cells present in or near the CNS can be found in (Ransohoff and Brown, 2012; Lopez-Atalaya et al., 2018). Considering the role of each of these immune cell types in PD neuroinflammation is important.

As the brain's resident phagocytic immune cells, microglia are responsible for effective clearance of debris, including misfolded and aggregated α-synuclein (Hickman et al., 2018). In addition to DA neuron loss, formation of LBs that primarily consist of aggregated α-synuclein and Lewy neurites that form in the axons, are key neuropathological hallmarks of PD. A better understanding of the relationship between microglial antigen presentation and α-synuclein accumulation and formation of LBs will further our understanding of PD and could guide development of immunomodulatory treatments to prevent or delay this disease. Furthermore, increased microglial HLA-DR (a human MHCII molecule) expression occurs in many neurological diseases characterized by chronic neuroinflammation including Alzheimer's, Huntington's, and Pick's disease, broadening the relevance of work on antigen presentation in the CNS (McGeer et al., 1988a).

Lymphocyte presence in the CNS has been reported in PD (McGeer et al., 1988a; Brochard et al., 2009). The precise function of T cells in the brain in PD is not fully understood, but their function has been implicated in learning and memory (Ziv et al., 2006; Kipnis et al., 2012; Radjavi et al., 2014) as well as neurodegeneration (reviewed in (Sommer et al., 2017)). In general, CD8+ T cells recognize and respond to antigen presented in complex with the MHC class I protein (MHCI), which can be expressed by all cells. CD8+ T cells can kill neurons by several different mechanisms including engagement of Fas and TNF signaling pathways, release of granzymes and perforins following recognition of their cognate antigen-MHCI complex (Appel et al., 2010; Coque et al., 2019). Neurons in the SN and locus coeruleus (LC) are reported to up-regulate MHCI in an α-synuclein overexpression model of PD neuropathology, flagging themselves for cell killing mediated by antigen-specific CD8+ T cells (Cebrian et al., 2014). Both CD8+ and CD4+ T cells are more abundant in the brains of PD patients and those of MPTP-intoxicated mice than controls, where the T cell infiltration is known to appear subsequent to gliosis and is evinced by the presence of T cells proximal to blood vessels and melanized DA neurons (Brochard et al., 2009). How adaptive immune cells from the periphery gain access to the brain parenchyma is a matter of controversy. It may be the case that the fluid portion of the CSF drains into the blood via arachnoid granulations, a feature of the meninges localized along sinuses. In this model, immune cells and proteins in CSF could drain through dural lymphatics and into deep cervical lymph nodes, even in the absence of disease, but never enter the parenchyma. However, the presence of T cells within the brain parenchyma in studies of mouse and rat models of PD pathology and in post-mortem PD tissue, contradicts this proposed structural separation (Theodore et al., 2008; Brochard et al., 2009; Sanchez-Guajardo et al., 2010).

In animal models of PD and in *in vitro* systems, microglia can respond to overexpressed, misprocessed (nitrated), WT or mutant α-synuclein, and this reaction occurs prior to neuron death (Croisier et al., 2005; Klegeris et al., 2008; Theodore et al., 2008; Watson et al., 2012; Tansey and Romero-Ramos, 2019). There is evidence to suggest that prion-like, aggregated, or oxidized proteins including α-synuclein may act as immunogenic stimuli in PD, setting off a signaling cascade resulting in neurodegeneration. Pathogenic α-synuclein forms appear to be permitted to accumulate and have been proposed to spread throughout the brain, based on experiments using rodents: rat- (Kirik et al., 2002; Klein et al., 2002; Lo Bianco et al., 2002; Lauwers et al., 2003; Chung et al., 2009; Koprich et al., 2010), mouse- (Lauwers et al., 2003; Theodore et al., 2008; Oliveras-Salva et al., 2013). Comparison of viral vector-mediated α-synuclein expression in rat relative to the intra-striatal delivery of the chemical neurotoxin 6-OHDA model found that both the level of dopamine loss and motor deficits seen after α-synuclein overexpression are similar in extent to that seen after 6-OHDA, but the timing of degeneration and development of motor deficits were progressive, developing over the course of 8-16 weeks post AAV virus injection (Lindgren et al., 2012). Due to the more protracted nature of DA loss and neuron death in the α-synuclein model, viral vector-based models can be regarded as more closely representing the key aspects of PD than the 6-OHDA oxidative neurotoxin model. Importantly, PD is typically diagnosed in the clinic when 60% of SN neurons have been lost (Dauer and Przedborski, 2003), and viral vector mediated overexpression of WT α-synuclein has, at high titers in rats, been shown to produce similar degree of DA neuron loss (Fischer et al., 2016).

High expression of human α-synuclein as compared to green fluorescent protein (GFP) in rodent brain produces notable upregulation of MHCII. In addition to their antigen presenting capacity, brain-resident and peripheral immune cells also release cytokines and chemokines that can not only communicate between immune cells, but can act directly on neurons, causing the activation of caspases and cell death pathways. In order to better understand the role of different immune cells in an α-synuclein-based model of disease, an early study examined recombinant adeno-associated viral vector (rAAV2/5) to drive expression of human, wild-type (WT) α-synuclein in female rats (Sanchez-Guajardo et al., 2010). By adjusting the viral titer, researchers were able to distinguish between ongoing neuron death- or non-death-associated inflammation. Transient increases in microglia cell number occurred in the presence of α-synuclein pathology, independent of cell death (Sanchez-Guajardo et al., 2010). This transient increase in microglia number was followed by long term induction of MHCII expression on Mac1+ cells (macrophages or microglia) (Sanchez-Guajardo et al., 2010). Interestingly, T cell infiltration was associated with the degree of neuron loss such that CD3+ cell counts in the SN were higher when neuron death occurred (Sanchez-Guajardo et al., 2010).

T cell responses have been characterized in other animal models of PD-like degeneration as well. After dopaminergic degeneration induced by MPTP, T cells are present in the SN, specifically those with expression of the transcription factor RORγT, which is found in the CD4+ T cell subset known as Th17's (Liu et al., 2017). Manipulation of T cell functionality, as in RAG1KO mice, can be protective in mice treated with MPTP (Benner et al., 2008). In a mouse model where the CSF1R-targeted compound PLX3397 was used to deplete microglia, increased leukocyte infiltration was observed in the brain following MPTP (Yang et al., 2018). This indicates that, in PD, microglia may act to limit the infiltration of T cells, B cells, and other peripheral immune cells into the brain parenchyma. Microglial depletion, and the associated increase in leukocyte infiltration, exacerbated MPTP-induced DA neuron loss (Yang et al., 2018). It is conceivable, then, that in PD there is either microglial loss-of-function, creating an environment permissive of T cell infiltration, or a T cell migration/activation gain-of-function that supersedes the homeostatic “brakes” offered by microglia. The molecular mechanisms of such processes remain to be understood and future work should prioritize *in vivo* experimental systems where all of these cell types are represented, and their interactions can be studied accordingly.

The results of studies that have examined brain inflammation and infiltration by peripheral immune cells suggest the following cascade of system level events possibly occurs in PD: α-synuclein burden in neurons increases in response to aging and/or some insult, creating a local environment of immune activation and inflammation. Microglia and peripheral immune cells that are present in the brain perivascular space or within the parenchyma itself release proinflammatory cytokines and chemokines and upregulate their antigen presentation proteins. Antigen presentation occurs followed by T cell activation and differentiation. T cells release inflammatory cytokines, entering into a positive feedback loop with innate immune cells. T cells are recruited to the brain perivascular space and potentially into the brain parenchyma. Neurons die, whether by direct mechanisms relating to α-synuclein burden and/or via the effects of downstream of inflammatory cytokine signaling/oxidative stress resulting from immune cell activation. The contribution of various immune cells to neuron dysfunction and, ultimately, death, indicates a complex web of neuron-immune cell interactions. As others have argued, we cannot assume the cascade of events performed by the immune system in response to age-related neurological diseases has been optimized by evolution via natural selection and is thus, adaptive (Cookson, 2012). In summary, there is abundant evidence for innate and adaptive immune system changes in PD in the CNS.

It is not clear whether the immune response in PD most closely resembles an autoimmune disease or the typical response to tissue injury, gone awry within the brain parenchyma. There have been reviews arguing that PD is not the result of an autoimmune response (Moller et al., 1989), but more recent reviews argue the opposite (Benkler et al., 2009; Benkler et al., 2012; De Virgilio et al., 2016; Garretti et al., 2019). That there is tissue injury in PD is not doubted, and acute head injuries increase risk for PD, although the majority of PD cases are not associated with head injury (Nicoletti et al., 2017). As stated above, the neuron death observed in idiopathic PD could be inflicted by immune cells gaining access to the other side of the BBB or immune cells secreting cytokines that maladaptively and continuously activate microglia, astrocytes, and neurons from afar. In animal models of the disease, immune activation can be observed prior to the death of SN DA neurons, thus suggesting that PD need not emerge from a neuron-autonomous process and could be, relatively purely, a result of chronic immune cell activation related to aging plus environmental triggers. The next section will review studies that have attempted to characterize the state of the immune system in PD patients.

1.1c) PD immunophenotype

PD, as a disease of aging, co-exists with the ongoing processes of inflammaging and immunosenescence. Inflammaging refers to the state of chronic, low-grade inflammation present with aging, thought to lead to an immune system “primed” to strongly and rapidly respond to stimulation with previously-experienced antigens (Franceschi and Campisi, 2014). Immunosenescence is the immune system’s decline in naïve cells with age, leading to higher incidence of infections, dysregulated cell proliferation, and autoimmune disease (Aw et al., 2007; Gustafson et al., 2018). Specifically, the CD45RO+CD4+ population, a subset of T helper cells, increases with age (Douek et al., 1998). On top of these ongoing changes in the aging immune system, PD-specific shifts have been identified in certain immune cell frequencies and functionalities, described below.

The existence of inflammation-related differences between PD patients and controls in both the brain and peripheral immune system has been reviewed elsewhere (Deleidi and Gasser, 2013; Kannarkat et al., 2013; Su and Federoff, 2014; Chen et al., 2016; Joshi and Singh, 2018). In studies of peripheral immunophenotype, there is great variability between groups, and specifically the directionality of changes in markers such as IFNγ and TNF in cerebrospinal fluid (CSF, the filtrate of fenestrated blood vessels in the choroid plexus of the brain’s ventricles) and serum has varied enormously. Previously, our lab reported that the variability in human biofluid immune markers may be in part attributable to differences in protocols of biofluid collection and processing or patient disease severity and their comorbidities (Eidson et al., 2017). Our study established that, within an individual, serum IFNγ, IL-8, neutrophil gelatinase-associated lipocalin (NGAL), and TNF as well as CSF IL-8, NGAL, and TNF were relatively stable throughout a day despite diurnal fluctuations in cortisol and other factors affecting inflammatory cytokine release (Eidson et al., 2017). Furthermore, in comparing PD and age-matched healthy control serum, we observed that PD patients have increased NGAL and decreased IFNγ and TNF relative to control subjects (Eidson et al., 2017). In the CSF, PD patients displayed greater fluctuation than controls in levels of the neurodegeneration/aggregation-associated proteins α-synuclein, Aβ40, and Aβ42 throughout the day (Eidson et al., 2017). Most importantly, this study from our group demonstrated that serum TNF combined with CSF α-synuclein levels can correctly sort subjects into PD or control categories with high specificity and sensitivity, suggesting this combination, rather than each biomarker alone, could be used to better asses disease severity, monitor progression, and biofluid inflammation in PD.

Changes in levels of inflammatory cytokines can affect immune cell frequencies in the blood. Comparisons between PD and age-matched control subject immune cell frequencies have revealed changes in T cells, identified by the surface marker CD3. T cells are often divided into two categories based on expression of either CD4 or CD8 coreceptor protein which stabilize the T cell receptor. As discussed above, CD4+ T cells recognize antigen in complex with MHCII, while CD8+ T cells recognize antigen on MHCI. MHCII expression is restricted to professional antigen presenting cells, while MHCI can be expressed by all cell types. CD4+ T cells are reduced relative to CD8+ T cells in PD patient blood (Bas et al., 2001; Baba et al., 2005; Stevens et al., 2012). Those CD4+ T cells that do persist in PD patient blood are more likely to secrete IFNγ, rather than IL-4 (Baba et al., 2005; Stevens et al., 2012). PD subjects have an increase in effector memory (Tem) CD4+T cells that are CD45RO+Fas+ relative to control subjects (Saunders et al., 2012). There is a moderate positive correlation between Unified Parkinson’s Disease Rating Scale III (UPDRSIII) and the frequency of CD45RO+CD4+ T cells (Saunders et al., 2012). A decrease in CD31+α4β7+ CD4+ T cells and diminished IL-9 and IL-6 mRNA in CD4+ T cells was also observed in immune cells isolated from PD patient blood (Saunders et al., 2012). These T cell surface markers have been associated with homing to gut associated lymphoid tissues, which is noteworthy given the gastrointestinal (GI) dysfunction and inflammation associated with PD (Houser and Tansey, 2017). There is also a functional association between DA receptor, specifically D3, expression on CD4+ T cells and neurodegeneration in that D3 knock-out was neuroprotective in an MPTP mouse model, but protection was lost with adoptive transfer of WT CD4+ T cells (Gonzalez et al., 2013; Elgueta et al., 2019). Some evidence suggests that signaling downstream of dopamine receptor D3 in CD4+ T cells is associated with differentiation into Th1-type effector cells (Contreras et al., 2016). Overall studies of PD T cells have suggested that the subset of T cells capable of rapidly responding to re-stimulation are more frequent in PD, making the specific identity of possible stimulating antigen(s) of great interest to the field.

T cell response to specific antigens is important for host defense but can drive tissue damage if sustained. Resolution of an inflammatory response is the function of regulatory T cells (Tregs). Tregs are an immunosuppressive T cell subset characterized by surface expression of the IL-2 receptor CD25 and intracellular expression of the transcription factor FOXP3. Tregs maintain self-tolerance, prevent autoimmunity, and regulate inflammatory responses to injury and pathogens. These functions are accomplished through mechanisms including anti-inflammatory (IL-35, IL-10, and TGF-β) cytokine release, suppression of CD8+ T cells' granzyme functions, "absorbing" IL-2 in the extracellular milieu thereby preventing proliferation of other T cells in the area, and driving downregulation of CD80 and CD86 (co-stimulatory molecules on antigen presenting cells) via CTLA-4 action (reviewed in (Duffy et al., 2018b)). The suppressive functions of Tregs limit the proliferation and effector functions of CD4+ and CD8+ T cells and can inhibit antigen presenting cells as well (Sakaguchi et al., 2008). Several animal studies with the neurotoxin MPTP have indicated that Tregs may play an important role in nigrostriatal dopaminergic neurodegeneration. Interventions that increase Treg frequency result in decreased infiltration of CD4+ T cells into the brain and improved SN DA neuron survival of MPTP treatment. Such treatments include adoptive transfer of Tregs and injection of a compound that promotes Treg proliferation into MPTP-treated mice (Reynolds et al., 2007). In a study where rats were immunized against α-synuclein prior to viral vector-mediated overexpression of α-synuclein, the vaccine's protection against DA neuron loss was associated with increased presence of Tregs in the brain (Sanchez-Guajardo et al., 2013). A potential causal link between increased Tregs and DA neuron survival may be the ability of Tregs to decrease microglial metabolism, migration, protein transport, and redox functions, decreasing the neuroinflammatory damage microglia are capable of (Reynolds et al., 2009). Treg development is, interestingly, regulated to some extent by the PD-related gene *PINK1* (Ellis et al., 2013). One study has reported that the Tregs of patients with PD are limited in their suppressive potential compared to control subjects' Tregs (Chen et al., 2015). Enhancing Treg function may be a therapeutic strategy employed to achieve neuroprotection in PD patients in the future. Administration of the cytokine granulocyte-macrophage colony-stimulating factor (GM-CSF) or adoptive transfer of Tregs from GM-CSF-treated donor mice was used for this type of intervention in MPTP-intoxicated mice (Kosloski et al., 2013; Schutt et al., 2018). T cell subset frequency may serve as a biomarker of sorts, although the relationship between peripheral immunophenotype and central inflammation is not yet fully understood deserve further investigation.

In 2017, a highly influential finding was published reporting that there exist T cells in the peripheral blood mononuclear cell (PBMC) population from PD patients that recognize α-synuclein-derived peptides (Sulzer et al., 2017). A major research question for PD researchers in the future will be understanding how such apparently auto-reactive T cells develop in PD. While there is still some uncertainty regarding precisely which antigens are immunogenic in PD, *in vitro* and *in vivo* studies have suggested that microglia have the capacity to phagocytose certain species of α-synuclein as well as debris released by degenerating DA neurons (Zhang et al., 2005; Park et al., 2008; Marinova-Mutafchieva et al., 2009; Zhang et al., 2011). Intraneuronal inclusions (Lewy bodies and neurites) are comprised of possible immunogenic antigens that become extracellular as neurons die, and these could serve as the stimulus the T cells identified in (Sulzer et al., 2017). While α-synuclein is expressed beginning at least as early as embryonic day 9.5, it is possible that abnormal processing emerging later in life, such as phosphorylation, nitration, and aggregation, renders the protein “foreign” to the immune system (Zhong et al., 2010).

Alternatively, increases in BBB permeability with aging may give immune cells increased access to epitopes shielded earlier in life. Subsequently, α-synuclein-derived epitopes would be loaded for antigen presentation into major histocompatibility complex proteins and presented to low affinity CD4+ T cells that evaded negative thymic selection, as has been hypothesized for other autoimmune disorders (Marrack and Kappler, 2012). Autoimmune reactions can emerge as a result of a) loss of tolerance to self-antigens due to a problem in the thymus' process of T cell selection and the action of regulatory T cells; or b) immune cell receptors with increased sensitivity. It has been hypothesized that loss of self-tolerance can be triggered by environmental factors such as injury or infection (Croisier et al., 2005; Chervonsky, 2010). Indeed, a recent GWAS suggested there are common genetic pathways shared by PD and autoimmune diseases (Witoelar et al., 2017).

What cells could present the possible neoantigens derived from α-synuclein or other neuronal components? Dendritic cells (DCs) are specialized antigen presenting cells that can be divided into two subsets: lymphoid and myeloid. The presence of DCs in the CNS is thought to be low under homeostatic conditions, but DCs are upregulated in the brain parenchyma under inflammatory conditions. It is not known whether the DCs present in inflamed CNS parenchyma arise from the periphery, from differentiated microglia or monocytes, or from immature DCs that normally reside in the meninges (Koutsilieri et al., 2013). DCs have both tolerogenic (induction of T cell anergy, induction of regulatory T cells) and immunogenic functions (migration to lymph nodes, antigen presentation) depending on their stage of maturation. Once in the

CNS, DCs are capable of migrating to the periphery and presenting autoantigens from the CNS, thus priming naïve T cells against proteins in brain tissue (de Vos et al., 2002) (Karman et al., 2004) (Kivisakk et al., 2004). Specifically, neuromelanin has been proposed as a CNS antigen capable of inducing DC activation. Despite the fact that blood DC frequency is reduced in PD and that B cells are known to be reduced in PD patient blood, antibodies against melanin proteins have been identified in PD patients (Bas et al., 2001; Double et al., 2009). In a study of post-mortem tissue from patients with idiopathic or dominantly-inherited PD, IgG binding was observed on DA neurons, and in particular Lewy bodies, and nearby microglia were positive for the IgG receptor FcγRIII (Croisier et al., 2005). Antibodies against α-synuclein and GM1 ganglioside, also a neuronal protein, have been identified in other studies of PD post-mortem tissue (Zappia et al., 2002; Papachroni et al., 2007; Yanamandra et al., 2011). These findings suggest robust antigen presentation and the launching and sustaining of an adaptive immune response against neuronal components. One hypothesis put forth by Koutsilieri et al. states that DCs that have phagocytosed neuron-derived components such as α-synuclein or neuromelanin, migrate to the deep cervical lymph nodes where they can perform antigen presentation to the adaptive immune cells (Koutsilieri et al., 2013). In this way, T cells could be “instructed” to carry out clearance of DA neurons, and B cells could mature into plasma cells capable of producing antibodies directed against proteins derived from DA neurons. The labeling of SN DA neurons with these auto-antibodies could drive complement-mediated neuron destruction and activation of microglial inflammatory functions (reviewed in (De Virgilio et al., 2016).

PD is associated with altered protein processing, creating an opportunity for neo-antigen production. The PD immunophenotype is characterized by changes in inflammatory cytokine levels and the types of T cells, especially CD4+ T cells circulating in the blood. Possible PD biomarkers may be identified by further investigation of immune cell frequencies in PD, particularly auto-reactive T cells. How early in disease progression such cells are present remains to be determined. Understanding when the autoimmune-like features of the immune system first emerge in PD progression will greatly inform the field's understanding of the role of immune cells in PD pathogenesis.

1.1d) PD genetic factors with known immune system effects

Historically, PD was regarded as a disease without any significant genetic component, as multiple twin studies indicated no role for genetic risk (Duvoisin et al., 1981; Ward et al., 1983; Eldridge and Ince, 1984). The field's focus on genetic factors shifted in 1997 with the identification of a rare, highly penetrant mutation that caused monogenic PD within a family (Polymeropoulos et al., 1997). This mutation was identified in *SNCA*, the gene encoding α-synuclein. Subsequently, mutations in 15 different genes have been identified as monogenic causes of PD, including *PARKIN, PINK1,* and *DJ1* (Kitada et al., 1998; Valente et al., 2001; Bonifati et al., 2003). In 3-5% of idiopathic or genetically complex cases of PD, a variation in one of those 15 genes is present (Billingsley et al., 2018). However, monogenic cases make up less than 10% of all PD cases (Ross, 2013). Current understanding of PD genetics proposes that there is a continuum from monogenic disease to complex inheritance featuring combinations of risk factors (Billingsley et al., 2018). GWAS have so far indicated that the frequency of a genetic risk factor within the population is, in general, inversely correlated with the conferred risk of disease, and this appears to be the case for PD (McCarthy et al., 2008; Kumaran and Cookson, 2015). As reviewed in (Billingsley et al., 2018), PD may emerge in people carrying one of several rare variations that moderately increase risk; or it may be the case that PD occurs in people who possess multiple, common genetic variants, each independently conferring a small increase in risk that, together, have a significant cumulative effect. Within some loci, both rare and common variants associated with disease have been identified, including *SNCA* and *LRRK2*. We will focus the next portion of this review on the relationship between three genetic risk factors and their influence on immune function. These three genes were chosen because they are highly expressed within immune cells. The broader immunogenetics of PD are more thoroughly reviewed in (Jimenez-Ferrer and Swanberg, 2018).

ALPHA-SYNUCLEIN

SNCA duplications, triplications, mutations, and variations are all associated with PD. Variations in the *SNCA* gene have been described and are associated with “idiopathic or genetically complex PD (Simon-Sanchez et al., 2009); (Consortium et al., 2011) (Lill et al., 2012) (Nalls et al., 2014) (Chang et al., 2017) are associated with “idiopathic” or genetically complex PD. The REP1 263-base pair allele has been associated with PD, as have the single-nucleotide polymorphisms (SNPs) rs356219, rs356165, rs11931074, and rs7684318 (in

White and Asian populations) (Mizuta et al., 2006; Ross et al., 2007) (Maraganore et al., 2006; Myhre et al., 2008). An analysis of 36 articles in 2018 found 7 SNPs in *SNCA* that significantly increase risk for PD in the overall population (Zhang et al., 2018). The specific effects of each of these variations on the immune system remains to be studied, but some general points of importance are reviewed here.

SNCA encodes α-synuclein, an acidic, heat resistant, and unstructured protein made up of 140 amino acids (Ueda et al., 1993; Lavedan, 1998; Kahle et al., 2002). Highly expressed in brain tissue, α-synuclein can be localized at the pre-synaptic terminal. Structurally, the protein has 3 regions: the N terminal region (amino acids 1-60) containing KTKEGV repeats that form amphipathic alpha helices, similar to the lipid binding domains of apolipoproteins; the Central region (61-95 amino acids) containing a very hydrophobic non-amyloid-beta-component of Alzheimer's disease region; and finally the acidic C terminal region (96-140 amino acids). In humans with and without PD, α-synuclein can be found in the neuronal cytoplasm as well as in extracellular biofluids including cerebrospinal fluid (CSF) and blood plasma. In mice, transport of α-synuclein has been reported from blood to brain following injection of radiolabeled α-synuclein into the jugular vein, and from brain to blood following intracerebroventricular delivery (Sui et al., 2014). This suggests that, at least in mice, peripheral, extracellular α-synuclein could be dynamically related to central levels of the protein.

Importantly, the brain is not the only source of α-synuclein. In the intestinal tissue, mucosa of the appendix, and the cells of the enteric nervous system, α-synuclein can be detected in non-PD and PD cases (Bottner et al., 2012; Gold et al., 2013; Gray et al., 2014). Multiple studies report levels of α-synuclein in PD gut are higher than in controls (Forsyth et al., 2011; Shannon et al., 2012; Gold et al., 2013). In a mouse line where α-synuclein is overexpressed under the Thy1 promoter, blockage of the colon and severe distension was observed in 9-12 month-old mice, suggesting high α-synuclein expression impairs gut motility, consistent with the reports of frequent constipation in PD patients (Hallett et al., 2012). Interestingly, α-synuclein was localized specifically within the intra-lysosomal compartment of macrophages within the appendix, in one study, possibly suggesting homeostatic consumption of α-synuclein by phagocytes in the gut, or lysosomal localization of α-synuclein (Gray et al., 2014).

Immune cells elsewhere are known to express α-synuclein under basal conditions, specifically erythroid precursors and megakaryocytes in bone marrow and peripheral blood (Hashimoto et al., 1997; Nakai et al., 2007). Circulating human B, T, and NK cells as well as monocytes all express α-synuclein (Shin et al., 2000; Kim et al., 2004). In hematopoiesis and B cell lymphopoiesis, α-synuclein plays a necessary role, as identified in a study on α-synuclein knock-out mice (Xiao et al., 2014). α-synuclein KO mice exhibit anemia and abnormal B cell development and synthesis of IgG, but not IgM (Xiao et al., 2014). Additionally, α-synuclein KO mice have increased numbers of CD3+ CD4-CD8- thymocytes and fewer single positive (CD4+ or CD8+) T cells (Shameli et al., 2016). Knock-out of α-synuclein was also found to affect IL-2 production of CD4+ T cells and the frequency of Tregs (Shameli et al., 2016). These observations are consistent with the hypothesis that α-synuclein affects the affinity of T cell receptors (TCRs) for peptide-MHC complexes, as Treg development is the result of high-affinity peptide-antigen binding. Furthermore, if α-synuclein function is lost in PD, due to aberrant post-translational modification, mis-localization, oligomerization, or aggregation, TCR:peptide-MHC interactions could be disrupted in a manner analogous to that of the α-synuclein KO mice.

The mechanism mediating the TCR:peptide-MHC connection is similar to the function α-synuclein performs in neurons. There, α-synuclein is a chaperone for the soluble N-ethylmalemide-sensitive factor attachment protein receptor (SNARE) complex and contributes to assembly/disassembly of vesicle fusion with the plasma membrane (Bendor et al., 2013; Diao et al., 2013). Oligomerization of α-synuclein interrupts this process through binding with synaptobrevin-2 (Choi et al., 2013). Transgenic mice overexpressing human α-synuclein display decreased neurotransmitter release (Nemani et al., 2010). SNARE complexes are important in T cells as well. In T cells, SNARE complex is essential for localizing TCRs, proper formation of the "immunological synapse" with peptide-MHC complexes, and the exocytic release of lytic granules in CD8+T cells (and NK cells) (Das et al., 2004; Pattu et al., 2012). Thus, disruptions in the SNARE-binding function of α-synuclein could conceivably have extensive effects on T cells.

Despite the fact the α-synuclein is expressed throughout development, several forms of the protein or species derived from it have been observed to elicit an immune response, possibly giving rise to the autoreactive T cells specific for α-synuclein discussed above. In murine primary cultures, the scavenger receptor CD36 contributes to α-synuclein-induced microglial activation (Su et al., 2008). In 2009, a specific amino acid sequence motif within the C terminal of α-synuclein was found to elicit dose-dependent TNF secretion in a mouse macrophage cell line (Lee et al., 2009). This is further evidence for the existence of a cascade in which microglia recognize extracellular α-synuclein, resulting in release of inflammatory cytokines.

Rodent models of PD pathology relying on viral vector-mediated α-synuclein expression (WT or with the A53T mutation) or injection of pre-formed fibrils of α-synuclein in the SN have demonstrated that the immune system launches an innate and adaptive response to α-synuclein in its fibrilized or full-length, monomeric forms (Sanchez-Guajardo et al., 2010; Barkholt et al., 2012; Nash et al., 2015; Thome et al., 2015; Harms et al., 2017; Duffy et al., 2018a; Olesen et al., 2018; Williams et al., 2018). Microglial morphology changes following experimental α-synuclein expression in animal models (Joers et al., 2017). NFκB increases, upregulation of TLR2 and TLR3, and increased inflammatory cytokine production have been reported in various rodent studies (Theodore et al., 2008; Cao et al., 2010; Fellner et al., 2013; Allen Reish and Standaert, 2015; Duffy et al., 2018a; Jimenez-Ferrer and Swanberg, 2018; Wang et al., 2018; Williams et al., 2018). Toll-like receptors on microglia, especially

TLR2 and 4, have been associated with microglial response to α-synuclein (Fellner et al., 2013; Dzamko et al., 2017). The evidence from animal models conclusively demonstrates the capacity for α-synuclein, at high levels of expression or in WT form, to induce a robust innate and adaptive immune response.

In peripheral blood of PD patients, T cells that recognize and respond to α-synuclein were reported by Sulzer et al. as discussed above, corroborating the ample evidence from animal models that α-synuclein can act as an immune stimulus (Sulzer et al., 2017). This apparent autoimmune response, as in other autoimmune diseases, could result in diffuse inflammation, proliferation of antigen-specific T cells, and a B lymphocyte response with production of antibodies against autoantigens. Progress in our understanding of α-synuclein as an immunogenic protein and regulator of neuronal and immune cell function benefits not only PD patients with rare *SNCA* mutations or polymorphisms, but idiopathic PD patients as well, as they too present with abnormal expression and post-translational modification of α-synuclein.

LEUCINE-RICH REPEAT KINASE 2

While some cases of PD arise from known variations or mutations in the gene for Leucine-rich Repeat Kinase 2 (LRRK2), idiopathic cases exhibit changes in LRRK2 expression and function. Mutations in *LRRK2* are the most common monogenic form of PD and are autosomal dominantly inherited (Paisan-Ruiz et al., 2004; Zimprich et al., 2004). The gene encodes a 286 kDa, 2527 amino acid protein. LRRK2 has at least 7 functional domains including a ROC (Ras of complex) GTPase domain as well as a kinase domain. LRRK2 is thought to interact with many other proteins via its leucine rich repeat domain, C-terminal W40 repeat domain, and armadillo and ankyrin repeat domains. LRRK2 structure and functional domains are detailed in (Mata et al., 2006).

LRRK2 has been reported to regulate many cellular functions including vesicle trafficking (Migheli et al., 2013; Carrion et al., 2017; Choudhary et al., 2017; Pan et al., 2017; Rassu et al., 2017), monocyte adhesion to endothelial cells (Hongge et al., 2015), ceramide metabolism (Ferrazza et al., 2016), autophagy (Plowey et al., 2008; Ramonet et al., 2011), macroautophagy (Manzoni, 2017), and lysosomal formation and acidification (Schapansky et al., 2015; Wallings et al., 2019). LRRK2 is a negative regular of nuclear factor of activated T cells (NFAT), which functions in innate immune activation, T cell cytokine production, and neuronal differentiation (Rao et al., 1997; Graef et al., 2003; Gardet et al., 2010; Greenblatt et al., 2010; Liu et al., 2011). Wnt and nuclear factor-κB cell signaling pathways also involve LRRK2, and LRRK2 negatively regulates protein kinase A (Parisiadou et al., 2014; Russo et al., 2015; Berwick et al., 2017). The gene *LRRK2* is also known as *Park8* and dardarin and is expressed in monocytes, dendritic cells, macrophages, B cells, and T cells in addition to neurons. Its expression in microglia at baseline and following inflammatory stimulation has been inconsistently reported (Moehle et al., 2012; Kozina et al., 2018). Expression in leukocytes was reported to be low at baseline, but inducible with IFNγ, and, to some extent, IFNβ, TNF or IL-6 (Gardet et al., 2010; Hakimi et al., 2011; Thevenet et al., 2011). In macrophages, LRRK2's upregulation in response to inflammatory stimulus is mediated by JAK/STAT and ERK5 (Kuss et al., 2014). It is important to consider, in targeting LRRK2 for PD treatment, that LRRK2's function and responsiveness appears to be highly cell-type-dependent.

Patients who carry the G2019S mutation in *LRRK2* have increased inflammatory cytokines in the sera (Dzamko et al., 2016), specifically IL-1β. In rats with the G2019S LRRK2 mutation, increased inflammatory cytokine levels were observed ten months after intracortical delivery of the highly immunogenic compound lipopolysaccharide (LPS) (Schildt et al., 2019). Consistent with this observation, LRRK2 KO rats are resistant to α-synuclein or LPS-induced DA neurodegeneration, suggesting inhibiting LRRK2 function or expression may support DA neuron survival (Daher et al., 2014). Inducing intestinal and systemic inflammation in G2019S rats elicits dampened CD4 helper responses, especially Th17 responses in the colon, brain, and blood (Park et al., 2017). This suggests that the increased kinase activity associated with the G2019S LRRK2 mutation promotes the generation of more suppressive immune cells and a decreased frequency of Th17 T cells. In mice overexpressing the LRRK2 mutations dosed with peripheral LPS, there was a shift in inflammatory cytokine production (Kozina et al., 2018). While WT mice experienced no nigral cell death following the LPS treatment, LRRK2 mutant mice did display DA neuron loss (Kozina et al., 2018). Thus, the G2019S LRRK2 mutation drives shifts in immune cell frequencies and function.

B cells and T cells from PD patients have higher expression of LRRK2 than healthy controls, independent of any known LRRK2 variation or mutation. In previous work from our lab, peripheral blood mononuclear cells from human PD patients and healthy controls were compared (Cook and Tansey, 2017). CD16+ non classical monocytes, also called alternatively activated or patrolling monocytes, displayed higher LRRK2 expression in PD patients than in controls (Cook and Tansey, 2017). Inflammatory cytokine secretion from monocytes was greater in PD patients than in controls and correlated with LRRK2 expression in T cells in PD patients (but not HCs) (Cook and Tansey, 2017). The work suggests that the function of LRRK2 in immune cells is altered in PD and should be considered in research regarding the role of LRRK2 in PD pathogenesis, along with the role of LRRK2 in DA neurons. For an in-depth review of LRRK2 function in immune cells see (Cook and Tansey, 2017).

MAJOR HISTOCOMPATIBILITY COMPLEX CLASS II

As discussed above, antigen presentation relies the MHC proteins, class I and II. MHC genes, called human leukocyte antigen (HLA) genes, are expressed in a coordinated fashion following induction by cytokines or other immune activation signals. The MHC locus, located on chromosome 6 in humans, is the most highly polymorphic gene cluster in the human genome and its expression is highly regulated by epigenetic mechanisms. The expression of all genes for MHCII are primarily controlled by a promoter proximal element called the W-X-Y box region. Constitutively expressed transcription factors bind the W-X-Y box region and form a scaffold for the master-regulator of MHCII expression called CIITA (class II transactivator) (Choi et al., 2011). CIITA expression is cytokine dependent, and MHCII protein levels are directly proportional to CIITA expression (Choi et al., 2011). Thus the local concentration of cytokines will influence CIITA and MHCII expression, making a cell's antigen presentation capacity dynamic. MHCII is expressed as an α-β heterodimer. The α- and β- chain genes are encoded by *HLA-DR*, *-DP*, and *-DQ*. The *HLA-DRB1*, *HLA-DQA1,* and *HLA-DQB1* genes are among the most highly variable human genes, allowing for diversity in the human population's antigen presenting capacity.

In a healthy CNS, MHCII expression is difficult to detect. In PD brains, where inflammatory cytokines are abundant, there is expression of the human MHCII protein HLA-DR detectable by immunohistochemical stain (McGeer et al., 1988b). One study in 2013 reported an association between PD and an MHCII haplotype present in 15% of the general population including MHCII gene alleles DRB5*01 and DRB1*15:01 (Wissemann et al., 2013). Several GWAS have identified single nucleotide polymorphisms in the MHC as variations associated with increased risk of PD (Hamza et al., 2010; Guo et al., 2011; Hill-Burns et al., 2011; International Parkinson Disease Genomics et al., 2011; Ahmed et al., 2012; Sun et al., 2012; Wissemann et al., 2013).

Our group previously reported that the *GG* genotype at the single nucleotide polymorphism *rs3129882* in the first intron of *HLA-DRA* is associated with PD and increased baseline expression in homozygous individuals regardless of disease and is also associated with greater inducibility of MHCII on B cells and monocytes in *GG* individuals with PD (Kannarkat et al., 2015). On the basis of these findings, we hypothesized that high expression of MHCII on brain myeloid cells is detrimental to DA neurons in the SN, while diminished antigen presentation capacity should be neuroprotective (**Figure 1**). Supporting this, in a study of MHCII KO mice, it was observed that DA neurons were less susceptible to α-synuclein-induced neuroinflammation and degeneration (Harms et al., 2013). Similarly, CIITA KO mice displayed the same attenuation of α-synuclein-induced lesion (Williams et al., 2018). In rats, increased numbers of MHCII+ cells in the SN following the overexpression of human α-synuclein was associated with greater DA neuron loss (Jimenez-Ferrer and Swanberg, 2018). Thus, increased antigen presentation via MHCII appears to promote PD pathology. Therefore, while there have been no reports of mutations in MHCII linked to monogenic forms of PD, several relatively common genetic variants in *HLA* genes increase risk for PD.

Figure 1. Working model of innate and adaptive immune crosstalk via MHCII in PD

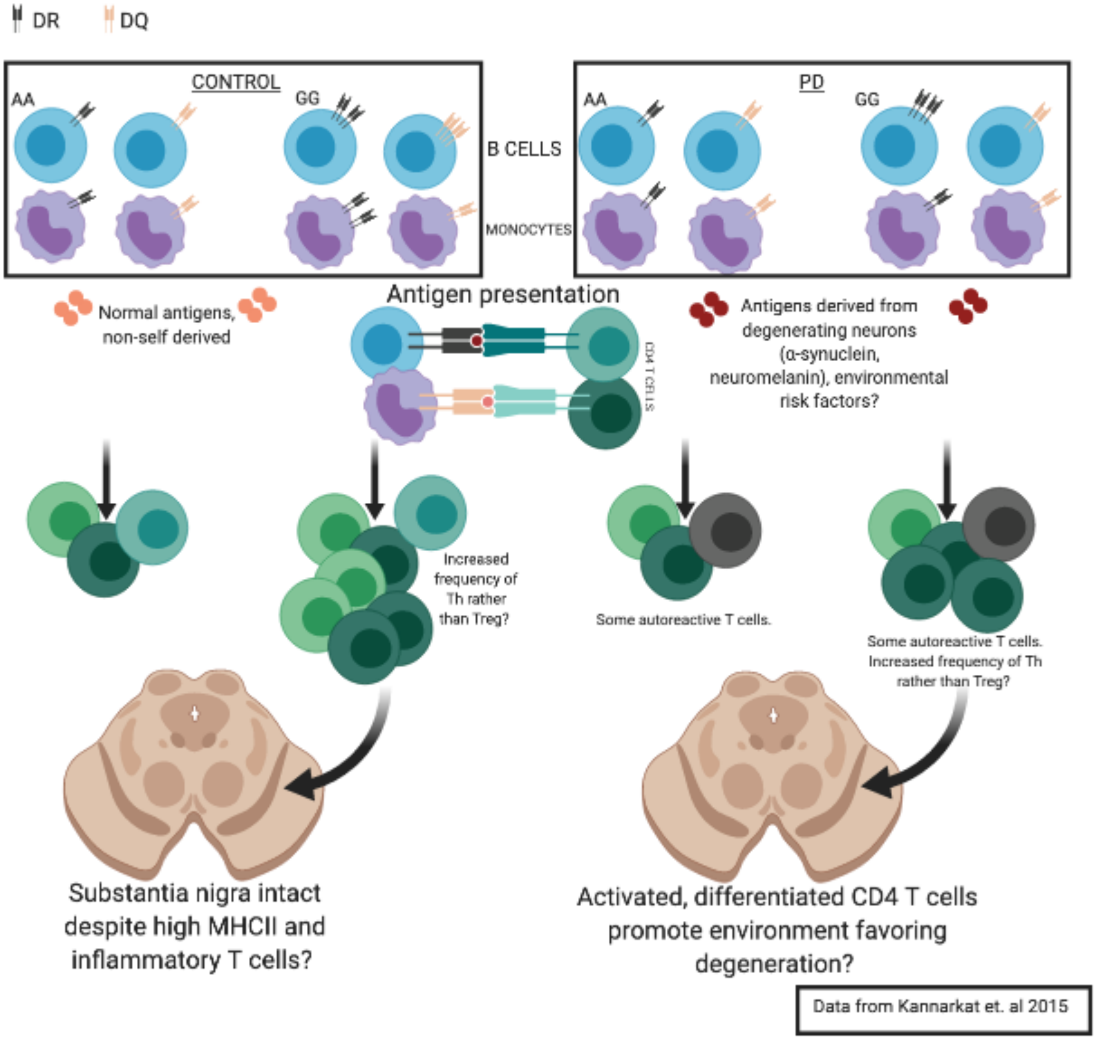

1.1e) PD environmental risk factors with known immune system effects

While most cases of PD involve no clear heritable genetic cause, the contributions of genetic risk factors are significant and have enhanced our ability to model the disease and better understand the underlying biology. Genes, however, cannot be the complete story of PD pathogenesis. PD occurs in both members of a pair of dizygotic twins as often as it occurs in both members of a pair of monozygotic twins, indicating there exist non-genetic factors contributing to disease (Di Monte, 2003). Ideal therapeutic interventions for PD would compensate for functional changes induced by genetic risk factors, but with the exception of theoretical CRISPR or gene therapy technologies, altering genetic risk is not an option. Modifying environmental exposures is often, though not always, more feasible, and several environmental risk factors have been associated with PD.

What constitutes an environmental factor is often unclear. Some clarity has been achieved through use of the term exposome, defined by Dr. Gary Miller as the "cumulative measure of environmental influences and associated biological processes" (Miller, 2014). The environment can include, but certainly is not limited to, chemicals we encounter, nutrients, physical activities, psychological factors such as stress, infectious agents, the climate, and experiences emerging from our race, gender, or socioeconomic status. As Dr. Miller's definition emphasizes, it is crucial to consider the biological processes downstream of an exposure when considering disease risk assessment. In response to an exposure or experience, epigenetic regulation can occur and the resulting cell signaling cascades could contribute to disease pathogenesis. Importantly, because neurons are long lived, environmental exposures throughout the lifespan may influence their health. In the immune system where there is ample cell turnover, early life exposures may still have long lasting effects as the phenomenon of immunological memory forms a record of epitopes that have activated innate and adaptive immune cells. It is also possible that the same factor encountered at different timepoints throughout the lifespan carries varying degrees of disease risk. Here we will specifically consider environmental exposures that elicit known processes within the immune system and are associated with PD, with the caveat that there surely exist many other factors yet to be identified.

Environmental factors may disrupt immune homeostasis by activating immune cells directly, causing tissue damage that releases DAMPs that are then recognized by PRRs, or via the process of molecular mimicry. Molecular mimicry occurs when a pathogen possesses components with similar amino acid sequences to a self-antigen. Any immune activation in response to such a pathogen spills over the organism's own tissues and can lead to tissue damage, eliciting DAMP release and a persistence of immune activation. For some of the environmental risk factors discussed here, the association with PD has been established, but the field is still investigating the downstream biological processes following exposure.

PYRETHROID PESTICIDES

Multiple epidemiological studies have reported a link between insecticide exposure and incidence of PD (Semchuk et al., 1992; Butterfield et al., 1993;

Gorell et al., 1998). The pesticide cypermethrin is, globally, one of the most commonly used agricultural and domestic insecticides (Crawford et al., 1981). A synthetic class II pyrethroid, cypermethrin has the chemical abstract name: (***RS***)-α-cyano-3-phenoxybenzyl(1***RS***,3***RS***; 1***RS***,3***SR***)-3-(2,2-dichlorovinyl)-2,2-dimethylcyclopropanecarboxylate and the international union of pure and applied chemistry name (***RS***)-α-cyano-3-phenoxybenzyl (1RS)*cis*-trans-3-(2,2-dichlorovinyl)-2,2-dimethyl-cyclopropane carboxylate. Used to control termite, cockroach, and other household and agricultural pests, cypermethrin is manufactured as an emulsifiable concentrate, powder, or ultra-low volume formulation for spray delivery. Because pesticides are most often formulated in mixtures of multiple classes of chemicals, establishing the specific health risks of individual components has been challenging for public health researchers. Nonetheless, cypermethrin has been identified as one of the important pesticide components that can be associated with health risks (Liao et al., 2011).

Human are primarily exposed to pyrethroids via skin contact, but ingestion through food and water consumption is also possible. This emphasizes the point that exposures are not only a hazard for those employed in pest control professions. A 2017 study of French children found that pyrethroids are detectable in the urine following a meal of locally grown foods (Glorennec et al., 2017). Pyrethroid residues in soil, water, and vegetables have been reported (Del Prado-Lu, 2015). The half-lives of various pyrethroids have been assessed in neuronal tissue (9-23 hours for permethrin I), plasma (11.5 hours for deltamethrin II), and fat (2.5 days for alpha-cypermethrin II). Metabolites are primarily excreted in urine and feces.

The mechanism of toxicity of cypermethrin and other pyrethroids in insects is to extend the opening of voltage-gated sodium channels, leading to depolarization of neurons and, thus, sustained excitation (Eells and Dubocovich, 1988; Brown and Narahashi, 1992; Singh et al., 2012a). In dopaminergic neurons, cypermethrin can induce free radical production and oxidative damage (Singh et al., 2011b), and its neurotoxicity is reviewed in (Nasuti et al., 2013; Nasuti et al., 2014; Costa, 2015). Additionally, cypermethrin is thought to be able to engage multiple neurotransmitter systems. A study with the similar pyrethroid deltamethrin reported that the concentration of gamma aminobutyric acid (GABA) in the brain was significantly reduced following a single oral dose of 150mg/kg in rats (Manna et al., 2006). Whether this reduction in GABA ought to be attributed to increases in GABA breakdown or decreased synthesis remains to be determined. Short term exposure to the pyrethroid cypermethrin was not reported to affect GABA and the long-term effects within the nigrostriatal tissues have not been examined (Singh et al., 2012b). The depletion of serotonin in the prefrontal cortex of rats has also been reported following cypermethrin treatment (Martinez-Larranaga et al., 2003). The developing brain seems to be particularly sensitive to cypermethrin exposures, and studies have been done comparing multiple dosing regimens in various rat strains. Effects range from no change to decreased dopamine levels and SN cell loss depending on dose, exposure duration, route of exposure, and strain (Malaviya et al., 1993; Gupta et al., 1999; Shafer et al., 2005; Tiwari et al., 2010; Singh et al., 2011b). Adulthood responses to cypermethrin exposure are larger if animals were exposed during development (Tiwari et al., 2010; Singh et al., 2012a).

To what extent might cypermethrin and other pyrethroids act directly on immune cells via sodium ion channels? Immune cells express a variety of ion channels to maintain and regulate their negative membrane potential and the influx of divalent ions that act as secondary messengers (Ca^{2+}, Mg^{2+}). Human T cells are not thought to express voltage-gated sodium channels (Na_v) though some cell line research indicates $Na_v1.5$ expression by CD4+ T cells may play a role in positive selection (Verheugen et al., 1994) (Lo et al., 2012; Feske et al., 2015). Phagocytosis is regulated by Na_v channels, specifically $Na_v1.5$ and 1.6 in macrophages and 1.7 in human dendritic cells (Craner et al., 2005; Zsiros et al., 2009). Importantly, GABA receptors are expressed by immune cells as well, indicating another pathway by which pyrethroids could alter immune cell function. Several studies have reported immunotoxic effects of pyrethroids on mouse splenocytes, thymic immune cells, and rat neutrophils (Gabbianelli et al., 2009; Kumar et al., 2015; Kumaran and Cookson, 2015). Female mice given 1 dose of permethrin (1100 mg/kg, topically) exhibited a 32% decrease in spleen T cell and thymic cell proliferation relative to untreated mice (Chrustek et al., 2018). Signs of apoptosis were observed in CD8+ and CD4-CD8- thymocytes following permethrin treatment (Chrustek et al., 2018). Oral administration of permethrin is associated with neutrophil abnormalities as well (Gabbianelli et al., 2009). In mouse splenocytes or rat thymic cells, deltamethrin has been reported to induce apoptosis (Kumar et al., 2015; Kumar et al., 2016). Cypermethrin has been shown to decrease plasma IL-2, IL-8, IL-12, and IFNγ (Costa et al., 2013). In humans exposed to cypermethrin via their employment, a lower CD4/CD8 ratio was reported, as well as changes in IL-12, p70, IL-2, IL-8, and IFNγ (El Okda et al., 2017). Pyrethroids readily cross the blood-brain barrier, are lipophilic, and are capable of disrupting microglial function (Anadon et al., 1996; Singh et al., 2011a; Chrustek et al., 2018). Thus, in thinking about the mechanism by which pyrethroids increase risk for PD, considerations should not be limited to neurons.

AIR POLLUTION

While there have been somewhat conflicting results regarding air pollution's association with PD, a general trend has been reported such that areas with higher pollution have more PD cases. Air pollution consists of a complex mixture of highly variable and dynamic combinations of factors. Determining which are associated with disease processes is an extremely challenging task. A study of victims of premature death in Mexico City reported olfactory bulb α-synuclein aggregates, and an association between Mexico City's high pollution level and olfactory bulb pathology was proposed (Calderon-Garciduenas et al., 2018). Endothelial cell apoptosis and increased numbers of monocytes and T cells have been reported in association with fine particulate matter air pollution (Pope et al., 2016). Pollution from diesel exhaust, specifically, is known to act as an activator of the immune system and can contribute to neuroinflammation (Levesque et al., 2011a; Levesque et al., 2011b). In rats exposed to diesel exhaust via inhalation, many indicators of immune activation and inflammation were increased in the brain including IL-6, protein nitration, ionized calcium-binding adaptor molecule-1 (Iba-1), TNF, IL-1β, MIP-1α, and fractalkine, with the greatest increases observed in the midbrain (Levesque et al., 2011a). More work remains to be done on the association between components of air pollution, immune activation, and PD risk.

INFLUENZA VIRAL INFECTION

A member of the Orthomyxoviridae family, the influenza virus is a single-stranded, RNA virus with a genome encoding 11 proteins (Bouvier and Palese, 2008). Highly pathogenic strains of influenza have been associated with subsequent neurological complications, including neurodegeneration and neuroinflammation (Jang et al., 2009). Following the 1918 Spanish influenza pandemic, an outbreak of an encephalitic condition known as *encephalitis lethargica* (EL) occurred, causing high fever, mental confusion, lethargy, and vision problems in patients previously exposed to influenza (Henry et al., 2010). No clear biological mechanism has been identified as a causal connection between influenza and EL.

In 80% of people who survived EL, secondary parkinsonism was later described (Henry et al., 2010), although, as with influenza and EL, no clear causal factor has been identified and the association is contested by some (Vilensky et al., 2010). One possibility is that some direct viral invasion of the central nervous system and/or a systemic cytokine storm caused by influenza virus predisposes death of midbrain DA neurons. Individuals who were young at the time of the Spanish flu pandemic and may have been exposed to highly pathogenic influenza are reported to have had a 2-3-fold higher risk of developing PD (Jang et al., 2009).

In a study of C57/Bl6 mice, intranasal infection with the highly infectious and, in humans, fatal H5N1 influenza virus resulted in early infection of the enteric nervous system, the vagal nerve, and eventually widespread and persistent microgliosis in the brain and signs of neuron death (Jang et al., 2009). Interestingly, in every region where the H5N1 infection was detectable, there was upregulation of phosphorylated α-synuclein (Jang et al., 2009). Notably, the synuclein pathology reported in this study mirrors the progression of α-synuclein pathology hypothesized to occur in idiopathic PD (Braak et al., 2003). Intracerebral inoculation of mice with an influenza A virus known to be neurovirulent resulted in detection of viral antigens within the SN and hippocampus (Takahashi et al., 1995).

Whether neurovirulence is strictly necessary for influenza virus exposure to increase risk for PD remains to be fully understood. The biological mechanisms that distinguish between secondary parkinsonism (no LB pathology) and PD are not fully understood, but the existence of infectious-disease-associated degeneration of DA neurons in the SN suggests that infection, even non-neurotropic, can be an inflammatory hit to the CNS. For instance, the 1918 influenza virus contained no known sequence indicative of neurotropic potential (Taubenberger and Morens, 2006). Viral activation of the immune system, an incredibly common environmental exposure, is, perhaps, sufficient to threaten the integrity of the DA system. As this statement logically predicts, antiviral interventions can eliminate virus-related neurodegeneration and act as neuroprotective agents (Sadasivan et al., 2017).

Infection with the flu or other pathogens may elicit an autoimmune reaction resulting in immune system-driven neurodegeneration. This could occur through the production of cryptic antigens (antigens normally invisible to the immune system that become exposed due to disease processes). Also, differential processing of self-proteins by infection-related protease action could produce neoantigens potentially recognized by existing T cells. As proposed in (Delogu et al., 2011), various mechanisms for infection-induced autoimmunity exist and are not mutually exclusive: molecular mimicry and the adjuvant effects of infectious pathogens may function early in the development of an autoimmune reaction in the pathogenesis of PD, followed by bystander activation and epitope spreading as inflammation persists. Bystander action occurs when there is proliferation of a previously small population of activated, autoreactive T cells due to chronic inflammation triggered by a pathogen or tissue damage. Epitope spreading is defined as the case in which a healthy, effective immune response, initially directed against some portion of an antigen, shifts to include a different portion of the same protein or a different protein. If this new antigen is similar to a self-protein, there can be cross recognition resulting in the destruction of self-tissue. It is possible of that the immune response to certain influenza strains in certain human populations could produce this type of induced autoimmunity, putting SN DA neurons at risk.

MANGANESE

Manganese (Mn) is a trace element in the human body and participates in enzymatic reactions as a cofactor. Protein and lipid synthesis require Mn.

Manganism is the accumulation of Mn in organs such as the kidney, liver, or brain, and this condition can be neurotoxic. South African mine workers chronically exposed to Mn developed a parkinsonism characterized by gait abnormalities and tremor (Gonzalez-Cuyar et al., 2014). Elevated manganese in the air has been associated with PD (Finkelstein and Jerrett, 2007).

In mice, Mn stimulates activation of microglia, resulting in neuroinflammation and DA neuron loss. Interventions that quiet microglial response to Mn have been described as neuroprotective (Chen et al., 2018).

1.1f) PD gene-environment interactions with known effects on the immune system

MAJOR HISTOCOMPATIBILITY COMPLEX CLASS II AND PYRETHROIDS

As mentioned above, a single nucleotide polymorphism (SNP) at *rs31229882* within the gene for MHCII was reported to be associated with a 1.7 fold increase in risk for PD, and the high-risk genotype (*GG*) at *rs3129882* is over-represented (46%) in patients with idiopathic PD compared to the age-matched healthy control population (40%) (Hamza et al., 2010). Functionally, our group demonstrated that *GG* homozygosity at this SNP is associated with greater baseline mRNA and surface MHCII protein expression in monocytes and B cells (Kannarkat et al., 2015). Monocytes and B cells from *GG* individuals with PD display 200-300 greater inducibility of MHCII expression following inflammatory cytokine exposure compared to *AA* individuals with PD (Kannarkat et al., 2015). This is significant because expression of MHCII must be sufficient to activate T cells when needed, but levels above the homeostatic range are linked to autoimmune diseases and accompanied by abnormal ratios of T cell subsets (Nepom and Erlich, 1991).

The mechanism by which pyrethroid exposure enhances risk for PD is not yet understood. It may be the case that pyrethroids, through their action on voltage gated sodium channels or, in the case of type II pyrethroids, chloride ion channels as well, alter antigen presenting cells' efficacy as activators of the adaptive immune system. Fully functional T cell activation requires that antigen presenting cells express, along with the peptide antigen-MHCII complex, costimulatory molecules that bind coreceptors on the CD4+ T cell (Tao et al., 1997). There is also a crucial contribution of cytokines secreted by antigen presenting cells that "instruct" the CD4+ T cells' differentiation into a functionally specific T helper cell (Th1, Th2, Th17, Treg, etc.) (Luckheeram et al., 2012; Yamane and Paul, 2012). Work done in THP1 and Jurkat cell lines suggests that the pyrethroid permethrin can affect the rate of T cell proliferation (Kannarkat and Tansey, 2016). Possible routes by which pyrethroid exposure may augment PD risk resulting from *rs3129882* genotype include further increasing MHCII expression, increasing costimulatory molecule expression, driving sustained cytokine secretion, or increasing the proliferation rate of T cells, perhaps those activated by a PD-related antigen such as α-synuclein.

We do not yet know the biological connection between increased MHCII expression related to *rs3129882 GG* genotype and pyrethroid exposure. Future work should explore the extent to which human immune cells from patients with or without PD and with or without the high risk MHCII SNP genotype respond to pyrethroid exposure.

1.1g) Conclusion

The work that follows focuses on genetic variation in MHCII and exposure to cypermethrin (**Chapter 3** and **4**). As described in section **1.1f**, previous work uncovered an increase in PD risk resulting from synergy between a *G* allele at rs3129882 and exposure to pyrethroids (Kannarkat et al., 2015). Because the *G* genotype at *rs3129982* is associated with both increased baseline MHCII expression on monocytes and risk for PD, we predicted that deletion of MHCII on monocytes and other peripheral myeloid cells would be neuroprotective in a mouse model of PD pathology (**Chapter 3**). This prediction was based on the hypothesis that MHCII expression level will drive shifts in the frequencies of CD4+ T cell subsets. Depending on the direction of such shifts, we hypothesize an immune environment is created either permitting or preventing dopaminergic neurodegeneration. Others have tested similar hypotheses in the past by globally deleting or decreasing MHCII (Harms et al., 2013) (Williams et al., 2018); (Jimenez-Ferrer and Swanberg, 2018). The studies presented in **Chapter 3** advance the field in that we describe a mouse line in which the deletion of MHCII is peripheral myeloid-specific and does not blunt T cell development, as is the case in global MHCII KO. Previous work investigated the effect of MHCII deletion or decrease in viral-vector-mediated α-synuclein overexpression models. We combine the same type of synuclein overexpression with cypermethrin treatment, enabling the investigation of the mechanistic connection between PD-relevant genetic and environmental factors.

Previous work by Kannarkat et al. examined the effects of *rs3129882* genotype on MHCII expression (Kannarkat et al., 2015). Because MHCII mediates crosstalk between antigen presenting cells in the innate immune system and the activation and differentiation of CD4+ T cells, we set out to characterize the relationship between *rs3129882* genotype and CD4+ T cell subset frequencies. We hypothesized that the increased MHCII expression in *GG* individuals and the dramatic increase in MHCII inducibility in PD *GG* individuals would dial up distinct types of CD4+ T cells. This hypothesis is tested in the studies presented in **Chapter 4.**

As the field moves forward investigating immunomodulatory therapeutic options, it is crucial to consider the patient subpopulations created by combinations of genetic variations and environmental exposures. Failure to do so could lead to findings of futility for treatments that could profoundly benefit a cluster of PD patients with a particular immunophenotype, inflammatory status, degree of autoimmunity, etc. To best design experiments so that true impacts of our interventions may be detected, we must be mindful of the exposome context each patient brings to a given PD therapy. It is likely that no single drug will be able to address the vast array of underlying pathologies involved in PD. It is also likely that it will be more feasible to prevent the degeneration of neurons rather than regenerate the SN and other affected nuclei. This requires a thorough understanding of the genetic and environmental factors converging on the immune system to increase risk for PD.

1.2 Mixed lineage kinase 3

Mixed lineage kinase (MLK) proteins are part of the MAP kinase kinase kinase family (MAP3Ks). Phosphorylation of c-Jun amino terminal kinase (JNK) is reported to occur downstream of all known MLKs (Gallo and Johnson, 2002).

Apoptotic stimuli including TNF, DNA damage, heat shock, ischemia-reperfusion, oxidative stress, hyperosmolarity, axonal injury, and trophic factor withdrawal can drive phosphorylation of JNK, potentially by MLKs (Xu et al., 2001). In another MAPK phosphorelay module, MLK3 phosphorylates MKK3/6, which in turn phosphorylates p38 (Gallo and Johnson, 2002). JNK and p38 are components of cell stress pathways. MLKs role in cell stress pathways were first described in a series of experiments conducted with the antibiotic cycloheximide (reviewed in (Kyriakis and Avruch, 2001)). Subsequently it was observed that many cellular stimuli, including heat shock, inhibition of glycosylation, inflammatory cytokines, and ultraviolet radiation are all capable of initiating cell responses that converge on JNK and p38, making MLKs key regulators of a cell's response to stress and potential for survival (Kyriakis and Avruch, 2001).

MLKs phosphorylate their targets at serine and threonine residues. MLKs are evolutionarily conserved enzymes, and are present in *Caenorhabditis elegans* and *Drosophila melanogaster*, important model organisms in biological research. In terms of cellular and tissue localization, MLK1 is found in mammalian epithelial cells (Gallo and Johnson, 2002). MLK2 has been found in brain, skeleton muscles, and the testes, while MLK3 is expressed in many kinds of mammalian tissues (Gallo and Johnson, 2002). MLK3 overexpression in Jurkat cells (human leukemia T cell line) led to increased expression of IL2 and TNF (Hoffmeyer et al., 1998; Hoffmeyer et al., 1999). Overexpression of MLKs in a rat chromaffin cell line (PC12 cells) and primary sympathetic neurons was reported to drive apoptosis that can be blocked with CEP-1347, an inhibitor of several MLKs (Xu et al., 2001). These studies suggest that high levels of MLK activity may be damaging in some tissues, creating interest in inhibition of MLK signaling as a therapeutic strategy.

In 2005, the MLK inhibitor CEP-1347 was shown to mediate neuroprotection against methamphetamine-exposed human mesencephalic-derived neurons, *in vitro* (Lotharius et al., 2005). CEP-1347 also prevented motor deficits and DA neuronal degeneration in a mouse 1-methyl-4-phenyl-1,2,3,6-tetrahydropyridine (MPTP) model of nigral degeneration (Hudkins et al., 2008). While results from these models were promising and CEP-1347 was found to be safe and well tolerated over 4 weeks in subjects with PD, clinical trials with CEP-1347 failed in a Phase II trial of 806 PD patients due to futility (Parkinson Study Group, 2007). This raised questions about the CNS pharmacokinetic properties and target selectivity of CEP-1347. Specifically, CEP-1347 likely failed due to its poor brain penetrance (brain/plasma ratio < 0.2 in mice) (Parkinson Study Group, 2007). Furthermore, interpreting the efficacy of specific MLK inhibition as a therapeutic strategy was complicated by off-target effects of CEP-1347 (50% inhibition of 185 other kinases at 1uM) (Goodfellow et al., 2013).

Later iterations of MLK inhibitors have shown somewhat more promise and efficacy in other disease models, and possibly mediate their neuroprotective effects via inhibition of MLKs in non-neuronal cell types. For example, MLK inhibition's effects on microglia have been investigated. The broad-spectrum MLK inhibitor URMC-099 was reported to modulate activated microglia in the mouse experimental autoimmune encephalomyelitis (EAE) hippocampus (Bellizzi et al., 2018). While no changes in activated morphology of Iba-1+ cells were induced by MLK inhibitor treatment, both URMC-099 and CLFB-1134, an MLK3-specific inhibitor, prevented increased CD68 expression (a lysosomal marker associated with phagocytosis) (Bellizzi et al., 2018). Furthermore, URMC-099 decreased canonical markers associated with microglial activation: iNOS, immunoglobulin receptor FCγR1/CD64, and the co-stimulatory molecule CD86 (Bellizzi et al., 2018). Overall the study suggests that MLK inhibition shifts brain microglia toward a less inflammatory and phagocytic phenotype, with broad-spectrum MLK inhibition favoring synaptic preservation in EAE. The extent to which MLK inhibition is protective in a Parkinson’s disease model is the topic of **Chapter 2**.

CHAPTER 2. THE SECOND GENERATION MIXED-LINEAGE KINASE-3 (MLK3) INHIBITOR CLFB-1134 PROTECTS AGAINST NEUROTOXIN-INDUCED NIGRAL DOPAMINERGIC NEURON LOSS

This chapter contains previously published material (Kline et al., 2019).

2.1 Introduction

Depletion of striatal dopamine (DA) due to death of substantia nigra DA neurons has been known for decades to be the cause of Parkinson's disease (PD) motor symptoms, yet no disease modifying therapies exist. The drivers of DA degeneration in PD are not fully understood, and many cellular processes have been implicated. Mixed lineage kinases (MLKs) in neurons are part of a signaling cascade thought to activate cell death machinery in PD. In PD, distinctions between apoptosis, necroptosis, and other forms of programmed cell death have been difficult to establish. Thus, while there is extensive death of DA and norepinephrine neurons in PD, the mechanistic interplay between programmed cell death pathways and cell-non-autonomous killing events remains to be fully elucidated. Molecular markers of apoptosis, such as increased expression of p53, CD95, caspases-3, -8 and -9, and activity of caspases-1 and -3 have been reported in human PD post-mortem brain (de la Monte et al., 1998; Hartmann et al., 2000; Mogi et al., 2000; Andersen, 2001). The consensus is that there is a proapoptotic environment in the substantia nigra, as reviewed in (Lev et al., 2003). In the MPTP mouse model of PD specifically, MPTP's neurotoxic derivative MPP+ kills cells by mitochondrial complex I inhibition which initiates apoptosis (Fall and Bennett, 1999). MLKs belong to the mitogen-activated kinase kinase kinase (MAP3K) family of serine/threonine kinases. Phosphorylation of c-

Jun N-terminal kinase (JNK), downstream of MLKs, activates the transcription factor c-Jun which regulates expression of cell death genes. Phosphorylated JNK (pJNK) inhibits pro-survival factors and activates Bad and Bim, apoptotic signaling molecules. In genetic and neurotoxin-based models of PD, JNK activation has been observed (Cha et al., 2005; Burke, 2007), and neuroprotection has been achieved with inhibition of JNK (Zhang et al., 2004). Furthermore, pJNK has been observed in cytoplasmic granules adjacent to intranuclear inclusions (Lewy bodies) in post-mortem PD brain (Ferrer et al., 2001).

Mixed-lineage kinase-3 (MLK3), encoded by the *MAP3K11* gene, preferentially activates MAPK8/JNK and functions as a positive regulator of the JNK signaling pathway. MLK3 can directly phosphorylate and activate JNK and p38MAPK and is involved in the transcriptional activity of AP1 mediated by Rho family GTPases and Cdc42 (Kant et al., 2011). Though redundancy exists in MLK pathways, specific inhibition of MLK3 has been associated with neuronal health and protection in multiple *in vitro* and *in vivo* systems (Handley et al., 2007). MLK3 has been implicated in apoptosis after nerve growth factor withdrawal in rat sympathetic neurons (Mota et al., 2001).

The objective of the current study was to test a more potent and highly selective MLK3 inhibitor called CLFB-1134 with improved pharmacokinetic properties (brain/plasma ratio ~1.0) in a sub-acute mouse model of MPTP intoxication that induces nigrostriatal dopaminergic pathology. The structure of CLFB-1134 is presented in **Figure 2**.

2.2 Materials and Methods

2.2a) Screening pharmacokinetics in mice and rats

Four mice or rats were used for each time point. Male C57/BL/6 mice or Sprague-Dawley rats were dosed IV (intravenously), PO (orally), and IP (intraperitoneally) at the doses indicated (**Table 2A, B, C**). Total concentrations of the compound were determined by liquid chromatography–tandem mass spectrometry (LC-MS/MS), following plasma protein precipitation with acetonitrile and injection of the supernatant onto the column (XTerra®MS C18, 5 µm, 4.6 × 50 mm). The LC system comprised an Agilent (Agilent Technologies Inc., USA) 1100 series liquid chromatography equipped with G1379A degasser, G1311A Quantpump, G1313A autosampler and G1316A Column Oven. Mass spectrometric analysis was performed using an API4000 (triple-quadrupole) instrument from AB Inc. (Canada) with an ESI interface. Brains were collected at the time points indicated, rinsed with ice-cold saline, weighed, and stored at −80°C until analysis. For compound quantitation, brains were homogenized in 5 volumes of water. The homogenates were extracted by protein precipitation with acetonitrile. LC-MS/MS analysis was conducted as described for the plasma. Brain homogenate concentrations were converted to brain concentrations for the calculations of brain to plasma ratios.

2.2b) 1-methyl-4-phenyl-1, 2, 3, 6-tetrahydropyridine studies

Eight-week old male C57BL/6J mice purchased from Charles River (Ashland, OH) were used in all studies. Mice were maintained on a 12:12 light/dark cycle and standard rodent chow and tap water were available ad libitum. Animals were sacrificed by live decapitation. All procedures were conducted in accordance with the Guide for Care and Use of Laboratory Animals (National Institutes of Health) and have been approved by the Institutional Animal Care and Use Committee at Emory University.

CLFB-1134 was formulated in 5% DMSO, 40% PEG-400 at 2 mg/mL and administered intraperitoneally except where otherwise noted (pharmacokinetic study). 5% DMSO, 40% PEG-400 vehicle solution is referred to throughout as drug vehicle and was also administered intraperitoneally. MPTP was formulated in sterile saline and administered subcutaneously. Sterile saline is referred to throughout at neurotoxin vehicle and was also administered subcutaneously. 1-methyl-4-phenyl-1,2,3,6-tetrahydropyridine (MPTP) was purchased from Sigma-Aldrich (St. Louis, MO). CLFB-1134 was synthesized by Califia Bio, Inc. (**Figure 2**).

In the target-engagement study, mice simultaneously treated with the neurotoxin vehicle and CLFB-1134 were compared to those treated with neurotoxin vehicle and drug vehicle. CLFB-1134 (30 mg/kg) or the drug vehicle was administered by intraperitoneal (i.p.) injection 30 minutes prior to subcutaneous (s.c.) neurotoxin vehicle injection.

To investigate the neuroprotective effect of MLK3 inhibition against MPTP-induced nigrostriatal pathology (**Figures 4-6**), mice were divided into the treatment groups described in **Table 1**, with the addition of untreated animals housed under identical conditions for the high performance liquid chromatography experiment described in the next section. CLFB-1134 was formulated as described above. CLFB-1134 or drug vehicle was administered via i.p. injection twice daily (8:00 am and 8:00 pm). MPTP or the neurotoxin vehicle was administered via subcutaneous s.c. injection once per day (1:00 pm). Groups are summarized in **Table 1**.

Table 1. Experimental groups for MPTP studies.

Group	Treatment Description	Figures
MPTP + CLFB-1134 (Co-dosed)	Mice received 20mg/kg MPTP once per day (s.c.; 1:00pm) and 30mg/kg CLFB-1134 twice per day (i.p.; 8:00 am and 8:00 pm) for 5 consecutive days. Sacrifice was 3 hours after the final MPTP dose.	**Figure 1**
MPTP + drug vehicle (Co-dosed)	Mice received 20mg/kg MPTP once per day (s.c.; 1:00pm) and DMSO/PEG vehicle twice per day (i.p.; 8:00 am and 8:00 pm) for 5 consecutive days. Sacrifice was 3 hours after the final MPTP dose.	**Figure 1**
Neurotoxin vehicle + CLFB-1134	Mice received a single i.p. injection of CLFB-1134 and were given s.c. saline 30 minutes later.	**Figure 2**
Neurotoxin vehicle + drug vehicle	Mice received a single i.p. injection of DMSO/PEG vehicle and were given s.c. saline 30 minutes later.	**Figure 2**
MPTP + drug vehicle	Mice received a single i.p. injection of DMSO/PEG vehicle and were given s.c. MPTP 30 minutes later.	**Figure 2**
MPTP + CLFB-1134	Mice received a single i.p. injection of CLFB-1134 and were given s.c. MPTP 30 minutes later.	**Figure 2**
Neurotoxin vehicle	Mice received a single daily injection of saline (s.c.) for 5 consecutive days. Mice were sacrificed 3 weeks following the last injection.	**Figures 3** and **4**
MPTP	Mice received a single daily injection of 20 mg/kg MPTP (s.c.) for 5 days in a row. Mice were sacrificed 3 weeks following the last injection.	**Figures 3, 4,** and **5**
MPTP + CLFB-1134 (Co-Dosed)	Mice were treated with a single daily injection of 20 mg/kg MPTP (s.c.) and two daily injections of CLFB-1134 (i.p.) for 5 days. CLFB-1134 injections continued on the same schedule for 3 more weeks following MPTP completion. Mice were sacrificed following the last CLFB-1134 injection.	**Figures 3, 4,** and **5**
MPTP + drug vehicle (Co-dosed)	Mice were concurrently treated with a single daily injection of 20 mg/kg MPTP (s.c.) and two daily injections of DMSO/PEG (i.p.) for 5 days. DMSO/PEG injections continued on the same schedule for 3 more weeks. Mice were sacrificed following the last injection.	**Figures 3** and **4**
MPTP + CLFB-1134 (Post MPTP)	Mice received a single daily injection of 20 mg/kg MPTP (s.c.) for 5 consecutive days. Mice then received two daily injections of CLFB-1134 (i.p.) for 3 weeks. Mice were sacrificed following the last injection.	**Figures 3, 4,** and **5**

2.2c) High performance liquid chromatography of striatal neurochemistry

HPLC analysis of neurochemistry was performed as previously described (Caudle et al., 2007). Monoamine standards for DA, dihydroxyphenylacetic acid (DOPAC), homovanillic acid (HVA), and norepinephrine (NE) were purchased from Sigma-Aldrich (St. Louis, MO). Briefly, dissected striata were sonicated in 0.1 M perchloric acid. Homogenates were centrifuged at 15,000×g and the supernatant filtered through a 0.22 µm filter by centrifugation at 15,000×g. The supernatants were analyzed for levels of DA, DOPAC, HVA, and NE. Quantification was made by reference to calibration curves made with individual standards.

MPP+ levels in the striatum were evaluated as previously described (Richardson et al., 2008). Mice were sacrificed 3 hours following the last dose of MPTP. Bilateral striata were sonicated in 5% trichloroacetic acid and centrifuged for 10 minutes at 14,000xg. MPP^+ levels were determined in the supernatants by HPLC with UV detection at 290 nm using a reverse-phase Altima C18 column (Alltech Associates Inc., Deerfield, Illinois, USA) and a mobile phase consisting of 89% 50 mM KH_2PO_4 and 11% acetonitrile. MPP^+ was identified and quantified by comparison of retention time with known standards.

2.2d) Phospho-JNK and total JNK immunoassay

The levels of JNK phosphorylation at Thr183 and Tyr185 in midbrain tissue was measured using the Phospho-JNK (Thr183/Tyr185) whole cell lysate assay kit (Meso Scale Discovery, Gaithersburg, MD). The assay was performed according to the manufacturer’s instructions and all samples were analyzed in duplicate. In brief, dissected mouse midbrain tissues were homogenized in 1X complete lysis buffer. Lysates were centrifuged at 10,000xg, at 4°C for 10 minutes and supernatant was collected. Total protein concentration in the lysate was determined using a BCA protein assay (Thermo Scientific). The Meso Scale Discovery plate was prepared according to the manufacturer's protocol, using lysate at a concentration of 0.2 μg/μL. The Meso Scale Discovery plate was read on the SECTOR Imager 2400 instrument (Meso Scale Discovery). Data represent background-subtracted chemiluminescent signal units.

2.2e) Western blot

Western blots were used to quantify the expression of tyrosine hydroxylase (TH) present in samples of striatal tissue from treated and control mice. Analysis was performed as previously described (Caudle et al., 2006). Briefly, unilateral striatum samples were homogenized, a BCA protein assay kit from Pierce (Rockford, IL) was used, and 5 ug (in 5 uL) of striatal protein were subjected to polyacrylamide gel electrophoresis. Following electrophoretic transfer to polyvinylidene difluoride membranes, nonspecific sites were blocked in 7.5% nonfat dry milk in Tris-buffered saline. Membranes were incubated overnight in a polyclonal antibody to TH (Immunostar, Hudson, WI, 1:1000). TH antibody binding was detected using a goat anti-rabbit horseradish peroxidase secondary antibody (1:10,000) and enhanced chemiluminescence. The luminescence signal was captured on an Alpha Innotech Fluorochem imaging system and stored as a digital image. Membranes were stripped for 15 minutes at room temperature with Pierce Stripping Buffer and sequentially re-probed with β-actin (1:3,000) antibody. Immunoreactivity of TH was normalized to β-actin levels to ensure equal protein loading across samples. Monoclonal mouse anti-β-actin antibodies were purchased from Sigma-Aldrich (St. Louis, MO). Secondary antibodies conjugated to horseradish peroxidase were obtained from Jackson Immunoresearch Laboratories (West Grove, PA). SuperSignal West Dura Extended duration substrate and stripping buffer were obtained from Pierce (Rockford, IL).

2.2f) Histology and stereology

Tissue staining and cell counts were performed as described previously (Caudle et al., 2007). Briefly, midbrain blocks from control and treated mice were immersion fixed in 4% paraformaldehyde for 24 h at 4°C and equilibrated in 30% sucrose in PBS at 4°C before being cryosectioned (40 μm, coronal slice). Sections were incubated with a polyclonal anti-TH antibody overnight (EMD Millipore, Billerica, MA). TH signal was amplified with an ABC Elite kit (Vector Laboratories, Burlingame, CA) and then sections were incubated in a biotinylated goat anti-rabbit secondary antibody for 1 hour at 4°C. Visualization was performed using 3,3'-diaminobenzedine with nickel enhancement (Sigma-Aldrich, St. Louis, MO) for 3 minutes at room temperature. Sections were then incubated with monoclonal anti-NeuN antibody overnight (EMD Millipore, Billerica, MA). NeuN signal was amplified with ABC Elite kit (Vector Laboratories) and sections were incubated with biotinylated goat anti-mouse secondary antibody for 1 hour at 4°C. Visualization was performed using 3,3-diaminobenzidine for 3 minutes at room temperature. For cresyl violet stained tissue, a 0.1% aqueous cresyl violet solution (from *Poly Scientific R&D Corp, New York*) was used followed by de-stain and dehydration in ethanol and xylenes.

Unbiased stereological estimates of TH+ and total (NeuN+ or cresyl violet) neurons were performed using the optical fractionator method in StereoInvestigator analysis software with sampling parameters chosen to maintain a coefficient of error under 0.12 (MicroBrightField, Williston, VT). The substantia nigra pars compacta (SNpc) was delineated using previously described criteria (West et al., 1991). After delineation at low magnification, every sixth section was sampled at 40x oil-immersion objective on a Nikon 90i microscope (Nikon Melville, NY).

2.2g) Statistics

GraphPad Prism (version 6) was used. When comparing only two groups, unpaired, two-tailed t-tests were used. Comparison across more than two treatment groups was carried out by one-way analysis of variance (ANOVA), followed by the multiple comparisons q (Newman-Keul's) test. Throughout analysis, $p < 0.05$ was considered statistically significant.

2.3 Results

2.3a) CLFB-1134 displays a favorable pharmacokinetic profile with high brain penetrance in rats and mice

Studies were performed in mice and rats to determine the half-life (T ½) and brain penetrance of the drug when dosed intravenously (I.V.), orally (P.O.), or intraperitoneally (I.P.). Dosing orally in mice achieved a longer half-life compared to i.v. dosing. The brain:plasma ratio is slightly increased when dosed i.v., although both dosing routes gave ratios of nearly one (**Table 2A**). Acute or sub-chronic IP dosing in rats achieved similar half-lives as IV dosing in mice but much longer half-lives in brain compared to mice (**Table 2B, C**). Under all dosing paradigms, the brain:plasma ratios were consistently greater than 1, indicating excellent brain penetrance. An IP dosing paradigm was selected for the MPTP studies (**Table 1**).

Table 2A. CLFB-1134 pharmacokinetic properties in C57BL/6J mice.

	IV Dose 10mg/kg	**PO Dose 30 mg/kg** *30% solutol in saline
PLASMA		
AUC	5575	7854
T ½ (hr)	2.6	3.3
V2 (mL/kg)	6745	1255
CLZ (mL/hr/kg)	1793	2.0
%F		47
BRAIN		
AUC	7286	7185
T ½ (hr)	1.4	3.3
V2 (mL/kg)	2858	765
CLZ (mL/hr/kg)	1372	2.0

Table 2B. CLFB-1134 (single dose) pharmacokinetic properties in Sprague-Dawley rats.

	IP Dose 10mg/kg *30% solutol in saline
PLASMA	
AUC	5630
T ½ (hr)	2.5
CLZ (mL/hr/kg)	1775
Cmax	2135
Tmax	0.25
BRAIN	
AUC	2870
T ½ (hr)	3.6
Cmax	517
Tmax	2

CLFB-1134 displays a favorable pharmacokinetic profile in mice with high brain penetrance. CLFB-1134's concentration in plasma and in brain following intravenous (IV), oral (PO), or intraperitoneal (IP) dosing, as indicated. AUC=area under curve, T ½ (hr) = half life time in hours. V2 = compartment volume.

Table 2C. CLFB-1134 chronic dosing pharmacokinetic properties in Sprague-Dawley rats.

Male	Day	Plasma (ng/mL)	Brain (ng/g)	B / P
7 Day 10mg/kg	Day 1	714	881	1.2
	Day 7	255	446	1.7
	% of Day 1	35%	51%	
7 Day 20mg/kg	Day 1	1496	1695	1.1
	Day 7	453	543	1.2
	% of Day 1	30%	32%	
35 Day 20mg/kg	Day 1	1496	1695	1.2
	Day 35	292	359	1.2
	% of Day 1	20%	21%	

Female	Day	Plasma (ng/mL)	Brain (ng/g)	B / P
7 Day 10 mg/kg	Day 1	240	494	2
	Day 7	104	157	1.5
	% of Day 1	43%	31%	
7 Day 20 mg/kg	Day 1	1051	640	0.61
	Day 7	234	441	1.9
	% of Day 1	22%	68%	

2.3b) MLK3 inhibition in vivo with CLFB-1134 does not interfere with MPTP metabolism to MPP+

The use of MPTP has long been the gold standard for generating a mouse model of the nigrostriatal dopaminergic pathway degeneration characteristic of parkinsonism. Critical to this process is the metabolism of MPTP to its neurotoxic metabolite, MPP+ by astrocytes (Javitch et al., 1985; Ransom et al., 1987) and the selective transport of MPP+ into the DA terminal by the DA transporter (DAT). Given these dynamics, it is imperative to ensure that any intervention, especially one that is viewed as neuroprotective, does not affect the processing of MPP+, leading to an artificial interpretation of neuroprotection. Striatal MPP+ levels were not different in mice concurrently dosed with MPTP + drug vehicle and those that received MPTP + CLFB-1134 (**Figure 2**). These data demonstrate that treatment with CLFB-1134 does not impair or enhance the metabolism of MPTP to MPP+, providing a reliable model to evaluate neuroprotection by MLK3 inhibition.

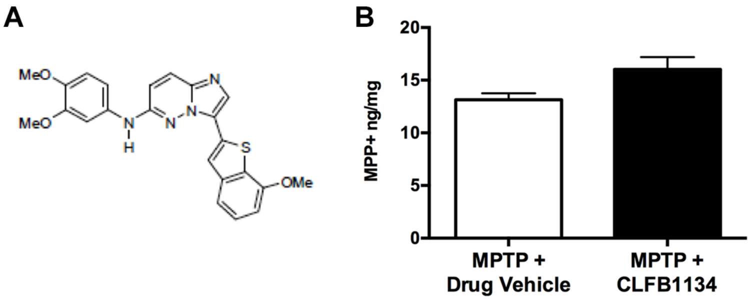

Figure 2. CLFB-1134 does not interfere with MPTP metabolism. A. Structure of CLFB-1134. CLFB-1134 (Imidazo[1,2-*b*]pyridazine). IC_{50} = 42nM. **B. CLFB-1134 does not interfere with MPTP metabolism.** Following 5 days of MPTP + CLFB-1134 or MPTP + drug vehicle treatment, striatal MPP+ levels were quantified using HPLC. MPP+ levels did not differ between mice concurrently dosed with MPTP + drug vehicle and those that received MPTP + CLFB-1134. MPTP + drug vehicle group mean ± SEM: 13.14ng/mg ± 0.6258, (n=9). MPTP + CLFB-1134 group mean ± SEM: 16.02 ± 1.175 (n=12). p=0.0648, by unpaired, two-tailed t test.

2.3c) **In vivo** ***administration of CLFB-1134 engages the target MLK3 and results in attenuated JNK phosphorylation***

Prior to embarking on neuroprotection experiments, we dosed two cohorts of mice with CLFB-1134 (or drug vehicle as a control) just prior to either an MPTP or neurotoxin vehicle injection as described in the Methods. As a downstream measure of target engagement, we measured pJNK at Thr183/Tyr185 by multiplexed immunoassay. While previous work has shown JNK phosphorylation following MPTP treatment in mice, in our hands, MPTP treatment did not increase pJNK relative to the other treatment groups (Tatton and Kish, 1997). The addition of CLFB-1134 produced a 13% reduction in the background-subtracted pJNK chemiluminescent signal relative to neurotoxin vehicle-treated animals that also received drug vehicle (**Figure 3**).

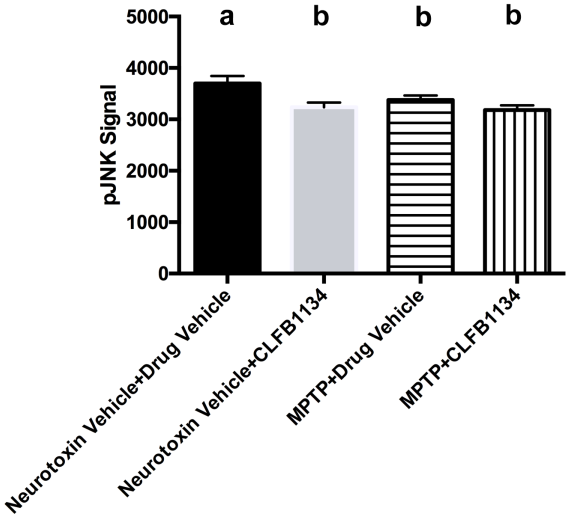

Figure 3. *In vivo* target engagement by CLFB-1134. As a measure of MLK3 inhibition, JNK phosphorylation was quantified in mouse brain tissue. CLFB-1134 treatment was associated with decreased pJNK signal relative to drug vehicle, although MPTP also was associated with decreased pJNK signal relative to the neurotoxin vehicle condition. Mean ±SEM in background-subtracted chemiluminescent units: Neurotoxin vehicle + drug vehicle: 3699±144.0 (n=7), Neurotoxin vehicle + CLFB-1134 group: 3234±93.2 (n=7), MPTP + drug vehicle group: 3378±87.82 (n=8), MPTP + CLFB-1134 group: 3179±93.78 (n=8). Different letters indicate that there is a statistically significant difference between groups.

2.3d) CLFB-1134 protects against MPTP-induced loss of striatal dopaminergic terminals

A hallmark pathological feature of PD is loss of markers of dopaminergic terminal integrity and function in the striatum. As previously published (Tillerson et al., 2002; Jackson-Lewis and Przedborski, 2007; Meredith et al., 2008) exposure to 20 mg/kg MPTP for 5 days resulted in an approximately 50% reduction in striatal TH expression, compared with animals that received only neurotoxin vehicle or drug vehicle (**Figure 4**). A similar reduction was measured when MPTP was co-administered with the drug vehicle. These reductions were absent when CLFB-1134 was administered *in vivo* simultaneously with MPTP or following the MPTP regimen (**Figure 4**).

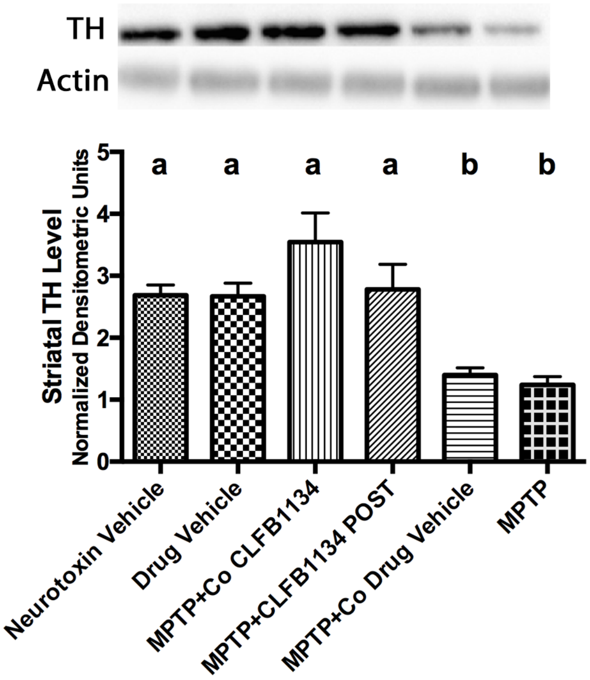

Figure 4. CLFB-1134 protects against MPTP-induced loss of striatal TH. Immunoblotting analysis of TH (and actin control) in striatum of mice that received MPTP and concurrent or delayed treatment with CLFB-1134. Order of samples in immunoblot matches the groups on the x axis of graph. Ordinary one-way ANOVA with Newman-Keuls multiple comparisons test. Bars represent mean±SEM. Neurotoxin vehicle n=7. Drug vehicle n=6. MPTP + Co-CLFB-1134 n=7. MPTP + CLFB-1134-Post n=10. MPTP + Co-Drug Vehicle n=5. MPTP n=5. *Co*- indicated co-dosing. *Post*- indicates CLFB-1134 dosing was initiated after MPTP dosing was completed. Different letters indicated statistically significant differences between groups.

2.3e) MLK3 inhibition in vivo with CLFB-1134 did not protect against MPTP-induced striatal DA depletion

The classic motor deficits observed in PD are routinely attributed to a significant loss of DA in the striatum. MPTP treatment reliably mimics this dramatic DA depletion. Our treatment with MPTP induced an approximately 50% reduction in striatal dopamine, compared with mice treated with neurotoxin vehicle or drug vehicle (**Figure 5**). Delayed treatment with CLFB-1134 following MPTP did not protect against loss of striatal DA relative to vehicle, and HVA and DOPAC levels were not restored to untreated levels.

2.3f) MLK3 inhibition in vivo with CLFB-1134 protects against MPTP-induced nigral dopaminergic degeneration

In addition to damage to terminals in the striatum, loss of dopaminergic neurons in the substantia nigra pars compacta (SNpc) is a classic feature of PD neuropathology. With our MPTP paradigm, we were able to demonstrate a dramatic reduction (approximately 84%) in the number of TH+ neurons in the SNpc of MPTP-treated mice, compared with neurotoxin vehicle or drug vehicle controls (**Figure 6**). Consistent with the striatal TH analysis, unbiased stereological estimate of total neurons in the SNpc confirmed that reductions were a result of loss of TH+ neurons, rather than a reduction or masking of the TH epitope (**Figure 6**). In contrast, CLFB-1134 provided robust protection from MPTP-induced nigral dopaminergic cell loss.

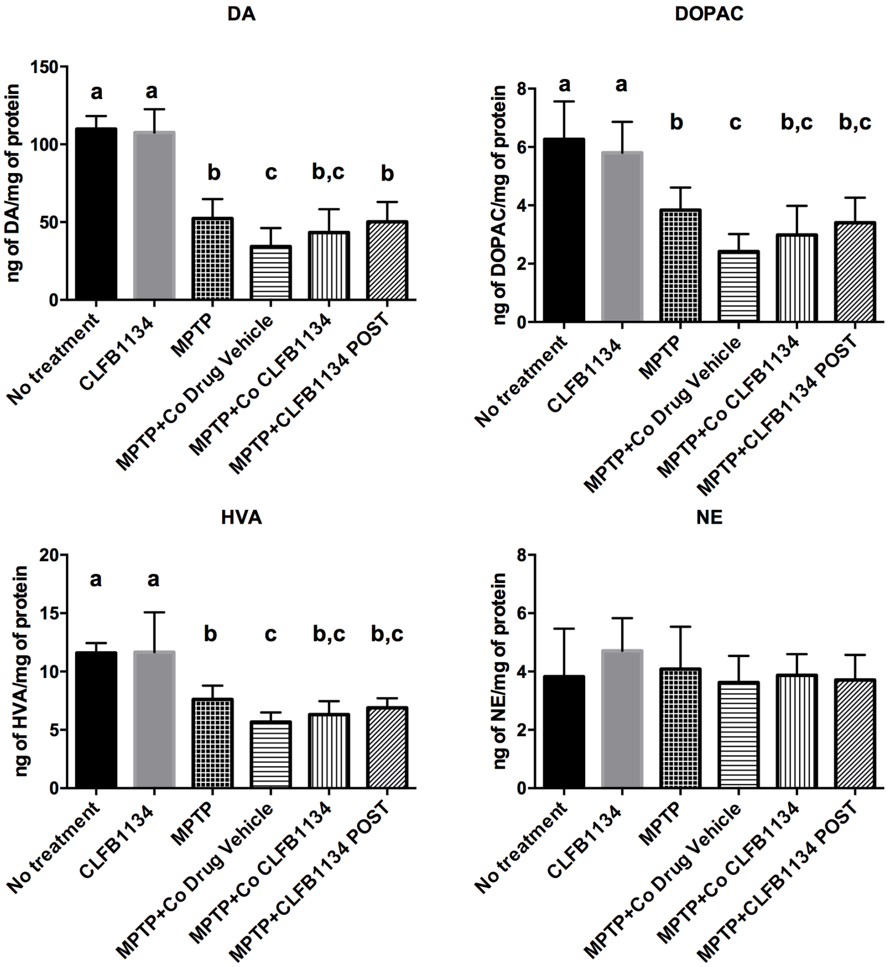

Figure 5. CLFB-1134 does not protect against MPTP-induced striatal DA depletion. DA (dopamine), DOPAC (3,4-dihydroxy-phenylacetic acid), HVA (homovanillic acid), and NE (norepinephrine) were assessed by high performance liquid chromatography. For each analyte, an ordinary one-way ANOVA with Newman-Keuls multiple comparisons test was used for analysis. Bars represent mean±SEM. No treatment n=6. CLFB-1134 n=8. MPTP n=12. MPTP + Co-Drug Vehicle n=10. MPTP + Co-CLFB-1134 n=9. MPTP + CLFB-1134-Post n=10. Different letters indicate that there is a statistically significant difference between groups.

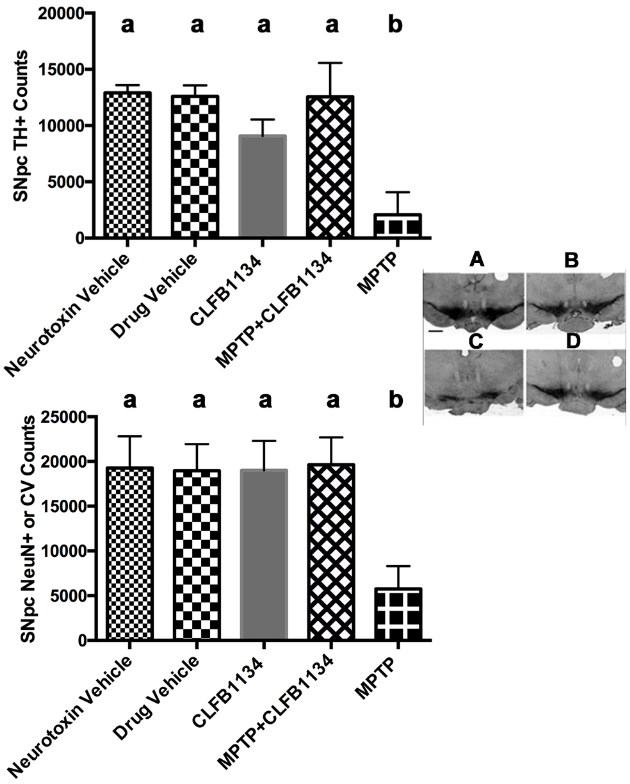

Figure 6. CLFB-1134 protects against MPTP-induced nigral dopaminergic cell loss. Stereological counts of TH+ and NeuN+ (or cresyl violet for CLFB-1134 group) cells in the substantia nigra. Representative micrographs depict nigral sections double-stained for TH and NeuN (2x). **A.** Vehicle, **B.** MPTP + Co-CLFB-1134, **C.** MPTP, **D.** MPTP + CLFB-1134-Post. Scale bar = 300μm. Bars in graphs represent mean±SEM. Ordinary one-way ANOVA. Neurotoxin vehicle n=4. Drug vehicle n=4. CLFB-1134 n=3. MPTP + CLFB-1134 n=5. MPTP n=3. Different letters indicate that there is a statistically significant different between groups.

2.4 Discussion

It has long been known that dopaminergic neurodegeneration drives the motor phenotypes of PD. Because of the cell cycle, apoptotic signaling, and immune activation effects of MLK inhibition, several MLK inhibitors have been tested in models of dopaminergic degeneration and in PD patients (Saporito et al., 1999; Saporito et al., 2002; Mathiasen et al., 2004; Lotharius et al., 2005; Parkinson Study Group, 2007). Using a compound more specific for MLK3 and with better brain penetrance than the earlier inhibitor CEP-1347, we hoped to improve upon previous MLK inhibition work. We found that, indeed, CLFB-1134 does cross the blood-brain barrier (BBB) and achieves physiologically relevant concentrations following oral, intravenous, or intraperitoneal dosing in mice and rats (**Table 2**). An IP dosing paradigm was selected for the MPTP/CLFB-1134 studies.

Dosing regimens used in previous work, including once daily dosing (i.p.) have been sufficient to achieve therapeutic effects in other studies with MLK inhibition (Dong et al., 2016; Gnanadhas et al., 2017; Tomita et al., 2017). We then verified that the neuroprotective capacity of CLFB-1134 can be tested in the MPTP-induced dopaminergic degeneration model because it does not interfere with the conversion of MPTP to MPP+ (**Figure 3**). While MPTP was not, at the timepoint selected, associated with increases in pJNK, CLFB-1134 was found to engage MLK3 and produce a 13% decrease in phosphorylation of JNK (comparing saline-treated groups, **Figure 4**). The lack of MPTP-induced pJNK increase could be due to the transience of MPTP-induced phosphorylation of JNK. The cascade engaging MLK3 and resulting in increased pJNK set off by

MPTP may, by time of sacrifice, have been erased by protein turnover and phosphatase activity altering JNK's status. Nevertheless, CLFB-1134, prior to animal sacrifice, had the opportunity to interrupt the cascade and diminish pJNK. An earlier sacrifice, closer to MPTP treatment, may have revealed increased pJNK as in (Huang et al., 2016), where elevated pJNK following MPTP was reported at 6 hours post neurotoxin injection.

Whether given simultaneously or after MPTP treatment, CLFB-1134 preserves striatal dopaminergic terminals expressing TH as well as nigral TH+ soma (**Figure 4, Figure 6**). The modest decrease in JNK phosphorylation achieved by MLK3 inhibition is the simplest explanation for the preservation of TH nigral cell bodies following CLFB-1134 treatment. Because MLK3, a MAPKKK, is part of a signaling cascade, MLK3 inhibition has far reaching consequences as pJNK in turn acts on many transcription factors and other signaling molecules. Thus, a slight change in MLK3-associated phosphorylation can be amplified and, as we interpret in this case, elicit robust protection of nigral TH+ neurons, and this is similar to what has been previously published with MLK inhibition. Treatment with the broad spectrum MLK inhibitor, URMC-099, in mice was associated with a 21.5, 17.3, and 23.7% decrease in phosphorylation of p38, p46-JNK, and p54-JNK (Dong et al., 2016).

By HPLC, our findings indicate that while there was a significantly greater amount of DA in MPTP + CLFB1134 POST animals than in MPTP + drug vehicle animals, there was no significant difference between concentrations of DA or its metabolites in MPTP, MPTP + Co CLFB1134 or MPTP + CLFB1134 POST groups (**Figure 5**). Achieving nigral neuroprotection in the absence of striatal DA restoration has been reported in other studies using MPTP to model PD neuropathology. Others have proposed that the discrepancy between persistent neurotransmitter depletion and the complete preservation of terminals and soma is due to MPTP's rapid effect on dopaminergic terminals and the more gradual, microglia-dependent action in the SNpc (Liberatore et al., 1999; Zhang et al., 2004; Hu et al., 2008). Loss of DA from the striatum in our paradigm may be related to loss of mitochondrial energetics as induced by MPTP directly, rather than the downstream apoptotic and necroptotic signaling that damages terminals and cell bodies. Specifically, TH is activated by phosphorylation, an event which requires ATP (Daubner et al., 2011). The depletion of ATP achieved by MPTP may prevent activation of TH and thus block proper DA synthesis. Neuroprotective interventions given post-MPTP would thus have a greater chance of affecting the SNpc rather than DA synthesis in striatal terminals. Another possible explanation of the discrepancy between terminal rescue in the absence of neurochemical recovery may be that MPTP damages elements of DA synthesis that are not regulated by MLK/JNK signaling pathways and thus cannot be mitigated by MLK inhibition with CLFB-1134. For example, MPTP treatment decreases the activity of aromatic L-amino acid decarboxylase (King et al., 2011) and the activity of this enzyme may not recover following inhibition of MLK3.

In our own work, **Figure 4** suggests that at the height of MPTP toxicity, CLFB-1134 is capable of preserving the dopaminergic phenotype of the vulnerable nigrostriatal terminals. Preservation of tyrosine hydroxylase expression is necessary for DA production, so while DA and its metabolites were decreased in CLFB-1134-treated mice relative to untreated and CLFB-1134-alone groups, the synthetic machinery (TH) necessary for neurotransmitter production remains expressed. Counts of dopaminergic cell bodies in the substantia nigra further support the conclusion that CLFB-1134 protects neuronal potential to produce dopamine, despite DA levels at the time of sacrifice appearing relatively depleted. The endpoint in this study was 3 weeks post-MPTP, and it is possible that more complete neurochemical recovery could have been observed given more time. However, because spontaneous recovery from MPTP has been observed given increased time post-toxin (Mitsumoto et al., 1998), our limited time course is most informative for specifically evaluating CLFB-1134's neuroprotective capacity.

The early findings from pre-clinical models with first generation MLK inhibitors were promising, yet clinical trials with CEP-1347 failed in a Phase II trial for early PD due to futility (Parkinson Study Group, 2007). It was proposed that another way to improve upon the function of MLK3 inhibitors would be to provide additional support from neurotropic factors such as brain-derived neurotrophic factor (BDNF) signaling via tropomyosin receptor kinase B (TrkB) receptors (Wang and Johnson, 2008). This recommendation is based on the fact that MLK3 inhibition increases the expression of Trk receptors. For dopaminergic neurons in SNpc, the Trk receptors expressed are type B and cannot activate in the absence of their ligand. Once activated, as by BDNF, TrkB receptors lead to the activation of the PI3k signaling cascade, engaging Akt and, ultimately, inhibition of GSK3β. The efficacy of GSK3β inhibition alone as a neuroprotective treatment in an MPTP model of dopaminergic degeneration has been previously described, although the study was limited in translational relevance as a pre-MPTP dosing schedule was used (Wang et al., 2007). Nonetheless, the GSK3β inhibitor did protect dopaminergic soma and terminals. Similar to our own results, the DA concentration in the striatum remained low relative to the control condition, despite the anatomical preservation achieved by GSK3β inhibition. This suggests that targeting the signaling cascade downstream of TrkB may not restore DA levels beyond what was achieved with MLK3 inhibition. Thus, MLK3 inhibition, even on its own, warrants further investigation.

Here, we demonstrated that CLFB-1134 has a favorable brain penetrance and, as evinced from our studies, penetrates the BBB sufficiently to engage its target and dampen the downstream pJNK signal that can be measured by immunoassay in brain lysates from mice treated with drug *in vivo*. This target engagement is then the basis for the robust protection of striatal TH terminals and DA neurons in the SNpc from MPTP-induced damage.

CHAPTER 3. PERIPHERAL MYELOID CELL MHCII EXPRESSION IN MICE AFFECTS IMMUNOPHENOTYPE AND RESPONSE TO HUMAN WT α-SYNUCLEIN

Technical assistance with qPCR, Western blots, and Mesoscale Discovery multiplex enzyme linked immunosorbent assays provided by Sean Kelly, Mary K. Herrick (rAAV2/9 study only), and Jianjun Chang respectively. Stereotaxic surgeries, cypermethrin treatment, flow cytometry, histology, and all analyses performed by Elizabeth Marie Kline.

3.1 Introduction

Evidence from multiple studies suggests an association between changes in the immune system and the hallmark neuropathologies of Parkinson’s disease (PD), specifically age-related dopaminergic degeneration and α-synuclein aggregation. The brain’s resident immune cells, microglia, are activated in rodent models of transgene- and viral-vector-mediated α-synuclein overexpression (Su et al., 2008; Theodore et al., 2008; Su et al., 2009; Sanchez-Guajardo et al., 2010; Watson et al., 2012), as well as in the post-mortem (McGeer et al., 1988c; McGeer et al., 1988b; Banati et al., 1998; Imamura et al., 2003) and living brains of PD patients (Gerhard et al., 2006). Cytokines such as IL-1β, TNF, and IL-6 are secreted by activated microglia and promote an inflammatory environment in the brain, as seen in PD substantia nigra pars compacta (SN, locus of neurodegeneration), and striatum (Mogi et al., 1994b; Mogi et al., 1994a). Adaptive immune system alterations have also been identified in PD, including extensive infiltration of CD4+ and CD8+ T cells into the central nervous system in human patients and rodent models (Baba et al., 2005; Brochard et al., 2009).

Autoantibodies against dopaminergic (DA) neuron proteins in PD patient serum and cerebrospinal fluid have also been observed (Defazio et al., 1994), as have T cells capable of recognizing synuclein-derived antigens (Sulzer et al., 2017). Despite what we have learned about the state of the immune system in PD, the mechanism by which immune system function influences risk for PD remains unclear.

One key immune system function of interest in PD is the process of antigen presentation, which is the nexus between the innate and adaptive immune systems. The way in which antigen presentation regulates the status of the immune system specifically in PD is not yet fully understood. Antigen presentation relies on major histocompatibility complex proteins (MHC) proteins which display antigen peptides to T cells, prompting T cell activation and differentiation. Differentiated T cells promote pathogen clearance and the formation of immunological memory. Microglia and other specialized antigen presenting cells display peptides derived from engulfed pathogens and intracellular debris using MHC class II (MHCII), recognized by CD4+ T cells. In *in vitro* and *in vivo* studies, microglia have been shown to have the capacity to phagocytose certain species of α-synuclein as well as debris released by degenerating DA neurons (Zhang et al., 2005; Park et al., 2008; Marinova-Mutafchieva et al., 2009; Zhang et al., 2011). Coupled with the observation that MHCII expression in PD brain correlates with deposition of α-synuclein (Croisier et al., 2005) and is increased relative to control brains (McGeer et al., 1988b), the current evidence suggests the possibility that immune cells phagocytose and present α-synuclein-derived peptides or antigens from α-synuclein-burdened, degenerating neurons to CD4+ T cells in PD. While the precise location of such antigen presentation (within the brain parenchyma, in the perivascular space, or more distant from the central nervous system) is a subject of debate, the fact that antigen presentation is an important process in PD is accepted.

Consistent with post-mortem observations and studies with animal models of PD in which MHCII is upregulated in the brain, a single nucleotide polymorphism (SNP), *rs3129882*, within the gene for MHCII was reported to be associated with a 1.7-fold increase in risk for PD (Hamza et al., 2010). The high-risk genotype (*GG*) at *rs3129882* is over-represented (46%) in patients with idiopathic PD compared to its frequency in an age-matched healthy control population (40%). Functionally, our group demonstrated that *GG* homozygosity at this SNP is associated with greater baseline mRNA and surface MHCII protein expression in monocytes and B cells (see **Figure 1**). This suggests that the high-risk genotype may also be associated with increased antigen presentation throughout the lifespan, increasing risk for PD as antigenic load increases with age (De Martinis et al., 2005). It may be the case that genotype differences *rs3129882* may also be associated with differences in T cell activation and differentiation.

Because immune activation, including upregulation of MHCII, is associated with neurodegeneration, there has been interest in targeting MHCII for PD treatment, with the goal of blocking antigen presentation to prevent neurodegeneration. Indeed, while some expression of MHCII is necessary to activate T cells when needed to fight an infection, for example, levels above the homeostatic range are linked to autoimmune diseases and accompanied by abnormal ratios of T cell subsets (Nepom and Erlich, 1991). The work presented here was done in an effort to determine the extent to which deletion of MHCII on peripheral myeloid cells alters T cell frequencies and, thus, impacts dopamine (DA) neuron integrity. Towards this effort, we used a model of PD pathology in which a recombinant adeno-associated viral vector drives human α-synuclein expression in mouse SN. To understand the contributions of peripheral myeloid cell MHCII-mediated antigen presentation to α-synuclein-induced inflammation and degeneration, mice with peripheral myeloid deletion of MHCII (LysMCre+I-Ab$^{fl/fl}$) were used in these experiments.

Insertion of Cre recombinase into the endogenous M lysozyme locus has previously been used to create myeloid-specific gene recombination (Clausen et al., 1999). In the original study, deletion efficiency in mature macrophages was 83-98% and nearly 100% in granulocytes, with 16% deletion in splenic CD11c+ dendritic cells (Clausen et al., 1999). LysM is found in a subset of lymphoid and erythroid cells, but no significant deletion was observed in B or T lymphocytes (Clausen et al., 1999). In LysMCre mice, Cre is expressed under the control of the endogenous Lyz2 promoter/enhancer elements. *Lyz2* encodes lysozyme, an enzyme which cleaves peptidoglycans of the bacterial cell wall (Cross et al., 1988). Expression of *Lyz2* varies among cell types and with immune activation. Microglia do not express *Lyz2* at baseline (Wohleb et al., 2013; Zeisel et al., 2015); thus, recombination in microglia is not efficient in LysMCre mice. The LysMCre mouse line crossed with I-Ab$^{fl/fl}$ mice was provided to the Tansey lab by Dr. Tim Denning. In our work, deletion of MHCII under the LysM promoter was first confirmed in naïve LysMCre+I-Ab$^{fl/fl}$ animals relative to LysMCre-I-Ab$^{fl/fl}$ mice. Based on a study of tdTomato expression under LysM, the LysMCre mouse line is expected to drive gene deletion in (at least half of) peripheral myeloid cells, with the possibility of some deletion occurring under inflammatory conditions in microglia as well (Orthgiess et al., 2016).

In what is referred to throughout as the higher-titer rAAV2/9 experiment, rAAV2/9 human WT α-synuclein was delivered to the left SN of LysMCre+ and Cre- I-Ab$^{fl/fl}$ mice to assess the effects of peripheral myeloid cell MHCII expression on α-synuclein-induced degeneration and inflammation. We describe here the DA terminal damage produced by rAAV2/9 human WT α-synuclein and characterize the immune reaction in the striatum. The immunophenotypic differences between LysMCre+ and Cre-I-Ab$^{fl/fl}$ mice are also reported. In order to understand the interactions between α-synuclein, variations in MHCII expression, and a PD-relevant environmental exposure, the second experiment presented in this chapter describes a "double-hit" model in which LysMCre- and Cre+I-Ab$^{fl/fl}$ mice were given rAAV2/5 human WT α-synuclein (left SN) followed by a brief treatment with the pyrethroid pesticide cypermethrin. This study is referred to throughout as the rAAV 2/5 experiment.

The combination of varying MHCII expression (normal in Cre- animals, deleted in some cell types in Cre+ animals) and exposure to a pyrethroid allowed us to investigate the mechanism behind the observation reported in (Kannarkat et al., 2015). Specifically, the high-risk *rs3129882* genotype was associated with increased risk for PD in humans who had also been exposed to 1 or more pyrethroids (Kannarkat et al., 2015). Humans with the high-risk single nucleotide polymorphism (SNP) genotype (*GG*) at *rs3129882* in the first intron of the human

MHCII gene *HLA-DRA* have high expression of MHCII on monocytes and B cells relative to those with the low risk SNP genotype (Kannarkat et al., 2015). While we did not take the approach of mimicking the increase in MHCII expression observed in high-risk genotype individuals, we can compare the conditions in mice with relative higher (Cre-) MHCII levels to those with the cell-specific deletion. Immunomodulatory PD treatments aimed at decreasing MHCII expression have been proposed (Williams et al., 2018), suggesting our comparison is translationally relevant.

3.2 Materials and Methods

3.2a) Mice

Male LysMCre+I-Ab$^{fl/fl}$ and control LysMCre-I-Ab$^{fl/fl}$ mice were used in this study. Mice were housed in the facilities in the Whitehead Biomedical Research building in the Division of Animal Resources at Emory University with *ad libitum* access to food and water. The animal facility is on a 12-hour light/dark cycle. Experimental procedures were approved by the Institutional Animal Care and Use Committee of Emory University and performed in compliance with the National Institutes of Health guide for the care and use of laboratory animals. Mice that received stereotaxic injection were 2-3 months old (young adult) at the time of stereotaxic injection. Mice were euthanized by intraperitoneal Euthasol (Virbac Animal Health, Fort Worth, TX) for the rAAV2/5 and higher titer rAAV9 studies. Mice were euthanized by isoflurane-anesthetized cervical dislocation for the verification of MHCII deletion experiment.

For the rAAV2/5 study, cypermethrin (CHEM SERVICE, Inc. N-11545-100mg, lot 6593600, certified on 11.10/2015) was formulated in sterile corn oil

(Mazola, ACH Food Companies, Inc. Oakbrook Terrace, IL) at 5mg/mL in a light safe vial. Dosing began 8-9 months following stereotaxic surgery with rAAV2/5 human WT α-synuclein and was carried out twice per week for three weeks (6 total injections, intraperitoneal). The solution of cypermethrin and the vehicle were vortexed prior to drawing up solution for each injection. Animals were sacrificed within 1 week following the final injection. Animals treated with cypermethrin or vehicle were co-housed to avoid confounding cage effects.

The verification of MHCII deletion in peripheral myeloid cell experiment included n=3 LysMCre+I-Ab$^{fl/fl}$ mice and n=3 LysMCre-I-Ab$^{fl/fl}$ mice. The rAAV9 higher titer experiment included n=16 LysMCre-I-Ab$^{fl/fl}$ and n= 11 LysMCre+I-Ab$^{fl/fl}$. The rAAV2/5 double hit experiment with cypermethrin treatment included all male mice, LysMCre+I-Ab$^{fl/fl}$ + vehicle n=6, LysMCre+I-Ab$^{fl/fl}$ + cypermethrin n=8, LysMCre-I-Ab$^{fl/fl}$ + vehicle n=9, LysMCre-I-Ab$^{fl/fl}$ + cypermethrin n=9. The rAAV9 higher-titer study included all male mice, LysMCre-I-Ab$^{fl/fl}$ n=16. LysMCre+I-Ab$^{fl/fl}$ n=11.

3.2b) Virus and stereotaxic injection

Viruses were generously provided by Dr. Frederic Manfredsson at Michigan State University (Stock Titer: rAAV9 2.1x10^{12}, rAAV2/5 2.9x10^{11}). Mice were unilaterally injected (2µL) under stereotaxic guidance to the left SN as in (Theodore et al., 2008). Surgery was performed under 1-2% isoflurane anesthesia. Mice were placed into stereotaxic frame and injection coordinates for the SN were determined relative to bregma: AP -3.2mm, ML +1.2mm, DV -4.6mm from dura. The virus was delivered via handmade glass microcapillary pipette affixed to an 80000 Hamilton syringe (Hamilton Company, Reno, Nevada) coated in Sigmacote

(Millipore Sigma, Darmstadt, Germany). Post-operative pain relief was provided using buprenorphine (Reckitt Benckiser, NDC 12496-0757-1, 0.1mg/kg, intraperitoneal).

3.2c) Immunofluorescence

For rAAV2/5 and higher titer rAAV2/9 studies, following Euthasol injection, mice were saline perfused for five minutes. Brains were extracted and the caudle portion of the brain (posterior of striatum) was placed in 4% paraformaldehyde at 4°C for 24 hours. Tissue was transferred to a 30% sucrose solution in phosphate buffered saline (PBS) and stored until sliced. Sectioning was performed on a freezing stage microtome (Leica SM 2010R, Leica Biosystems Inc., Buffalo Grove IL) and 40μm coronal slices were stored in 0.1% PBS with sodium azide at 4°C until stained. Free floating staining of SN brain sections was performed as follows. Slices were washed in Tris buffered saline (TBS) and incubated in a solution of 4% normal goat serum and 0.25% Triton-x-100 in TBS for 60 min at room temperature to block non-specific labeling. Sections incubated with primary antibody for 24 hours in TBS with 0.25% Triton-X-100 and 2% normal goat serum. For primary and secondary antibody concentrations, staining conditions, and catalog numbers, see antibody table. Following TBS wash, secondary antibody incubations were carried out at room temp for 2.5 hours with normal goat serum (2%). Secondary-only controls were used to confirm the specificity of the staining. Images of co-labeling of tyrosine hydroxylase and α-synuclein were captured using 4x-20x objective lenses on a Nikon 90i fluorescence microscope and the Nikon Elements 5 software (Nikon, Melville, NY) for the rAAV2/5 study. Images for the higher tier rAAV9 study were captured on a Keyence BZ-X700.

3.2d) Western blot

Following Euthasol injection and saline perfusion, brains were extracted, and the left and right striatum were dissected and flash frozen in liquid nitrogen for the rAAV2/5 and the higher-titer rAAV9 studies. Tissue was stored at -80°C until processed for Western blot. Tissue was homogenized using a pestle motor mixer in RIPA buffer with protease and phosphatase inhibitors. Following a bicinchoninic acid protein assay, samples were diluted in water and 2x Laemmli buffer. Samples were boiled for 5min and run immediately for Western blot. Pre-cast, 15-well 10% mini-PROTEAN® TGX™ polyacrylamide gels from Bio-Rad were loaded with 10μg of protein from each sample. Gel electrophoresis was performed at 100V for 110 min. Methanol-activated PVDF membranes were used for protein transfer via the Trans-Blot Turbo System (Bio-Rad). The high molecular weight, 10 min setting was used to transfer protein. REVERT stain (LI-COR Biosciences) for detection of total protein was performed and membranes were imaged in the 700 channel, 30 second exposure. The membrane was then blocked in 5% Triton-X-100 in TBS with milk for 1 hour at room temperature. Primary antibodies against mouse dopamine transporter (DAT), and TH were used at the concentrations indicated in the antibody table. Blots were incubated in 5% Triton-X-100 in TBS with milk at 4°C overnight. Blots were then washed and incubated with secondary antibodies at room temperature for 1 hour. Following additional washes in TBS with Triton-X-100 and TBS, blots were developed using West Pico Chemiluminescent Substrate or SuperSignal West Femto Chemiluminescent Substrate (Thermo Scientific, Waltham, MA). Band intensity was measured using an Azure c400 (Azure Biosystems, Dublin, CA) and analysis was performed using ImageStudio Software (Li-Cor Biosciences, Lincoln NE).

3.2e) Immune cell isolation and flow cytometry

In order to assess the extent of MHCII deletion in the peripheral myeloid cells of LysMCre+I-Ab$^{fl/fl}$ relative to LysMCre-I-Ab$^{fl/fl}$ mice, splenocytes, peritoneal macrophages from naïve animals and prepared for flow cytometry. Spleens were placed in 1xHBSS and passed through a 40μm cell strainer to create a single cell suspension. Following centrifugation and removal of supernatant, red blood cells were lysed using ACK buffer. RPMI media was used to wash away ACK buffer, and splenocytes were counted using a hemacytometer and Trypan blue exclusion. Splenocytes were loaded into the autoMACS Pro Separator (Miltenyi Biotec, Bergisch Gladbach, Germany) for CD11b+ cell selection. Peritoneal macrophages were harvested by following a protocol similar to the one published in (Ray and Dittel, 2010). Briefly, peritoneal lavage was performed using an 18g needle and 5mL of RPMI 1640. Cells were recovered, counted, and went through the autoMACS CD11b+ isolation described for spleen. Cells were stained for flow cytometry using **Panel 1** for splenocytes and **Panel 2** for peritoneal macrophage (see antibody table). For both panels, cells were incubated with Live/Dead Fixable Red (1:2000, Thermo Fischer L34971) and anti-mouse Fc block (CD16/CD32) (1:100, 14-0161085 eBioscience) along with cell surface markers in PBS. Samples were run on an LSRII (BD Bioscience) and analyzed using FlowJo_V10. The gating strategies for **Panels 1** and **2** are presented in **Figures 7.**

As part of the low titer rAAV2/5 and higher-titer rAAV2/9 studies, the following procedure was used to assess circulating immune cells in mouse blood and the immune cells within the deep cervical lymph nodes. Approximately 200µL of whole blood was collected from cheek bleeds prior to Euthasol injection. Blood was collected in EDTA coated tubes (Coidien 8881311248) and 100µL was treated with Biolegend 1x red blood cell lysis buffer (420301) in order to isolate peripheral blood mononuclear cells (PBMCs). The remaining 100µL of blood was centrifuged for plasma collection. Plasma was flash frozen in liquid nitrogen and then stored at -80°C until processing. The right and left deep cervical lymph nodes (DCLNs) were removed each mouse and placed into 1xHanks Balanced Salt Solution with 5% fetal bovine serum. A single cell suspension was made by grinding the tissue through a 70µm filter. All cells isolated from DCLNs were plated and stained as follows for multi-color flow cytometry using the mouse T cell subset panel (**Panel 3**, see antibody table). PBMCs were divided into two wells. One well was stained using the mouse T cell subset panel and the other was stained using the mouse immunophenotyping panel (**Panel 4**, see antibody table). For both panels, cells were incubated with Live/Dead Fixable Aqua (1:2000, L34957 Invitrogen) and anti-mouse Fc block (CD16/CD32) (1:100, 14-0161085 eBioscience) in PBS. Following incubation with surface markers, intracellular staining was performed for the mouse T cell subset panel samples. To fix and permeablize, the Invitrogen intracellular staining kit was used as per the manufacturer's protocol (00-5223-56, 00-5123-43), 00-8333-56). Spherobeads (BD Biosciences) and OneComp beads (eBiosciences) were used to set voltages on the cytometer and compensation settings and to standardize the 4 cohorts within the rAAV2/5 study and 3 cohorts in the rAAV2/9 study (animals staggered based on breeding). Samples were immediately run on an LSRII (BD Bioscience) following staining. FlowJo_V10 was used for analysis. The gating strategy for each panel is depicted in **Figure 9**.

In the samples, 10μL of counting beads were added prior to running on the cytometer (AccuCheck Counting Beads, Invitrogen, PCB100). The counts of each population of interest were calculated using FlowJo. To determine the counts of a certain cell type in a particular tissue, the following calculation was performed: ((population count from FlowJo / bead count from FlowJo) x ((bead concentration x bead volume) / flow sample volume) x tissue volume.

3.2f) Mesoscale Discovery multiplex enzyme linked immunosorbent assay

Plasma samples were run on a multiplexed immunoassay according to the manufacturers protocol in order to detect TNF, CXCL1, IL-6, IL-5, IL-4, IL-2, IL-1, IL-12, IL-10, and IFNγ (Meso Scale Discovery, Gaithersburg, MD). Samples were run in duplicate (10μL each) by an experimentalist blinded to mouse genotype and treatment. Meso Scale Discovery integrated data analysis software was used to convert data into pg/mL. The following mice were included in the multiplexed immune assay from the lower titer rAAV2/5 study: LysMCre-I-Ab$^{fl/fl}$ vehicle-treated n=4, cypermethrin treated n=3; LysMCre+I-Ab$^{f/f/}$ vehicle treated n=4, cypermethrin treated n=3, randomly selected. For the higher titer rAAV2/9 study, n=6 LysMCre-I-Ab$^{fl/fl}$ and n=8 LysMCre+I-Ab$^{fl/fl}$ mice were used, randomly selected.

3.2g) Quantitative real time polymerase chain reaction

In the higher titer rAAV9 experiment, to complement our understanding of protein level changes to the nigrostriatal DA system following viral vector-mediated expression of human α-synuclein, RNA was isolated from the same left and right striatal samples used for Western blots. RNA was isolated using TRIzol™ reagent according to the manufacturer's protocol (15596018, ThermoFischer Scientific). Reverse transcription was performed to make cDNA as published (Kannarkat et al., 2015). cDNA was used with the primer sets in **Table 3** for qPCR (GAPDH used as housekeeping control for normalization).

Table 3.

Gene	Forward 5'-3'	Reverse 5'-3'
Human α-synuclein	CAG GAA GGA ATT CTG GAA GAT	TAG TCT TGA TAC CCT TCC TCA
Mouse CD4	GTG AGC TGG AGA ACA GGA AAG AG	GGC TGG TAC CCG GAC TGA
Mouse TNF	CTG AGG TCA ATC TGC CCA AGT AC	CTT CAC AGA GCA ATG ACT CCA AAG
Mouse CD68	GGA CTA CAT GGC GGT GGA ATA	GAT GAA TTC TGC GCC ATG AA
Mouse CCL2	CTT CCT CCA CCA CCA TGC A	CCA GCC GGC AAC TGT GA
Mouse iNOS	CAG GAG GAG AGA GAT CCG ATT TA	GCA TTA GCA TGG AAG CAA AGA
Mouse MHCII (I-Ab)	CAG GAG TCA GAA AGG ACC TC	AGT CTG AGA CAG TCA ACT GAG
Mouse IL-1beta	CAA CCA ACA AGT GAT ATT CTC CAT G	GAT CCA CAC TCT CCA GCT GCA
Mouse IL-6	CAC AAG TCG GAG GCT TAA T	AAT TGC CAT TGC ACA ACT C
Mouse MHCI (H2-Ab1)	TGC TAC TTC ACC AAC GGG AC	CAC AGT GAT GGG GCT CTT CA
Mouse GAPDH	CAA GGT CAT CCA TGA CAA CTT TG	GGC CAT CCA CAG TCT TCT GG

3.2h) Statistics

In the rAAV2/5 study, values were compared across genotypes (LysMCre+ and Cre– I-Ab$^{fl/fl}$) and treatment conditions (cypermethrin or vehicle) using ordinary two-way ANOVA with Sidak's multiple comparison's test. In the higher-titer rAAV2/9 study, values were compared between genotypes using normal, 2 tailed Student's t test. To compare left and right brain hemispheres (α-synuclein virus-injected and uninjected sides, respectively) as well as the two genotypes, ordinary two-way ANOVA was performed. When post-hoc analyses were performed, the Sidak's multiple comparison's test was used. GraphPad Prism 6 software was used for all statistical analysis, with the exception of Grubbs' test to detect outliers, which was performed using the calculator at https://www.graphpad.com/quickcalcs/grubbs1/. Significance for all comparisons was set at $p \leq 0.05$. Data is presented throughout as mean±SEM.

3.3 Results

3.3a) Verification of MHCII deletion in peripheral myeloid cells in LysMCre+ I-Ab$^{fl/fl}$ mice

Studies were performed in naïve (no stereotaxic surgery) LysMCre+I-Ab$^{fl/fl}$ and LysMCre-I-Ab$^{fl/f}$ mice to determine the extent to which Cre expression under the LysM promoter affected MHCII protein expression on CD11b+ cells, positively selected using the autoMACS Pro Separator. Cells from spleen and the peritoneal cavity were assessed. The frequency of MHCII+ cells in the LD-CD11b+CD45+CD3-Ly6G-CD11c+ and in the LD-CD11b+CD45+CD3-Ly6G-CD11c- populations was statistically significantly decreased in the LysMCre+I-Ab$^{fl/fl}$ mice relative to LysMCre-I-Ab$^{fl/fl}$ (**Figure 8.A** and **B**). In CD11b+

peritoneal immune cells (positively selected using autoMACS), LysMCre+I-Ab$^{fl/fl}$ mice similarly displayed a decrease in the frequency of MHCII+ cells in both CD11b MID and HI populations, regardless of Ly6C expression (**Figure 8.C-F**). LysMCre genotype did not affect the frequency or counts of cells within any other gate. These data indicate that LysMCre+I-Ab$^{fl/fl}$ have a deletion of MHCII+ myeloid (CD11b+) cells in peripheral tissues.

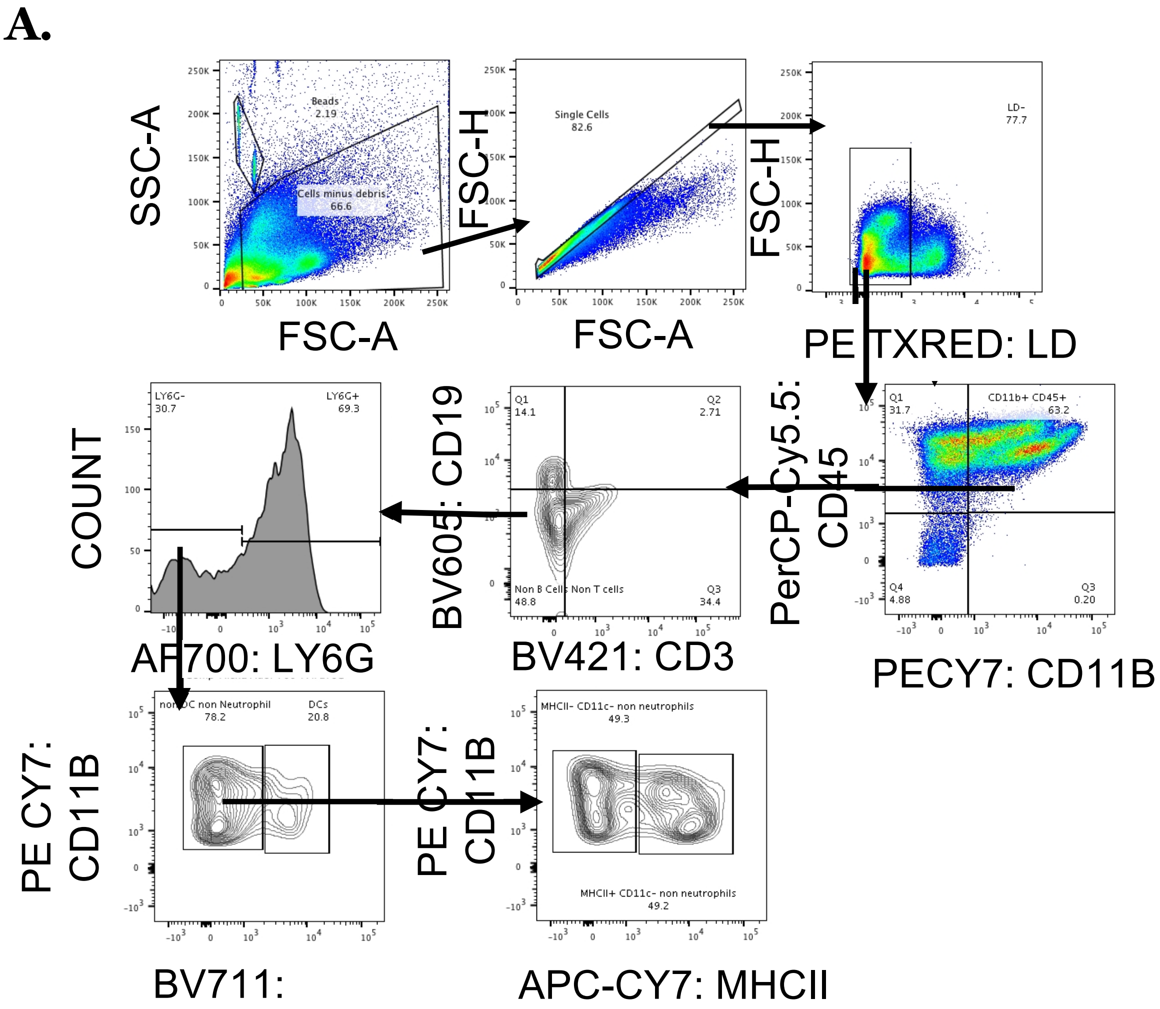

Figure 7A. Flow cytometry gating strategies for mouse splenocytes, Panel 1. Live cell population was identified as LD-. The myeloid immune cell population (CD11b+CD45+) was then identified and gated on CD3 (T cells) and CD19 (B cells) to further purify the myeloid population. Ly6G+ gate was used to identify neutrophils. Ly6G- cells were gated on CD11c as a marker of a subset of dendritic cells. CD11c+ and CD11c- populations were both gated on MHCII (vs CD11b for clarify) to determine the frequency of MHCII+ cells.

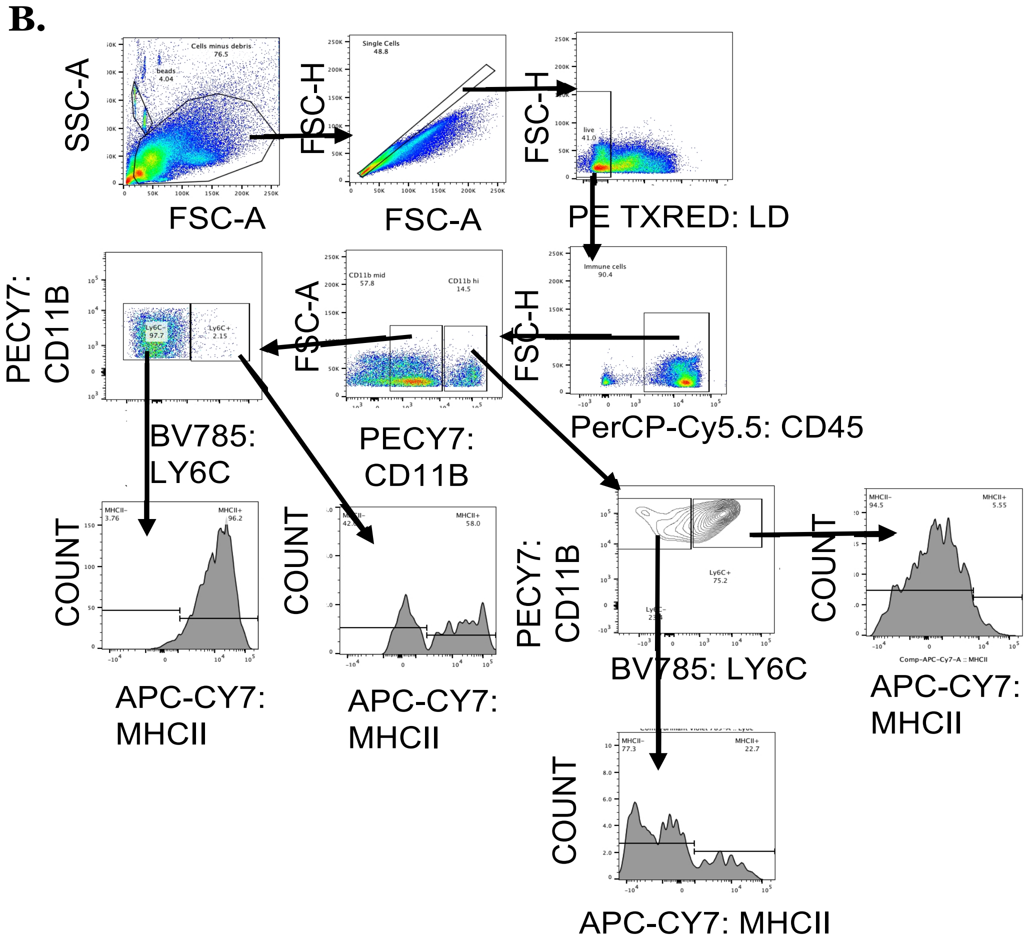

Figure 7B. Flow cytometry gating strategies for mouse peritoneal immune cells, Panel 2. Live cell population was identified as LD-. The CD45+ population (plotted versus FSC-H for clarity) was gated on CD11b (versus FSC-A for clarity), and CD11b HI (large peritoneal macrophage) and CD11b MID (small peritoneal macrophage) populations were identified. Within both the CD11bHI and MID populations, cells were gated on Ly6C to identify infiltrating (Ly6C+) and circulating (Ly6C-) cells, and both Ly6C+ and Ly6C- populations were then gated on MHCII. For both **A.** and **B.,** standardization and compensation with Sphero beads and OneComp beads was performed, and gates were drawn based on isotype antibody controls.

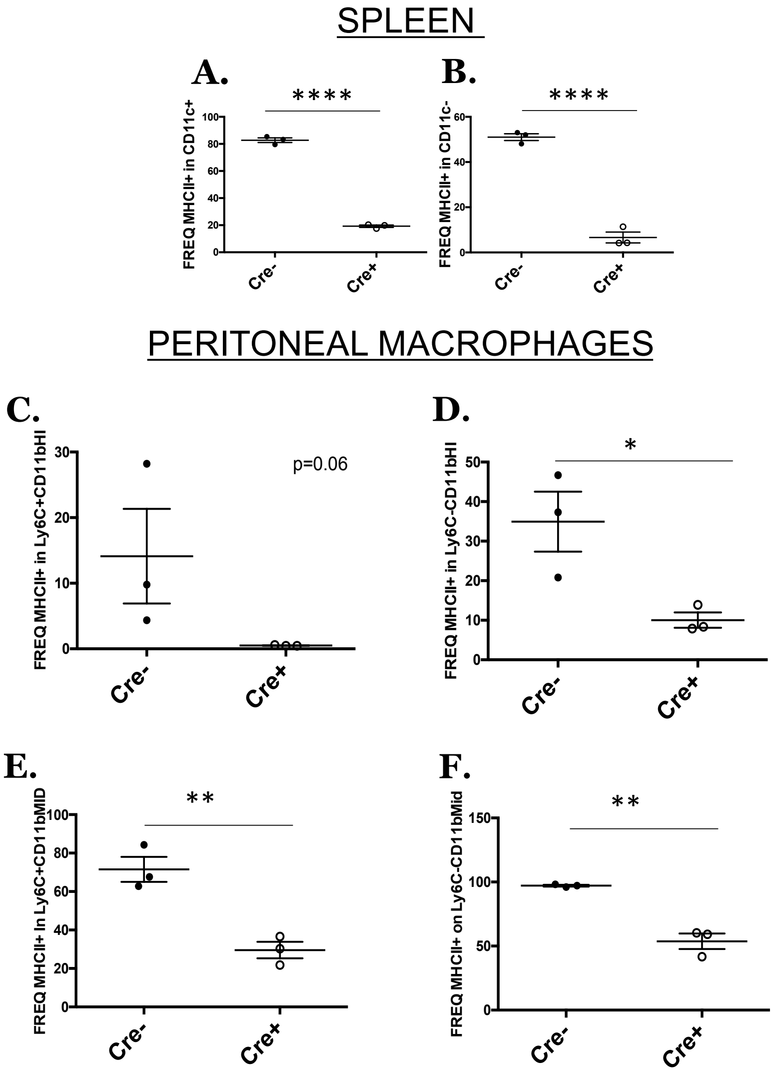

Figure 8. MHCII deletion in peripheral myeloid cells of naïve LysMCre+I-Ab$^{fl/fl}$ mice. Gating strategy presented in Figure 7. The frequency of MHCII+ cells was measured by surface staining for flow cytometry on CD11b+ positively selected cells from (**A** and **B**) the spleen and the peritoneal macrophages (**C-F**) of naïve LysMCre- (CRE-, filled circles) and LysMCre+ (CRE+, open circles) I-Ab$^{fl/fl}$ mice. Data are plotted as mean +/- standard error of the mean (SEM). P-values are indicated for two-tailed t-test: ****$p<0.0001$, **$p<0.01$, *$p<0.05$. See **Panels 1** and **2**.

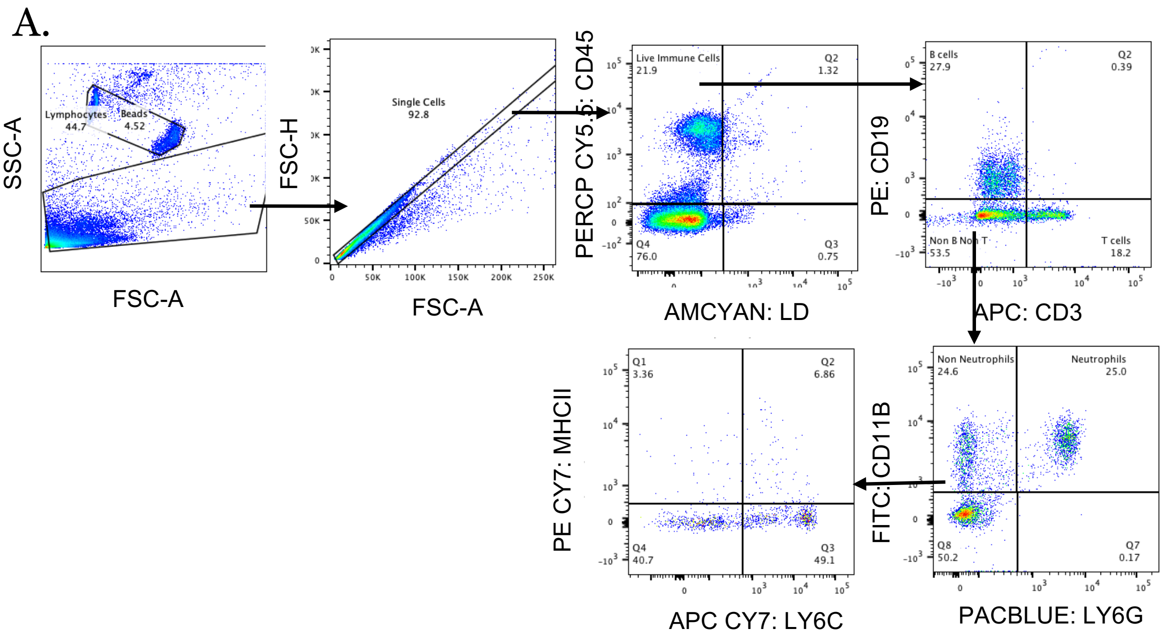

Figure 9A. Flow cytometry gating strategies for mouse PBMC general immune cell types, Panel 4. Live immune cells (LD-CD45+) were gated on CD3 versus CD19 to identify the T cell (CD3+CD19-), B cell (CD3-CD19+), and non-T cell, non-B cell populations (CD3-CD19-). The non-T non-B population was gated on Ly6G versus CD11b to identify neutrophils (Ly6G+CD11b+) and non-neutrophils (Ly6G-CD11b+). Non-neutrophils were then gated on Ly6C versus MHCII to identify the MHCII+ infiltrating (Ly6C+) or circulating (Ly6C-) cells. For both **A.** and **B.,** standardization and compensation with Sphero beads and OneComp beads was performed, and gates were drawn based on isotype antibody controls.

B.

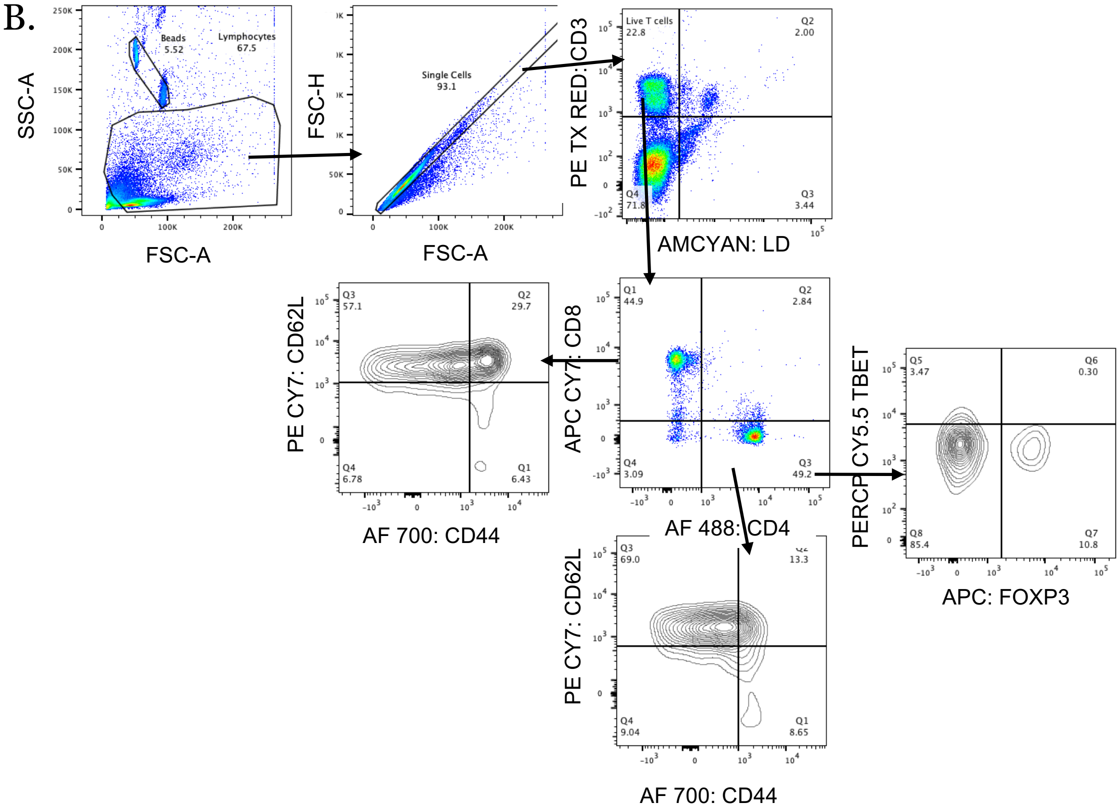

Figure 9B. Flow cytometry gating strategies for mouse PBMC and DCLN T cell subsets, Panel 3. The live T cell population was identified as LD-CD3+. Live T cells were then gated on CD4 and CD8. CD8+ cells were then gated on CD44 versus CD62L to identify naïve CD8 (CD44-CD62L+), central memory CD8 (CD44+CD62L+), and effector memory CD8 (CD44+CD62L-) populations. CD4+ Cells were gated on FoxP3 versus Tbet to identify Th1's (Tbet+, FoxP3-) and regulatory T cells (Tregs, Tbet-, FoxP3+).

3.3b) Immunophenotyping of LysMCre±I-Ab$^{fl/fl}$ mouse peripheral blood mononuclear cells

In mice that had received unilateral nigral rAAV2/9 human WT α-synuclein, to investigate whether peripheral myeloid deletion of MHCII alters general immunophenotype, we analyzed the frequencies and counts of immune cell subsets in the peripheral blood. The frequency of B cells (**Figure 10.A**), T cells (**Figure 10.B**), neutrophils (**Figure 10.C**), and non-neutrophil CD11b+ cells (**Figure 10.D**) did not differ between LysMCre- and LysMCre+I-Ab$^{fl/fl}$ mice, nor did the number of each subset. There was a significant decrease in the frequency and number of Ly6C-MHCII+ and Ly6C+MHCII cells in LysMCre+I-Ab$^{fl/fl}$ mice relative to Cre- (**Figure 10.E-F**). Thus, as in the spleen and peritoneal immune cell population, the *LysMCre* genotype properly deletes MHCII in peripheral myeloid cells. Ly6C+ is a surface marker of immune cells that will migrate to areas of inflammation, such as the brain during an ongoing α-synuclein burden. The results of this experiment indicate that, in LysMCre+I-Ab$^{fl/fl}$ mice, we have deleted MHCII in peripheral myeloid cells without disrupting the overall frequency or number of T and B cells.

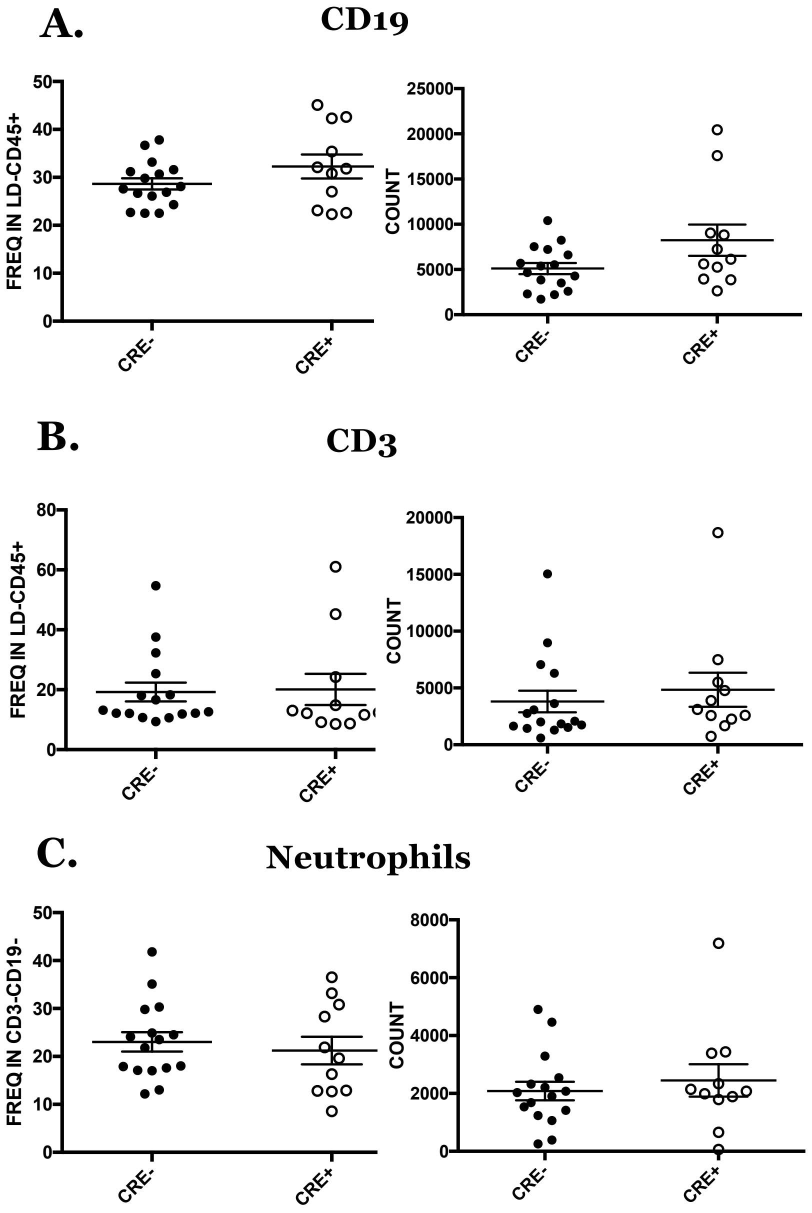

Figure 10.A-C. MHCII deletion in LysMCre+I-Ab$^{fl/fl}$ PBMCs. Peripheral blood mononuclear cells were isolated from LysMCre- I-Ab$^{fl/fl}$ (CRE-, filled circles) and LysMCre+ I-Ab$^{fl/fl}$ (CRE+, open circles) mice 4 months after stereotaxic injection of rAAV2/9 human WT α-synuclein to the SN. Gating strategy presented in Figure 9.A. Data are plotted as mean +/- standard error of the mean (SEM).

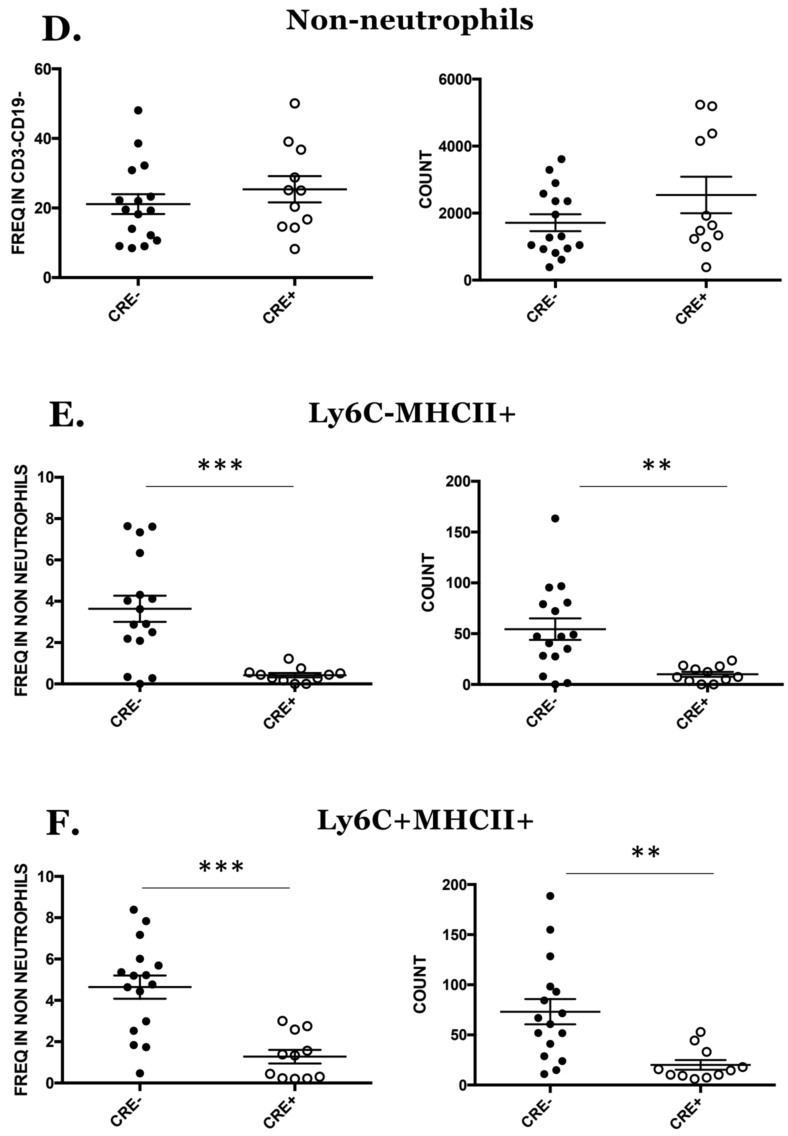

Figure 10.D-F. MHCII deletion in LysMCre+I-Ab$^{fl/fl}$ PBMCs. Peripheral blood mononuclear cells were isolated from LysMCre- I-Ab$^{fl/fl}$ (CRE-, filled circles) and LysMCre+ I-Ab$^{fl/fl}$ (CRE+, open circles) mice 4 months after stereotaxic injection of rAAV2/9 human WT α-synuclein to the SN. Gating strategy presented in Figure 9.A. The frequency and count of MHCII+ cells were measured by surface staining for flow cytometry (see **Panel 4**). Data are plotted as mean +/- standard error of the mean (SEM). P-values are indicated for two-tailed t-test: **p<0.01, ***p<0.001.

3.3c) Immunophenotyping of LysMCre±I-Ab$^{fl/fl}$ following 3 weeks of cypermethrin treatment

In mice that had received unilateral rAAV2/5 human WT α-synuclein, to investigate whether peripheral myeloid deletion of MHCII in the presence or absence of cypermethrin treatment alters general immunophenotype, we analyzed the frequencies and counts of immune cell subsets in the peripheral blood. The frequency of B cells (**Figure 11.A**), T cells (**Figure 11.B**), neutrophils (**Figure 11.C**), and non-neutrophil CD11b+ cells (**Figure 11.D**) did not differ between LysMCre- and LysMCre+I-Ab$^{fl/fl}$ mice, nor did the cell count for each subset. There was no significant difference in the frequency and number of Ly6C-MHCII+ and Ly6C+MHCII cells in LysMCre+I-Ab$^{fl/fl}$ mice relative to Cre- (**Figure 11.E-F**). Injection of the vehicle (corn oil) and cypermethrin treatment affected the frequency and counts of MHCII+ cells such that the ablation of MHCII protein expression observed in the untreated animals (no cypermethrin or vehicle, **Figure 10**), was not detected. Without additional markers, it cannot be confirmed whether this is due to expansion of a CD19-CD3- CD11b+Ly6G- cell subset that expresses MHCII but not LysM, but this conclusion is supported by the fact that the average frequencies of Ly6C-MHCII+ and Ly6C+MHCII+ cells for both LysMCre- and LysMCre+I-Ab$^{fl/fl}$ animals were increased in this experiment relative to the rAAV9 higher-titer experiment.

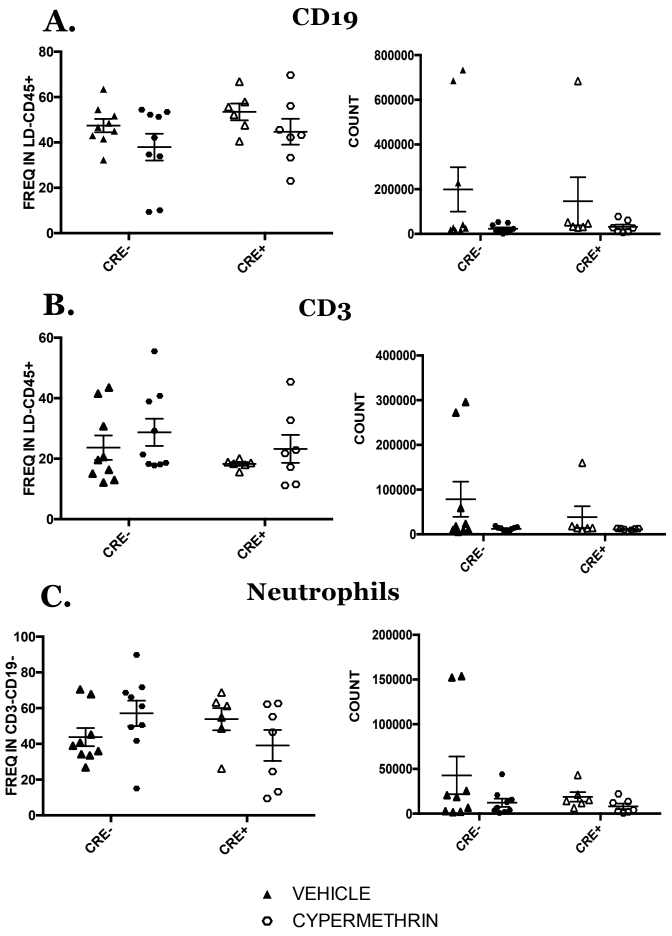

Figure 11.A-C. No difference in MHCII+ cell frequency or number between LysMCre-I-Ab$^{fl/fl}$ and LysMCre+I-Ab$^{fl/fl}$ PBMCs following 3 weeks of cypermethrin or vehicle treatment. Peripheral blood mononuclear cells were isolated from LysMCre- I-Ab$^{fl/fl}$ (CRE-, filled triangles and circles) and LysMCre+ I-Ab$^{fl/fl}$ (CRE+, open triangles and circles) mice 8-9 months after stereotaxic injection of rAAV2/5 human WT α-synuclein to the SN, following 3 weeks of twice-weekly cypermethrin (circles) or vehicle (triangles) treatment. Gating strategy presented in Figure 9.B. Data are plotted as mean +/- standard error of the mean (SEM).

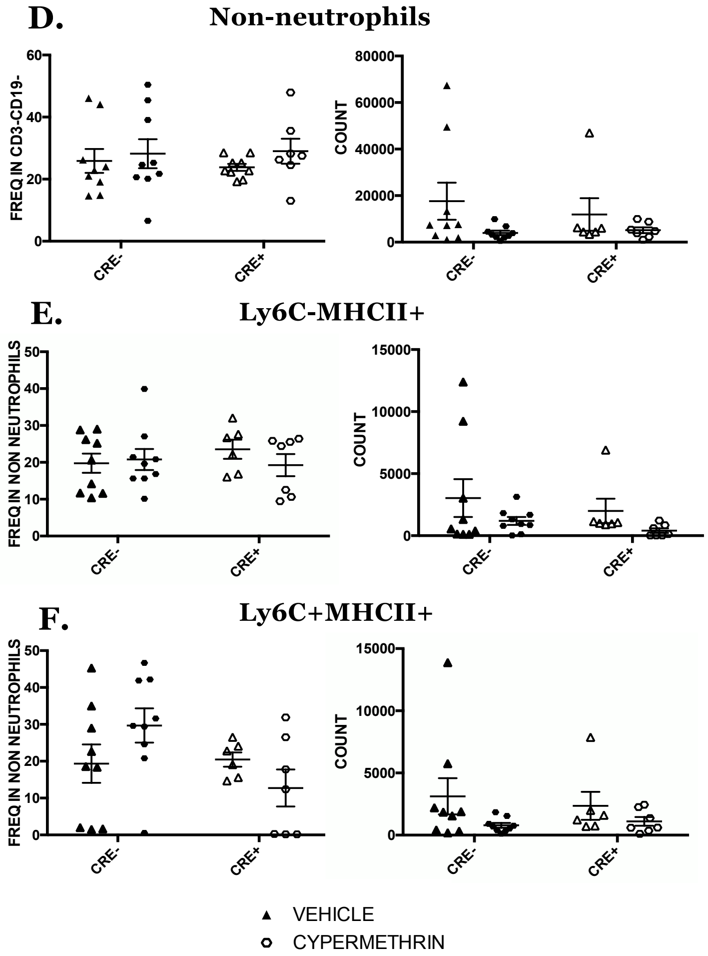

Figure 11.D-F. No difference in MHCII+ cell frequency or number between LysMCre-I-Ab$^{fl/fl}$ and LysMCre+I-Ab$^{fl/fl}$ PBMCs following 3 weeks of cypermethrin or vehicle treatment. Peripheral blood mononuclear cells were isolated from LysMCre- I-Ab$^{fl/fl}$ (CRE-, filled triangles and circles) and LysMCre+ I-Ab$^{fl/fl}$ (CRE+, open triangles and circles) mice 8-9 months after stereotaxic injection of rAAV2/5 human WT α-synuclein to the SN, following 3 weeks of twice-weekly cypermethrin (circles) or vehicle (triangles) treatment. Gating strategy presented in Figure 9.B. The frequency and count of MHCII+ cells were measured by surface staining for flow cytometry (see **Panel 4**). Data are plotted as mean +/- standard error of the mean (SEM).

3.3d) T cell subsets in the peripheral blood and deep cervical lymph nodes of LysMCre±I-Ab$^{fl/fl}$ mice

In an effort to determine the effect of peripheral myeloid MHCII deletion on T cell subset frequency, PBMCs were isolated from LysMCre- and LysMCre+I-Ab$^{fl/fl}$ four months after stereotaxic injection with higher tier rAAV9 human WT α-synuclein to the SN. T cell subsets were identified as described in **Figure 9.B**. We observed a statistically significant decrease in the frequency of Tregs (CD4+Tbet-FoxP3+) in LysMCre+I-Ab$^{fl/fl}$ mice (**Figure 12.D**), which is consistent with the decreases in MHCII expression reported in **Figure 10.E-F**, given that CD4+ T cell activation and differentiation is dependent on antigen presentation via MHCII. Similarly, the statistically significant decreases in the frequencies of effector memory (chronically activated, CD4+CD44+CD62L-) and central memory (CD4+CD44+CD62L+) and increased naïve CD4+ T cell frequency (CD4+CD44-CD62L+) is consistent with the decreased MHCII expression on LysMCre+I-Ab$^{fl/fl}$ myeloid subsets.

The deep cervical lymph nodes are the central nervous system-draining lymph nodes. In immune cells isolated from these small structures, we report a decreased frequency of CD4+ effector memory (CD4+ Cd44+CD62L-, **Figure 13.F**). The CD4+ T cell population shifts present in LysMCre+I-Ab$^{fl/fl}$ PBCMs but not deep cervical lymph nodes suggest peripheral myeloid deletion of MHCII has a tissue-dependent effect on CD4 T cell frequencies.

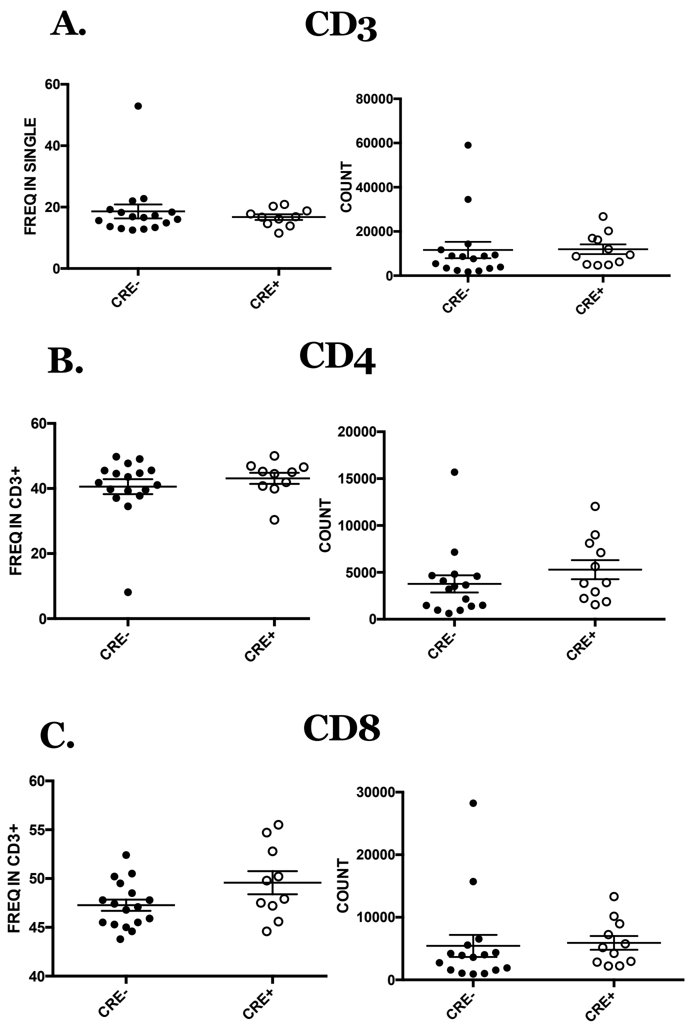

Figure 12.A-C. CD4+ T cell subsets are affected by LysMCre-mediated deletion of MHCII. Peripheral blood mononuclear cells were isolated from LysMCre- I-Ab$^{fl/fl}$ (CRE-, filled) and LysMCre+ I-Ab$^{fl/fl}$ (CRE+, open) mice 4 months after stereotaxic injection of rAAV2/9 human WT α-synuclein to the SN. Gating strategy presented in Figure 9B. The frequency and count of T cell subsets were measured by surface staining for flow cytometry using the markers listed in **Panel 3**. Data are plotted as mean +/- standard error of the mean (SEM).

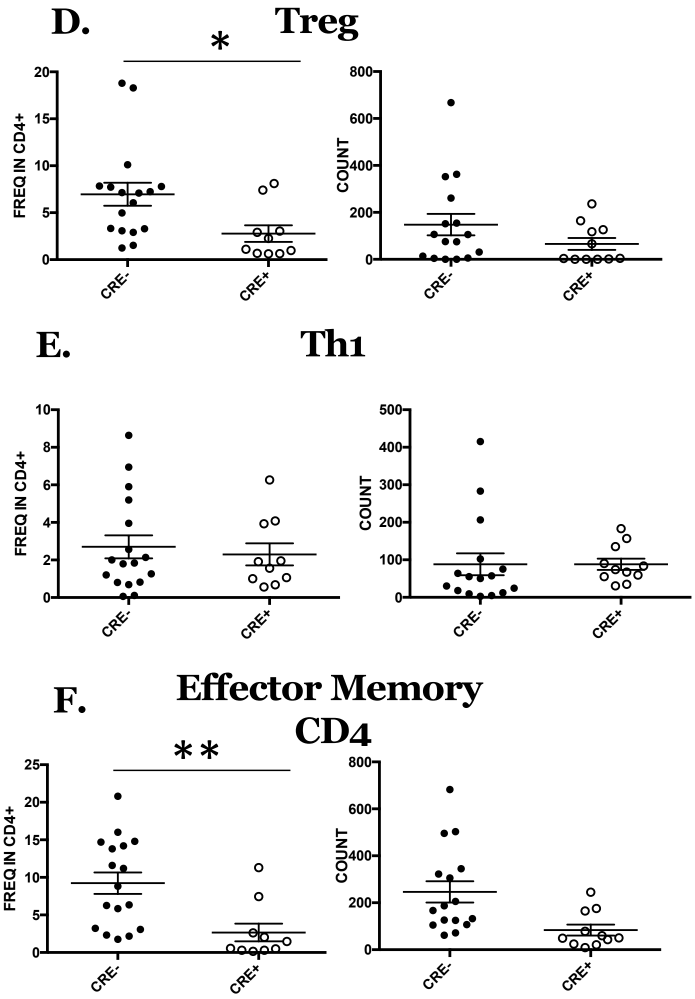

Figure 12.D-F. CD4+ T cell subsets are affected by LysMCre-mediated deletion of MHCII. Peripheral blood mononuclear cells were isolated from LysMCre- I-Ab$^{fl/fl}$ (CRE-, filled) and LysMCre+ I-Ab$^{fl/fl}$ (CRE+, open) mice 4 months after stereotaxic injection of rAAV2/9 human WT α-synuclein to the SN. Gating strategy presented in Figure 9B. The frequency and count of T cell subsets were measured by surface staining for flow cytometry using the markers listed in **Panel 3**. Data are plotted as mean +/- standard error of the mean (SEM). P-values are indicated for two-tailed t-test: *p<0.05, **p<0.01, ***p<0.001.

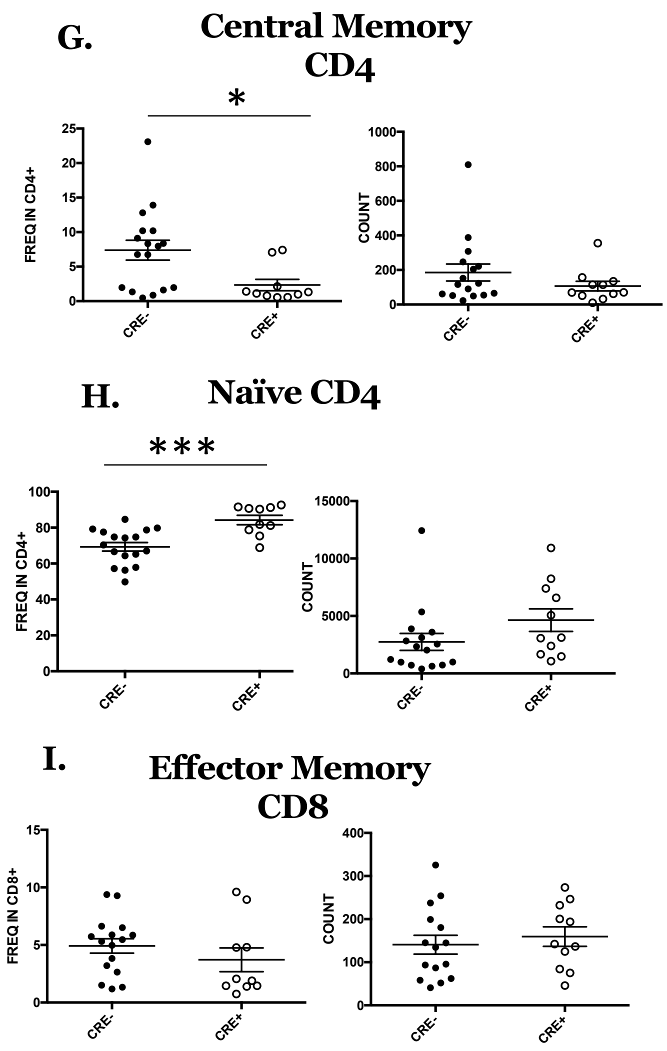

Figure 12.G-I. CD4+ T cell subsets are affected by LysMCre-mediated deletion of MHCII. Peripheral blood mononuclear cells were isolated from LysMCre- I-Ab$^{fl/fl}$ (CRE-, filled) and LysMCre+ I-Ab$^{fl/fl}$ (CRE+, open) mice 4 months after stereotaxic injection of rAAV2/9 human WT α-synuclein to the SN. Gating strategy presented in Figure 9B. The frequency and count of T cell subsets were measured by surface staining for flow cytometry using the markers listed in **Panel 3**. Data are plotted as mean +/- standard error of the mean (SEM). P-values are indicated for two-tailed t-test: *p<0.05, **p<0.01, ***p<0.001.

J. Central Memory CD8

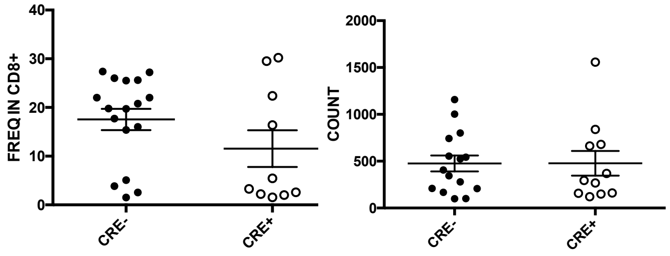

K. Naïve CD8

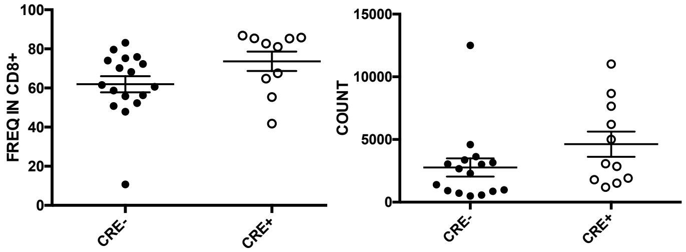

Figure 12.J-K. CD4+ T cell subsets are affected by LysMCre-mediated deletion of MHCII. Peripheral blood mononuclear cells were isolated from LysMCre- I-Ab$^{fl/fl}$ (CRE-, filled) and LysMCre+ I-Ab$^{fl/fl}$ (CRE+, open) mice 4 months after stereotaxic injection of rAAV2/9 human WT α-synuclein to the SN. Gating strategy presented in Figure 9B. The frequency and count of T cell subsets were measured by surface staining for flow cytometry using the markers listed in **Panel 3**. Data are plotted as mean +/- standard error of the mean (SEM). P-values are indicated for two-tailed t-test: $^{*}p<0.05$, $^{**}p<0.01$, $^{***}p<0.001$.

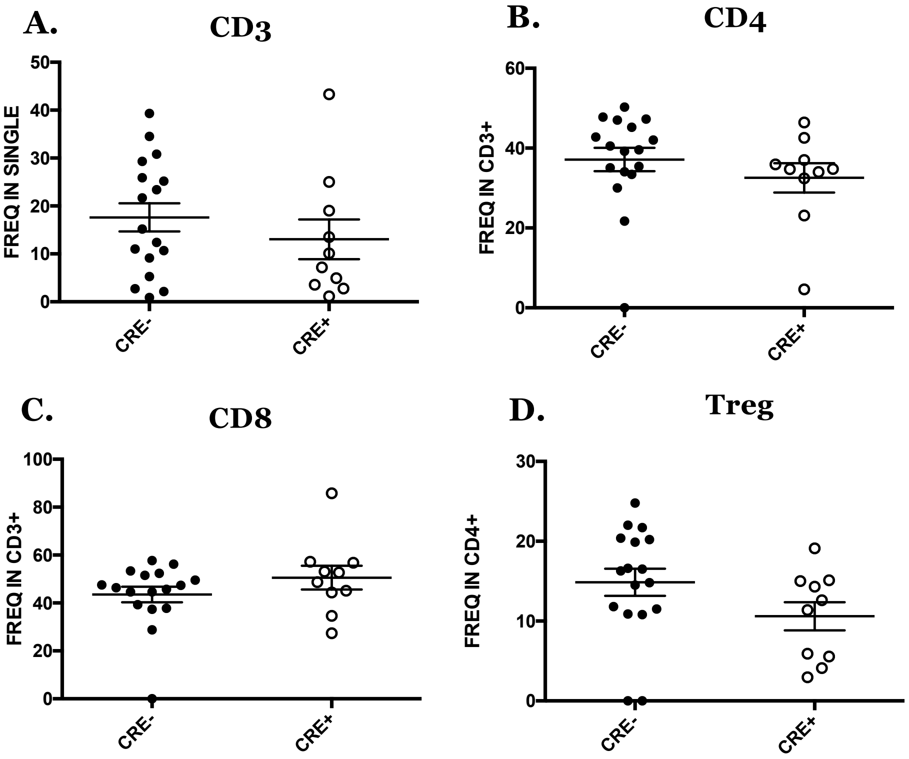

Figure 13.A-D The frequency of effector memory CD4+ T cells in mouse deep cervical lymph nodes is affected by LysMCre-mediated deletion of MHCII. Immune cells from the left and right deep cervical lymph nodes were isolated from LysMCre- I-Ab$^{fl/fl}$ (CRE-, filled) and LysMCre+ I-Ab$^{fl/fl}$ (CRE+, open) mice 4 months after stereotaxic injection of rAAV2/9 human WT α-synuclein to the SN. Gating strategy presented in Figure 9B. The frequency and count of T cell subsets were measured by surface staining for flow cytometry using the markers listed in **Panel 3**. Data are plotted as mean +/- standard error of the mean (SEM). P-values are indicated for two-tailed t-test: $*p<0.05$.

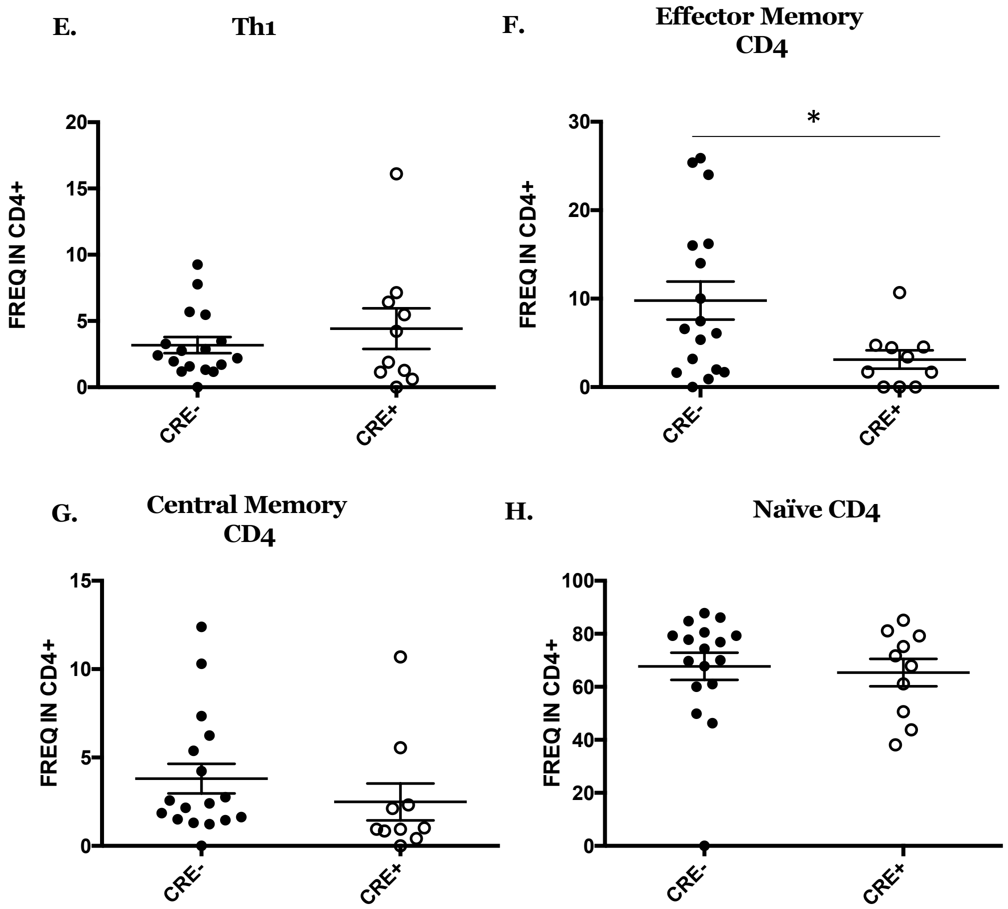

Figure 13.E-H. The frequency of effector memory CD4+ T cells in mouse deep cervical lymph nodes is affected by LysMCre-mediated deletion of MHCII. Immune cells from the left and right deep cervical lymph nodes were isolated from LysMCre- I-Ab$^{fl/fl}$ (CRE-, filled) and LysMCre+ I-Ab$^{fl/fl}$ (CRE+, open) mice 4 months after stereotaxic injection of rAAV2/9 human WT α-synuclein to the SN. Gating strategy presented in Figure 8A. The frequency and count of T cell subsets were measured by surface staining for flow cytometry using the markers listed in **Panel 3**. Data are plotted as mean +/- standard error of the mean (SEM). P-values are indicated for two-tailed t-test: *p<0.05.

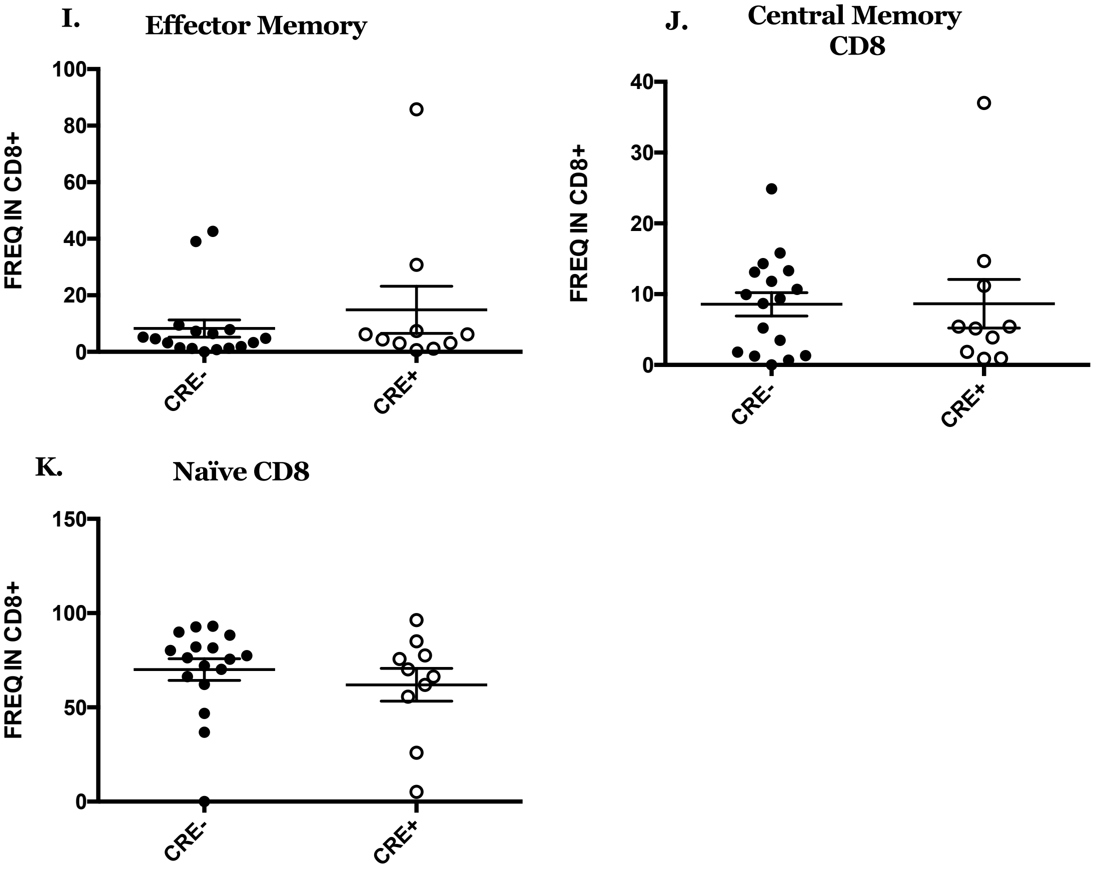

Figure 13.I-K The frequency of effector memory CD4+ T cells in mouse deep cervical lymph nodes is affected by LysMCre-mediated deletion of MHCII. Immune cells from the left and right deep cervical lymph nodes were isolated from LysMCre- I-Ab$^{fl/fl}$ (CRE-, filled) and LysMCre+ I-Ab$^{fl/fl}$ (CRE+, open) mice 4 months after stereotaxic injection of rAAV2/9 human WT α-synuclein to the SN. Gating strategy presented in Figure 8A. The frequency and count of T cell subsets were measured by surface staining for flow cytometry using the markers listed in **Panel 3**. Data are plotted as mean +/- standard error of the mean (SEM). P-values are indicated for two-tailed t-test: *p<0.05.

3.3e) T cell subsets of LysMCre±I-Ab$^{fl/fl}$ mice following 3 weeks of cypermethrin treatment

The pyrethroid cypermethrin is a commonly used household pesticide. Because pyrethroid exposure is known to compromise DA neuron health (Singh et al., 2012a) and exposure synergizes as an environmental risk factor with a common variant in the gene for MHCII (Kannarkat et al., 2015), we set out to determine the immunological impact of cypermethrin treatment on mouse immune cells *in vivo*, within the context of an ongoing α-synuclein burden. T cell subsets were identified as described in **Figure 8.A**. In the PBMC samples, we observed a statistically significant effect interaction between genotype and cypermethrin treatment on the frequency of CD3+ T cells, as well as specifically in the Treg population (CD4+Tbet-FoxP3, **Figure 14.D**). Cypermethrin treatment, regardless of genotype, was associated with a decreased frequency of effector memory CD4+ T cells (CD4+ Cd44+CD62L-, **Figure 14.F**) The LysMCre+I-Ab$^{fl/fl}$ genotype was associated with an increased frequency of naïve CD4+ T cells (CD4+CD44-CD62L+), matching what was observed in the absence of cypermethrin or vehicle treatment in the rAAV2/9 higher titer study (**Figure 12.H**).

In the deep cervical lymph nodes, we report a decreased frequency of CD3+ T cells in LysMCre+I-Ab$^{fl/fl}$ mice (**Figure 15.A**). There was also a statistically significant interaction between LysMCre genotype and exposure to cypermethrin affecting the frequency of central memory CD4+ T cells in the deep cervical lymph nodes (**Figure 15.G**).

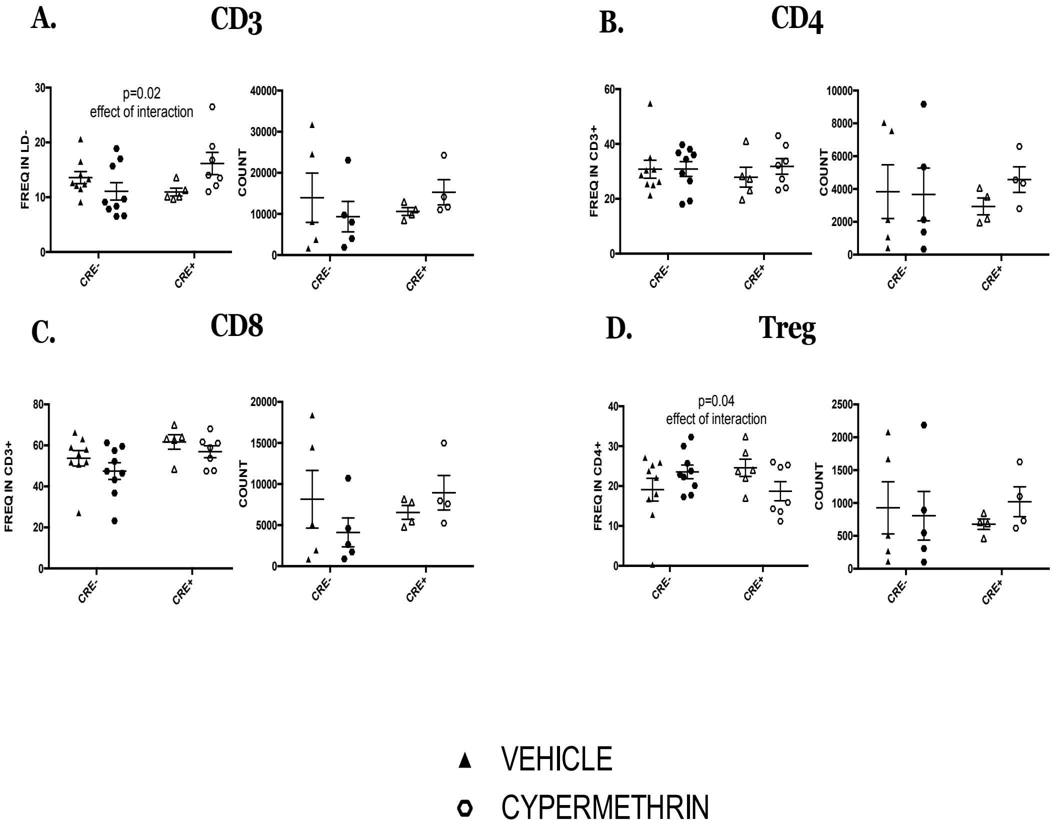

Figure 14A-D. Cypermethrin and LysMCre genotype affect PBMC T cell frequencies. Peripheral blood mononuclear cells were isolated from LysMCre- I-Ab$^{fl/fl}$ (CRE-, filled) and LysMCre+ I-Ab$^{fl/fl}$ (CRE+, open) mice 8-9 months after stereotaxic injection of rAAV2/5 human WT α-synuclein to the SN. Gating strategy presented in Figure 8.A. The frequency and count of T cell subsets was measured by surface staining for flow cytometry with intracellular staining for FoxP3 (see **Panel 3**). Data are plotted as mean +/- standard error of the mean (SEM). P-values are indicated above applicable graphs.

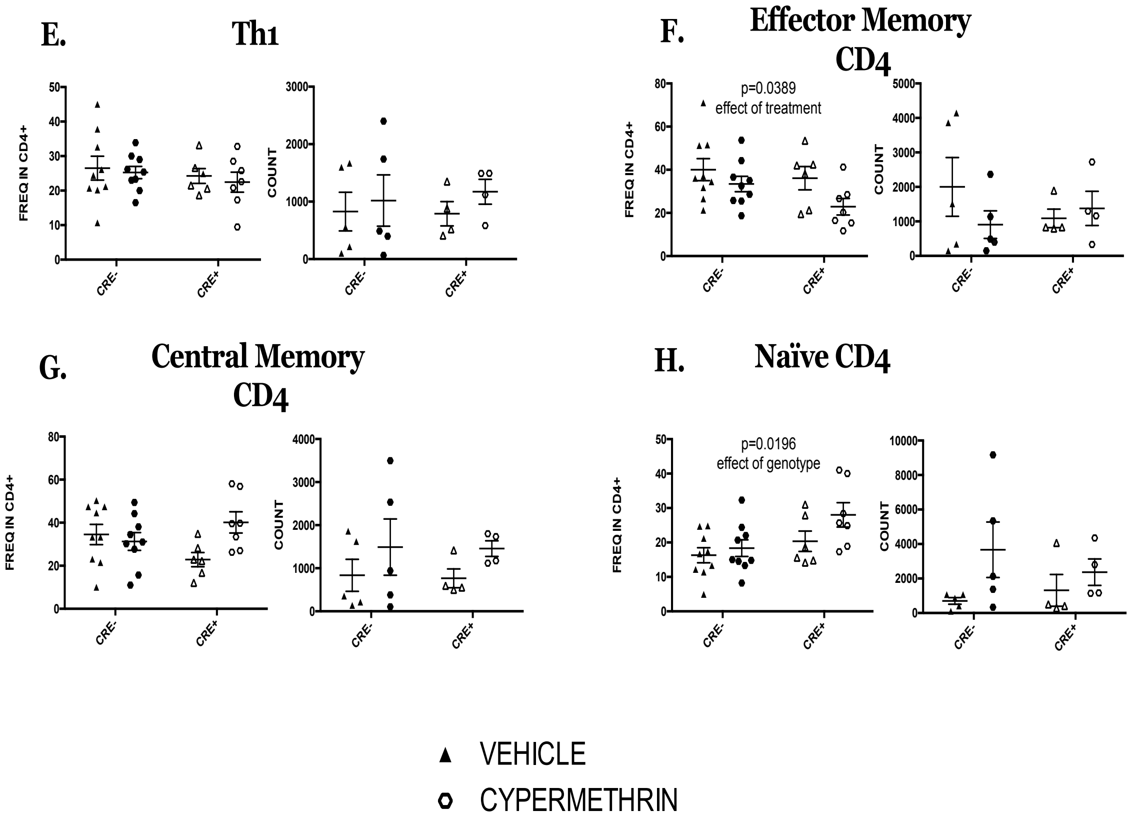

Figure 14E-H. Cypermethrin and LysMCre genotype affect PBMC T cell frequencies. Peripheral blood mononuclear cells were isolated from LysMCre- I-Ab$^{fl/fl}$ (CRE-, filled) and LysMCre+ I-Ab$^{fl/fl}$ (CRE+, open) mice 8-9 months after stereotaxic injection of rAAV2/5 human WT α-synuclein to the SN. Gating strategy presented in Figure 8.A. The frequency and count of T cell subsets was measured by surface staining for flow cytometry with intracellular staining for FoxP3 (see **Panel 3**). Data are plotted as mean +/- standard error of the mean (SEM). P-values are indicated above applicable graphs.

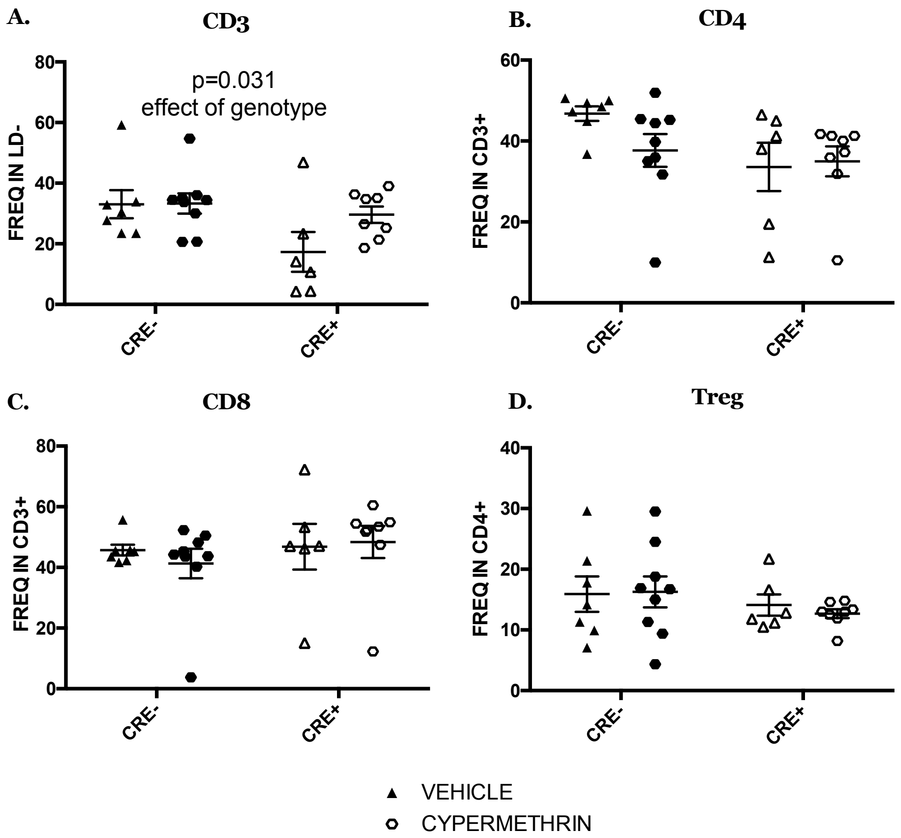

Figure 15.A-D. Cypermethrin and LysMCre genotype affect the frequency of total T cells and central memory CD4s in the deep cervical lymph nodes. Immune cells were isolated from the deep cervical lymph nodes of LysMCre-I-Ab$^{fl/fl}$ (CRE-, filled) and LysMCre+ I-Ab$^{fl/fl}$ (CRE+, open) mice 8-9 months after stereotaxic injection of rAAV2/5 human WT α-synuclein to the SN. Gating strategy presented in Figure 8.A. The frequency and count of T cell subsets was measured by surface staining for flow cytometry with intracellular staining for FoxP3 (see **Panel 3**). Data are plotted as mean +/- standard error of the mean (SEM). P-values are indicated above applicable graphs.

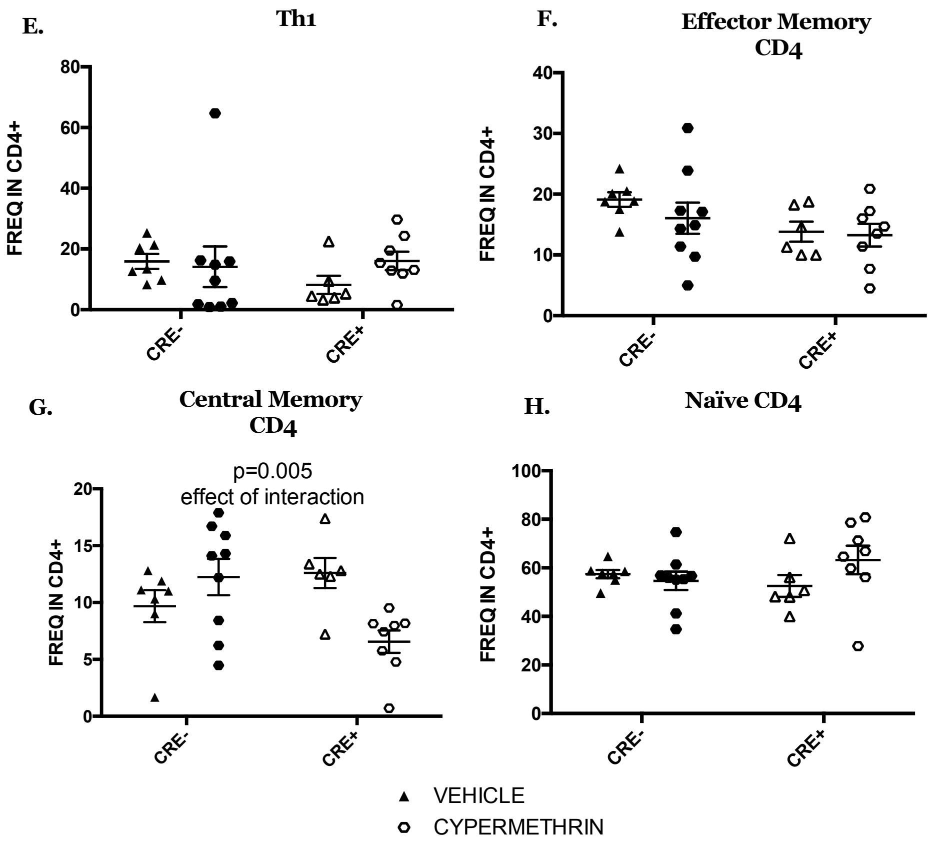

Figure 15.E-F. Cypermethrin and LysMCre genotype affect the frequency of total T cells and central memory CD4s in the deep cervical lymph nodes. Immune cells were isolated from the deep cervical lymph nodes of LysMCre-I-Ab$^{fl/fl}$ (CRE-, filled) and LysMCre+ I-Ab$^{fl/fl}$ (CRE+, open) mice 8-9 months after stereotaxic injection of rAAV2/5 human WT α-synuclein to the SN. Gating strategy presented in Figure 8.A. The frequency and count of T cell subsets was measured by surface staining for flow cytometry with intracellular staining for FoxP3 (see **Panel 3**). Data are plotted as mean +/- standard error of the mean (SEM). P-values are indicated above applicable graphs.

3.3f) LysMCre±I-Ab$^{fl/fl}$ mice do not differ in plasma levels of inflammatory cytokines 4 months post-rAAV2/9 human WT α-synuclein injection.

We investigated the circulating levels of cytokines and chemokines in order to determine whether there are any effects of peripheral myeloid MHCII deletion on systemic inflammation. The levels of immunomodulatory cytokines and chemokines were assessed via multiplexed chemiluminescent immunoassay (**Figure 16**). LysMCre- and LysMCre+I-Ab$^{fl/fl}$ did not differ in their plasma levels of IFNγ, IL-10, IL-1β, IL-2, IL-5, IL-6, CXCL1, and TNF.

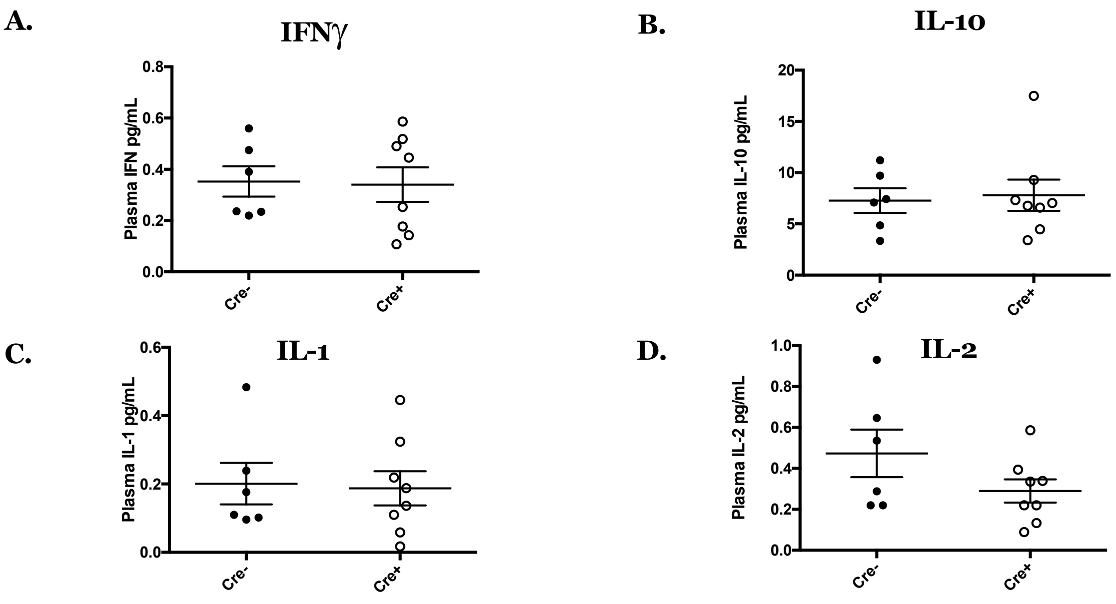

Figure 16. A-D. Plasma cytokine and chemokine levels do not differ between LysMCre- and LysMCre+I-Ab$^{fl/fl}$ mice. Mesoscale Discovery (MSD) Multi-Array immunoassay technology measured the levels of the indicated cytokines and CXCL1 in plasma. Data are plotted as mean +/- standard error of the mean (SEM).

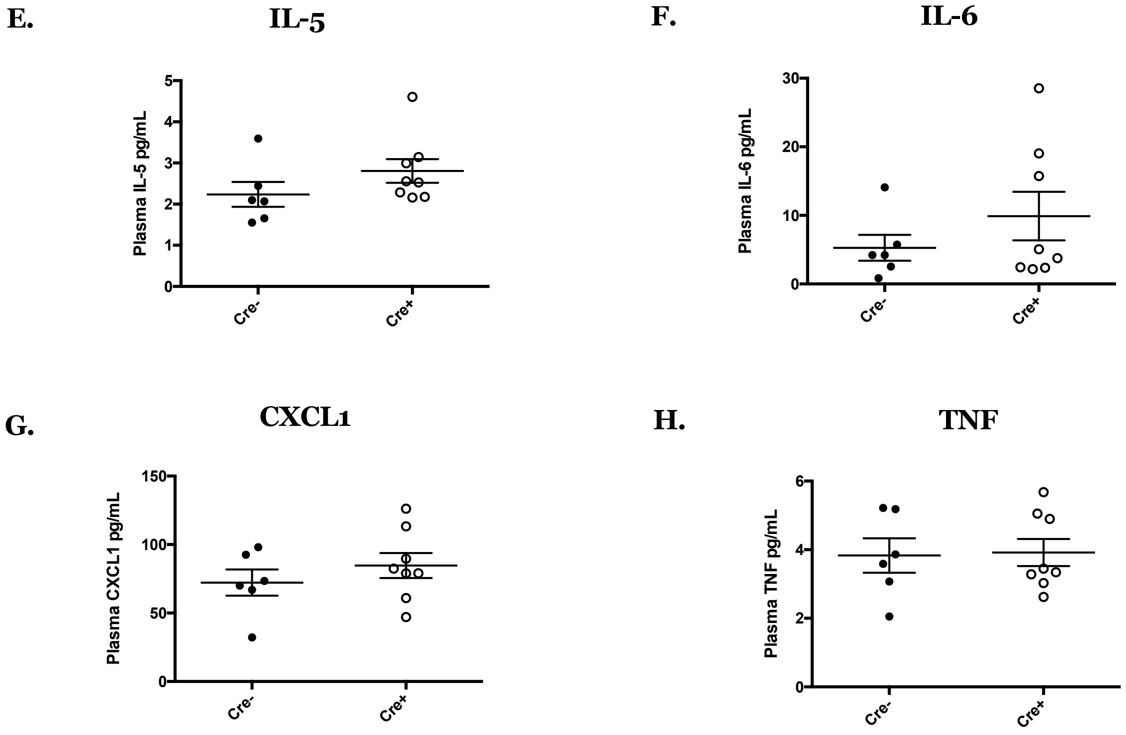

Figure 16. E-F. Plasma cytokine and chemokine levels do not differ between LysMCre- and LysMCre+I-Ab$^{fl/fl}$ mice. Mesoscale Discovery (MSD) Multi-Array immunoassay technology measured the levels of the indicated cytokines and CXCL1 in plasma. Data are plotted as mean +/- standard error of the mean (SEM).

3.3g) Cypermethrin treatment increases plasma IL-1β **in LysMCre+I-Ab$^{fl/fl}$ mice.**

To understand the immune effects of acute treatment with cypermethrin, plasma cytokines and chemokines were assessed via multiplexed chemiluminescent immunoassay (**Figure 17**). LysMCre- and LysMCre+I-Ab$^{fl/fl}$ did not differ in their plasma levels of IFNγ, IL-10, IL-2, IL-5, IL-6, CXCL1 , and

TNF, but there was an interaction between genotype and treatment affecting IL-1β (**Figure 17.C**).

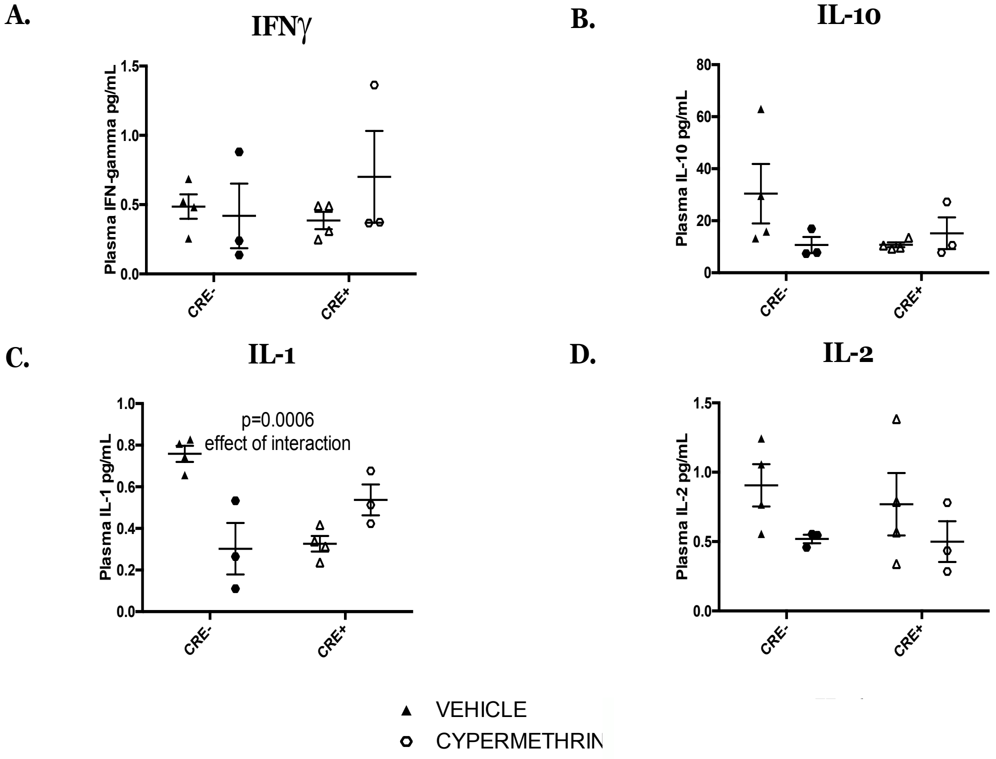

Figure 17.A-D. Plasma IL-1β levels increase with cypermethrin treatment in LysMCre+I-Ab$^{fl/fl}$ mice. Mesoscale Discovery (MSD) Multi-Array immunoassay technology measured the levels of the indicated cytokines and CXCL1 in plasma isolated from LysMCre- (closed triangles and circles) and LysmCre+ (open triangles and circles) I-Ab$^{fl/fl}$ mice. Treatment with corn oil vehicle (triangles) or cypermethrin (circles) interacted with LysMCre genotype, affecting IL-1β levels. Data are plotted as mean +/- standard error of the mean (SEM). P-values are indicated above applicable graph.

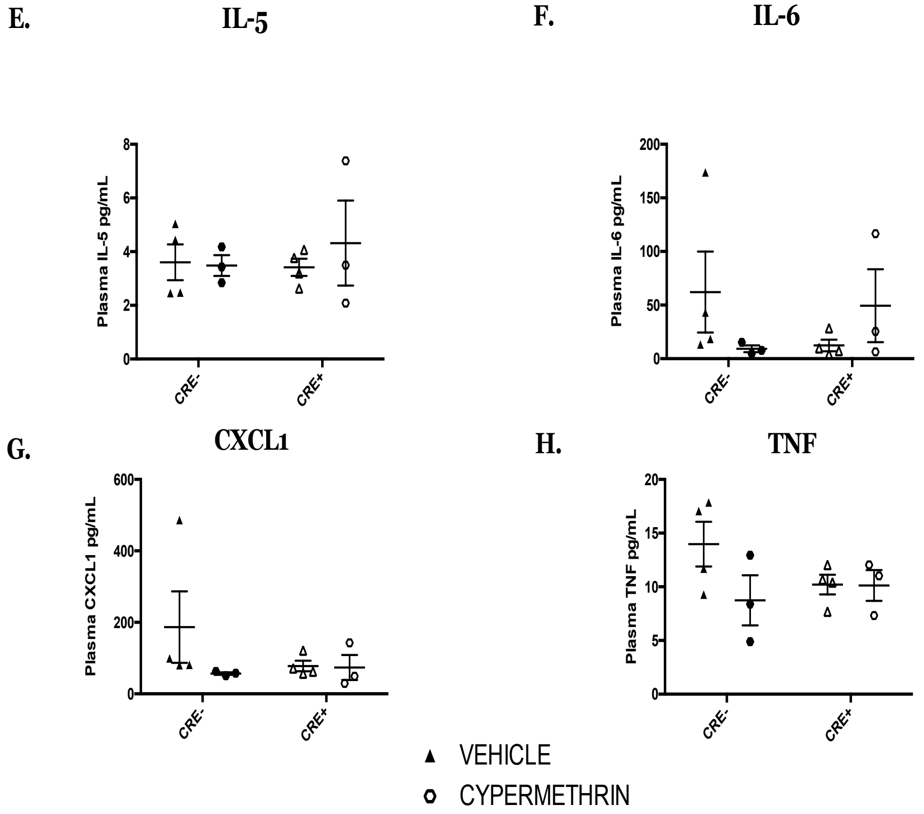

Figure 17.E-H. Plasma IL-1β levels increase with cypermethrin treatment in LysMCre+I-Ab$^{fl/fl}$ mice. Mesoscale Discovery (MSD) Multi-Array immunoassay technology measured the levels of the indicated cytokines and CXCL1 in plasma isolated from LysMCre- (closed triangles and circles) and LysmCre+ (open triangles and circles) I-Ab$^{fl/fl}$ mice. Treatment with corn oil vehicle (triangles) or cypermethrin (circles) interacted with LysMCre genotype, affecting IL-1β levels. Data are plotted as mean +/- standard error of the mean (SEM). P-values are indicated above applicable graph.

3.3h) Demonstration of human α-synuclein expression in the SN following viral vector injection

Unilateral intranigral injection of higher titer rAAV2/9 human WT α-synuclein or rAAV2/5 human WT α-synuclein was performed in young adult male LysMCre- and LysMCre+I-Ab$^{fl/fl}$ mice. Immunofluorescent staining was performed to confirm the proper targeting and expression of human α-synuclein to the left SN. Representative images illustrate the presence of α-synuclein within and adjacent to TH-immunoreactive neurons. For both rAAV2/9 and rAAV2/5, the absence of human α-synuclein immunoreactivity on the uninjected side suggests virus did not cross midline.

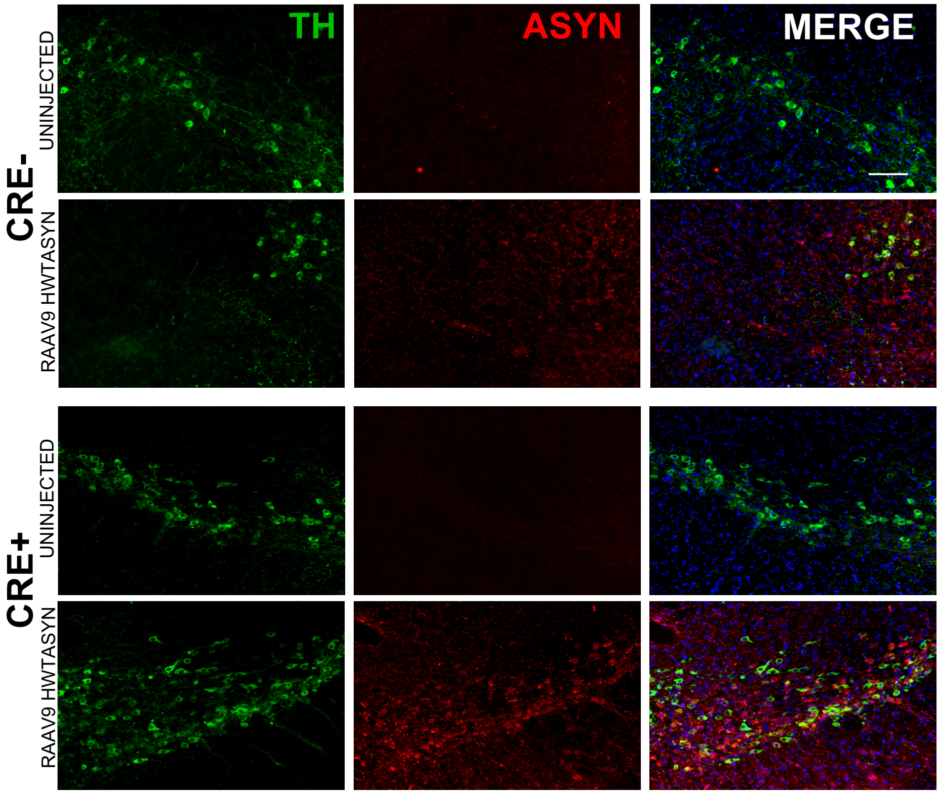

Figure 18. Targeting of rAAV2/9 human WT α-synuclein to the mouse substantia nigra. Human WT α-synuclein (ASYN, red) is expressed in the substantia nigra 4 months after unilateral rAAV2/9-human WT α-synuclein injection. Immunofluorescent staining of α-synuclein, tyrosine hydroxylase (TH, green), and DAPI (blue). Images of LysMcre-I-Ab$^{fl/fl}$ (CRE-, top) and LysMCre+I-Ab$^{fl/fl}$ (CRE+, bottom) 40μm-thick slices were taken at 20x. Scale bar = 100μm.

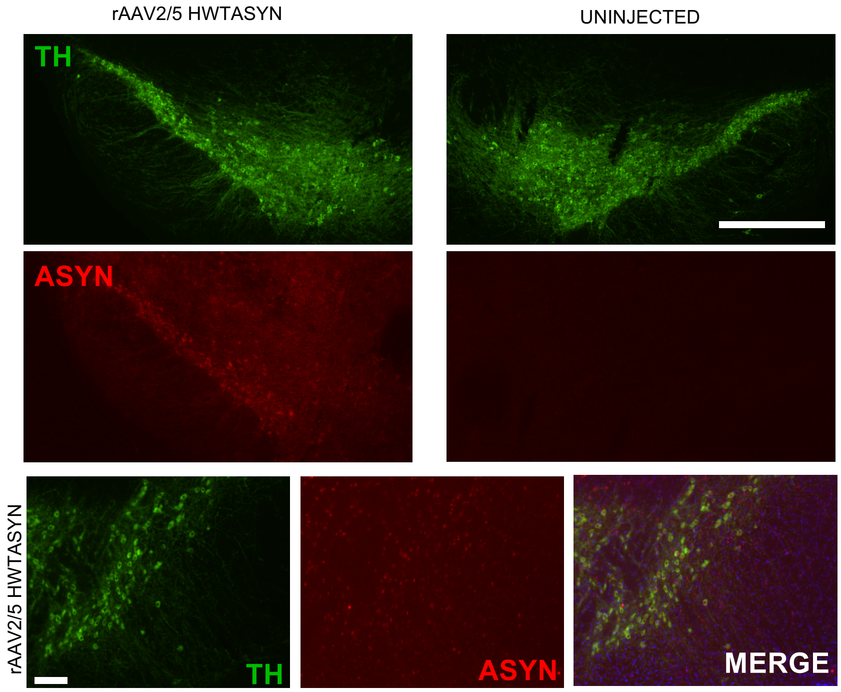

Figure 19. Targeting of rAAV2/5 human WT α-synuclein to the mouse substantia nigra. Human WT α-synuclein (ASYN, red) is expressed in the substantia nigra 8 months after unilateral rAAV2/9-human WT α-synuclein injection in a Cre- mouse. Immunofluorescent staining of α-synuclein, tyrosine hydroxylase (TH, green). 40μm-thick slices were taken at 4x (top) and 10x (bottom row). Scale bar=0.25mm top right, 30μm bottom left.

3.3i) Inflammatory gene expression in the striatum 4 months after nigral rAAV2/9 human WT α-synuclein injection

Having confirmed expression of human WT α-synuclein via immunofluorescent staining in DA neuron soma, we then investigated the transcriptional levels of several immune markers in order to characterize the inflammatory status of the striatum, where nigral DA neurons terminate. RT-PCR was performed to detect transcript levels of human α-synuclein, surface makers of immune cells (CD4, MHCII, MHCI), intracellular markers (iNOS, CD68), and the immune signals TNF, CCL2, IFNγ, IL-6, and IL-1β. In both LysMCre- and LysMCre+I-Ab$^{fl/fl}$, we observed a positive fold change for human α-synuclein mRNA for all animals (striatum ipsilateral to nigral injection divided by contralateral striatum), indicating α-synuclein mRNA from the rAAV2/9 virus was present in the striatum. There were no statistically significant effects of either the viral injection or LysMCre genotype on CD4, TNF, CCL2, MHCII, MHCI, and IL-1β mRNA level. The striatum ipsilateral to the rAAV2/9 human WT α-synuclein injection had increased CD68 (lysosomal marker) gene expression in both LysMCre- and LysMCre+I-Ab$^{fl/fl}$ mice (**Figure 20.F**), suggesting an increase in phagocytosis in the presence of human WT α-synuclein. LysMCre+I-Ab$^{fl/fl}$ animals displayed increased iNOS levels in both striatal hemispheres relative to LysMCre-I-Ab$^{fl/fl}$ mice, suggesting peripheral myeloid MHCII deletion has an effect on immune nitrosative stress-related gene expression in the brain.

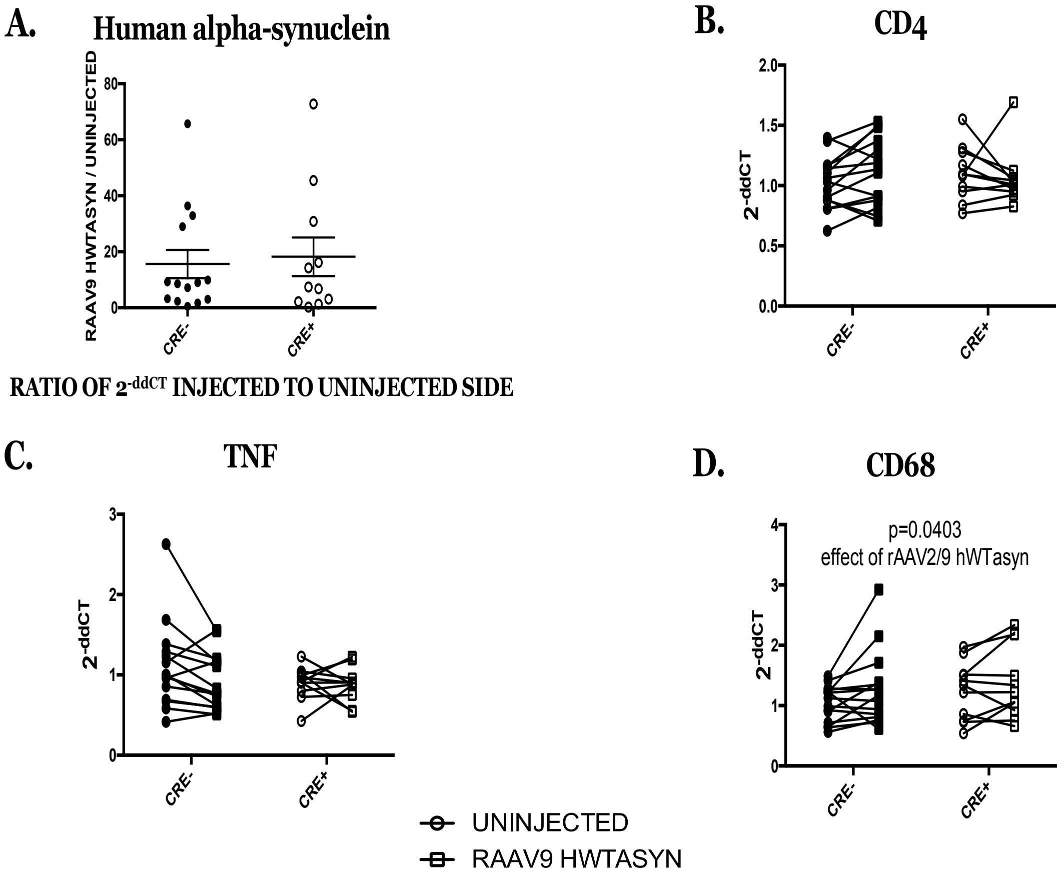

Figure 20.A-D Inflammatory gene expression in the striatum 4 months after nigral rAAV2/9 human WT α-synuclein injection. RNA isolated from striatum. Gene expression was quantified relative to GAPDH with RT-PCR. P-values indicated above applicable graphs.

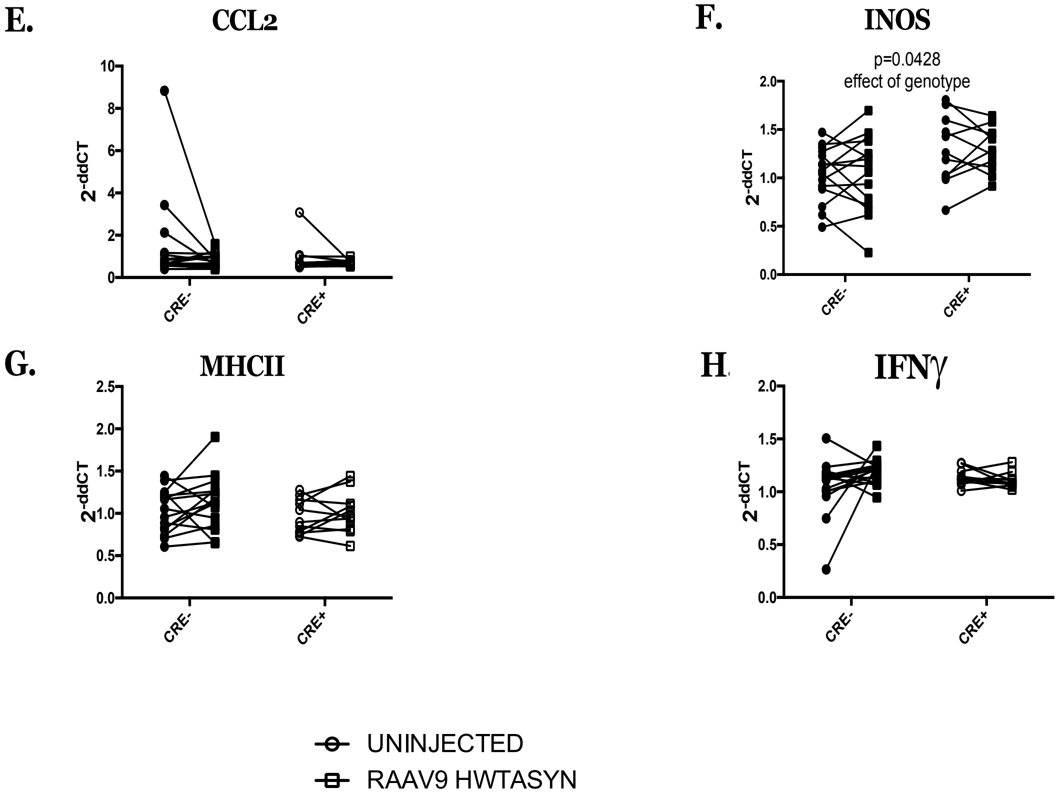

Figure 20.E-H Inflammatory gene expression in the striatum 4 months after nigral rAAV2/9 human WT α-synuclein injection. RNA isolated from striatum. Gene expression was quantified relative to GAPDH with RT-PCR. P-values indicated above applicable graphs.

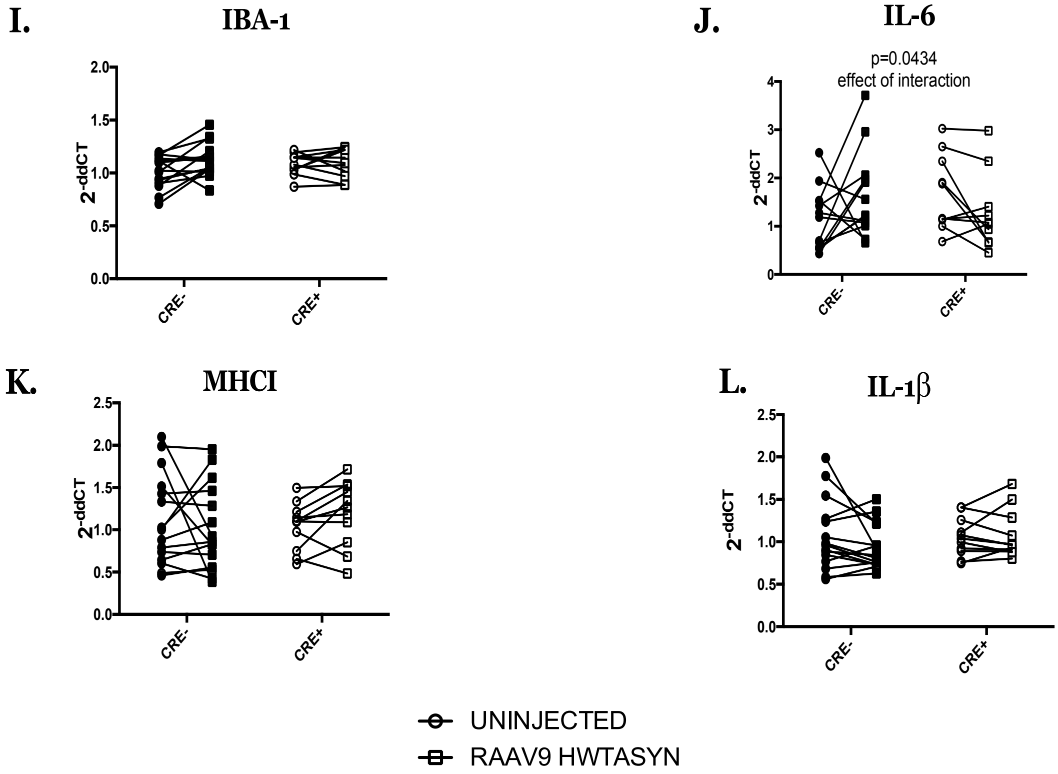

Figure 20.I-L Inflammatory gene expression in the striatum 4 months after nigral rAAV2/9 human WT α-synuclein injection. RNA isolated from striatum. Gene expression was quantified relative to GAPDH with RT-PCR. P-values indicated above applicable graphs.

3.3j) Assessment of striatal dopaminergic terminals 4 months after rAAV2/9 human WT α-synuclein injection

The loss of tyrosine hydroxylase expression in the striatum following nigral rAAV2/9 human WT α-synuclein in mice has been reported elsewhere (Castro-Sanchez et al., 2018). Here, we confirmed that in our hands, at a titer of $2.1x10^{12}$, DA neuron phenotype of the striatum was compromised, as indicated by a significant decrease in dopamine transporter (DAT) protein expression (**Figure 21.B**) in both LysMCre-I-$Ab^{fl/fl}$ mice. While DAT protein indicates a lesion was produced by the virus, the expression of tyrosine hydroxylase (TH) is informative as well as it catalyzes the rate-limiting step of dopamine neurotransmitter synthesis. TH protein expression was significantly decreased by rAAV2/9 human WT α-synuclein in LysMCre- but not LysMCre+I-$Ab^{fl/fl}$ mice. These data suggest deletion of peripheral myeloid MHCII deletion is associated with maintenance of DA neuron phenotype (DAT and TH expression, capacity to synthesize dopamine) despite ongoing α-synuclein burden in mice with peripheral myeloid deletion of MHCII.

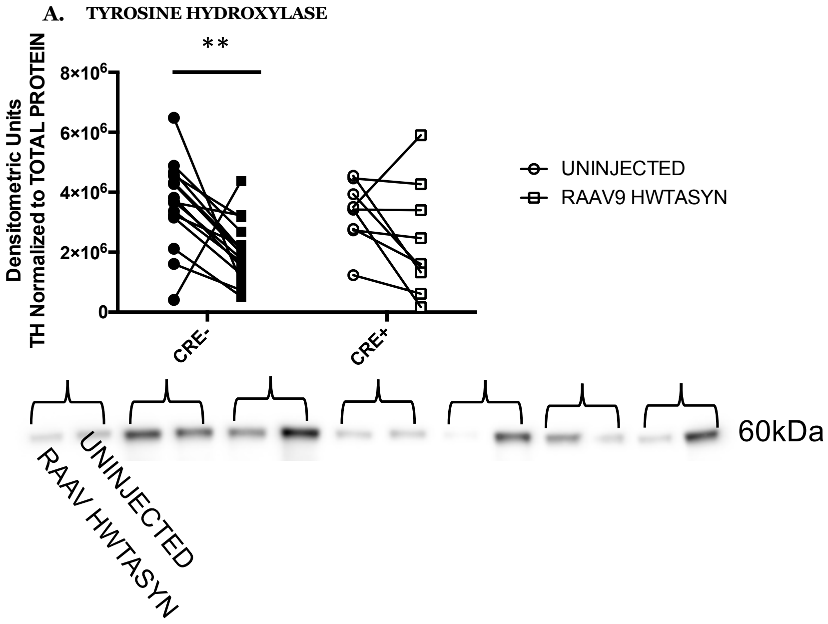

Figure 21.A. Tyrosine hydroxylase protein expression is decreased ipsilateral to rAAV2/9 human WT α-synuclein injection in LysMCre-I-Ab$^{fl/fl}$ striatum. Soluble protein lysates from the left (RAAV9 HWTASYN, squares) and right (UNINJECTED, circles) striatal tissues LysMCre- and LysMCre+I-Ab$^{fl/fl}$ (filled and open shapes, respectively) were analyzed for protein levels of TH (**A**), normalized to total protein identified by REVERT stain. Data are plotted to show the paired striatal samples for each animal. P-values for post-hoc comparisons are indicated (**p<0.01).

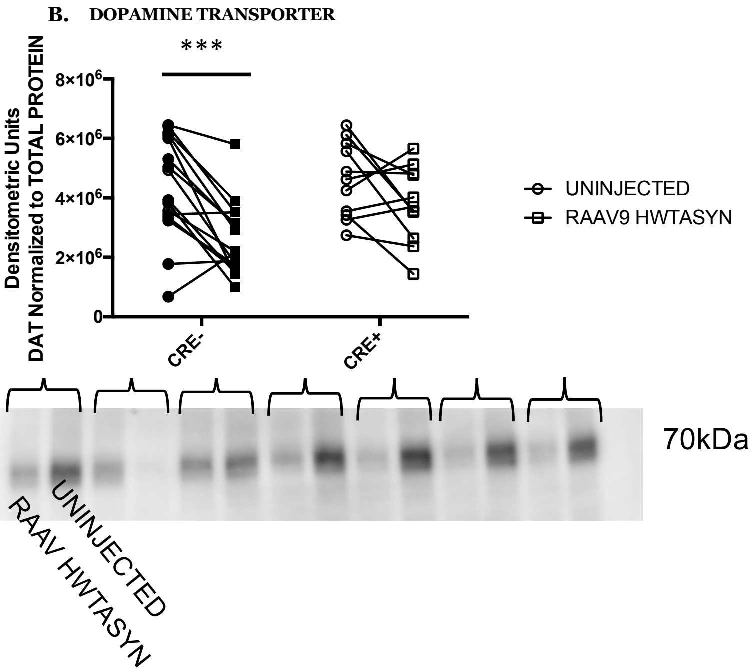

Figure 21.B. Dopamine transporter protein expression is decreased ipsilateral to rAAV2/9 human WT α-synuclein injection in LysMCre-I-Ab$^{fl/fl}$ striatum. Soluble protein lysates from the left (RAAV9 HWTASYN, squares) and right (UNINJECTED, circles) striatal tissues LysMCre- and LysMCre+I-Ab$^{fl/fl}$ (filled and open shapes, respectively) were analyzed for protein levels of DAT (**B**), normalized to total protein identified by REVERT stain. Data are plotted to show the paired striatal samples for each animal. P-values for post-hoc comparisons are indicated (***p<0.001).

3.3k) Short-term cypermethrin exposure does not decrease tyrosine hydroxylase or dopamine transporter protein expression, even in the presence of human WT α-synuclein

The loss of tyrosine hydroxylase expression in the striatum following nigral rAAV2/5 human WT α-synuclein in mice has been reported elsewhere in rats (Gorbatyuk et al., 2008; Febbraro et al., 2013; Gombash et al., 2013). Here, we found that, at a titer of 2.9×10^{11}, DA neuron phenotype of the striatum was not affected by human WT α-synuclein at the ~10month post-injection time point (**Figure 22**) in both LysMCre- and LysMCre+I-Ab$^{fl/fl}$ mice. While DAT protein indicates a lesion was produced by the virus, the expression of tyrosine hydroxylase (TH) is informative as well as it catalyzes the rate-limiting step of dopamine neurotransmitter synthesis. TH protein expression was significantly decreased by rAAV9 human WT α-synuclein in LysMCre- but not LysMCre+I-Ab$^{fl/fl}$ mice. These data suggest deletion of peripheral myeloid MHCII is associated with maintenance of DA neuron phenotype (TH expression, capacity to synthesize dopamine) despite ongoing α-synuclein burden.

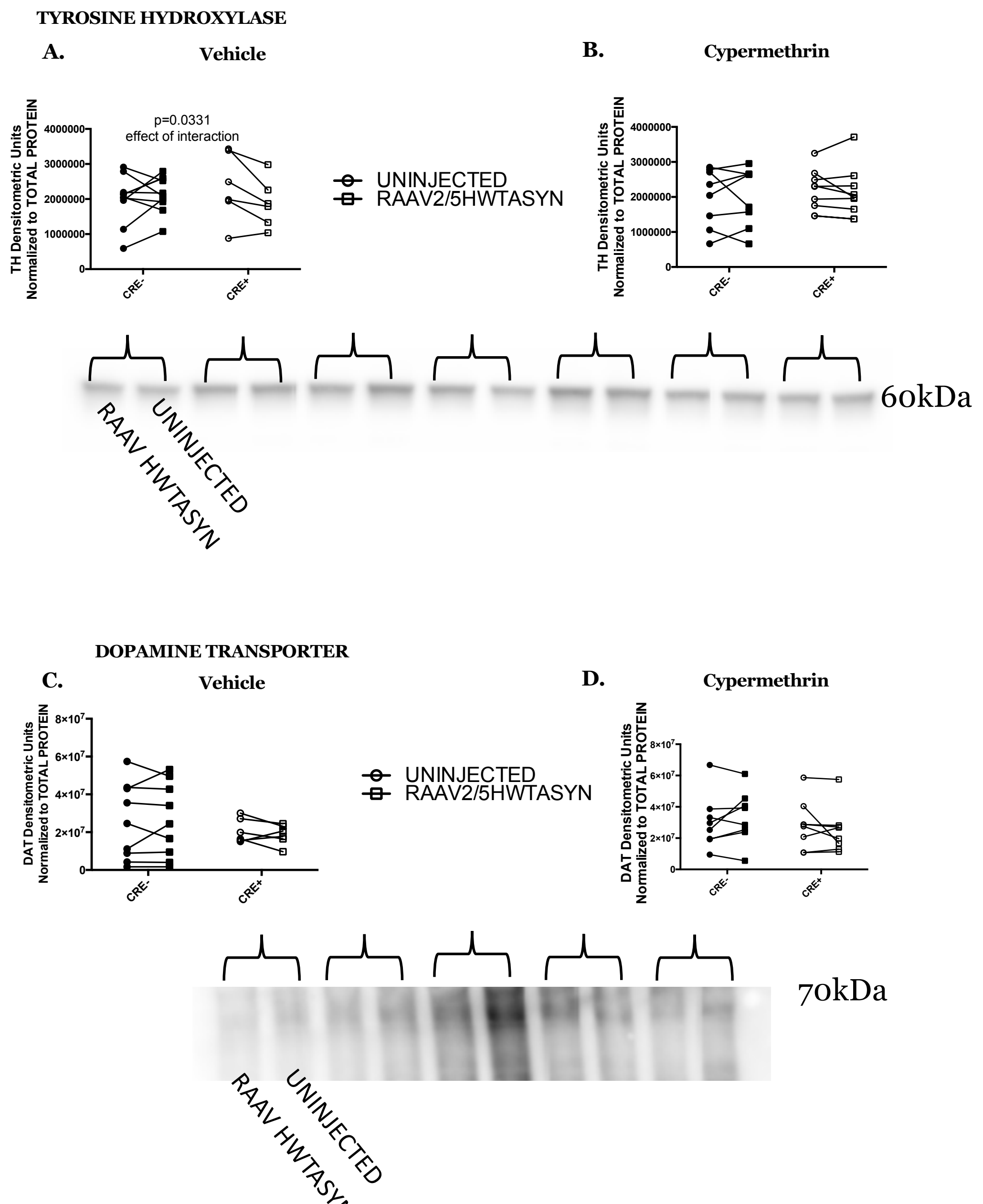

Figure 22. Short-term cypermethrin exposure does not decrease tyrosine hydroxylase or dopamine transporter protein expression, even in the presence of human WT α-synuclein. Soluble protein lysates from the left (RAAV2/5 HWTASYN, squares) and right (UNINJECTED, circles) striatal tissues LysMCre- and LysMCre+I-Ab$^{fl/fl}$ (filled and open shapes, respectively) were analyzed for protein levels of TH (**A**) and DAT (**B**), normalized

to total protein identified by REVERT stain. Data are plotted to show the paired striatal samples for each animal. P-values are indicated above relevant graphs.

3.4 Discussion

This work was motivated by the observation that a common variation in the gene for MHCII is associated with increased risk for PD and our group's observation that individuals with the high-risk genotype at *rs312988* displayed monocytes in blood with higher surface MHCII protein expression and hyper-responsiveness to an immune challenge in conjunction with PD status (Kannarkat et al., 2015). Therefore, we set out to investigate the role of MHCII protein expression in a mouse model of PD-like pathology. Previous work using an α-synuclein nigral overexpression mouse model reported that MHCII was necessary for α-synuclein-induced dopaminergic degeneration (Harms et al., 2013; Williams et al., 2018). While these studies were informative, they examined the immune response in a context in which CD4 T cells were not able to develop normally (global MHCII KO), complicating interpretation of results. Previous work was not designed to address different contributions to antigen presentation by peripheral versus brain-resident immune cells. This is of critical importance and translational relevance when one considers the challenges of developing therapeutics to prevent or treat PD that have minimal penetrance across the blood-brain barrier; yet, if they can be shown to engage the peripheral immune system, they may still have protective and therapeutic effect. Based on the data reported in (Kannarkat et al., 2015), we hypothesized that decreased MHCII expression in peripheral immune cells would be beneficial to the health of dopaminergic neurons, specifically by decreasing effector CD4+ T cell frequency of cells that may traffic to the brain, thereby protecting dopaminergic neurons from an adaptive immune response directed against α-synuclein or other immunogenic neuron-derived antigens.

We investigated the role of peripheral myeloid cell MHCII in a viral-vector-mediated α-synuclein overexpression model of PD pathology because rAAV models allow for targeting α-synuclein to neurons known to degenerate and express LBs in PD. Viral vector models similar to the ones used in our studies have shown an increase in α-synuclein expression of around 2-4 times endogenous levels following SN injection, and the transduction of SN neurons can be long-lasting (Kirik et al., 2002; Klein et al., 2002).

To test our hypothesis that diminished antigen presentation capacity on peripheral immune cells can protect dopaminergic neurons by preventing CD4 T cell-mediated inflammatory immune responses, we performed our experiments using LysmCre- and LysMCre+I-Ab$^{fl/fl}$ mice. We first assessed the extent of MHCII deletion in LysMCre+I-Ab$^{fl/fl}$ mice. We demonstrated that LysMCre+I-Ab$^{fl/fl}$ have deletion of MHCII on peritoneal macrophages, spleen-derived myeloid cells, and PBMC CD11b+Ly6G- cells (**Figure 9**, **Figure 10.I-L**). There were no statistically significant differences in the frequency or number of B cells, T cells, neutrophils, or Ly6G-CD11b+ cells (non-neutrophils) between LysMCre- and LysMCre+I-Ab$^{fl/fl}$ mice in the peripheral blood (**Figure 10.A-H**).

In previous work from our lab, it was observed that the high-risk SNP genotype at *rs3129882* synergizes with exposure to pyrethroid pesticides to increase risk for PD (Kannarkat et al., 2015). To investigate the interaction between MHCII expression and the pyrethroid cypermethrin, we treated LysMCre±I-Ab$^{fl/fl}$ mice with cypermethrin or vehicle for 3 weeks, beginning 8-9 months after rAAV2/5 injection. As in the rAAV2/9 study, the B cells, T cells, neutrophils, and non-neutrophil population were not affected by LysMCre genotype. However, unexpectedly, following vehicle or cypermethrin treatment twice per week for three weeks, the deletion of MHCII observed in LysMCre+I-Ab$^{fl/fl}$ PBMCs from the rAAV2/9 study was not reproduced. One possible explanation for this observation is that the vehicle impairs the health of peripheral immune cells and causes downregulation of homeostatic genes, including *LysM*. Myeloid immune cells in the blood have a relatively short lifespan. Monocytes for example have a half-life of 22h (van Furth and Cohn, 1968). Throughout our short-term treatment, there may be a failure to express Cre under *LysM*, and, thus, we detected MHCII expression in CD11b+Ly6G- cells in LysMCre+I-Ab$^{fl/fl}$ mice. We could test this possibility in the future by staining for lysozyme M or Cre and performing RT-PCR for *LysM* on PBMCs isolated from mice treated with vehicle or cypermethrin. We observed an increase in the frequency of naïve CD4+ T cells in LysMCre+I-Ab$^{fl/fl}$ mice in the rAAV2.5 study, which is consistent with the idea of pre-treatment deletion of MHCII (**Figure 14.H**). It is possible that in our mice, prior to treatment, Cre under the control of *LysM* blocked the contributions of peripheral myeloid cell antigen presentation to the immune response to the human WT α-synuclein driven by rAAV2/5 in the SN. Future work should assess MHCII expression before and after vehicle or cypermethrin exposure.

In the rAAV2/9 study, we tested whether peripheral myeloid MHCII deletion affected the frequency of Th1s, Tregs, central memory, effector memory, and naïve CD4+ T cells. We observed a decrease in the frequency of Tregs in LysMCre+I-Ab$^{fl/fl}$ mice (**Figure 12.D**). Tregs suppress inflammation (Luckheeram et al., 2012), suggesting inflammatory immune responses in LysMCre+I-Ab$^{fl/fl}$ mice may last longer and/or involve increased levels of cytokine release relative to LysMCre-I-Ab$^{fl/fl}$ controls. Because we did not collect blood samples throughout the post-injection period, only at the time of sacrifice, we cannot assess the effect altered Treg frequency had on the acute inflammatory response to human α-synuclein in the nigra, but future work could be done to assess the presence of CD4 T cells, even Tregs specifically, in the brain by flow cytometry at time points closer to the onset of α-synuclein expression. In addition to the shift in Treg frequency, LysMCre+I-Ab$^{fl/fl}$ mice have decreased frequencies of effector memory and central memory CD4+ T cells and an increase in the frequency of naïve CD4+ T cells (**Figure 12.F-H**). PD patients are known to have increased frequency of CD45RO+ T cells (marker of memory subsets) (Fuzzati-Armentero et al., 2019). If we assume the T cell frequencies of a PD patient are disease-promoting or at least permissive, our data indicate that the deletion of MHCII on peripheral myeloid cells is beneficial, in that it promotes the development of a T cell compartment lacking the characteristics seen in PD. In **Figure 13**, we showed that, similar to PBMCs, the frequency of effector memory CD4+ T cells in mouse deep cervical lymph nodes is decreased in LysMCre+I-Ab$^{fl/fl}$ mice. These observations are consistent our finding that MHCII is deleted on peripheral myeloid cells and provide confirmation that the deletion in *LysM*-expressing cells is sufficient to affect CD4+ T cells.

Following 3 weeks of cypermethrin treatment in mice that had received rAAV2/5 human WT α-synuclein, we observed an effect of treatment (cypermethrin versus vehicle) x genotype (LysMCre±I-Ab$^{fl/fl}$) interaction such that cypermethrin decreased CD3+ T cell frequency in LysMCre-, but increased in LysMCre+I-Ab$^{fl/fl}$ mice (**Figure 14.A**). This suggests the possibility that cypermethrin has a toxic effect on T cells that is mitigated in LysMCre+I-Ab$^{fl/fl}$ mice. We cannot attribute this observation to the absence of MHCII in peripheral myeloid cells, however, because, at the time of the experiment, as discussed above, the LysMCre+I-Ab$^{fl/fl}$ mice showed no MHCII deletion. There is previous research showing immunotoxicity of pyrethroid pesticides. In female mice treated with the pyrethroid permethrin, a 32% decrease in spleen T cell proliferation was observed (Chrustek et al., 2018). In mouse splenocytes and rat thymic cells, another pyrethroid, deltamethrin, has been reported to induce apoptosis (Kumar et al., 2015; Chauhan et al., 2016). Future work could assess apoptotic marker expression in T cells isolated from cypermethrin treated mice to further compare the compound's immunotoxicity between LysMCre+ and LysMCre-I-Ab$^{fl/fl}$ mice. A treatment x genotype interaction also influenced Treg frequency such that cypermethrin-treated LysMCre-I-Ab$^{fl/fl}$ mice showed an increased frequency of Tregs, while LysMCre+I-Ab$^{fl/fl}$ mice showed the opposite (**Figure 14.D**). The results could be explained by an immune response in LysMCre-I-Ab$^{fl/fl}$ mice that differentially affects some CD4+ T cells subsets so that the relative frequency of Tregs increases. This is consistent with the data in **Figure 14.F** where we showed that cypermethrin decreases the frequency of effector memory CD4+ T cells, a cell type associated with chronic immune activation. The mechanism behind how cypermethrin interacts with T cells remains to be investigated. Work done in THP1 and Jurkat cell lines suggests that the pyrethroid permethrin increases the rate of T cell proliferation, but this may not be the case uniformly across all T cell subsets (Kannarkat and Tansey, 2016). Future work should investigate the extent to which cypermethrin can increase the proliferation rate of autoreactive T cells i.e. those specific for a PD-related antigen such as α-synuclein.

The deep cervical lymph nodes drain the meningeal lymphatic vessels (Louveau et al., 2018). We were interested in sampling the deep cervical lymph nodes as a read-out of the CNS adaptive immune response. Cypermethrin and LysMCre genotype affected the frequencies of T cell subsets within the deep cervical lymph nodes as well (**Figure 15**). Specifically, we observed a decrease in CD3+ T cells in LysMCre+I-Ab$^{fl/fl}$ mice (**Figure 15.A**), and a treatment x genotype interaction affecting the frequency of central memory CD4+ T cells such that cypermethrin increased central memory frequency in the LysMCre-I-Ab$^{fl/fl}$ mice (**Figure 15.G**). Conversely, in the LysMCre+I-Ab$^{fl/fl}$ animals, cypermethrin decreased central memory CD4+ frequency. This suggests that MHCII expression level and cypermethrin exposure could interact to influence T cells. The frequency of some CD4 T cell subsets has been shown to vary over time in other models of dopaminergic degeneration in rats, suggesting that future work interested in elucidating the role of CD4+ T cells in pathogenesis should consider collecting tissue at multiple timepoints (Ambrosi et al., 2017).

In order to determine the molecular mediators involved in the immune response to LysMCre-mediated MHCII deletion or, in the rAAV2/5 study, cypermethrin, we assessed plasma cytokine and chemokine levels at the time of sacrifice. No differences were observed in any of the assayed plasma markers in the rAAV2/9 higher titer study (**Figure 16**), suggesting that deletion of peripheral myeloid MHCII alone does not alter cytokine secretion. In the presence of cypermethrin, however, we found that IL-1β was affected by a treatment x genotype interaction such that LysMCre+I-Ab$^{fl/fl}$ mice treated with cypermethrin have increased plasma IL-1β (**Figure 17.C**). Shifts in IL-1β are interesting given that PD patient blood and brain contains increased IL-1β relative to controls, among other cytokine increases (Fuzzati-Armentero et al., 2019). However, in previous work characterizing the effect of *rs3129882* genotype on the immune system, no difference in IL-1β was observed (only in MIP-1α in PD *GG* individuals, (Kannarkat et al., 2015)). More work is needed to thoroughly interrogate the relationship between altered antigen presentation, pyrethroid exposures, and cytokine release.

Having assessed peripheral immune cell frequencies and secreted factors, we next characterized the nigrostriatal systems in our LysMCre±I-Ab$^{fl/fl}$ mice following rAAV-mediated human WT α-synuclein expression. In **Figures 18** and **19** we present double labeling of the mouse SN for TH and human α-synuclein. Four months post-rAAV2/9 and 8-9 months post-rAAV2/5, we were able to detect expression of the virus within the nigra and did not observe contralateral expression. In other studies with rAAV-α-synuclein, progressive loss of dopaminergic neurons in the nigra and the TH+ terminals in the striatum have been reported (Koprich et al., 2010; Lundblad et al., 2012). In previous work specifically with rAAV2/9 human WT α-synuclein in mice, approximately 50% of TH+ cells were lost in the SN, and 20% of the TH in the striatal terminals was lost on the injected side 1 month after surgery (Castro-Sanchez et al., 2018). In that study, microgliosis as evinced by increased SN Iba-1-immunoreactive cell number, Iba-1 and GFAP mRNA, as well as mRNA levels of IL-1β and TNF. For this study, we characterized the striatal inflammatory environment by Western blot and qRT-PCR. We found that four months after rAAV2/9 human WT α-synuclein, there is an upregulation of CD68 mRNA in the striatal hemisphere ipsilateral to stereotaxic injection (**Figure 20.D**). CD68 is a lysosomal marker known to be expressed in monocytes and macrophages (Pulford et al., 1990). LysMCre genotype did not affect CD68 upregulation. Treatment of primary microglia with α-synuclein fibrils has been shown to increase expression of iNOS, which can be prevented with global CIITA KO (Williams et al., 2018). Deletion of MHCII would, thus, be expected to similarly decrease α-synuclein-related iNOS expression; however, we observed the opposite. In **Figure 20.F**, the data show an effect of genotype on iNOS mRNA level. One possible explanation for this observation is microglial-specific upregulation of iNOS in LysMCre+I-Ab$^{fl/fl}$, There was an rAAV2/9 x genotype interaction that significantly affected IL-6 mRNA levels (**Figure 20.J**). In LysMCre-I-Ab$^{fl/fl}$ mice, rAAV2/9 human WT α-synuclein drove increased IL-6 levels, while LysMCre+I-Ab$^{l/fl}$ mice displayed a decrease. Because IL-6 is an inflammatory cytokine increased in the blood of PD patients relative to controls

(Fuzzati-Armentero et al., 2019), its decrease in LysMCre+I-Ab$^{fl/fl}$ mice suggests a some aspects of neuroinflammation may be mitigated by peripheral myeloid MHCII deletion.

We also examined protein markers of nigrostriatal axon terminals by Western blot (**Figures 21** and **22**). Neither short-term cypermethrin treatment nor lower-titer human WT α-synuclein affected TH or DAT expression, with the exception of an effect of interaction in vehicle treated animals (**Figure 22.A**). Following rAAV2/5 and cypermethrin treatment, we observed an effect of genotype x rAAV2/5 interaction on TH protein expression in vehicle-treated animals. Because LysMCre+I-Ab$^{fl/fl}$ deletion of MHCII has been called into question following cypermethrin or vehicle treatment (**Figure 11.I-L**), and due to the variability in TH levels in our samples, the meaning of this result is difficult to ascertain. Results of the rAAC2/9 study's Western blots were more straightforward. Following rAAV2/9, we observed a statistically significant decrease in DAT and TH in LysMCre-I-Ab$^{fl/fl}$ mice on the injected side. No such decrease was observed in LysMCre+I-Ab$^{fl/fl}$ mice. This suggests that peripheral myeloid MHCII deletion protected dopaminergic terminals, sparing them from human α-synuclein-induced lesion. Overall, the data from the rAAV2/9 higher-tier study suggests there may be some benefit, in terms of neuroinflammation and maintenance of dopaminergic phenotype, to minimizing MHCII expression on peripheral myeloid cells.

In this chapter, we report our efforts to understand the biological mechanisms driving the synergy between MHCII expression in an α-synuclein lesion, and exposure to the pyrethroid pesticide cypermethrin. While our findings yielded important insights, they also motivate additional experiments. First, characterization of the synuclein-induced lesion at the level of the nigra should be performed to determine the extent of nigral dopaminergic neuron loss. The striatum is a large and heterogenous structure, and the quantification of TH+ soma in the nigra will more precisely inform us regarding the extent of synuclein-induced lesion with each of the serotypes. Therefore, we will be able to determine whether the maintenance of TH protein content in the striatum in LysMCre+I-Ab$^{fl/fl}$ is accompanied by increased nigral neuron survival. Next, more chronic dosing of cypermethrin would be of interest, and a dosing route that is more translationally relevant than intraperitoneal injection. It would also be beneficial to perform experiments similar to those presented here in animals with upregulation of MHCII, mimicking the immune systems of humans with the high-risk *rs3129882* genotype. Antigen presentation capacity is dynamic, and likely interacts with other environmental factors beyond pyrethroid exposure. More work remains to be done on this promising target for future immunomodulatory interventions to treat PD.

CHAPTER 4. CHARACTERIZATION OF T CELL SUBSETS ASSOCIATED WITH *rs3129882* GENOTYPE IN PARKINSON'S DISEASE PATIENTS AND CONTROLS

Saliva and blood samples collected by collaborators at the University of Florida. Peripheral blood mononuclear cell isolation and cryopreservation performed by the McFarland lab at the University of Florida. DNA extraction was performed by Yuan Yang. Flow cytometry and analysis performed by Elizabeth Marie Kline.

4.1 Introduction

Several studies have linked single nucleotide polymorphisms (SNPs) in the gene for major histocompatibility complex class II (MHCII) to risk for the neurodegenerative disease Parkinson's disease (PD) (Hamza et al., 2010; International Parkinson Disease Genomics et al., 2011; Ahmed et al., 2012; Nalls et al., 2014). One SNP, *rs3129882,* has been of particular interest to our lab. A *G* allele at *rs3129882* is associated with a 1.7-fold increase in risk for PD. Previous work from the Tansey lab reported that the high-risk genotype for this SNP (*GG*) synergizes with exposure to pyrethroid pesticides to increase risk for PD (Kannarkat et al., 2015). Furthermore, *GG* individuals were found to have increased MHCII expression on monocytes and B cells (see **Figure 1**) (Kannarkat et al., 2015).

Understanding the functional implications of an association between MHCII and PD requires an appreciation for the normal functions of the immune system and its interaction with the central nervous system (CNS). In order to clear pathogens, immune cells secrete inflammatory cytokines, upregulate surface activation markers, perform antigen presentation, migrate, proliferate, and perform a variety of other immune processes depending on the specific cell type. To maintain homeostasis, eventually, the immune system's tone shifts towards the resolution of inflammation and tissue repair, which is, in part, regulated by the effector functions regulatory T cells (Tregs). During the process of pathogen clearance and resolution of inflammation, the effects of the immune system on the nervous system may be indirect, via secreted factors for which neurons have receptors, or more direct. For example, CD8+ T cells can directly kill neurons through engagement of Fas and TNF signaling pathways (Coque et al., 2019).

There is ample evidence for the involvement of the adaptive immune system in the pathophysiology of PD. Studies of human post-mortem tissue demonstrated CD4+ and CD8+ T cells within the brain parenchyma, specifically in the SN, in PD patients, but not healthy controls (McGeer et al., 1988b; Croisier et al., 2005; Orr et al., 2005; Miklossy et al., 2006). CD4+ T cells are associated with dopaminergic (DA) neuron loss in that CD4-/- mice are protected in an MPTP model of degeneration (Brochard et al., 2009). CD4+ and CD8+ T cells within PD brains are found in close contact with blood vessels or melanized dopamine (DA) neurons (Brochard et al., 2009) (Campos-Acuna et al., 2019; Garretti et al., 2019). Removal of CD4+ but not CD8+ T cells can significantly reduce the DA degeneration induced by MPTP intoxication. Overall the existing evidence suggests that the nature of the adaptive immune system, specifically in the presences of certain T cells, can influence DA neuron health.

Exposure to the neuronal protein, α-synuclein, although it is normally expressed throughout development, can elicit an innate and adaptive immune response. Section ***1.1d*** reviews the immunogenic nature of α-synuclein in more detail. Neurons are reported to up-regulate the antigen presentation molecule major histocompatibility class I (MHCI) in an α-synuclein overexpression model of PD neuropathology, emphasizing the importance of antigen presentation and its effect on T cell recruitment to the brain (Cebrian et al., 2014). Neuronal MHCI has also been observed in human PD SN and locus coeruleus (Cebrian et al., 2014).

Peripheral dysregulation of the adaptive immune system has been characterized in flow cytometry studies where PBMCs were isolated from PD patients (see section ***1.1c***). Within the PBMC population, some studies report that PD patients have an increased frequency of CD8 T cells and decreased frequency of CD4 T cells (Bas et al., 2001; Baba et al., 2005; Stevens et al., 2012). Specific decreases in the frequency and suppressive abilities of Tregs has been associated with PD (Saunders et al., 2012; Chen et al., 2015). T cell-driven inflammation of the gut mucosa is involved in inflammatory bowel diseases, which have been positively correlated with PD (Campos-Acuna et al., 2019). In line with this observation, shifting inflammatory factors secreted by T cells has been considered as an approach for the treatment of PD (Hirsch and Hunot, 2009; Mosley et al., 2012). In PD, there has been increasing evidence that Th17's, another CD4+ T cell subset, may play an important role (Bolte and Lukens, 2018; Storelli et al., 2019). Th17's are distinguishable by their expression of CCR6 and the transcription factor RORγT. Th17s are known for their role in autoimmunity, making their function in PD particularly interesting given the evidence for α-synuclein and neuromelanin as putative auto-antigens (Garretti et al., 2019).

Th17s and the other CD4+ T cell subtypes recognize antigen presented via the antigen presentation protein MHCII, connecting them to the observation that *rs3129882* genotype affects MHCII expression. We and others have hypothesized that PD may feature excessive killer T cell function and/or failure of regulatory T cells to arrest inflammation and auto-reactivity.

Because of the connection between innate and adaptive immunity via antigen presentation, we hypothesized that antigen presentation via MHCII impacts dopamine neurons by skewing T cell frequency and function. We set out to determine the extent to which individuals with the high- versus low-risk allele at *rs3129882* with, or without, PD display differences in T cell subset frequency, predicting that high MHCII expression would be associated with increased frequencies of inflammatory CD4+ T cells relative to those with the low-risk SNP genotype and lower MHCII protein expression and transcript levels.

4.2 Materials and Methods

4.2a) Cohort and subject recruitment and genotyping

PD patients and healthy control subjects were recruited through a collaboration with Dr. Nicholas McFarland at the University of Florida through a protocol approved by the IRB's of Emory University and the University of Florida. All participants were of white, European background. No participants listed Jewish religious or ethnic background. Some but not all of the control subjects were spouses of PD participants. To identify the *rs3129882* genotype of all participants, saliva was collected using Oragene DNA OG-500 kit and DNA isolated according to the manufacturers protocol (DNA genotek). Taqman SNP Genotyping Assay (Life Technologies) was used to determine genotype. Subjects provided an approximately 40mL blood sample. A questionnaire was administered at the time of blood collection to assess disease status, medication use, demographic background, family history, and any inflammation-related exposures. Caffeine, NSAID, and nicotine use data was collected as well.

4.2b) Peripheral blood mononuclear cell isolation, cryopreservation, and thaw

Blood was drawn via venipuncture from participants at the University of Florida into BD Vacutainer Cell Preparation Tubes (CPT) with sodium heparin from BD Biosciences (362761). Following density centrifugation, the plasma layer was removed and frozen in liquid nitrogen. PBMCs were cryopreserved in 90% heat-inactivated fetal bovine serum (FBS, Sigma) in 10% DMSO at a concentration of $10x10^6$ cells per 1mL. Cryovials of 1mL were frozen down in a room temperature Mr. Frosty™ (ThermoFischer Scientific) placed in a -80°C freezer for 24 hours and then shipped on dry ice to Emory University where vials were stored in liquid nitrogen until time of experiment. To thaw, 1 cryovial per participant was placed in a water bath (37°C) and just prior to full thaw, 1mL of 10% FBS in RPMI-1640 (Corning) was added. The diluted, thawed cell solution was then transferred into 30mL of 10%FBS in RPMI and centrifuged for 10 minutes at 400rcf. The pellet was resuspended in RPMI sith 10% FBS and cells were counted. For flow cytometry, 250000 cells were plated per subject in a 96-well V-bottom plate.

4.2c) Flow cytometry

To stain for flow cytometry, cells were incubated in PBS with Live-Dead stain, Fc block, and anti-CD25 antibody in phosphate buffered saline on ice for

30 minutes. Following a wash step, cells were incubated with anti-CCR7 antibody in FACS buffer (1% bovine serum albumin, 0.1% sodium azide, 1mM EDTA) for 15 minutes at 37°C. Following another wash step, cells were incubated with antibodies against all other surface makers in FACS buffer on ice for 25 minutes. Cells were washed with FACS, fixed with 0.1% paraformaldehyde, washed again, and then transferred into FACS tubes and stored at 4°C until run on the LSRII flow cytometer within 48 hours (BD Biosciences). Antibody details are listed in the antibody table. Data analysis was performed using FlowJo v10.

4.2d) Study approval

Informed consent was received in writing from all participants prior to inclusion in the study. Procedures were approved by the Institutional Review Boards of Emory University in Atlanta, Georgia and the University of Florida in Gainesville, Florida.

4.2e) Statistics

Comparison among the four groups (Control AA, Control AG/GG, PD AA, PD AG/GG) was analyzed by two-way ANOVA followed by Sidak's *post-hoc* multiple comparison's test for *p* values. GraphPad Prism v6 was used for analysis. Data is reported in table and figure as mean ± SEM.

4.3 Results

4.3a) Characteristics of study population

Subjects were sorted into Control AA, Control AG/GG, PD AA, and PD AG/GG groups in order to assess the effect of one or more copies of the high-risk SNP allele (*G)* relative to those with only the *A* allele. The general characteristics of the study participants are presented in **Table 4**. Because brain injury is a risk factor for PD (Taylor et al., 2016) (reviewed in (Tansey et al., 2007)), subjects were asked whether they had ever had a head injury that caused loss of consciousness or required medical care. In the PD group, a total of 9 head injuries were reported (14 total participants), while only 3 head injuries were reported in the control group (11 total participants). There were no statistically significant differences between controls and PD subjects in age (unpaired two-tailed Student's t test). PD *AA* and *AG/GG* subjects did not differ in age of onset or number of years since diagnosis (unpaired two-tailed Student's t test). The control group included more females than the PD group.

Table 4.

A.	**Age at time of study (years)**	**Range (years)**	**Total number of head injuries**	**Number of males, females**
Control (n=11)	66.36 ± 2.064	55-76	3	3, 8
AA (n=6)	64 ± 2.582	55-71	0	1,5
AG/GG (n=5)	69.2 ± 3.121	58-74	3	2, 3

B.	**Age at time of study (years)**	**Range (years)**	**Age at diagnosis (years)**	**Years since diagnosis**	**Total number of head injuries**	**Number of males, females**
PD (n=14)	70.21 ± 2.22	46-79	60.65 ± 2.567	8.13 ± 1.715	9	11, 3
AA (n=5)	70 ± 1.643	66-75	64.6 ± 2.657	5.4 ± 2.015	4	4, 1
AG/GG (n=9)	70.33 ± 3.424	46-79	58.19 ± 3.684	10.07 ± 2.406	5	7, 2

4.3b) High-risk rs3129882 genotype is associated with decreased numbers of Tregs, and interactions between SNP and PD affect effector memory subset counts

To assess the effect of *rs3129882* on T cell subset frequency, PBMCs from PD and healthy control subjects were prepared for flow cytometry. We hypothesized that, due to increased expression of MHCII on monocytes and B cells in *GG* individuals, there would be alterations in CD4+ T cell subsets in the *AG/GG* group relative to the *AA* group. Furthermore, we predicted interactions between genotype and treatment, given that mRNA level of MHCII was affected by an interaction between genotype and disease status (Kannarkat et al., 2015). We observed no differences in overall frequencies of total T cells, CD4+ T cells, or CD8+ T cells among our four groups (**Figure 24.A-C**). We observed that PD participants had an increase in Treg frequency, while the *GG rs3129882* genotype significantly decreased the number of Tregs and increased CD4 and CD8 effector memory T cells (**Figure 24.D, H, L**).

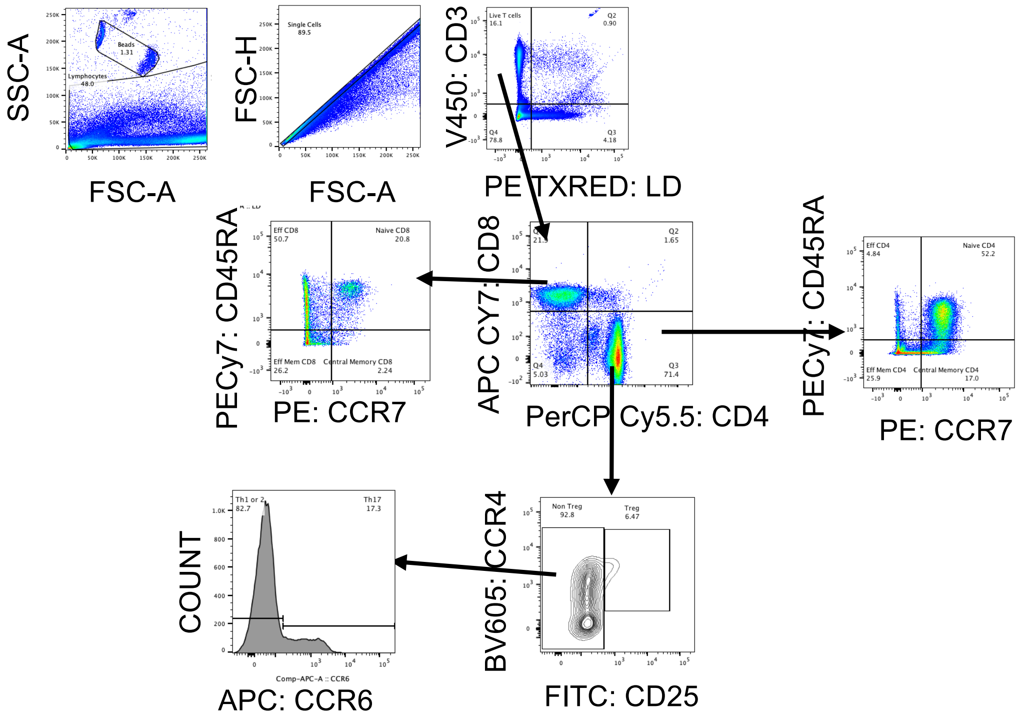

Figure 23. Human T cell subset gating strategy. Cryopreserved PBMCs were stained for flow cytometry and analyzed on an LSRII after standardization and compensation with Sphero beads and OneComp beads. Gates were placed based on staining with fluorescence-minus-one and isotype control antibodies. Analysis was performed and plots were generated using FlowJo software. Live T cells were identified as LD-CD3+, and then gated on CD4 versus CD8. CD4+ live T cells were then gated on 1. CCR7 versus CD45RA and 2. CD25 versus CCR4. Naïve CD4 T cells: CCR7+CD45RA+. Central memory CD4 T cells: CCR7+CD45RA-. Effector CD4 T cells: CCR7-CD45RA+. Effector memory CD4 T cells: CCR7-CD45RA-. Tregs: CD25+CCR4+. Non-Tregs were gated on CCR6. Th17: CCR6+. Th1 or Th2: CCR6-. The same memory marker combinations were used to identify subsets of CD8+ T cells. Surface markers were chosen based on the recommendations of the Human Immunology Project (Maecker et al., 2012).

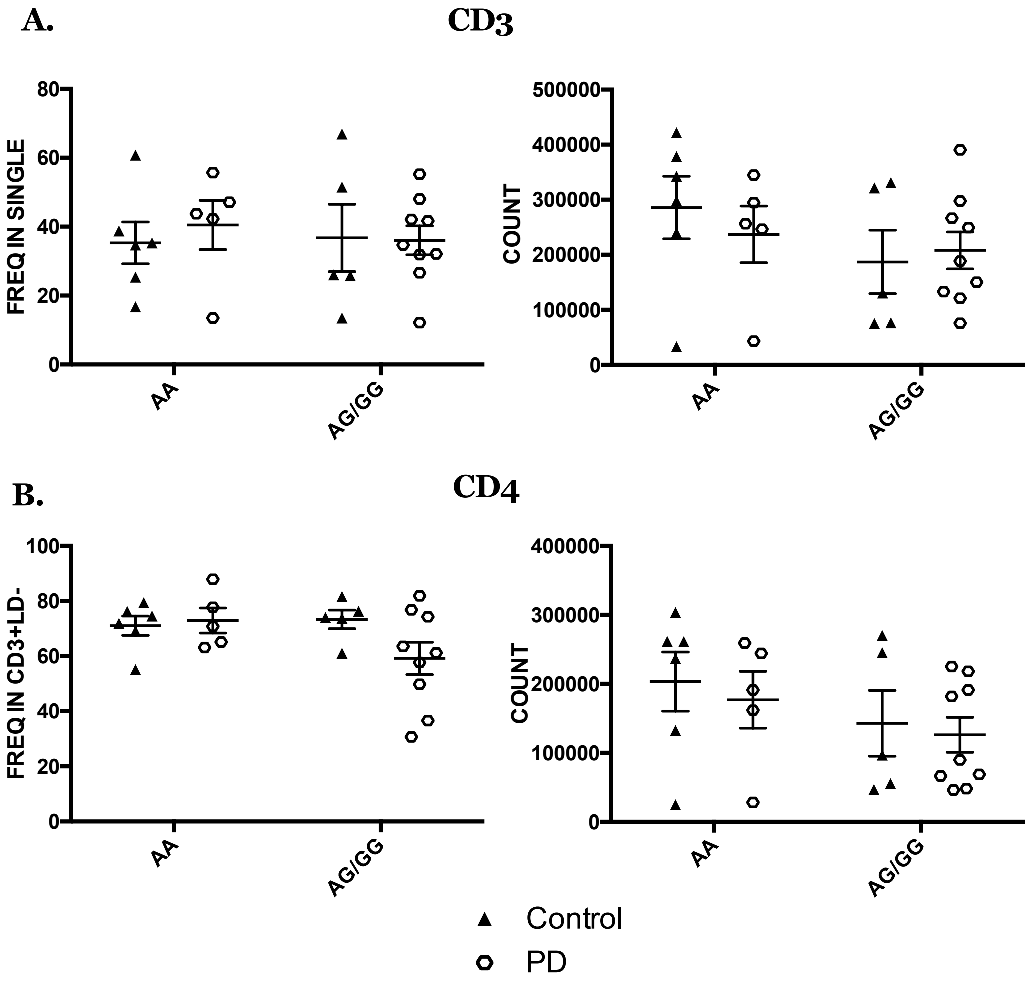

Figure 24.A-B. **High-risk *rs3129882* genotype is associated with decreased number of Tregs, and interactions between SNP genotype and PD affect effector memory subset counts.** Flow cytometry staining was used to determine frequencies and counts of T cells in cryopreserved PBMC samples. Two-way ANOVA was used to test for significant differences between control (triangles) AA, p values are indicated above applicable graphs.

C. **CD8**

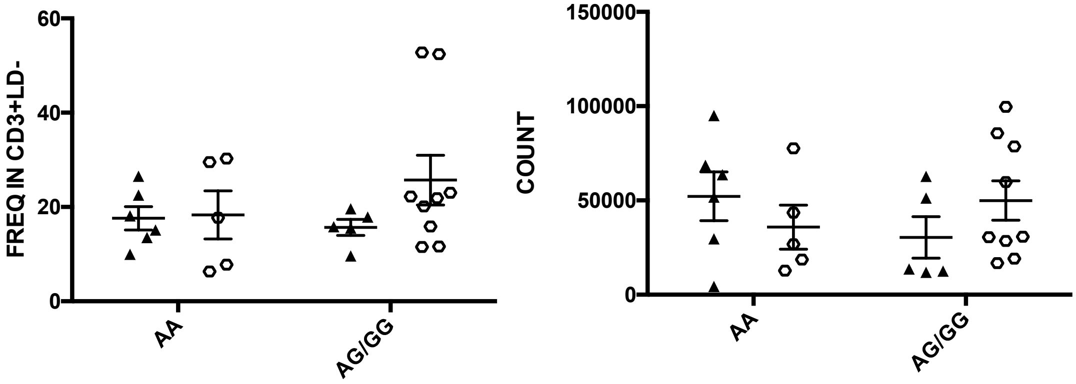

D. **Treg**

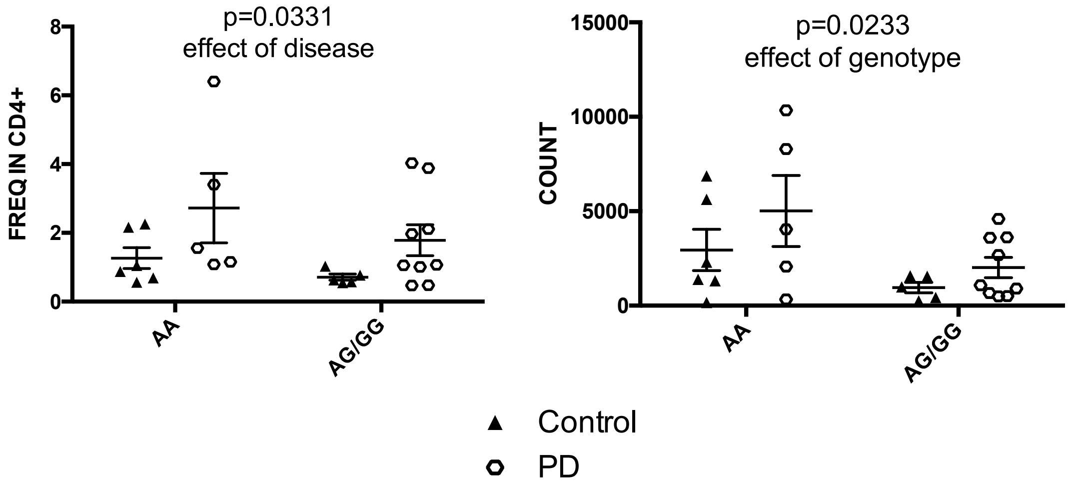

Figure 24.C-D. High-risk *rs3129882* genotype is associated with decreased number of Tregs, and interactions between SNP genotype and PD affect effector memory subset counts. Flow cytometry staining was used to determine frequencies and counts of T cells in cryopreserved PBMC samples. Two-way ANOVA was used to test for significant differences between control (triangles) AA, p values are indicated above applicable graphs.

E. Th17

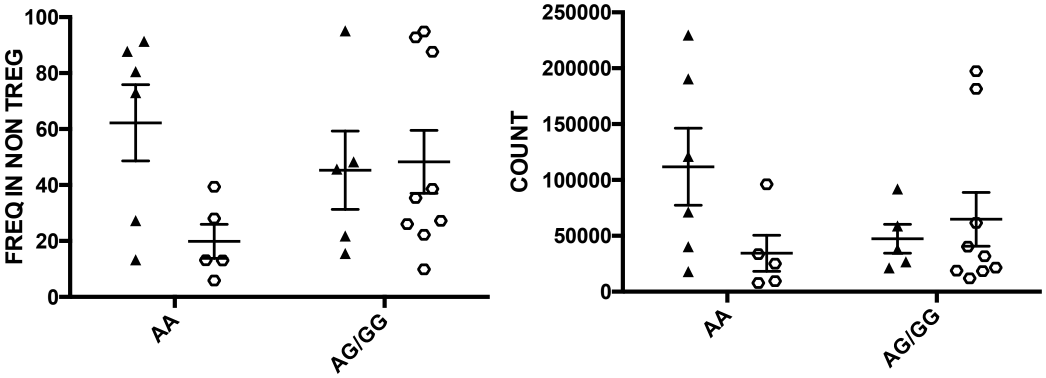

F. Th 1 or 2

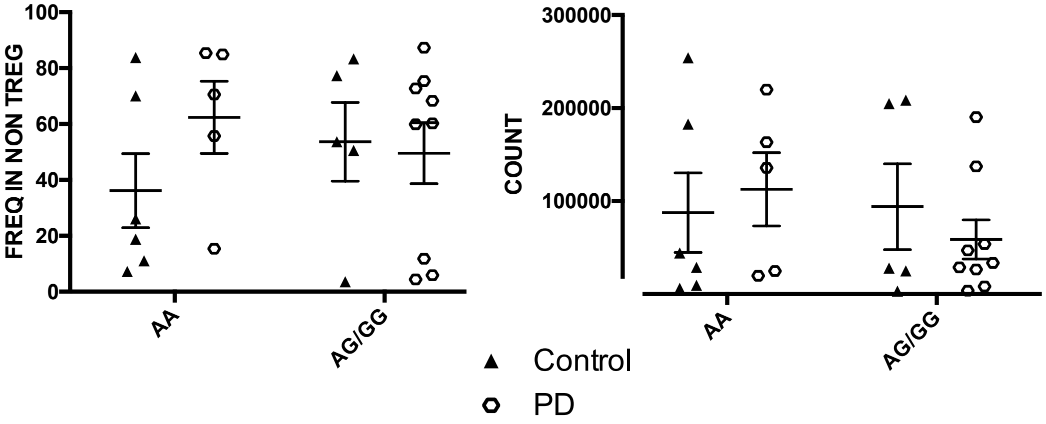

Figure 24.E-F. **High-risk *rs3129882* genotype is associated with decreased number of Tregs, and interactions between SNP genotype and PD affect effector memory subset counts.** Flow cytometry staining was used to determine frequencies and counts of T cells in cryopreserved PBMC samples. Two-way ANOVA was used to test for significant differences between control (triangles) AA, p values are indicated above applicable graphs.

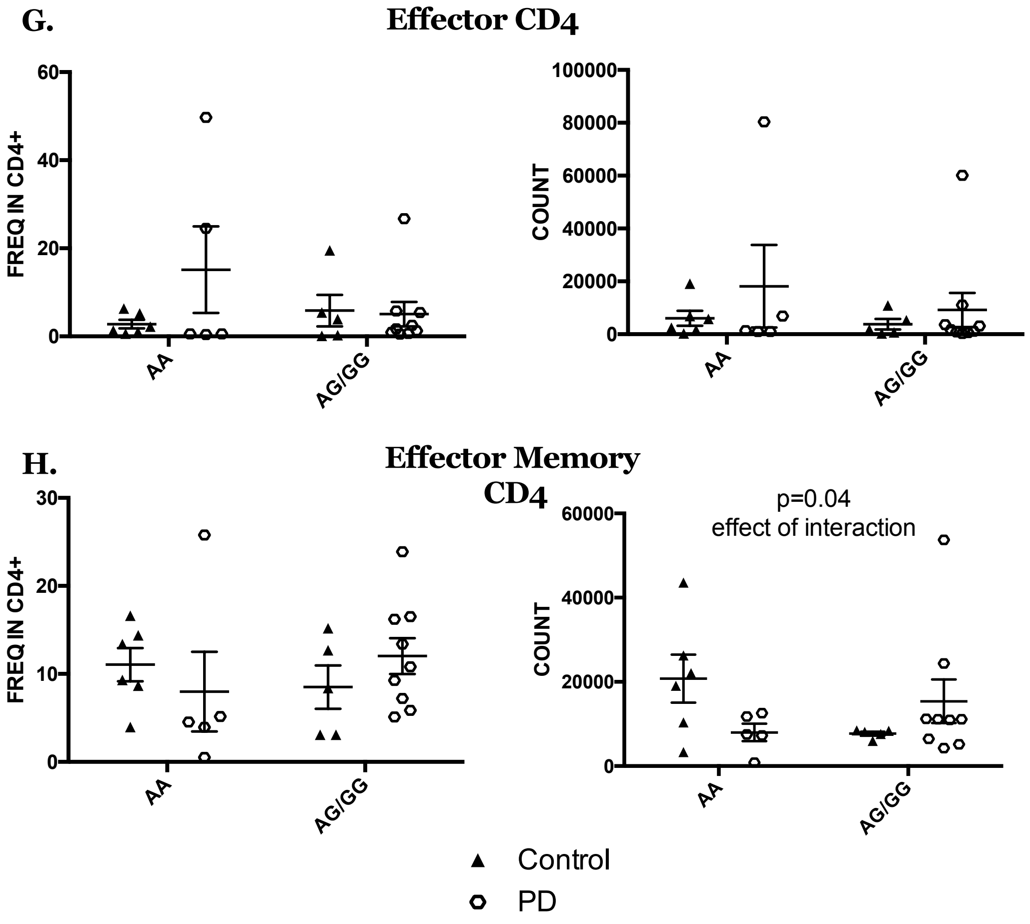

Figure 24.G-H. High-risk *rs3129882* genotype is associated with decreased number of Tregs, and interactions between SNP genotype and PD affect effector memory subset counts. Flow cytometry staining was used to determine frequencies and counts of T cells in cryopreserved PBMC samples. Two-way ANOVA was used to test for significant differences between control (triangles) AA, p values are indicated above applicable graphs.

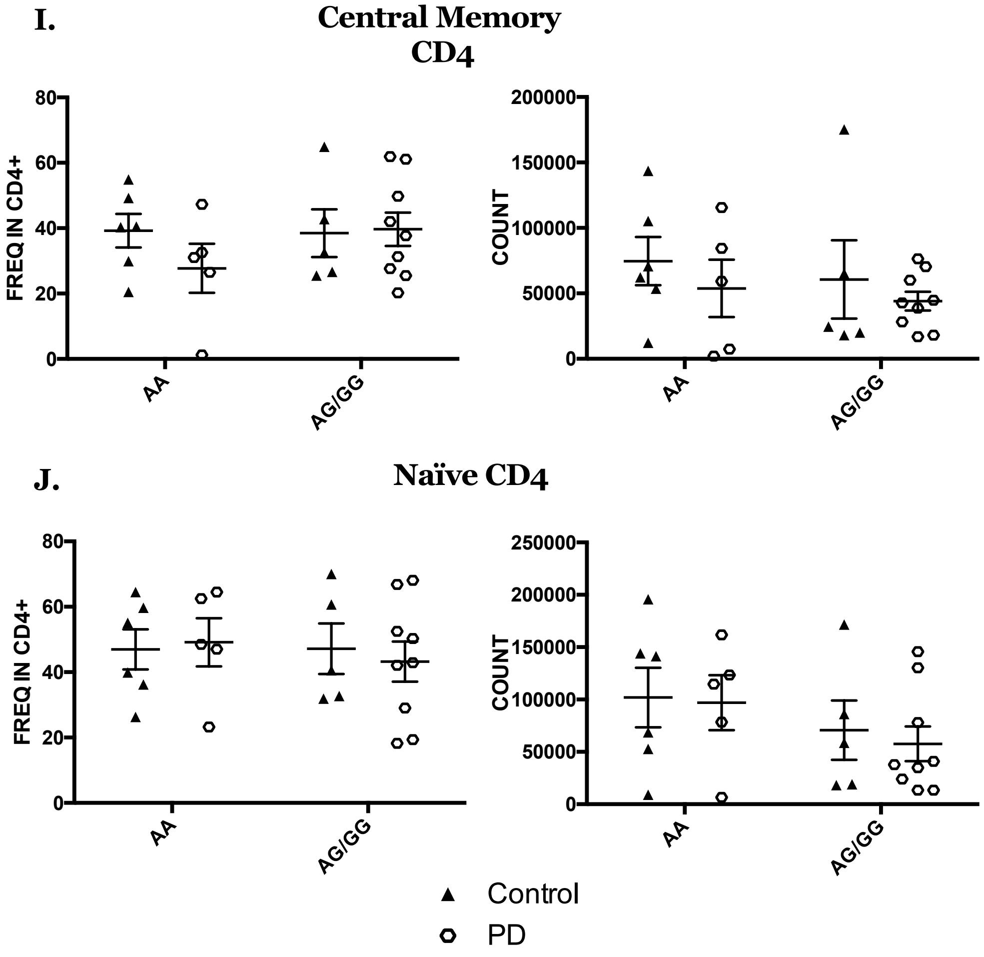

Figure 24.I-J. **High-risk *rs3129882* genotype is associated with decreased number of Tregs, and interactions between SNP genotype and PD affect effector memory subset counts.** Flow cytometry staining was used to determine frequencies and counts of T cells in cryopreserved PBMC samples. Two-way ANOVA was used to test for significant differences between control (triangles) AA, p values are indicated above applicable graphs.

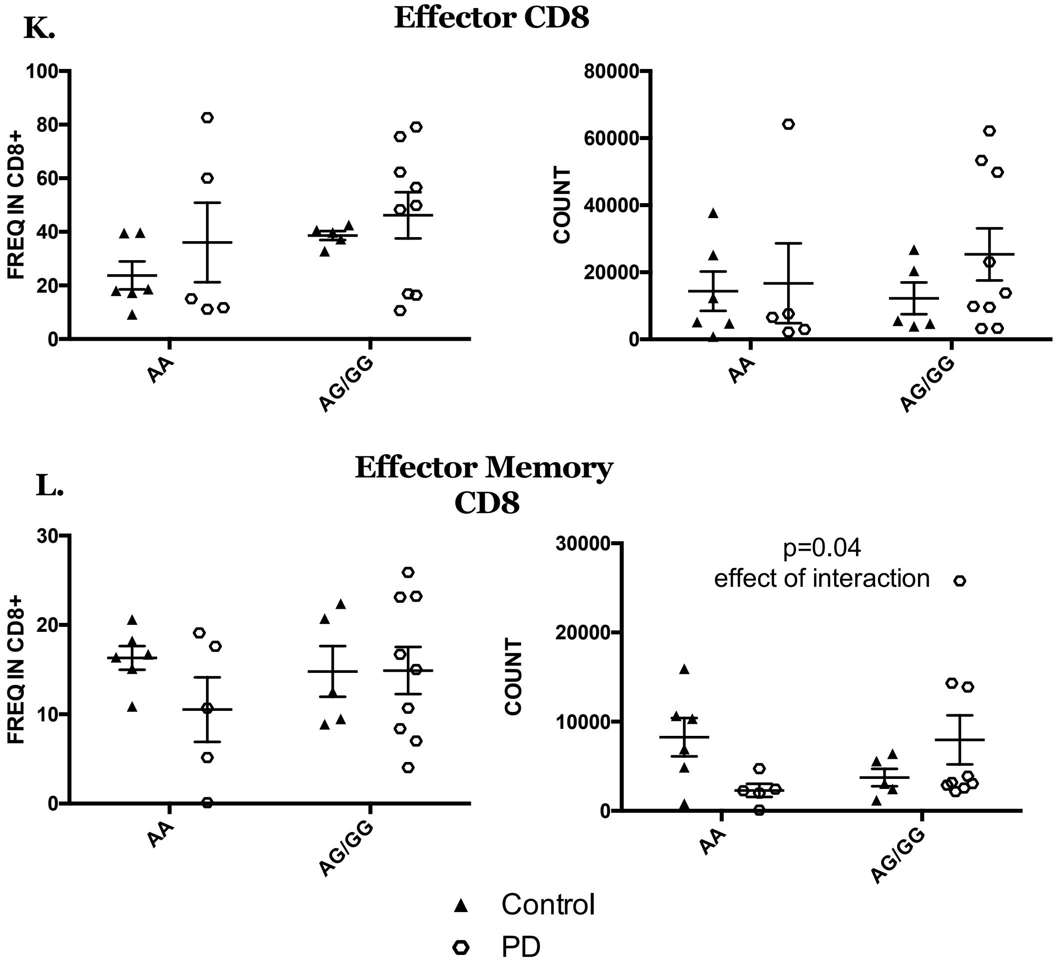

Figure 24.K-L. High-risk *rs3129882* genotype is associated with decreased number of Tregs, and interactions between SNP genotype and PD affect effector memory subset counts. Flow cytometry staining was used to determine frequencies and counts of T cells in cryopreserved PBMC samples. Two-way ANOVA was used to test for significant differences between control (triangles) AA, p values are indicated above applicable graphs.

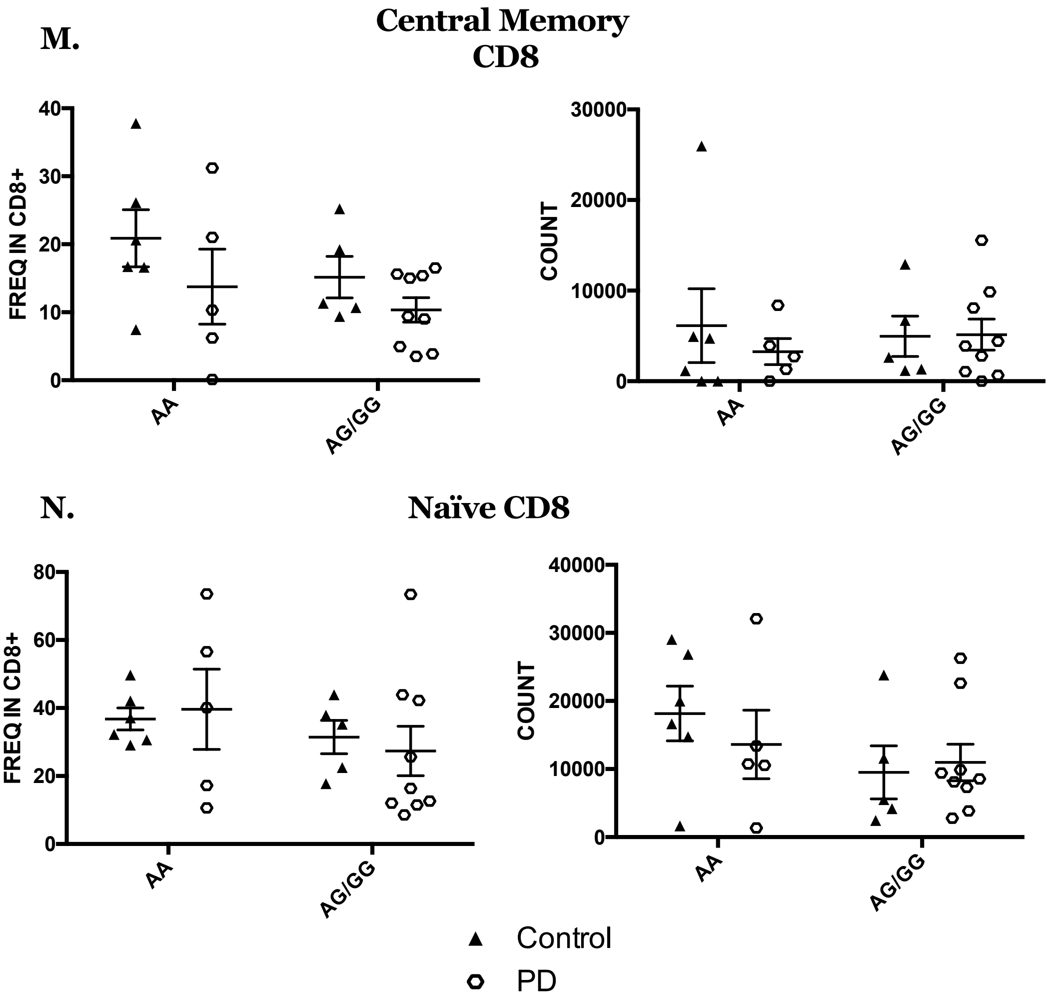

Figure 24.M-N. **High-risk *rs3129882* genotype is associated with decreased number of Tregs, and interactions between SNP genotype and PD affect effector memory subset counts.** Flow cytometry staining was used to determine frequencies and counts of T cells in cryopreserved PBMC samples. Two-way ANOVA was used to test for significant differences between control (triangles) AA, p values are indicated above applicable graphs.

4.4 Discussion

In a population of PD and control participants recruited from the University of Florida, we report that the high-risk *rs3129882* genotype is associated with decreased number of Tregs (**Figure 24.D**). Tregs are an immunosuppressive T cell subset which maintain self-tolerance, prevent autoimmunity, and regulate inflammatory responses to injury and pathogens. Individuals with 1 or more *G* alleles at *rs3129882* showed decreased number of Tregs. Interestingly, in our study PD was associated with an increased frequency of Tregs, in contrast to previous reports (Saunders et al., 2012; Chen et al., 2015). This could be due to a number of different possibilities including age and ethnic differences and/or the effects of medications (**Figure 24.D**). Treg functions include anti-inflammatory (IL-35, IL-10, and TGF-β) cytokine release, suppression of CD8+ T cells' granzyme functions, "absorbing" IL-2 in the extracellular milieu thereby preventing proliferation of other T cells in the area, and driving downregulation of CD80 and CD86 (co-stimulatory molecules on antigen presenting cells) via CTLA-4 action (reviewed in (Duffy et al., 2018b)). The suppressive functions of Tregs limit the proliferation and effector functions of CD4+ and CD8+ T cells and can inhibit antigen presenting cells as well (Sakaguchi et al., 2008). Decreased number of Tregs, then, could create an immune environment permissive of the runaway inflammation thought to promote neurodegeneration.

We also observed an interaction between SNP genotype and PD affecting effector memory subset counts (**Figure 24.H** and **L**). In controls, having one or more *G* allele was associated with decreased number of effector memory CD4+ or effector memory CD8+ T cells. Conversely, in PD cases, *AG/GG* individuals displayed increased counts of effector memory CD4+ and CD8+ T cells. One possible explanation for this finding may be that in controls, other compensatory mechanisms prevent high MHCII expression related to a high-risk *rs3129882* genotype from driving increases in effector memory subset numbers. This is consistent with the observation that PD *GG*, but not control *GG* individuals had increased inducibility of MHCII (Kannarkat et al., 2015). Environmental exposures or other genetic factors may account for this difference.

As discussed in **Chapter** 1, there exist T cells in the peripheral blood mononuclear cell (PBMC) population from PD patients that recognize α-synuclein-derived peptides (Sulzer et al., 2017). As the study population expands and recruitment continues, increases in the frequency or number of Th17 in the *AG/GG* population are predicted to be identified. In addition to changes in T helper cells, shifts in memory cell frequency may also play an important role in PD risk or progression. Historically memory T cells have been divided into subsets on the basis of surface marker expression, as was done in the work presented below. Doing so implies that phenotypic differences between the defined subsets are cleanly associated with distinct immune functions. The appeal of such divisions of cell subsets is that shifts in one or the other can be quantified and associated with a disease state or genotype of interest. Nevertheless, the field of T cell memory research is shifting toward regarding T cells on a continuum, rather than as members of discrete types (Jameson and Masopust, 2018). This is an important caveat that must be kept in mind when interpreting the work presented here and future experiments on memory subsets.

Functions of memory T cells may vary within populations with matching surface markers. For example the trafficking, durability, and effector functions of CD8+CD62L- T cells, traditionally classified as effector memory CD8 T cells, may be heterogeneous as many cells within that population will actually be resident, non-circulating memory T cells (Sathaliyawala et al., 2013). The extent to which the perivascular space in the brain or the parenchyma itself has such a population of resident memory T cells remains to be investigated, and will be critical for our understanding of the adaptive immune systems contributions to PD.

In conclusion, these data point towards an association between *rs3129882* genotype and the frequencies of CD4+ T cells subsets; however, more research is needed in a larger cohort. It remains to be investigated by what mechanism the *rs3129882* SNP, in a non-coding region of the *HLA-DR* locus, increases MHCII expression, and future studies will address the hypothesis that *rs3129882* is linked to a *cis*-regulatory element. The *cis*-regulatory element could directly regulate MHC-II gene expression or an epigenetic state controlling the expression of genes within the *HLA* locus. Future studies should also investigate whether the groups included in the work presented here are characterized by differences in the frequencies of certain antigen-specific T cells. By continuing this line of research, future studies will push the field toward a more complete understanding of the pathogenesis of PD and new therapeutic strategies may emerge that engage the immune system to prevent or slow the progression of PD.

CHAPTER 5. CONCLUSIONS

Parkinson's disease is a neurodegenerative movement disorder characterized by degeneration of dopaminergic neurons in the substantia nigra and aggregation of α-synuclein. Currently, no disease-modifying therapies exist for this progressive disorder. The cause of Parkinson's disease (PD) is unknown, although genetic and environmental risk factors have been identified and are reviewed in detail in **Chapter 1**. The signaling pathways downstream of mixed lineage kinases and antigen presentation regulate a multitude of neuronal and immune functions and are of interest in PD.

In **Chapter 2**, we presented a series of experiments testing an inhibitor of mixed lineage kinase 3 in a neurotoxin model of PD. Mixed lineage kinases (MLKs) are upstream of cell death pathways, and previous work focused on inhibition as a possible neuroprotective strategy, potentially blocking apoptotic cascades. The studies presented were motivated by the observation that the MLK inhibitor CEP-1347 mediates neuroprotection against methamphetamine in human mesencephalic-derived neurons (Lotharius et al., 2005). CEP-1347 also prevented motor deficits and DA neuronal degeneration in a mouse 1-methyl-4-phenyl-1,2,3,6-tetrahydropyridine (MPTP) model of nigral degeneration (Hudkins et al., 2008). While results from these models were promising and CEP-1347 was found to be safe and well tolerated over 4 weeks in subjects with PD, clinical trials with CEP-1347 failed in a Phase II trial of 806 PD patients due to futility (Parkinson Study Group, 2007). The failure of CEP-1347 to have beneficial effect in PD patients was attributed to poor brain penetrance (brain/plasma ratio < 0.2 in mice) and off-target effects (Parkinson Study

Group, 2007) (Goodfellow et al., 2013). We hypothesized that a more specific MLK inhibitor with greater brain penetrance may be more effective than CEP-1347. While this hypothesis will ultimately need to be tested in human PD patients and compared to healthy controls, we initiated investigation in a mouse MPTP model to assess the protective capacity of the mixed lineage kinase 3 (MLK3) inhibitor CLFB-1134. We found that CLFB-1134 protected dopaminergic cell bodies and terminals against MPTP (**Figure 4** and **6**). However, striatal levels of dopamine were not restored to the level observed in control animals (**Figure 5**). As discussed in section **2.4**, the presence of neuroprotection without restoring dopamine levels to those seen in controls has been observed in other MPTP models (Liberatore et al., 1999; Zhang et al., 2004; Hu et al., 2008). As a complex-I inhibitor, MPTP effects mitochondrial energetics and, by depleting ATP, may prevent the activation of dopamine-synthesizing enzymes (tyrosine hydroxylase). Another possible explanation of our observation may be the effects of MPTP on pathways other than those regulated by MLK3.

Future expansion of this work should investigate the effect of CLFB-1134 on microglia, brain-infiltrating peripheral immune cells, and astrocytes, as these cell types express MLK3. This may provide insight into the role of MLK3 in neuroinflammation and neurodegeneration. Supporting this idea, URMC-099, another MLK3 inhibitor, has been shown to successfully inhibit lipopolysaccharide induction of tumor necrosis factor release from microglia and facilitates microglial clearance of amyloid beta *ex vivo* (Dong et al., 2016). Thus, in addition to direct neuronal action, the capacity for MLK inhibition to engage glia may contribute to the neuroprotective effect observed in our studies with CLFB-1134.

In **Chapter 3,** we investigated the role of peripheral myeloid cell antigen presentation in a mouse model of human α-synuclein expression. Antigen presentation via the protein major histocompatibility complex class II (MHCII) is suspected to contribute to PD pathology based on genome-wide association studies, post-mortem histology, and evidence from animal models of PD. Previous work showed that global deletion of MHCII or CIITA was protective in a mouse model of PD pathology in which human α-synuclein is expressed in the SN (Harms et al., 2013; Williams et al., 2018). Importantly, full deletion of MHCII prevents normal T cell development. Therefore, the neuroprotection observed in Harms et al. and Williams et al. is achieved by preventing antigen presentation in combination with blunted adaptive immune system function (Harms et al., 2013); (Williams et al., 2018). Because work from Kannarkat et al. demonstrated an association between PD risk and increased baseline MHCII expression on monocytes in the peripheral blood, we wanted to know whether specific MHCII deletion on peripheral myeloid cells is sufficient to achieve neuroprotection against a nigral α-synuclein lesion (Kannarkat et al., 2015). Through the work presented in **Chapter 3,** we advanced the field by demonstrating that mice with peripheral myeloid deletion of MHCII maintain dopaminergic terminals to a greater extent than animals with intact MHCII in an rAAV2/9 human WT α-synuclein model (**Figure 21**). This suggests that manipulating MHCII on peripheral myeloid cells in PD patients may be sufficient to slow the progression of dopaminergic neuron loss.

The common genetic variation in *HLA-DRA, rs3129882*, synergizes with exposure to pyrethroid pesticides to increase risk for PD (Kannarkat et al., 2015). To characterize the effect of the pyrethroid cypermethrin on the immune system and its influence on the toxicity of α-synuclein, we performed a "double-hit" study, described in **Chapter 3.** Mice were given a unilateral injection of rAAV2/5 human WT α-synuclein as well as treatment with cypermethrin twice weekly for 3 weeks. The high-risk *rs3129882* genotype is associated with increased baseline MHCII expression, suggesting the combination of high MHCII and pyrethroid exposure produce increased risk for PD. We predicted that in the absence of peripheral myeloid MHCII, any inflammatory or neurotoxic effects of cypermethrin would be lessened. We found, however, that this level of cypermethrin exposure did not exacerbate inflammation or degeneration driven by human α-synuclein in the mouse nigra. Therefore, no clear relationship between cypermethrin and MHCII expression level could be discerned.

Overall, the data reported in **Chapter 3** motivate additional experiments. First, characterization of the synuclein-induced lesion at the level of the nigra should be performed. The striatum is a large and internally variable structure, and the quantification of nigral TH+ soma will more precisely inform us regarding the extent of synuclein-induced lesion. Furthermore, we will be able to determine whether the maintenance of dopaminergic phenotype in the striatum in LysMCre+I-Ab$^{fl/fl}$ mice in the rAAV2/9 study is accompanied by increased nigral neuron survival. Next, more chronic dosing of cypermethrin would be of interest. A dosing route that is more translationally relevant than intraperitoneal injection could be utilized. It would also be beneficial to perform experiments similar to those presented here in animals with upregulation of MHCII, mimicking the immune systems of humans with the high-risk *rs3129882* genotype.

While previous work indicated that deletion of MHCII is neuroprotective, those observations occurred in the context of arrested T cell development (Harms et al., 2013; Williams et al., 2018). Work from Jimenez-Ferrer et al. addressed global MHCII decrease, but not total ablation (Jimenez-Ferrer and Swanberg, 2018). Rats in this study are hypothesized to have relatively normal T cells, but lower expression of MHCII on monocytes, macrophages, dendritic cells, and microglia. The global decrease in MHCII was associated with more severe synuclein-induced degeneration and motor behavioral impairments (Jimenez-Ferrer and Swanberg, 2018). It may be the case that antigen presentation by microglia has a different functional outcome than antigen presentation by peripheral immune cells. This would account for the deleterious effects of global MHCII decrease and the striatal terminal protection we observed in mice with peripheral myeloid MHCII deletion.

In the study by Kannarkat et al., the effects of rs3129882 were only assessed on monocytes and B cells. Because MHCII mediates innate and adaptive immune system crosstalk, we were interested in the relationship between rs3129882-related MHCII expression levels and the types of CD4+ T cell subsets in circulation. **Chapter 4** presented work in its early stages on human PD patients and healthy controls. The data generated suggest that there may be an association between *rs3129882* genotype and the frequencies of certain CD4+ T cells subsets (Tregs, effector and central memory T cells, **Figure 24**). More research is needed in a larger cohort. Due to the abovementioned synergy between pyrethroid exposure and rs3129882 genotype, the environmental exposure history of our cohort should be interrogated to determine if the association with pyrethroid exposure replicates in our study population. Future studies should also investigate whether the groups included in the work presented here are characterized by differences in the frequencies of certain antigen-specific T cells. This recommendation is based on the fact that T cells specific for α-synuclein-derived peptide have been identified in PD patients (Sulzer et al., 2017). The abundance of such antigen-specific T cells may be greater in individuals with greater antigen presentation capacity (*GG* individuals).

MHCII antigen presentation and MLK3 kinase function regulate key immune and neuronal functions that appear to influence the neurodegenerative process in PD. Anti-inflammatory therapeutic interventions that attempt to diminish MHCII expression and inhibition of MLK3 represent different approaches to preserve nigrostriatal dopamine and prevent the progression of degeneration in PD.

	Antibody	Manufacturer	Catalog Number	Dilution
	Rb anti-tyrosine hyrdoxylase	Millipore	AB152	1:500 IF, 1:1500 WB
	Ms anti-alpha-synuclein	BioLegend	807801	1:500 IF
	Ms anti-alpha-synuclein	ThermoFischer Scientific	32-8100	1:1000 WB
	Rt anti-dopamine transporter	Millipore	MAB369	1:5000 WB
	Gt anti-Ms IgG-HRP	BioLegend	405306	1:2000 WB
	Gt anti-Rt IgG-HRP	Jackson ImmunoResearch	112-035-006	1:2000 WB
	Gt anti-Rb IgG-HRP	Jackson ImmunoResearch	111-035-144	1:2000 WB
	Gt anti-Ms IgG-594	Invitrogen	A11020	1:1000 IF
	Gt anti-Rb IgG-488	Invitrogen	A11070	1:1000 IF
Panel 1	Rt anti-Ly6C-**FITC**	BioLegend	53-5932-82	1:100 Flow
	Rt anti-CD45-**PerCp-Cy5.5**	eBioscience	45-0451-80	1:100 Flow
	Rt anti-CD11b-**Pe-Cy7**	BioLegend	101215	1:200 Flow
	Rt anti-Ly6G-**AF700**	eBioscience	56-5931-80	1:100 Flow
	Arm Ham anti-CD11c-**BV711**	BioLegend	117349	1:100 Flow
	Rt anti-MHCII-**APC Cy7**	BioLegend	107627	1:200 Flow
	Rt anti-CD3-**BV421**	BioLegend	100227	1:50 Flow
	Rat anti-CD19-**BV650**	BioLegend	115541	1:100 Flow
	Live/Dead Fixable Red **PE 610**	Life Technologies/Invitrogen Corp.	L23102_3625538389	1:2000 Flow
Panel 2	Rt anti-CD45-**PerCp-Cy5.5**	eBioscience	45-0451-80	1:100 Flow
	Rt anti-CD11b-**PE-Cy7**	BioLegend	101215	1:200 Flow
	Rt anti-Ly6C-**BV785**	BioLegend	128041	1:100 Flow
	Rt anti-Ly6G-**AF700**	eBioscience	56-5931-80	1:100 Flow
	Arm Ham anti-CD11c-**BV711**	BioLegend	117349	1:100 Flow
	Rt anti-MHCII-**APC Cy7**	BioLegend	107627	1:200 Flow
	Live/Dead Fixable Red **PE 610**	Life Technologies/Invitrogen Corp.	L23102_3625538389	1:2000 Flow
Panel 3	Arm Ham anti-CD3-**PE610**	eBioscience	61-0031	1:100 Flow
	Rt anti-CD4-**FITC**	eBioscience	53-0041	1:100 Flow
	Rt anti-CD8b-**APC-e780**	eBioscience	47-0083-82	1:100 Flow
	Rt-anti-CD62L-**Pe-Cy7**	eBioscience	25-0621-81	1:200 Flow
	Rt anti-CD44-**AF700**	BioLegend	103026	1:100 Flow
	Rt anti-FoxP3-**APC**	eBioscience	17-5773	1:20 Flow
	Ms anti-Tbet-**PerCp-Cy5.5**	BioLegend	644805	1:20 Flow
	Live/Dead Fixable Aqua **AmCyan**	Molecular Probes	L34957	1:2000 Flow
Panel 4	Rt anti-CD11b-**FITC**	eBioscience	11-0112	1:50 Flow
	Rt anti-CD19-**PE**	eBioscience	12-0193-81	1:500 Flow
	Rt anti-CD45-**PerCp-Cy5.5**	eBioscience	45-0451-80	1:100 Flow
	Rt anti-MHCII-**PE-Cy7**	eBIoscience	25-5321-80	1:500 Flow
	Arm Ham anti-CD3-**APC**	eBioscience	17-0031-81	1:100 Flow
	Rt anti-Ly6C-**APC Cy7**	BioLegend	128026	1:100 Flow
	Rt anti-Ly6G-**v450**	BioLegend	127611	1:50 Flow
	Live/Dead Fixable Aqua **AmCyan**	Molecular Probes	L34957	1:2000 Flow
Panel 5	Ms anti-CD3-**v450**	BioLegend	560365	1:20 Flow
	Ms anti-CD4-**PerCp-Cy5.5**	BioLegend	317428	1:100 Flow
	Ms anti-CD8-**APCH7**	BD Biosciences	560179	1:50 Flow
	Ms anti-CD45RA-**Pe-Cy7**	BioLegend	304126	1:100 Flow
	anti-CD25-**FITC**	BioLegend	302604	1:20 Flow
	Ms anti-CCR7-**PE**	BioLegend	353204	1:100 Flow
	Ms anti-CCR4-**BV605**	BD Biosciences	564906	1:50 Flow
	Ms anti-CCR6-**APC**	BioLegend	353416	1:20 Flow
	Live/Dead Fixable Red **PE 610**	Life Technologies/Invitrogen Corp.	L23102_3625538389	1:2000 Flow

Appendix 1. Antibodies used in Chapters 2-4.

References

Ahmed I, Tamouza R, Delord M, Krishnamoorthy R, Tzourio C, Mulot C, Nacfer M, Lambert JC, Beaune P, Laurent-Puig P, Loriot MA, Charron D, Elbaz A (2012) Association between Parkinson's disease and the HLA-DRB1 locus. Mov Disord 27:1104-1110.

Allen Reish HE, Standaert DG (2015) Role of alpha-synuclein in inducing innate and adaptive immunity in Parkinson disease. J Parkinsons Dis 5:1-19.

Alliot F, Godin I, Pessac B (1999) Microglia derive from progenitors, originating from the yolk sac, and which proliferate in the brain. Brain Res Dev Brain Res 117:145-152.

Ambrosi G, Kustrimovic N, Siani F, Rasini E, Cerri S, Ghezzi C, Dicorato G, Caputo S, Marino F, Cosentino M, Blandini F (2017) Complex Changes in the Innate and Adaptive Immunity Accompany Progressive Degeneration of the Nigrostriatal Pathway Induced by Intrastriatal Injection of 6-Hydroxydopamine in the Rat. Neurotoxicity research 32:71-81.

Anadon A, Martinez-Larranaga MR, Fernandez-Cruz ML, Diaz MJ, Fernandez MC, Martinez MA (1996) Toxicokinetics of deltamethrin and its 4'-HO-metabolite in the rat. Toxicol Appl Pharmacol 141:8-16.

Andersen JK (2001) Does neuronal loss in Parkinson's disease involve programmed cell death? BioEssays : news and reviews in molecular, cellular and developmental biology 23:640-646.

Appel SH, Beers DR, Henkel JS (2010) T cell-microglial dialogue in Parkinson's disease and amyotrophic lateral sclerosis: are we listening? Trends Immunol 31:7-17.

Aw D, Silva AB, Palmer DB (2007) Immunosenescence: emerging challenges for an ageing population. Immunology 120:435-446.

Baba Y, Kuroiwa A, Uitti RJ, Wszolek ZK, Yamada T (2005) Alterations of T-lymphocyte populations in Parkinson disease. Parkinsonism Relat Disord 11:493-498.

Banati RB, Myers R, Kreutzberg GW (1997) PK ('peripheral benzodiazepine')--binding sites in the CNS indicate early and discrete brain lesions: microautoradiographic detection of [3H]PK11195 binding to activated microglia. J Neurocytol 26:77-82.

Banati RB, Daniel SE, Blunt SB (1998) Glial pathology but absence of apoptotic nigral neurons in long-standing Parkinson's disease. Mov Disord 13:221-227.

Barkholt P, Sanchez-Guajardo V, Kirik D, Romero-Ramos M (2012) Long-term polarization of microglia upon alpha-synuclein overexpression in nonhuman primates. Neuroscience 208:85-96.

Bas J, Calopa M, Mestre M, Mollevi DG, Cutillas B, Ambrosio S, Buendia E (2001) Lymphocyte populations in Parkinson's disease and in rat models of parkinsonism. J Neuroimmunol 113:146-152.

Bellizzi MJ, Hammond JW, Li H, Gantz Marker MA, Marker DF, Freeman RS, Gelbard HA (2018) The Mixed-Lineage Kinase Inhibitor URMC-099 Protects Hippocampal Synapses in Experimental Autoimmune Encephalomyelitis. eneuro 5:ENEURO.0245-0218.

Benabid AL, Pollak P, Louveau A, Henry S, de Rougemont J (1987) Combined (thalamotomy and stimulation) stereotactic surgery of the VIM thalamic nucleus for bilateral Parkinson disease. Appl Neurophysiol 50:344-346.

Bendor JT, Logan TP, Edwards RH (2013) The function of alpha-synuclein. Neuron 79:1044-1066.

Benkler M, Agmon-Levin N, Shoenfeld Y (2009) Parkinson's disease, autoimmunity, and olfaction. Int J Neurosci 119:2133-2143.

Benkler M, Agmon-Levin N, Hassin-Baer S, Cohen OS, Ortega-Hernandez OD, Levy A, Moscavitch SD, Szyper-Kravitz M, Damianovich M, Blank M, Chapman J, Shoenfeld Y (2012) Immunology, autoimmunity, and autoantibodies in Parkinson's disease. Clin Rev Allergy Immunol 42:164-171.

Benner EJ, Banerjee R, Reynolds AD, Sherman S, Pisarev VM, Tsiperson V, Nemachek C, Ciborowski P, Przedborski S, Mosley RL, Gendelman HE (2008) Nitrated alpha-synuclein immunity accelerates degeneration of nigral dopaminergic neurons. PLoS One 3:e1376.

Berwick DC, Javaheri B, Wetzel A, Hopkinson M, Nixon-Abell J, Granno S, Pitsillides AA, Harvey K (2017) Pathogenic LRRK2 variants are gain-of-function mutations that enhance LRRK2-mediated repression of beta-catenin signaling. Mol Neurodegener 12:9.

Billingsley KJ, Bandres-Ciga S, Saez-Atienzar S, Singleton AB (2018) Genetic risk factors in Parkinson's disease. Cell Tissue Res 373:9-20.

Birkmayer W, Hornykiewicz O (1961) [The L-3,4-dioxyphenylalanine (DOPA)-effect in Parkinson-akinesia]. Wien Klin Wochenschr 73:787-788.

Boka G, Anglade P, Wallach D, Javoy-Agid F, Agid Y, Hirsch EC (1994) Immunocytochemical analysis of tumor necrosis factor and its receptors in Parkinson's disease. Neurosci Lett 172:151-154.

Bolte AC, Lukens JR (2018) Th17 Cells in Parkinson's Disease: The Bane of the Midbrain. Cell Stem Cell 23:5-6.

Bonifati V, Rizzu P, Squitieri F, Krieger E, Vanacore N, van Swieten JC, Brice A, van Duijn CM, Oostra B, Meco G, Heutink P (2003) DJ-1(PARK7), a novel gene for autosomal recessive, early onset parkinsonism. Neurol Sci 24:159-160.

Bottner M, Zorenkov D, Hellwig I, Barrenschee M, Harde J, Fricke T, Deuschl G, Egberts JH, Becker T, Fritscher-Ravens A, Arlt A, Wedel T (2012) Expression pattern and localization of alpha-synuclein in the human enteric nervous system. Neurobiol Dis 48:474-480.

Bouvier NM, Palese P (2008) The biology of influenza viruses. Vaccine 26 Suppl 4:D49-53.

Braak H, Del Tredici K, Rub U, de Vos RA, Jansen Steur EN, Braak E (2003) Staging of brain pathology related to sporadic Parkinson's disease. Neurobiol Aging 24:197-211.

Brochard V, Combadiere B, Prigent A, Laouar Y, Perrin A, Beray-Berthat V, Bonduelle O, Alvarez-Fischer D, Callebert J, Launay JM, Duyckaerts C, Flavell RA, Hirsch EC, Hunot S (2009) Infiltration of CD4+ lymphocytes into the brain contributes to neurodegeneration in a mouse model of Parkinson disease. J Clin Invest 119:182-192.

Brown LD, Narahashi T (1992) Modulation of nerve membrane sodium channel activation by deltamethrin. Brain research 584:71-76.

Burke RE (2007) Inhibition of mitogen-activated protein kinase and stimulation of Akt kinase signaling pathways: Two approaches with therapeutic potential in the treatment of neurodegenerative disease. Pharmacology & therapeutics 114:261-277.

Butterfield PG, Valanis BG, Spencer PS, Lindeman CA, Nutt JG (1993) Environmental antecedents of young-onset Parkinson's disease. Neurology 43:1150-1158.

Calderon-Garciduenas L, Gonzalez-Maciel A, Reynoso-Robles R, Kulesza RJ, Mukherjee PS, Torres-Jardon R, Ronkko T, Doty RL (2018) Alzheimer's disease and alpha-synuclein pathology in the olfactory bulbs of infants, children, teens and adults </=40 years in Metropolitan Mexico City. APOE4 carriers at higher risk of suicide accelerate their olfactory bulb pathology. Environ Res 166:348-362.

Campos-Acuna J, Elgueta D, Pacheco R (2019) T-Cell-Driven Inflammation as a Mediator of the Gut-Brain Axis Involved in Parkinson's Disease. Front Immunol 10:239.

Cao S, Theodore S, Standaert DG (2010) Fcgamma receptors are required for NF-kappaB signaling, microglial activation and dopaminergic neurodegeneration in an AAV-synuclein mouse model of Parkinson's disease. Mol Neurodegener 5:42.

Carrion MDP, Marsicano S, Daniele F, Marte A, Pischedda F, Di Cairano E, Piovesana E, von Zweydorf F, Kremmer E, Gloeckner CJ, Onofri F, Perego C, Piccoli G (2017) The LRRK2 G2385R variant is a partial loss-of-function mutation that affects synaptic vesicle trafficking through altered protein interactions. Sci Rep 7:5377.

Castro-Sanchez S, Garcia-Yague AJ, Lopez-Royo T, Casarejos M, Lanciego JL, Lastres-Becker I (2018) Cx3cr1-deficiency exacerbates alpha-synuclein-A53T induced neuroinflammation and neurodegeneration in a mouse model of Parkinson's disease. Glia 66:1752-1762.

Caudle WM, Richardson JR, Delea KC, Guillot TS, Wang M, Pennell KD, Miller GW (2006) Polychlorinated biphenyl-induced reduction of dopamine transporter expression as a precursor to Parkinson's disease-associated dopamine toxicity. Toxicol Sci 92:490-499.

Caudle WM, Richardson JR, Wang MZ, Taylor TN, Guillot TS, McCormack AL, Colebrooke RE, Di Monte DA, Emson PC, Miller GW (2007) Reduced vesicular storage of dopamine causes progressive nigrostriatal neurodegeneration. J Neurosci 27:8138-8148.

Cebrian C, Zucca FA, Mauri P, Steinbeck JA, Studer L, Scherzer CR, Kanter E, Budhu S, Mandelbaum J, Vonsattel JP, Zecca L, Loike JD, Sulzer D (2014) MHC-I expression renders catecholaminergic neurons susceptible to T-cell-mediated degeneration. Nat Commun 5:3633.

Cha GH, Kim S, Park J, Lee E, Kim M, Lee SB, Kim JM, Chung J, Cho KS (2005) Parkin negatively regulates JNK pathway in the dopaminergic neurons of Drosophila. Proc Natl Acad Sci U S A 102:10345-10350.

Chang D, Nalls MA, Hallgrimsdottir IB, Hunkapiller J, van der Brug M, Cai F, International Parkinson's Disease Genomics C, andMe Research T, Kerchner GA, Ayalon G, Bingol B, Sheng M, Hinds D, Behrens TW, Singleton AB, Bhangale TR, Graham RR (2017) A meta-analysis of genome-wide association studies identifies 17 new Parkinson's disease risk loci. Nat Genet 49:1511-1516.

Chauhan LK, Varshney M, Pandey V, Sharma P, Verma VK, Kumar P, Goel SK (2016) ROS-dependent genotoxicity, cell cycle perturbations and apoptosis in mouse bone marrow cells exposed to formulated mixture of cypermethrin and chlorpyrifos. Mutagenesis 31:635-642.

Chen J, Su P, Luo W, Chen J (2018) Role of LRRK2 in manganese-induced neuroinflammation and microglial autophagy. Biochem Biophys Res Commun 498:171-177.

Chen L, Mo M, Li G, Cen L, Wei L, Xiao Y, Chen X, Li S, Yang X, Qu S, Xu P (2016) The biomarkers of immune dysregulation and inflammation response in Parkinson disease. Transl Neurodegener 5:16.

Chen Y, Qi B, Xu W, Ma B, Li L, Chen Q, Qian W, Liu X, Qu H (2015) Clinical correlation of peripheral CD4+cell subsets, their imbalance and Parkinson's disease. Mol Med Rep 12:6105-6111.

Chervonsky AV (2010) Influence of microbial environment on autoimmunity. Nat Immunol 11:28-35.

Choi BK, Choi MG, Kim JY, Yang Y, Lai Y, Kweon DH, Lee NK, Shin YK (2013) Large alpha-synuclein oligomers inhibit neuronal SNARE-mediated vesicle docking. Proc Natl Acad Sci U S A 110:4087-4092.

Choi NM, Majumder P, Boss JM (2011) Regulation of major histocompatibility complex class II genes. Current opinion in immunology 23:81-87.

Choudhary B, Kamak M, Ratnakaran N, Kumar J, Awasthi A, Li C, Nguyen K, Matsumoto K, Hisamoto N, Koushika SP (2017) UNC-16/JIP3 regulates early events in synaptic vesicle protein trafficking via LRK-1/LRRK2 and AP complexes. PLoS Genet 13:e1007100.

Chrustek A, Holynska-Iwan I, Dziembowska I, Bogusiewicz J, Wroblewski M, Cwynar A, Olszewska-Slonina D (2018) Current Research on the Safety of Pyrethroids Used as Insecticides. Medicina (Kaunas) 54.

Chung CY, Koprich JB, Siddiqi H, Isacson O (2009) Dynamic changes in presynaptic and axonal transport proteins combined with striatal neuroinflammation precede dopaminergic neuronal loss in a rat model of AAV alpha-synucleinopathy. J Neurosci 29:3365-3373.

Clausen BE, Burkhardt C, Reith W, Renkawitz R, Forster I (1999) Conditional gene targeting in macrophages and granulocytes using LysMcre mice. Transgenic Res 8:265-277.

Consortium UKPsD et al. (2011) Dissection of the genetics of Parkinson's disease identifies an additional association 5' of SNCA and multiple associated haplotypes at 17q21. Hum Mol Genet 20:345-353.

Contreras F, Prado C, Gonzalez H, Franz D, Osorio-Barrios F, Osorio F, Ugalde V, Lopez E, Elgueta D, Figueroa A, Lladser A, Pacheco R (2016) Dopamine Receptor D3 Signaling on CD4+ T Cells Favors Th1- and Th17-Mediated Immunity. J Immunol 196:4143-4149.

Cook DA, Tansey MG (2017) LRRK2. In: Neuroimmune Pharmacology (Gendelman HE, Ikezu T, eds): Springer, Cham.

Cookson MR (2012) Evolution of neurodegeneration. Curr Biol 22:R753-761.

Coque E et al. (2019) Cytotoxic CD8(+) T lymphocytes expressing ALS-causing SOD1 mutant selectively trigger death of spinal motoneurons. Proc Natl Acad Sci U S A 116:2312-2317.

Costa C, Rapisarda V, Catania S, Di Nola C, Ledda C, Fenga C (2013) Cytokine patterns in greenhouse workers occupationally exposed to alpha-cypermethrin: an observational study. Environ Toxicol Pharmacol 36:796-800.

Costa LG (2015) The neurotoxicity of organochlorine and pyrethroid pesticides. Handb Clin Neurol 131:135-148.

Craner MJ, Damarjian TG, Liu S, Hains BC, Lo AC, Black JA, Newcombe J, Cuzner ML, Waxman SG (2005) Sodium channels contribute to microglia/macrophage activation and function in EAE and MS. Glia 49:220-229.

Crawford MJ, Croucher A, Hutson DH (1981) Metabolism of cis- and trans-cypermethrin in rats. Balance and tissue retention study. J Agric Food Chem 29:130-135.

Croisier E, Moran LB, Dexter DT, Pearce RK, Graeber MB (2005) Microglial inflammation in the parkinsonian substantia nigra: relationship to alpha-synuclein deposition. J Neuroinflammation 2:14.

Cross M, Mangelsdorf I, Wedel A, Renkawitz R (1988) Mouse lysozyme M gene: isolation, characterization, and expression studies. Proc Natl Acad Sci U S A 85:6232-6236.

Daher JP, Volpicelli-Daley LA, Blackburn JP, Moehle MS, West AB (2014) Abrogation of alpha-synuclein-mediated dopaminergic neurodegeneration in LRRK2-deficient rats. Proc Natl Acad Sci U S A 111:9289-9294.

Das V, Nal B, Dujeancourt A, Thoulouze MI, Galli T, Roux P, Dautry-Varsat A, Alcover A (2004) Activation-induced polarized recycling targets T cell antigen receptors to the immunological synapse; involvement of SNARE complexes. Immunity 20:577-588.

Daubner SC, Le T, Wang S (2011) Tyrosine hydroxylase and regulation of dopamine synthesis. Archives of biochemistry and biophysics 508:1-12.

Dauer W, Przedborski S (2003) Parkinson's disease: mechanisms and models. Neuron 39:889-909.

de la Monte SM, Sohn YK, Ganju N, Wands JR (1998) P53- and CD95-associated apoptosis in neurodegenerative diseases. Lab Invest 78:401-411.

De Martinis M, Franceschi C, Monti D, Ginaldi L (2005) Inflamm-ageing and lifelong antigenic load as major determinants of ageing rate and longevity. FEBS Lett 579:2035-2039.

De Virgilio A, Greco A, Fabbrini G, Inghilleri M, Rizzo MI, Gallo A, Conte M, Rosato C, Ciniglio Appiani M, de Vincentiis M (2016) Parkinson's disease: Autoimmunity and neuroinflammation. Autoimmun Rev 15:1005-1011.

de Vos AF, van Meurs M, Brok HP, Boven LA, Hintzen RQ, van der Valk P, Ravid R, Rensing S, Boon L, t Hart BA, Laman JD (2002) Transfer of central nervous system autoantigens and presentation in secondary lymphoid organs. J Immunol 169:5415-5423.

Defazio G, Dal Toso R, Benvegnu D, Minozzi MC, Cananzi AR, Leon A (1994) Parkinsonian serum carries complement-dependent toxicity for rat mesencephalic dopaminergic neurons in culture. Brain research 633:206-212.

Del Prado-Lu JL (2015) Insecticide residues in soil, water, and eggplant fruits and farmers' health effects due to exposure to pesticides. Environ Health Prev Med 20:53-62.

Deleidi M, Gasser T (2013) The role of inflammation in sporadic and familial Parkinson's disease. Cell Mol Life Sci 70:4259-4273.

Delogu LG, Deidda S, Delitala G, Manetti R (2011) Infectious diseases and autoimmunity. J Infect Dev Ctries 5:679-687.

Di Monte DA (2003) The environment and Parkinson's disease: is the nigrostriatal system preferentially targeted by neurotoxins? Lancet Neurol 2:531-538.

Diao J, Burre J, Vivona S, Cipriano DJ, Sharma M, Kyoung M, Sudhof TC, Brunger AT (2013) Native alpha-synuclein induces clustering of synaptic-vesicle mimics via binding to phospholipids and synaptobrevin-2/VAMP2. Elife 2:e00592.

Dong W, Embury CM, Lu Y, Whitmire SM, Dyavarshetty B, Gelbard HA, Gendelman HE, Kiyota T (2016) The mixed-lineage kinase 3 inhibitor URMC-099 facilitates microglial amyloid-beta degradation. J Neuroinflammation 13:184.

Dorsey ER, Constantinescu R, Thompson JP, Biglan KM, Holloway RG, Kieburtz K, Marshall FJ, Ravina BM, Schifitto G, Siderowf A, Tanner CM (2007) Projected number of people with Parkinson disease in the most populous nations, 2005 through 2030. Neurology 68:384-386.

Double KL, Rowe DB, Carew-Jones FM, Hayes M, Chan DK, Blackie J, Corbett A, Joffe R, Fung VS, Morris J, Riederer P, Gerlach M, Halliday GM (2009) Anti-melanin antibodies are increased in sera in Parkinson's disease. Exp Neurol 217:297-301.

Douek DC, McFarland RD, Keiser PH, Gage EA, Massey JM, Haynes BF, Polis MA, Haase AT, Feinberg MB, Sullivan JL, Jamieson BD, Zack JA, Picker LJ, Koup RA (1998) Changes in thymic function with age and during the treatment of HIV infection. Nature 396:690-695.

Duffy MF, Collier TJ, Patterson JR, Kemp CJ, Fischer DL, Stoll AC, Sortwell CE (2018a) Quality Over Quantity: Advantages of Using Alpha-Synuclein Preformed Fibril Triggered Synucleinopathy to Model Idiopathic Parkinson's Disease. Front Neurosci 12:621.

Duffy SS, Keating BA, Perera CJ, Moalem-Taylor G (2018b) The role of regulatory T cells in nervous system pathologies. J Neurosci Res 96:951-968.

Duvoisin RC, Eldridge R, Williams A, Nutt J, Calne D (1981) Twin study of Parkinson disease. Neurology 31:77-80.

Dzamko N, Rowe DB, Halliday GM (2016) Increased peripheral inflammation in asymptomatic leucine-rich repeat kinase 2 mutation carriers. Mov Disord 31:889-897.

Dzamko N, Gysbers A, Perera G, Bahar A, Shankar A, Gao J, Fu Y, Halliday GM (2017) Toll-like receptor 2 is increased in neurons in Parkinson's disease brain and may contribute to alpha-synuclein pathology. Acta Neuropathol 133:303-319.

Eells JT, Dubocovich ML (1988) Pyrethroid insecticides evoke neurotransmitter release from rabbit striatal slices. J Pharmacol Exp Ther 246:514-521.

Eidson LN, Kannarkat GT, Barnum CJ, Chang J, Chung J, Caspell-Garcia C, Taylor P, Mollenhauer B, Schlossmacher MG, Ereshefsky L, Yen M, Kopil C, Frasier M, Marek K, Hertzberg VS, Tansey MG (2017) Candidate inflammatory biomarkers display unique relationships with alpha-synuclein and correlate with measures of disease severity in subjects with Parkinson's disease. J Neuroinflammation 14:164.

El Okda ES, Abdel-Hamid MA, Hamdy AM (2017) Immunological and genotoxic effects of occupational exposure to alpha-cypermethrin pesticide. Int J Occup Med Environ Health 30:603-615.

Eldridge R, Ince SE (1984) The low concordance rate for Parkinson's disease in twins: a possible explanation. Neurology 34:1354-1356.

Elgueta D, Contreras F, Prado C, Montoya A, Ugalde V, Chovar O, Villagra R, Henriquez C, Abellanas MA, Aymerich MS, Franco R, Pacheco R (2019) Dopamine Receptor D3 Expression Is Altered in CD4(+) T-Cells From Parkinson's Disease Patients and Its Pharmacologic Inhibition Attenuates the Motor Impairment in a Mouse Model. Front Immunol 10:981.

Ellis GI, Zhi L, Akundi R, Bueler H, Marti F (2013) Mitochondrial and cytosolic roles of PINK1 shape induced regulatory T-cell development and function. Eur J Immunol 43:3355-3360.

Fall CP, Bennett JP, Jr. (1999) Characterization and time course of MPP+ -induced apoptosis in human SH-SY5Y neuroblastoma cells. J Neurosci Res 55:620-628.

Febbraro F, Sahin G, Farran A, Soares S, Jensen PH, Kirik D, Romero-Ramos M (2013) Ser129D mutant alpha-synuclein induces earlier motor dysfunction while S129A results in distinctive pathology in a rat model of Parkinson's disease. Neurobiol Dis 56:47-58.

Fellner L, Irschick R, Schanda K, Reindl M, Klimaschewski L, Poewe W, Wenning GK, Stefanova N (2013) Toll-like receptor 4 is required for alpha-synuclein dependent activation of microglia and astroglia. Glia 61:349-360.

Ferrazza R, Cogo S, Melrose H, Bubacco L, Greggio E, Guella G, Civiero L, Plotegher N (2016) LRRK2 deficiency impacts ceramide metabolism in brain. Biochem Biophys Res Commun 478:1141-1146.

Ferrer I, Blanco R, Carmona M, Puig B, Barrachina M, Gomez C, Ambrosio S (2001) Active, phosphorylation-dependent mitogen-activated protein kinase (MAPK/ERK), stress-activated protein kinase/c-Jun N-terminal kinase (SAPK/JNK), and p38 kinase expression in Parkinson's disease and Dementia with Lewy bodies. J Neural Transm (Vienna) 108:1383-1396.

Feske S, Wulff H, Skolnik EY (2015) Ion channels in innate and adaptive immunity. Annu Rev Immunol 33:291-353.

Finkelstein MM, Jerrett M (2007) A study of the relationships between Parkinson's disease and markers of traffic-derived and environmental manganese air pollution in two Canadian cities. Environ Res 104:420-432.

Fischer DL, Gombash SE, Kemp CJ, Manfredsson FP, Polinski NK, Duffy MF, Sortwell CE (2016) Viral Vector-Based Modeling of Neurodegenerative Disorders: Parkinson's Disease. Methods Mol Biol 1382:367-382.

Forsyth CB, Shannon KM, Kordower JH, Voigt RM, Shaikh M, Jaglin JA, Estes JD, Dodiya HB, Keshavarzian A (2011) Increased intestinal permeability correlates with sigmoid mucosa alpha-synuclein staining and endotoxin exposure markers in early Parkinson's disease. PLoS One 6:e28032.

Franceschi C, Campisi J (2014) Chronic inflammation (inflammaging) and its potential contribution to age-associated diseases. J Gerontol A Biol Sci Med Sci 69 Suppl 1:S4-9.

Fuzzati-Armentero MT, Cerri S, Blandini F (2019) Peripheral-Central Neuroimmune Crosstalk in Parkinson's Disease: What Do Patients and Animal Models Tell Us? Front Neurol 10:232.

Gabbianelli R, Falcioni ML, Cantalamessa F, Nasuti C (2009) Permethrin induces lymphocyte DNA lesions at both Endo III and Fpg sites and changes in monocyte respiratory burst in rats. J Appl Toxicol 29:317-322.

Gallo KA, Johnson GL (2002) Mixed-lineage kinase control of JNK and p38 MAPK pathways. Nat Rev Mol Cell Biol 3:663-672.

Gardet A, Benita Y, Li C, Sands BE, Ballester I, Stevens C, Korzenik JR, Rioux JD, Daly MJ, Xavier RJ, Podolsky DK (2010) LRRK2 is involved in the IFN-gamma response and host response to pathogens. J Immunol 185:5577-5585.

Garretti F, Agalliu D, Lindestam Arlehamn CS, Sette A, Sulzer D (2019) Autoimmunity in Parkinson's Disease: The Role of alpha-Synuclein-Specific T Cells. Front Immunol 10:303.

Gerhard A, Pavese N, Hotton G, Turkheimer F, Es M, Hammers A, Eggert K, Oertel W, Banati RB, Brooks DJ (2006) In vivo imaging of microglial activation with [11C](R)-PK11195 PET in idiopathic Parkinson's disease. Neurobiol Dis 21:404-412.

Ginhoux F, Lim S, Hoeffel G, Low D, Huber T (2013) Origin and differentiation of microglia. Front Cell Neurosci 7:45.

Glorennec P, Serrano T, Fravallo M, Warembourg C, Monfort C, Cordier S, Viel JF, Le Gleau F, Le Bot B, Chevrier C (2017) Determinants of children's exposure to pyrethroid insecticides in western France. Environ Int 104:76-82.

Gnanadhas DP, Dash PK, Sillman B, Bade AN, Lin Z, Palandri DL, Gautam N, Alnouti Y, Gelbard HA, McMillan J, Mosley RL, Edagwa B, Gendelman HE, Gorantla S (2017) Autophagy facilitates macrophage depots of sustained-release nanoformulated antiretroviral drugs. J Clin Invest 127:857-873.

Gold A, Turkalp ZT, Munoz DG (2013) Enteric alpha-synuclein expression is increased in Parkinson's disease but not Alzheimer's disease. Mov Disord 28:237-240.

Gombash SE, Manfredsson FP, Kemp CJ, Kuhn NC, Fleming SM, Egan AE, Grant LM, Ciucci MR, MacKeigan JP, Sortwell CE (2013) Morphological and behavioral impact of AAV2/5-mediated overexpression of human wildtype alpha-synuclein in the rat nigrostriatal system. PLoS One 8:e81426.

Gonzalez H, Contreras F, Prado C, Elgueta D, Franz D, Bernales S, Pacheco R (2013) Dopamine receptor D3 expressed on CD4+ T cells favors neurodegeneration of dopaminergic neurons during Parkinson's disease. J Immunol 190:5048-5056.

Gonzalez-Cuyar LF, Nelson G, Criswell SR, Ho P, Lonzanida JA, Checkoway H, Seixas N, Gelman BB, Evanoff BA, Murray J, Zhang J, Racette BA (2014) Quantitative neuropathology associated with chronic manganese exposure in South African mine workers. Neurotoxicology 45:260-266.

Goodfellow VS, Loweth CJ, Ravula SB, Wiemann T, Nguyen T, Xu Y, Todd DE, Sheppard D, Pollack S, Polesskaya O, Marker DF, Dewhurst S, Gelbard HA (2013) Discovery, synthesis, and characterization of an orally bioavailable, brain penetrant inhibitor of mixed lineage kinase 3. J Med Chem 56:8032-8048.

Gorbatyuk OS, Li S, Sullivan LF, Chen W, Kondrikova G, Manfredsson FP, Mandel RJ, Muzyczka N (2008) The phosphorylation state of Ser-129 in human alpha-synuclein determines neurodegeneration in a rat model of Parkinson disease. Proc Natl Acad Sci U S A 105:763-768.

Gorell JM, Johnson CC, Rybicki BA, Peterson EL, Richardson RJ (1998) The risk of Parkinson's disease with exposure to pesticides, farming, well water, and rural living. Neurology 50:1346-1350.

Graef IA, Wang F, Charron F, Chen L, Neilson J, Tessier-Lavigne M, Crabtree GR (2003) Neurotrophins and netrins require calcineurin/NFAT signaling to stimulate outgrowth of embryonic axons. Cell 113:657-670.

Gray MT, Munoz DG, Gray DA, Schlossmacher MG, Woulfe JM (2014) Alpha-synuclein in the appendiceal mucosa of neurologically intact subjects. Mov Disord 29:991-998.

Greenblatt MB, Aliprantis A, Hu B, Glimcher LH (2010) Calcineurin regulates innate antifungal immunity in neutrophils. J Exp Med 207:923-931.

Guo Y, Deng X, Zheng W, Xu H, Song Z, Liang H, Lei J, Jiang X, Luo Z, Deng H (2011) HLA rs3129882 variant in Chinese Han patients with late-onset sporadic Parkinson disease. Neurosci Lett 501:185-187.

Gupta A, Agarwal R, Shukla GS (1999) Functional impairment of blood-brain barrier following pesticide exposure during early development in rats. Hum Exp Toxicol 18:174-179.

Gustafson CE, Weyand CM, Goronzy JJ (2018) T follicular helper cell development and functionality in immune ageing. Clin Sci (Lond) 132:1925-1935.

Hakimi M, Selvanantham T, Swinton E, Padmore RF, Tong Y, Kabbach G, Venderova K, Girardin SE, Bulman DE, Scherzer CR, LaVoie MJ, Gris D, Park DS, Angel JB, Shen J, Philpott DJ, Schlossmacher MG (2011) Parkinson's disease-linked LRRK2 is expressed in circulating and tissue immune cells and upregulated following recognition of microbial structures. J Neural Transm (Vienna) 118:795-808.

Hallett PJ, McLean JR, Kartunen A, Langston JW, Isacson O (2012) alpha-Synuclein overexpressing transgenic mice show internal organ pathology and autonomic deficits. Neurobiol Dis 47:258-267.

Hamza TH, Zabetian CP, Tenesa A, Laederach A, Montimurro J, Yearout D, Kay DM, Doheny KF, Paschall J, Pugh E, Kusel VI, Collura R, Roberts J, Griffith A, Samii A, Scott WK, Nutt J, Factor SA, Payami H (2010) Common genetic variation in the HLA region is associated with late-onset sporadic Parkinson's disease. Nat Genet 42:781-785.

Handley ME, Rasaiyaah J, Chain BM, Katz DR (2007) Mixed lineage kinases (MLKs): a role in dendritic cells, inflammation and immunity? International journal of experimental pathology 88:111-126.

Harms AS, Delic V, Thome AD, Bryant N, Liu Z, Chandra S, Jurkuvenaite A, West AB (2017) alpha-Synuclein fibrils recruit peripheral immune cells in the rat brain prior to neurodegeneration. Acta Neuropathol Commun 5:85.

Harms AS, Cao S, Rowse AL, Thome AD, Li X, Mangieri LR, Cron RQ, Shacka JJ, Raman C, Standaert DG (2013) MHCII is required for alpha-synuclein-induced activation of microglia, CD4 T cell proliferation, and dopaminergic neurodegeneration. J Neurosci 33:9592-9600.

Hartmann A, Hunot S, Michel PP, Muriel MP, Vyas S, Faucheux BA, Mouatt-Prigent A, Turmel H, Srinivasan A, Ruberg M, Evan GI, Agid Y, Hirsch EC (2000) Caspase-3: A vulnerability factor and final effector in apoptotic death of dopaminergic neurons in Parkinson's disease. Proc Natl Acad Sci U S A 97:2875-2880.

Hashimoto M, Yoshimoto M, Sisk A, Hsu LJ, Sundsmo M, Kittel A, Saitoh T, Miller A, Masliah E (1997) NACP, a synaptic protein involved in Alzheimer's disease, is differentially regulated during megakaryocyte differentiation. Biochem Biophys Res Commun 237:611-616.

Henry J, Smeyne RJ, Jang H, Miller B, Okun MS (2010) Parkinsonism and neurological manifestations of influenza throughout the 20th and 21st centuries. Parkinsonism Relat Disord 16:566-571.

Hickman S, Izzy S, Sen P, Morsett L, El Khoury J (2018) Microglia in neurodegeneration. Nat Neurosci 21:1359-1369.

Hill-Burns EM, Factor SA, Zabetian CP, Thomson G, Payami H (2011) Evidence for more than one Parkinson's disease-associated variant within the HLA region. PLoS One 6:e27109.

Hirsch EC, Hunot S (2009) Neuroinflammation in Parkinson's disease: a target for neuroprotection? The Lancet Neurology 8:382-397.

Hoffmeyer A, Avots A, Flory E, Weber CK, Serfling E, Rapp UR (1998) The GABP-responsive element of the interleukin-2 enhancer is regulated by JNK/SAPK-activating pathways in T lymphocytes. The Journal of biological chemistry 273:10112-10119.

Hoffmeyer A, Grosse-Wilde A, Flory E, Neufeld B, Kunz M, Rapp UR, Ludwig S (1999) Different mitogen-activated protein kinase signaling pathways cooperate to regulate tumor necrosis factor alpha gene expression in T lymphocytes. The Journal of biological chemistry 274:4319-4327.

Hongge L, Kexin G, Xiaojie M, Nian X, Jinsha H (2015) The role of LRRK2 in the regulation of monocyte adhesion to endothelial cells. J Mol Neurosci 55:233-239.

Hostiuc S, Drima E, Buda O (2016) Shake the Disease. Georges Marinesco, Paul Blocq and the Pathogenesis of Parkinsonism, 1893. Frontiers in neuroanatomy 10:74.

Houser MC, Tansey MG (2017) The gut-brain axis: is intestinal inflammation a silent driver of Parkinson's disease pathogenesis? NPJ Parkinsons Dis 3:3.

Hu X, Zhang D, Pang H, Caudle WM, Li Y, Gao H, Liu Y, Qian L, Wilson B, Di Monte DA, Ali SF, Zhang J, Block ML, Hong JS (2008) Macrophage antigen complex-1 mediates reactive microgliosis and progressive dopaminergic neurodegeneration in the MPTP model of Parkinson's disease. J Immunol 181:7194-7204.

Huang Q, Du X, He X, Yu Q, Hu K, Breitwieser W, Shen Q, Ma S, Li M (2016) JNK-mediated activation of ATF2 contributes to dopaminergic neurodegeneration in the MPTP mouse model of Parkinson's disease. Exp Neurol 277:296-304.

Hudkins RL, Diebold JL, Tao M, Josef KA, Park CH, Angeles TS, Aimone LD, Husten J, Ator MA, Meyer SL, Holskin BP, Durkin JT, Fedorov AA, Fedorov EV, Almo SC, Mathiasen JR, Bozyczko-Coyne D, Saporito MS, Scott RW, Mallamo JP (2008) Mixed-lineage kinase 1 and mixed-lineage kinase 3 subtype-selective dihydronaphthyl[3,4-a]pyrrolo[3,4-c]carbazole-5-ones: optimization, mixed-lineage kinase 1 crystallography, and oral in vivo activity in 1-methyl-4-phenyltetrahydropyridine models. J Med Chem 51:5680-5689.

Imamura K, Hishikawa N, Sawada M, Nagatsu T, Yoshida M, Hashizume Y (2003) Distribution of major histocompatibility complex class II-positive microglia and cytokine profile of Parkinson's disease brains. Acta Neuropathol 106:518-526.

Ingelsson M (2016) Alpha-Synuclein Oligomers-Neurotoxic Molecules in Parkinson's Disease and Other Lewy Body Disorders. Front Neurosci 10:408.

International Parkinson Disease Genomics C, Nalls MA, Plagnol V, Hernandez DG, Sharma M, Sheerin UM, Saad M, Simon-Sanchez J, Schulte C, Lesage S, Sveinbjornsdottir S, Stefansson K, Martinez M, Hardy J, Heutink P, Brice A, Gasser T, Singleton AB, Wood NW (2011) Imputation of sequence variants for identification of genetic risks for Parkinson's disease: a meta-analysis of genome-wide association studies. Lancet 377:641-649.

Jackson-Lewis V, Przedborski S (2007) Protocol for the MPTP mouse model of Parkinson's disease. Nature protocols 2:141-151.

Jameson SC, Masopust D (2018) Understanding Subset Diversity in T Cell Memory. Immunity 48:214-226.

Jang H, Boltz D, Sturm-Ramirez K, Shepherd KR, Jiao Y, Webster R, Smeyne RJ (2009) Highly pathogenic H5N1 influenza virus can enter the central nervous system and induce neuroinflammation and neurodegeneration. Proc Natl Acad Sci U S A 106:14063-14068.

Javitch JA, D'Amato RJ, Strittmatter SM, Snyder SH (1985) Parkinsonism-inducing neurotoxin, N-methyl-4-phenyl-1,2,3,6 -tetrahydropyridine: uptake of the metabolite N-methyl-4-phenylpyridine by dopamine neurons explains selective toxicity. Proc Natl Acad Sci U S A 82:2173-2177.

Jimenez-Ferrer I, Swanberg M (2018) Immunogenetics of Parkinson's Disease. In: Parkinson's Disease: Pathogenesis and Clinical Aspects (Stoker TB, Greenland JC, eds). Brisbane (AU).

Joers V, Tansey MG, Mulas G, Carta AR (2017) Microglial phenotypes in Parkinson's disease and animal models of the disease. Prog Neurobiol 155:57-75.

Joshi N, Singh S (2018) Updates on immunity and inflammation in Parkinson disease pathology. J Neurosci Res 96:379-390.

Kahle PJ, Neumann M, Ozmen L, Muller V, Jacobsen H, Spooren W, Fuss B, Mallon B, Macklin WB, Fujiwara H, Hasegawa M, Iwatsubo T, Kretzschmar HA, Haass C (2002) Hyperphosphorylation and insolubility of alpha-synuclein in transgenic mouse oligodendrocytes. EMBO Rep 3:583-588.

Kannarkat GT, Tansey MG (2016) Pesticide-induced Immunotoxicity May Underlie Synergistic Gene-environment Interactions that Increase Parkinson’s Disease Risk for HIgh-risk Genotype Individuals at rs3129882 in the *HLA-DRA* Gene. Journal of Clinical and Cellular Immunology 7:5.

Kannarkat GT, Boss JM, Tansey MG (2013) The role of innate and adaptive immunity in Parkinson's disease. J Parkinsons Dis 3:493-514.

Kannarkat GT, Cook DA, Lee JK, Chang J, Chung J, Sandy E, Paul KC, Ritz B, Bronstein J, Factor SA, Boss JM, Tansey MG (2015) Common Genetic Variant Association with Altered HLA Expression, Synergy with Pyrethroid Exposure, and Risk for Parkinson's Disease: An Observational and Case-Control Study. NPJ Parkinsons Dis 1.

Kant S, Swat W, Zhang S, Zhang ZY, Neel BG, Flavell RA, Davis RJ (2011) TNF-stimulated MAP kinase activation mediated by a Rho family GTPase signaling pathway. Genes & development 25:2069-2078.

Karman J, Ling C, Sandor M, Fabry Z (2004) Initiation of immune responses in brain is promoted by local dendritic cells. J Immunol 173:2353-2361.

Kim S, Seo JH, Suh YH (2004) Alpha-synuclein, Parkinson's disease, and Alzheimer's disease. Parkinsonism Relat Disord 10 Suppl 1:S9-13.

King JM, Muthian G, Mackey V, Smith M, Charlton C (2011) L-Dihydroxyphenylalanine modulates the steady-state expression of mouse striatal tyrosine hydroxylase, aromatic L-amino acid decarboxylase, dopamine and its metabolites in an MPTP mouse model of Parkinson's disease. Life sciences 89:638-643.

Kipnis J, Gadani S, Derecki NC (2012) Pro-cognitive properties of T cells. Nature reviews Immunology 12:663-669.

Kirik D, Rosenblad C, Burger C, Lundberg C, Johansen TE, Muzyczka N, Mandel RJ, Bjorklund A (2002) Parkinson-like neurodegeneration induced by targeted overexpression of alpha-synuclein in the nigrostriatal system. J Neurosci 22:2780-2791.

Kitada T, Asakawa S, Hattori N, Matsumine H, Yamamura Y, Minoshima S, Yokochi M, Mizuno Y, Shimizu N (1998) Mutations in the parkin gene cause autosomal recessive juvenile parkinsonism. Nature 392:605-608.

Kivisakk P, Mahad DJ, Callahan MK, Sikora K, Trebst C, Tucky B, Wujek J, Ravid R, Staugaitis SM, Lassmann H, Ransohoff RM (2004) Expression of CCR7 in multiple sclerosis: implications for CNS immunity. Ann Neurol 55:627-638.

Klegeris A, Pelech S, Giasson BI, Maguire J, Zhang H, McGeer EG, McGeer PL (2008) Alpha-synuclein activates stress signaling protein kinases in THP-1 cells and microglia. Neurobiol Aging 29:739-752.

Klein RL, King MA, Hamby ME, Meyer EM (2002) Dopaminergic cell loss induced by human A30P alpha-synuclein gene transfer to the rat substantia nigra. Hum Gene Ther 13:605-612.

Kline EM, Butkovich LM, Bradner JM, Chang J, Gelbard H, Goodfellow V, Caudle WM, Tansey MG (2019) The second generation mixed lineage kinase-3 (MLK3) inhibitor CLFB-1134 protects against neurotoxin-induced nigral dopaminergic neuron loss. Exp Neurol 318:157-164.

Koprich JB, Johnston TH, Reyes MG, Sun X, Brotchie JM (2010) Expression of human A53T alpha-synuclein in the rat substantia nigra using a novel AAV1/2 vector produces a rapidly evolving pathology with protein aggregation, dystrophic neurite architecture and nigrostriatal degeneration with potential to model the pathology of Parkinson's disease. Mol Neurodegener 5:43.

Kosloski LM, Kosmacek EA, Olson KE, Mosley RL, Gendelman HE (2013) GM-CSF induces neuroprotective and anti-inflammatory responses in 1-methyl-4-phenyl-1,2,3,6-tetrahydropyridine intoxicated mice. J Neuroimmunol 265:1-10.

Koutsilieri E, Lutz MB, Scheller C (2013) Autoimmunity, dendritic cells and relevance for Parkinson's disease. J Neural Transm (Vienna) 120:75-81.

Kozina E, Sadasivan S, Jiao Y, Dou Y, Ma Z, Tan H, Kodali K, Shaw T, Peng J, Smeyne RJ (2018) Mutant LRRK2 mediates peripheral and central immune responses leading to neurodegeneration in vivo. Brain 141:1753-1769.

Kumar A, Sasmal D, Sharma N (2015) Immunomodulatory role of piperine in deltamethrin induced thymic apoptosis and altered immune functions. Environ Toxicol Pharmacol 39:504-514.

Kumar A, Sasmal D, Bhaskar A, Mukhopadhyay K, Thakur A, Sharma N (2016) Deltamethrin-induced oxidative stress and mitochondrial caspase-dependent signaling pathways in murine splenocytes. Environ Toxicol 31:808-819.

Kumaran R, Cookson MR (2015) Pathways to Parkinsonism Redux: convergent pathobiological mechanisms in genetics of Parkinson's disease. Hum Mol Genet 24:R32-44.

Kuss M, Adamopoulou E, Kahle PJ (2014) Interferon-gamma induces leucine-rich repeat kinase LRRK2 via extracellular signal-regulated kinase ERK5 in macrophages. J Neurochem 129:980-987.

Kyriakis JM, Avruch J (2001) Mammalian mitogen-activated protein kinase signal transduction pathways activated by stress and inflammation. Physiol Rev 81:807-869.

Langston JW, Forno LS, Tetrud J, Reeves AG, Kaplan JA, Karluk D (1999) Evidence of active nerve cell degeneration in the substantia nigra of humans years after 1-methyl-4-phenyl-1,2,3,6-tetrahydropyridine exposure. Ann Neurol 46:598-605.

Lauwers E, Debyser Z, Van Dorpe J, De Strooper B, Nuttin B, Baekelandt V (2003) Neuropathology and neurodegeneration in rodent brain induced by lentiviral vector-mediated overexpression of alpha-synuclein. Brain Pathol 13:364-372.

Lavedan C (1998) The synuclein family. Genome Res 8:871-880.

Lawson LJ, Perry VH, Dri P, Gordon S (1990) Heterogeneity in the distribution and morphology of microglia in the normal adult mouse brain. Neuroscience 39:151-170.

Lee SB, Park SM, Ahn KJ, Chung KC, Paik SR, Kim J (2009) Identification of the amino acid sequence motif of alpha-synuclein responsible for macrophage activation. Biochem Biophys Res Commun 381:39-43.

Lev N, Melamed E, Offen D (2003) Apoptosis and Parkinson's disease. Prog Neuropsychopharmacol Biol Psychiatry 27:245-250.

Levesque S, Surace MJ, McDonald J, Block ML (2011a) Air pollution & the brain: Subchronic diesel exhaust exposure causes neuroinflammation and elevates early markers of neurodegenerative disease. J Neuroinflammation 8:105.

Levesque S, Taetzsch T, Lull ME, Kodavanti U, Stadler K, Wagner A, Johnson JA, Duke L, Kodavanti P, Surace MJ, Block ML (2011b) Diesel exhaust activates and primes microglia: air pollution, neuroinflammation, and regulation of dopaminergic neurotoxicity. Environ Health Perspect 119:1149-1155.

Liao HT, Hsieh CJ, Chiang SY, Lin MH, Chen PC, Wu KY (2011) Simultaneous analysis of chlorpyrifos and cypermethrin in cord blood plasma by online solid-phase extraction coupled with liquid chromatography-heated electrospray ionization tandem mass spectrometry. J Chromatogr B Analyt Technol Biomed Life Sci 879:1961-1966.

Liberatore GT, Jackson-Lewis V, Vukosavic S, Mandir AS, Vila M, McAuliffe WG, Dawson VL, Dawson TM, Przedborski S (1999) Inducible nitric oxide synthase stimulates dopaminergic neurodegeneration in the MPTP model of Parkinson disease. Nature medicine 5:1403-1409.

Lill CM et al. (2012) Comprehensive research synopsis and systematic meta-analyses in Parkinson's disease genetics: The PDGene database. PLoS Genet 8:e1002548.

Lindgren HS, Lelos MJ, Dunnett SB (2012) Do alpha-synuclein vector injections provide a better model of Parkinson's disease than the classic 6-hydroxydopamine model? Exp Neurol 237:36-42.

Liu Z, Huang Y, Cao BB, Qiu YH, Peng YP (2017) Th17 Cells Induce Dopaminergic Neuronal Death via LFA-1/ICAM-1 Interaction in a Mouse Model of Parkinson's Disease. Mol Neurobiol 54:7762-7776.

Liu Z, Lee J, Krummey S, Lu W, Cai H, Lenardo MJ (2011) The kinase LRRK2 is a regulator of the transcription factor NFAT that modulates the severity of inflammatory bowel disease. Nat Immunol 12:1063-1070.

Lo Bianco C, Ridet JL, Schneider BL, Deglon N, Aebischer P (2002) alpha - Synucleinopathy and selective dopaminergic neuron loss in a rat lentiviral-based model of Parkinson's disease. Proc Natl Acad Sci U S A 99:10813-10818.

Lo WL, Donermeyer DL, Allen PM (2012) A voltage-gated sodium channel is essential for the positive selection of CD4(+) T cells. Nat Immunol 13:880-887.

Lopez-Atalaya JP, Askew KE, Sierra A, Gomez-Nicola D (2018) Development and maintenance of the brain's immune toolkit: Microglia and non-parenchymal brain macrophages. Dev Neurobiol 78:561-579.

Lotharius J, Falsig J, van Beek J, Payne S, Dringen R, Brundin P, Leist M (2005) Progressive degeneration of human mesencephalic neuron-derived cells triggered by dopamine-dependent oxidative stress is dependent on the mixed-lineage kinase pathway. J Neurosci 25:6329-6342.

Louveau A et al. (2018) CNS lymphatic drainage and neuroinflammation are regulated by meningeal lymphatic vasculature. Nat Neurosci 21:1380-1391.

Luckheeram RV, Zhou R, Verma AD, Xia B (2012) CD4(+)T cells: differentiation and functions. Clin Dev Immunol 2012:925135.

Lundblad M, Decressac M, Mattsson B, Bjorklund A (2012) Impaired neurotransmission caused by overexpression of alpha-synuclein in nigral dopamine neurons. Proc Natl Acad Sci U S A 109:3213-3219.

Maecker HT, McCoy JP, Nussenblatt R (2012) Standardizing immunophenotyping for the Human Immunology Project. Nature reviews Immunology 12:191-200.

Malaviya M, Husain R, Seth PK, Husain R (1993) Perinatal effects of two pyrethroid insecticides on brain neurotransmitter function in the neonatal rat. Vet Hum Toxicol 35:119-122.

Manna S, Bhattacharyya D, Mandal TK, Dey S (2006) Neuropharmacological effects of deltamethrin in rats. J Vet Sci 7:133-136.

Manzoni C (2017) The LRRK2-macroautophagy axis and its relevance to Parkinson's disease. Biochem Soc Trans 45:155-162.

Maraganore DM et al. (2006) Collaborative analysis of alpha-synuclein gene promoter variability and Parkinson disease. JAMA 296:661-670.

Marinova-Mutafchieva L, Sadeghian M, Broom L, Davis JB, Medhurst AD, Dexter DT (2009) Relationship between microglial activation and dopaminergic neuronal loss in the substantia nigra: a time course study in a 6-hydroxydopamine model of Parkinson's disease. J Neurochem 110:966-975.

Marrack P, Kappler JW (2012) Do MHCII-presented neoantigens drive type 1 diabetes and other autoimmune diseases? Cold Spring Harb Perspect Med 2:a007765.

Martinez-Larranaga MR, Anadon A, Martinez MA, Martinez M, Castellano VJ, Diaz MJ (2003) 5-HT loss in rat brain by type II pyrethroid insecticides. Toxicol Ind Health 19:147-155.

Mata IF, Wedemeyer WJ, Farrer MJ, Taylor JP, Gallo KA (2006) LRRK2 in Parkinson's disease: protein domains and functional insights. Trends Neurosci 29:286-293.

Mathiasen JR, McKenna BA, Saporito MS, Ghadge GD, Roos RP, Holskin BP, Wu ZL, Trusko SP, Connors TC, Maroney AC, Thomas BA, Thomas JC, Bozyczko-Coyne D (2004) Inhibition of mixed lineage kinase 3 attenuates MPP+-induced neurotoxicity in SH-SY5Y cells. Brain research 1003:86-97.

McCarthy MI, Abecasis GR, Cardon LR, Goldstein DB, Little J, Ioannidis JP, Hirschhorn JN (2008) Genome-wide association studies for complex traits: consensus, uncertainty and challenges. Nat Rev Genet 9:356-369.

McGeer PL, Itagaki S, McGeer EG (1988a) Expression of the histocompatibility glycoprotein HLA-DR in neurological disease. Acta Neuropathol 76:550-557.

McGeer PL, Itagaki S, Boyes BE, McGeer EG (1988b) Reactive microglia are positive for HLA-DR in the substantia nigra of Parkinson's and Alzheimer's disease brains. Neurology 38:1285-1291.

McGeer PL, Itagaki S, Akiyama H, McGeer EG (1988c) Rate of cell death in parkinsonism indicates active neuropathological process. Ann Neurol 24:574-576.

Meredith GE, Sonsalla PK, Chesselet MF (2008) Animal models of Parkinson's disease progression. Acta Neuropathol 115:385-398.

Michelucci A, Heurtaux T, Grandbarbe L, Morga E, Heuschling P (2009) Characterization of the microglial phenotype under specific pro-inflammatory and anti-inflammatory conditions: Effects of oligomeric and fibrillar amyloid-beta. J Neuroimmunol 210:3-12.

Migheli R, Del Giudice MG, Spissu Y, Sanna G, Xiong Y, Dawson TM, Dawson VL, Galioto M, Rocchitta G, Biosa A, Serra PA, Carri MT, Crosio C, Iaccarino C (2013) LRRK2 affects vesicle trafficking, neurotransmitter extracellular level and membrane receptor localization. PLoS One 8:e77198.

Miklossy J, Doudet DD, Schwab C, Yu S, McGeer EG, McGeer PL (2006) Role of ICAM-1 in persisting inflammation in Parkinson disease and MPTP monkeys. Exp Neurol 197:275-283.

Miller GW (2014) Exposome : a primer : the ex-POZE-ohm : a pr ĭ m'-er : the environmental equivalent of the genome. Amsterdam ; Boston: Elsevier/Academic Press.

Mitsumoto Y, Watanabe A, Mori A, Koga N (1998) Spontaneous regeneration of nigrostriatal dopaminergic neurons in MPTP-treated C57BL/6 mice. Biochem Biophys Res Commun 248:660-663.

Mittelbronn M, Dietz K, Schluesener HJ, Meyermann R (2001) Local distribution of microglia in the normal adult human central nervous system differs by up to one order of magnitude. Acta Neuropathol 101:249-255.

Mizuta I, Satake W, Nakabayashi Y, Ito C, Suzuki S, Momose Y, Nagai Y, Oka A, Inoko H, Fukae J, Saito Y, Sawabe M, Murayama S, Yamamoto M, Hattori N, Murata M, Toda T (2006) Multiple candidate gene analysis identifies alpha-synuclein as a susceptibility gene for sporadic Parkinson's disease. Hum Mol Genet 15:1151-1158.

Moehle MS, Webber PJ, Tse T, Sukar N, Standaert DG, DeSilva TM, Cowell RM, West AB (2012) LRRK2 inhibition attenuates microglial inflammatory responses. J Neurosci 32:1602-1611.

Mogi M, Kondo T, Mizuno Y, Nagatsu T (2007) p53 protein, interferon-gamma, and NF-kappaB levels are elevated in the parkinsonian brain. Neurosci Lett 414:94-97.

Mogi M, Harada M, Riederer P, Narabayashi H, Fujita K, Nagatsu T (1994a) Tumor necrosis factor-alpha (TNF-alpha) increases both in the brain and in the cerebrospinal fluid from parkinsonian patients. Neurosci Lett 165:208-210.

Mogi M, Harada M, Kondo T, Riederer P, Inagaki H, Minami M, Nagatsu T (1994b) Interleukin-1 beta, interleukin-6, epidermal growth factor and transforming growth factor-alpha are elevated in the brain from parkinsonian patients. Neurosci Lett 180:147-150.

Mogi M, Togari A, Kondo T, Mizuno Y, Komure O, Kuno S, Ichinose H, Nagatsu T (2000) Caspase activities and tumor necrosis factor receptor R1 (p55) level are elevated in the substantia nigra from parkinsonian brain. J Neural Transm (Vienna) 107:335-341.

Moller A, Perrild H, Pedersen H, Hoier-Madsen M (1989) Parkinson's disease and autoimmunity. Acta Neurol Scand 79:173-175.

Mosley RL, Hutter-Saunders JA, Stone DK, Gendelman HE (2012) Inflammation and adaptive immunity in Parkinson's disease. Cold Spring Harb Perspect Med 2:a009381.

Mota M, Reeder M, Chernoff J, Bazenet CE (2001) Evidence for a role of mixed lineage kinases in neuronal apoptosis. J Neurosci 21:4949-4957.

Myhre R, Toft M, Kachergus J, Hulihan MM, Aasly JO, Klungland H, Farrer MJ (2008) Multiple alpha-synuclein gene polymorphisms are associated with Parkinson's disease in a Norwegian population. Acta Neurol Scand 118:320-327.

Nakai M, Fujita M, Waragai M, Sugama S, Wei J, Akatsu H, Ohtaka-Maruyama C, Okado H, Hashimoto M (2007) Expression of alpha-synuclein, a presynaptic protein implicated in Parkinson's disease, in erythropoietic lineage. Biochem Biophys Res Commun 358:104-110.

Nalls MA et al. (2014) Large-scale meta-analysis of genome-wide association data identifies six new risk loci for Parkinson's disease. Nat Genet 46:989-993.

Nash KR, Moran P, Finneran DJ, Hudson C, Robinson J, Morgan D, Bickford PC (2015) Fractalkine over expression suppresses alpha-synuclein-mediated neurodegeneration. Mol Ther 23:17-23.

Nasuti C, Fattoretti P, Carloni M, Fedeli D, Ubaldi M, Ciccocioppo R, Gabbianelli R (2014) Neonatal exposure to permethrin pesticide causes lifelong fear and spatial learning deficits and alters hippocampal morphology of synapses. J Neurodev Disord 6:7.

Nasuti C, Carloni M, Fedeli D, Gabbianelli R, Di Stefano A, Serafina CL, Silva I, Domingues V, Ciccocioppo R (2013) Effects of early life permethrin exposure on spatial working memory and on monoamine levels in different brain areas of pre-senescent rats. Toxicology 303:162-168.

Nemani VM, Lu W, Berge V, Nakamura K, Onoa B, Lee MK, Chaudhry FA, Nicoll RA, Edwards RH (2010) Increased expression of alpha-synuclein reduces neurotransmitter release by inhibiting synaptic vesicle reclustering after endocytosis. Neuron 65:66-79.

Nepom GT, Erlich H (1991) MHC class-II molecules and autoimmunity. Annu Rev Immunol 9:493-525.

Nicoletti A, Vasta R, Mostile G, Nicoletti G, Arabia G, Iliceto G, Lamberti P, Marconi R, Morgante L, Barone P, Quattrone A, Zappia M (2017) Head trauma and Parkinson's disease: results from an Italian case-control study. Neurol Sci 38:1835-1839.

Olesen MN, Christiansen JR, Petersen SV, Jensen PH, Paslawski W, Romero-Ramos M, Sanchez-Guajardo V (2018) CD4 T cells react to local increase of alpha-synuclein in a pathology-associated variant-dependent manner and modify brain microglia in absence of brain pathology. Heliyon 4:e00513.

Oliveras-Salva M, Van der Perren A, Casadei N, Stroobants S, Nuber S, D'Hooge R, Van den Haute C, Baekelandt V (2013) rAAV2/7 vector-mediated overexpression of alpha-synuclein in mouse substantia nigra induces protein aggregation and progressive dose-dependent neurodegeneration. Mol Neurodegener 8:44.

Orr CF, Rowe DB, Mizuno Y, Mori H, Halliday GM (2005) A possible role for humoral immunity in the pathogenesis of Parkinson's disease. Brain 128:2665-2674.

Orthgiess J, Gericke M, Immig K, Schulz A, Hirrlinger J, Bechmann I, Eilers J (2016) Neurons exhibit Lyz2 promoter activity in vivo: Implications for using LysM-Cre mice in myeloid cell research. Eur J Immunol 46:1529-1532.

Ouchi Y, Yoshikawa E, Sekine Y, Futatsubashi M, Kanno T, Ogusu T, Torizuka T (2005) Microglial activation and dopamine terminal loss in early Parkinson's disease. Ann Neurol 57:168-175.

Paisan-Ruiz C et al. (2004) Cloning of the gene containing mutations that cause PARK8-linked Parkinson's disease. Neuron 44:595-600.

Pan PY, Li X, Wang J, Powell J, Wang Q, Zhang Y, Chen Z, Wicinski B, Hof P, Ryan TA, Yue Z (2017) Parkinson's Disease-Associated LRRK2 Hyperactive Kinase Mutant Disrupts Synaptic Vesicle Trafficking in Ventral Midbrain Neurons. J Neurosci 37:11366-11376.

Papachroni KK, Ninkina N, Papapanagiotou A, Hadjigeorgiou GM, Xiromerisiou G, Papadimitriou A, Kalofoutis A, Buchman VL (2007) Autoantibodies to alpha-synuclein in inherited Parkinson's disease. J Neurochem 101:749-756.

Papadopoulos V, Baraldi M, Guilarte TR, Knudsen TB, Lacapere JJ, Lindemann P, Norenberg MD, Nutt D, Weizman A, Zhang MR, Gavish M (2006) Translocator protein (18kDa): new nomenclature for the peripheral-type benzodiazepine receptor based on its structure and molecular function. Trends Pharmacol Sci 27:402-409.

Parisiadou L, Yu J, Sgobio C, Xie C, Liu G, Sun L, Gu XL, Lin X, Crowley NA, Lovinger DM, Cai H (2014) LRRK2 regulates synaptogenesis and dopamine receptor activation through modulation of PKA activity. Nat Neurosci 17:367-376.

Park J, Lee JW, Cooper SC, Broxmeyer HE, Cannon JR, Kim CH (2017) Parkinson disease-associated LRRK2 G2019S transgene disrupts marrow myelopoiesis and peripheral Th17 response. J Leukoc Biol 102:1093-1102.

Park JY, Paik SR, Jou I, Park SM (2008) Microglial phagocytosis is enhanced by monomeric alpha-synuclein, not aggregated alpha-synuclein: implications for Parkinson's disease. Glia 56:1215-1223.

Parkinson Study Group PI (2007) Mixed lineage kinase inhibitor CEP-1347 fails to delay disability in early Parkinson disease. Neurology 69:1480-1490.

Pattu V, Qu B, Schwarz EC, Strauss B, Weins L, Bhat SS, Halimani M, Marshall M, Rettig J, Hoth M (2012) SNARE protein expression and localization in human cytotoxic T lymphocytes. Eur J Immunol 42:470-475.

Pennock ND, White JT, Cross EW, Cheney EE, Tamburini BA, Kedl RM (2013) T cell responses: naive to memory and everything in between. Adv Physiol Educ 37:273-283.

Plowey ED, Cherra SJ, 3rd, Liu YJ, Chu CT (2008) Role of autophagy in G2019S-LRRK2-associated neurite shortening in differentiated SH-SY5Y cells. J Neurochem 105:1048-1056.

Poewe W, Seppi K, Tanner CM, Halliday GM, Brundin P, Volkmann J, Schrag AE, Lang AE (2017) Parkinson disease. Nat Rev Dis Primers 3:17013.

Polymeropoulos MH, Lavedan C, Leroy E, Ide SE, Dehejia A, Dutra A, Pike B, Root H, Rubenstein J, Boyer R, Stenroos ES, Chandrasekharappa S, Athanassiadou A, Papapetropoulos T, Johnson WG, Lazzarini AM, Duvoisin RC, Di Iorio G, Golbe LI, Nussbaum RL (1997) Mutation in the alpha-synuclein gene identified in families with Parkinson's disease. Science 276:2045-2047.

Pope CA, 3rd, Bhatnagar A, McCracken JP, Abplanalp W, Conklin DJ, O'Toole T (2016) Exposure to Fine Particulate Air Pollution Is Associated With Endothelial Injury and Systemic Inflammation. Circ Res 119:1204-1214.

Pulford KA, Sipos A, Cordell JL, Stross WP, Mason DY (1990) Distribution of the CD68 macrophage/myeloid associated antigen. Int Immunol 2:973-980.

Radjavi A, Smirnov I, Kipnis J (2014) Brain antigen-reactive CD4+ T cells are sufficient to support learning behavior in mice with limited T cell repertoire. Brain Behav Immun 35:58-63.

Ramonet D et al. (2011) Dopaminergic neuronal loss, reduced neurite complexity and autophagic abnormalities in transgenic mice expressing G2019S mutant LRRK2. PLoS One 6:e18568.

Ransohoff RM, Brown MA (2012) Innate immunity in the central nervous system. J Clin Invest 122:1164-1171.

Ransom BR, Kunis DM, Irwin I, Langston JW (1987) Astrocytes convert the parkinsonism inducing neurotoxin, MPTP, to its active metabolite, MPP+. Neurosci Lett 75:323-328.

Rao A, Luo C, Hogan PG (1997) Transcription factors of the NFAT family: regulation and function. Annu Rev Immunol 15:707-747.

Rassu M, Del Giudice MG, Sanna S, Taymans JM, Morari M, Brugnoli A, Frassineti M, Masala A, Esposito S, Galioto M, Valle C, Carri MT, Biosa A, Greggio E, Crosio C, Iaccarino C (2017) Role of LRRK2 in the regulation of dopamine receptor trafficking. PLoS One 12:e0179082.

Ray A, Dittel BN (2010) Isolation of mouse peritoneal cavity cells. J Vis Exp.

Reynolds AD, Stone DK, Mosley RL, Gendelman HE (2009) Proteomic studies of nitrated alpha-synuclein microglia regulation by CD4+CD25+ T cells. J Proteome Res 8:3497-3511.

Reynolds AD, Banerjee R, Liu J, Gendelman HE, Mosley RL (2007) Neuroprotective activities of CD4+CD25+ regulatory T cells in an animal model of Parkinson's disease. J Leukoc Biol 82:1083-1094.

Richardson JR, Caudle WM, Wang MZ, Dean ED, Pennell KD, Miller GW (2008) Developmental heptachlor exposure increases susceptibility of dopamine neurons to N-methyl-4-phenyl-1,2,3,6-tetrahydropyridine (MPTP)in a gender-specific manner. Neurotoxicology 29:855-863.

Roche PA, Furuta K (2015) The ins and outs of MHC class II-mediated antigen processing and presentation. Nature reviews Immunology 15:203-216.

Ross OA (2013) A prognostic view on the application of individualized genomics in Parkinson's disease. Curr Genet Med Rep 1:52-57.

Ross OA, Gosal D, Stone JT, Lincoln SJ, Heckman MG, Irvine GB, Johnston JA, Gibson JM, Farrer MJ, Lynch T (2007) Familial genes in sporadic disease: common variants of alpha-synuclein gene associate with Parkinson's disease. Mech Ageing Dev 128:378-382.

Russo I, Berti G, Plotegher N, Bernardo G, Filograna R, Bubacco L, Greggio E (2015) Leucine-rich repeat kinase 2 positively regulates inflammation and down-regulates NF-kappaB p50 signaling in cultured microglia cells. J Neuroinflammation 12:230.

Sadasivan S, Sharp B, Schultz-Cherry S, Smeyne RJ (2017) Synergistic effects of influenza and 1-methyl-4-phenyl-1,2,3,6-tetrahydropyridine (MPTP) can be eliminated by the use of influenza therapeutics: experimental evidence for the multi-hit hypothesis. NPJ Parkinsons Dis 3:18.

Sakaguchi S, Yamaguchi T, Nomura T, Ono M (2008) Regulatory T cells and immune tolerance. Cell 133:775-787.

Sanchez-Guajardo V, Febbraro F, Kirik D, Romero-Ramos M (2010) Microglia acquire distinct activation profiles depending on the degree of alpha-synuclein neuropathology in a rAAV based model of Parkinson's disease. PLoS One 5:e8784.

Sanchez-Guajardo V, Annibali A, Jensen PH, Romero-Ramos M (2013) alpha-Synuclein vaccination prevents the accumulation of parkinson disease-like pathologic inclusions in striatum in association with regulatory T cell recruitment in a rat model. J Neuropathol Exp Neurol 72:624-645.

Saporito MS, Hudkins RL, Maroney AC (2002) Discovery of CEP-1347/KT-7515, an inhibitor of the JNK/SAPK pathway for the treatment of neurodegenerative diseases. Prog Med Chem 40:23-62.

Saporito MS, Brown EM, Miller MS, Carswell S (1999) CEP-1347/KT-7515, an inhibitor of c-jun N-terminal kinase activation, attenuates the 1-methyl-4-

phenyl tetrahydropyridine-mediated loss of nigrostriatal dopaminergic neurons In vivo. J Pharmacol Exp Ther 288:421-427.

Satake W et al. (2009) Genome-wide association study identifies common variants at four loci as genetic risk factors for Parkinson's disease. Nat Genet 41:1303-1307.

Sathaliyawala T, Kubota M, Yudanin N, Turner D, Camp P, Thome JJ, Bickham KL, Lerner H, Goldstein M, Sykes M, Kato T, Farber DL (2013) Distribution and compartmentalization of human circulating and tissue-resident memory T cell subsets. Immunity 38:187-197.

Saunders JA, Estes KA, Kosloski LM, Allen HE, Dempsey KM, Torres-Russotto DR, Meza JL, Santamaria PM, Bertoni JM, Murman DL, Ali HH, Standaert DG, Mosley RL, Gendelman HE (2012) CD4+ regulatory and effector/memory T cell subsets profile motor dysfunction in Parkinson's disease. J Neuroimmune Pharmacol 7:927-938.

Schapansky J, Nardozzi JD, LaVoie MJ (2015) The complex relationships between microglia, alpha-synuclein, and LRRK2 in Parkinson's disease. Neuroscience 302:74-88.

Schildt A, Walker MD, Dinelle K, Miao Q, Schulzer M, O'Kusky J, Farrer MJ, Doudet DJ, Sossi V (2019) Single Inflammatory Trigger Leads to Neuroinflammation in LRRK2 Rodent Model without Degeneration of Dopaminergic Neurons. J Parkinsons Dis 9:121-139.

Schutt CR, Gendelman HE, Mosley RL (2018) Tolerogenic bone marrow-derived dendritic cells induce neuroprotective regulatory T cells in a model of Parkinson's disease. Mol Neurodegener 13:26.

Semchuk KM, Love EJ, Lee RG (1992) Parkinson's disease and exposure to agricultural work and pesticide chemicals. Neurology 42:1328-1335.

Shafer TJ, Meyer DA, Crofton KM (2005) Developmental neurotoxicity of pyrethroid insecticides: critical review and future research needs. Environ Health Perspect 113:123-136.

Shameli A, Xiao W, Zheng Y, Shyu S, Sumodi J, Meyerson HJ, Harding CV, Maitta RW (2016) A critical role for alpha-synuclein in development and function of T lymphocytes. Immunobiology 221:333-340.

Shannon KM, Keshavarzian A, Dodiya HB, Jakate S, Kordower JH (2012) Is alpha-synuclein in the colon a biomarker for premotor Parkinson's disease? Evidence from 3 cases. Mov Disord 27:716-719.

Shin EC, Cho SE, Lee DK, Hur MW, Paik SR, Park JH, Kim J (2000) Expression patterns of alpha-synuclein in human hematopoietic cells and in Drosophila at different developmental stages. Mol Cells 10:65-70.

Simon-Sanchez J et al. (2009) Genome-wide association study reveals genetic risk underlying Parkinson's disease. Nat Genet 41:1308-1312.

Singh AK, Tiwari MN, Prakash O, Singh MP (2012a) A current review of cypermethrin-induced neurotoxicity and nigrostriatal dopaminergic neurodegeneration. Curr Neuropharmacol 10:64-71.

Singh AK, Tiwari MN, Upadhyay G, Patel DK, Singh D, Prakash O, Singh MP (2012b) Long term exposure to cypermethrin induces nigrostriatal dopaminergic neurodegeneration in adult rats: postnatal exposure enhances the susceptibility during adulthood. Neurobiol Aging 33:404-415.

Singh AK, Tiwari MN, Dixit A, Upadhyay G, Patel DK, Singh D, Prakash O, Singh MP (2011a) Nigrostriatal proteomics of cypermethrin-induced dopaminergic neurodegeneration: microglial activation-dependent and -independent regulations. Toxicol Sci 122:526-538.

Singh P, Lata P, Patel S, Pandey AK, Jain SK, Shanker R, Dhawan A (2011b) Expression profiling of toxicity pathway genes by real-time PCR array in cypermethrin-exposed mouse brain. Toxicol Mech Methods 21:193-199.

Sommer A, Winner B, Prots I (2017) The Trojan horse - neuroinflammatory impact of T cells in neurodegenerative diseases. Mol Neurodegener 12:78.

Stevens CH, Rowe D, Morel-Kopp MC, Orr C, Russell T, Ranola M, Ward C, Halliday GM (2012) Reduced T helper and B lymphocytes in Parkinson's disease. J Neuroimmunol 252:95-99.

Storelli E, Cassina N, Rasini E, Marino F, Cosentino M (2019) Do Th17 Lymphocytes and IL-17 Contribute to Parkinson's Disease? A Systematic Review of Available Evidence. Front Neurol 10:13.

Su X, Federoff HJ (2014) Immune responses in Parkinson's disease: interplay between central and peripheral immune systems. Biomed Res Int 2014:275178.

Su X, Federoff HJ, Maguire-Zeiss KA (2009) Mutant alpha-synuclein overexpression mediates early proinflammatory activity. Neurotoxicity research 16:238-254.

Su X, Maguire-Zeiss KA, Giuliano R, Prifti L, Venkatesh K, Federoff HJ (2008) Synuclein activates microglia in a model of Parkinson's disease. Neurobiol Aging 29:1690-1701.

Sui YT, Bullock KM, Erickson MA, Zhang J, Banks WA (2014) Alpha synuclein is transported into and out of the brain by the blood-brain barrier. Peptides 62:197-202.

Sulzer D et al. (2017) T cells from patients with Parkinson's disease recognize alpha-synuclein peptides. Nature 546:656-661.

Sun C, Wei L, Luo F, Li Y, Li J, Zhu F, Kang P, Xu R, Xiao L, Liu Z, Xu P (2012) HLA-DRB1 alleles are associated with the susceptibility to sporadic Parkinson's disease in Chinese Han population. PLoS One 7:e48594.

Takahashi M, Yamada T, Nakajima S, Nakajima K, Yamamoto T, Okada H (1995) The substantia nigra is a major target for neurovirulent influenza A virus. J Exp Med 181:2161-2169.

Tansey MG, Romero-Ramos M (2019) Immune system responses in Parkinson's disease: Early and dynamic. Eur J Neurosci 49:364-383.

Tansey MG, McCoy MK, Frank-Cannon TC (2007) Neuroinflammatory mechanisms in Parkinson's disease: potential environmental triggers, pathways, and targets for early therapeutic intervention. Exp Neurol 208:1-25.

Tao X, Constant S, Jorritsma P, Bottomly K (1997) Strength of TCR signal determines the costimulatory requirements for Th1 and Th2 CD4+ T cell differentiation. J Immunol 159:5956-5963.

Tatton NA, Kish SJ (1997) In situ detection of apoptotic nuclei in the substantia nigra compacta of 1-methyl-4-phenyl-1,2,3,6-tetrahydropyridine-treated mice using terminal deoxynucleotidyl transferase labelling and acridine orange staining. Neuroscience 77:1037-1048.

Taubenberger JK, Morens DM (2006) 1918 Influenza: the mother of all pandemics. Emerg Infect Dis 12:15-22.

Taylor KM, Saint-Hilaire MH, Sudarsky L, Simon DK, Hersh B, Sparrow D, Hu H, Weisskopf MG (2016) Head injury at early ages is associated with risk of Parkinson's disease. Parkinsonism Relat Disord 23:57-61.

Theodore S, Cao S, McLean PJ, Standaert DG (2008) Targeted overexpression of human alpha-synuclein triggers microglial activation and an adaptive immune response in a mouse model of Parkinson disease. J Neuropathol Exp Neurol 67:1149-1158.

Thevenet J, Pescini Gobert R, Hooft van Huijsduijnen R, Wiessner C, Sagot YJ (2011) Regulation of LRRK2 expression points to a functional role in human monocyte maturation. PLoS One 6:e21519.

Thome AD, Standaert DG, Harms AS (2015) Fractalkine Signaling Regulates the Inflammatory Response in an alpha-Synuclein Model of Parkinson Disease. PLoS One 10:e0140566.

Tillerson JL, Caudle WM, Reveron ME, Miller GW (2002) Detection of behavioral impairments correlated to neurochemical deficits in mice treated with moderate doses of 1-methyl-4-phenyl-1,2,3,6-tetrahydropyridine. Exp Neurol 178:80-90.

Tiwari MN, Singh AK, Ahmad I, Upadhyay G, Singh D, Patel DK, Singh C, Prakash O, Singh MP (2010) Effects of cypermethrin on monoamine transporters, xenobiotic metabolizing enzymes and lipid peroxidation in the rat nigrostriatal system. Free Radic Res 44:1416-1424.

Tomita K, Kohli R, MacLaurin BL, Hirsova P, Guo Q, Sanchez LHG, Gelbard HA, Blaxall BC, Ibrahim SH (2017) Mixed-lineage kinase 3 pharmacological inhibition attenuates murine nonalcoholic steatohepatitis. JCI Insight 2.

Trowsdale J (1993) Genomic structure and function in the MHC. Trends Genet 9:117-122.

Ueda K, Fukushima H, Masliah E, Xia Y, Iwai A, Yoshimoto M, Otero DA, Kondo J, Ihara Y, Saitoh T (1993) Molecular cloning of cDNA encoding an unrecognized component of amyloid in Alzheimer disease. Proc Natl Acad Sci U S A 90:11282-11286.

Valente EM, Bentivoglio AR, Dixon PH, Ferraris A, Ialongo T, Frontali M, Albanese A, Wood NW (2001) Localization of a novel locus for autosomal recessive early-onset parkinsonism, PARK6, on human chromosome 1p35-p36. Am J Hum Genet 68:895-900.

van Furth R, Cohn ZA (1968) The origin and kinetics of mononuclear phagocytes. J Exp Med 128:415-435.

Verheugen JA, Oortgiesen M, Vijverberg HP (1994) Veratridine blocks voltage-gated potassium current in human T lymphocytes and in mouse neuroblastoma cells. J Membr Biol 137:205-214.

Vilensky JA, Gilman S, McCall S (2010) A historical analysis of the relationship between encephalitis lethargica and postencephalitic parkinsonism: a complex rather than a direct relationship. Mov Disord 25:1116-1123.

Wallings R, Connor-Robson N, Wade-Martins R (2019) LRRK2 interacts with the vacuolar-type H+-ATPase pump a1 subunit to regulate lysosomal function. Hum Mol Genet.

Wang J, Chen Z, Walston JD, Gao P, Gao M, Leng SX (2018) alpha-Synuclein activates innate immunity but suppresses interferon-gamma expression in murine astrocytes. Eur J Neurosci.

Wang LH, Johnson EM, Jr. (2008) Mixed lineage kinase inhibitor CEP-1347 fails to delay disability in early Parkinson disease. Neurology 71:462; author reply 462-463.

Wang W, Yang Y, Ying C, Li W, Ruan H, Zhu X, You Y, Han Y, Chen R, Wang Y, Li M (2007) Inhibition of glycogen synthase kinase-3beta protects dopaminergic neurons from MPTP toxicity. Neuropharmacology 52:1678-1684.

Ward CD, Duvoisin RC, Ince SE, Nutt JD, Eldridge R, Calne DB (1983) Parkinson's disease in 65 pairs of twins and in a set of quadruplets. Neurology 33:815-824.

Watson MB, Richter F, Lee SK, Gabby L, Wu J, Masliah E, Effros RB, Chesselet MF (2012) Regionally-specific microglial activation in young mice over-expressing human wildtype alpha-synuclein. Exp Neurol 237:318-334.

West MJ, Slomianka L, Gundersen HJ (1991) Unbiased stereological estimation of the total number of neurons in thesubdivisions of the rat hippocampus using the optical fractionator. Anat Rec 231:482-497.

Williams GP, Schonhoff AM, Jurkuvenaite A, Thome AD, Standaert DG, Harms AS (2018) Targeting of the class II transactivator attenuates inflammation and neurodegeneration in an alpha-synuclein model of Parkinson's disease. J Neuroinflammation 15:244.

Wissemann WT, Hill-Burns EM, Zabetian CP, Factor SA, Patsopoulos N, Hoglund B, Holcomb C, Donahue RJ, Thomson G, Erlich H, Payami H (2013) Association of Parkinson disease with structural and regulatory variants in the HLA region. Am J Hum Genet 93:984-993.

Witoelar A et al. (2017) Genome-wide Pleiotropy Between Parkinson Disease and Autoimmune Diseases. JAMA Neurol 74:780-792.

Wohleb ES, Powell ND, Godbout JP, Sheridan JF (2013) Stress-induced recruitment of bone marrow-derived monocytes to the brain promotes anxiety-like behavior. J Neurosci 33:13820-13833.

Xiao W, Shameli A, Harding CV, Meyerson HJ, Maitta RW (2014) Late stages of hematopoiesis and B cell lymphopoiesis are regulated by alpha-synuclein, a key player in Parkinson's disease. Immunobiology 219:836-844.

Xu Z, Maroney AC, Dobrzanski P, Kukekov NV, Greene LA (2001) The MLK family mediates c-Jun N-terminal kinase activation in neuronal apoptosis. Mol Cell Biol 21:4713-4724.

Yamane H, Paul WE (2012) Cytokines of the gamma(c) family control CD4+ T cell differentiation and function. Nat Immunol 13:1037-1044.

Yanamandra K, Gruden MA, Casaite V, Meskys R, Forsgren L, Morozova-Roche LA (2011) alpha-synuclein reactive antibodies as diagnostic biomarkers in blood sera of Parkinson's disease patients. PLoS One 6:e18513.

Yang X, Ren H, Wood K, Li M, Qiu S, Shi FD, Ma C, Liu Q (2018) Depletion of microglia augments the dopaminergic neurotoxicity of MPTP. FASEB J 32:3336-3345.

Zappia M, Crescibene L, Bosco D, Arabia G, Nicoletti G, Bagala A, Bastone L, Napoli ID, Caracciolo M, Bonavita S, Di Costanzo A, Gambardella A, Quattrone A (2002) Anti-GM1 ganglioside antibodies in Parkinson's disease. Acta Neurol Scand 106:54-57.

Zeisel A, Munoz-Manchado AB, Codeluppi S, Lonnerberg P, La Manno G, Jureus A, Marques S, Munguba H, He L, Betsholtz C, Rolny C, Castelo-Branco G, Hjerling-Leffler J, Linnarsson S (2015) Brain structure. Cell types in the mouse cortex and hippocampus revealed by single-cell RNA-seq. Science 347:1138-1142.

Zhang W, Wang T, Qin L, Gao HM, Wilson B, Ali SF, Zhang W, Hong JS, Liu B (2004) Neuroprotective effect of dextromethorphan in the MPTP Parkinson's disease model: role of NADPH oxidase. FASEB J 18:589-591.

Zhang W, Wang T, Pei Z, Miller DS, Wu X, Block ML, Wilson B, Zhang W, Zhou Y, Hong JS, Zhang J (2005) Aggregated alpha-synuclein activates microglia: a process leading to disease progression in Parkinson's disease. FASEB J 19:533-542.

Zhang W, Phillips K, Wielgus AR, Liu J, Albertini A, Zucca FA, Faust R, Qian SY, Miller DS, Chignell CF, Wilson B, Jackson-Lewis V, Przedborski S, Joset D, Loike J, Hong JS, Sulzer D, Zecca L (2011) Neuromelanin activates microglia and induces degeneration of dopaminergic neurons: implications for progression of Parkinson's disease. Neurotoxicity research 19:63-72.

Zhang Y, Shu L, Sun Q, Pan H, Guo J, Tang B (2018) A Comprehensive Analysis of the Association Between SNCA Polymorphisms and the Risk of Parkinson's Disease. Front Mol Neurosci 11:391.

Zhong SC, Luo X, Chen XS, Cai QY, Liu J, Chen XH, Yao ZX (2010) Expression and subcellular location of alpha-synuclein during mouse-embryonic development. Cell Mol Neurobiol 30:469-482.

Zimprich A et al. (2004) Mutations in LRRK2 cause autosomal-dominant parkinsonism with pleomorphic pathology. Neuron 44:601-607.

Ziv Y, Ron N, Butovsky O, Landa G, Sudai E, Greenberg N, Cohen H, Kipnis J, Schwartz M (2006) Immune cells contribute to the maintenance of neurogenesis and spatial learning abilities in adulthood. Nat Neurosci 9:268-275.

Zsiros E, Kis-Toth K, Hajdu P, Gaspar R, Bielanska J, Felipe A, Rajnavolgyi E, Panyi G (2009) Developmental switch of the expression of ion channels in human dendritic cells. J Immunol 183:4483-4492.